ROBUST ESTIMATION OF LIMIT LOADS OF PLATES USING SECANT RIGIDITY

CENTRE FOR NEWFOUNDLAND STUDIES

TOTAL OF 10 PAGES ONLY
MAY BE XEROXED

(Without Author's Permission)

AMAN AHMED BOLAR

INFORMATION TO USERS

This manuscript has been reproduced from the microfilm master. UMI films the text directly from the original or copy submitted. Thus, some thesis and dissertation copies are in typewriter face, while others may be from any type of computer printer.

The quality of this reproduction is dependent upon the quality of the copy submitted. Broken or indistinct print, colored or poor quality illustrations and photographs, print bleedthrough, substandard margins, and improper alignment can adversely affect reproduction.

In the unlikely event that the author did not send UMI a complete manuscript and there are missing pages, these will be noted. Also, if unauthorized copyright material had to be removed, a note will indicate the deletion.

Oversize materials (e.g., maps, drawings, charts) are reproduced by sectioning the original, beginning at the upper left-hand corner and continuing from left to right in equal sections with small overlaps.

ProQuest Information and Learning
300 North Zeeb Road, Ann Arbor, MI 48106-1346 USA
800-521-0600

UMI®

NOTE TO USERS

Page(s) not included in the original manuscript are unavailable from the author or university. The manuscript was microfilmed as received.

115 – 121
also
133 – 140

This reproduction is the best copy available.

UMI

National Library of Canada
Acquisitions and Bibliographic Services
395 Wellington Street
Ottawa ON K1A 0N4
Canada

Bibliothèque nationale du Canada
Acquisitions et services bibliographiques
395, rue Wellington
Ottawa ON K1A 0N4
Canada

Your file Votre référence

Our file Notre référence

The author has granted a non-exclusive licence allowing the National Library of Canada to reproduce, loan, distribute or sell copies of this thesis in microform, paper or electronic formats.

The author retains ownership of the copyright in this thesis. Neither the thesis nor substantial extracts from it may be printed or otherwise reproduced without the author's permission.

L'auteur a accordé une licence non exclusive permettant à la Bibliothèque nationale du Canada de reproduire, prêter, distribuer ou vendre des copies de cette thèse sous la forme de microfiche/film, de reproduction sur papier ou sur format électronique.

L'auteur conserve la propriété du droit d'auteur qui protège cette thèse. Ni la thèse ni des extraits substantiels de celle-ci ne doivent être imprimés ou autrement reproduits sans son autorisation.

0-612-73579-6

Canada

ROBUST ESTIMATION OF LIMIT LOADS OF PLATES USING SECANT RIGIDITY

by

Aman Ahmed Bolar, B.E.

A thesis submitted to the

School of Graduate Studies

in partial fulfillment of the

requirements for the degree of

Master of Engineering

Faculty of Engineering and Applied Science

Memorial University of Newfoundland

June 2001

St. John's **Newfoundland**

ABSTRACT

A robust method for the estimation of limit loads of structures has been adopted for plate structures. It involves the use of modified secant rigidity. The method makes use of repeated linear elastic analyses to predict limit behavior. The results from an initial elastic analysis are used to obtain the principal moments. A suitable yield criterion (such as Tresca or Von Mises) in terms of generalized forces is used. A set of equivalent moments is then computed for the plate. This is used to modify the secant rigidity of the plate. The modified structure is re-analyzed iteratively until convergence is reached. The moment distribution from the convergent analysis shows the collapse mechanism for the plate. The average of the equivalent moments along the collapse (or yield) lines of the plate is scaled to the plastic moment capacity of the section to obtain the limit load factor. The method has several advantages in comparison to other traditional methods.

This method has been implemented on ANSYS software using APDL routines. Problems solved include: simply supported and fixed square and circular plates with uniform and concentrated loads, plates with irregular boundary conditions and shapes as well as continuous plates with checkerboard loading. The results from the above analyses match analytical results very closely, thus demonstrating the usefulness of the method used.

Acknowledgements

The author is grateful to his supervisor, Dr. Seshu Madhava Rao Adluri for his active mentoring during the numerous technical discussions and personal care undertaken by him during the course of this program. The financial support provided by the School of Graduate Studies as well as NSERC are thankfully acknowledged.

Appreciation is extended to Dr. R.Seshadri, Dean of Faculty of Engineering and Dr.M.Haddara, Associate Dean of Faculty of Engineering for their support and encouragement during the course of the program.

The author also wishes to acknowledge the staff at C-CAE for their timely co-operation during difficulties faced with computers and software. Encouragement and moral support provided by my parents, sister Rubyana Bolar and brother-in-law Aamir Sait is gratefully acknowledged.

Lastly, acknowledgements are directed to all my friends at Memorial University and elsewhere for their guidance and support. Special thanks in this regard, to friends Raj Mannem and Rehan Sadiq.

Table of Contents

List of Figures

List of Tables

List of Symbols

a	side dimension of square plate, mm
	longer span of the individual panel in a continuous plate, mm
b	shorter span of the individual panel in a continuous plate, mm
	free length of a plate simply supported on three sides, mm
	breadth of a beam, mm
B_i	body force in the direction i
D	flexural rigidity of plate, N-mm
D_{old}	rigidity from previous (old) elastic analysis, N-mm
D_{new}	modified rigidity for the next analysis, N-mm
E	Young's (elastic) modulus, N/mm^2
E_o	original value of Young's modulus, N/mm^2
EI_o	Original flexural rigidity of beam, N-mm
E_p	plastic modulus, N/mm^2
E_R	revised young's modulus, N/mm^2
E_s	modified Young's modulus after second elastic (r-node) analysis, N/mm^2
	secant modulus, N/mm^2
E_t	tangent modulus, N/mm^2
$(E_s)_k$	Young's modulus in second analysis for element k, N/mm^2
f_y	Yield stress of the material, MPa
G	shear modulus, N/mm^2
h	depth of a beam or plate, mm
I_1	first invariant of stress tensor
i	degree of fixity,
	iteration number
i, j, k	Direction identifiers, e.g., x, y, z

J_2 and J_3	second and third invariants of deviatoric stress tensor
$\dot{K}_r, \dot{K}_\theta$	curvatures in the radial and tangential direction respectively
k_1, k_2	material constants
L	length of the plate, mm
l, m, n	direction cosines of normal to the exterior of face of tetrahedron
M	applied moment, N-mm/mm
M_a	arbitrary moment, N-mm/mm
M_{el}	elastic moment in a rectangular cross-section, N-mm/mm
M_{eq}	equivalent moment, N-mm/mm
$M_{eq\text{-}av}$	average equivalent moment, N-mm/mm
M_{max}	maximum equivalent moment, N-mm/mm
M_p	plastic moment capacity, N-mm/mm (or N-mm)
M_{Pxy}	plastic moment in x-y direction, N-mm/mm
$M_r, M_\theta, M_{r\theta}$	plate moments in cylindrical co-ordinate system, N-mm/mm
M_x, M_y, M_{xy}	plate moments in Cartesian system, N-mm/mm (or N-mm)
$M_x^{(T)}, M_y^{(T)}, M_z^{(T)}$	total moments in Cartesian co-ordinate system, N-mm
m	exact limit load factor (for applied load)
m_1 and m_2	principal moments, N-mm/mm
$\dot{m}$ and m^0	lower and upper bound load multipliers
m_x, m_y, m_{xy}	moments per unit length, N-mm/mm
n	number of r-node peaks
P, p	uniformly distributed load on the plate, N/mm^2
P_2	additional load borne by a propped cantilever beam after formation of first plastic hinge
P_L	limit load, N (or kN)
P_d	applied load set

P_z	external load normal to plate surface in z-direction
Q_x *and* Q_y	transverse shear forces, N
q	uniformly distributed load on the plate, N/mm^2
q_x *and* q_y	transverse shear forces per unit length, N/mm
R	degree of indeterminacy of a structure
	radius of circular plate, mm
r	radial distance, mm
SI	stress intensity
S_m	code allowable stress intensity
s_{ij}	deviatoric stress tensor
$T^{(x)}$, $T^{(y)}$, $T^{(z)}$	tractions along x, y and z directions, respectively
T_i^v	traction along direction i
t	thickness of the plate, mm
t_0	original thickness, mm
t_{new}	new thickness, mm
UDL	uniformly distributed load
u, v, w	deflection components, mm
V	volume of the structure
V_R	reference volume of a component or structure
V_T	total volume of a component or structure
$\dot{W}$	velocity field which is a function of distance r along the radius R
W_E	external work done
W_I	internal work done
w	distributed load on the plate, N/mm^2
x, y, z	co-ordinate axes
Z	distance through the thickness at which stress is integrated to get moments
α	angle between principal stress planes,

α	convergence accelerator parameter
δ	deflection at a point in a structure
ε	total strain
ε_{cr}	creep strain
ε^{e}	elastic strain
ε_{e1}	equivalent strain of highly stressed region
ε_{e2}	equivalent strain of local element after second analysis (ref. stress)
ε_{el}	elastic strain
ε^{p}, ε_{p}	plastic strain
ε_{t}	total strain
$\varepsilon_{x}, \varepsilon_{y}, \varepsilon_{z}$	strain component in x, y and z direction, respectively
γ_1 and γ_2	scaling parameters
γ_{xy}	shearing strain, MPa
$\kappa_{x}, \kappa_{y}, \chi$	changes of curvature of deflected middle surface
λ	constraint parameter
μ	poisson's ratio
μ_i	for an edge, is the ratio of the negative resisting moment to the positive moment of resistance of the slab
ν	poisson's ratio
ν_{ij}	direction cosines of the coordinate system of traction forces with respect to the reference axes of the stresses
ν_{x}, ν_{y} and ν_{z}	direction cosines of the co-ordinate system of traction with respect to reference axes of stresses
$\dot{\phi}_{x}, \dot{\phi}_{y}$	pure curvature rates about x and y axes
σ_0	yield stress in simple tension test, N/mm^2

$\sigma_1, \sigma_2, \sigma_3$	principal stresses, N/mm^2
σ_{arb}	arbitrary stress value, N/mm^2
$(\sigma_e)_{r-node}$	r-node equivalent stress, N/mm^2
σ_{e1}	equivalent stress of highly stressed region, N/mm^2
σ_{e2}	equivalent stress of local element after second analysis (ref. stress)
σ_{ei}	von Mises equivalent stress of the ith element, N/mm^2
σ_{i-1}	maximum unaveraged nodal equivalent stress associated with element from previous solution, N/mm^2
σ_{ij}	stress in the direction of i on the plane whose normal is along j
σ_n	combined r-node effective stress, N/mm^2
	nominal stress value, N/mm^2
σ_{nj}	r-node effective stress at plastic hinge location j, N/mm^2
$(\sigma_e^o)_k$	equivalent stress for any element k, N/mm^2
σ_{ref}	reference stress , N/mm^2
σ_R	maximum stress having lowest value after repeated analysis, N/mm^2
$\sigma_x, \sigma_y, \sigma_z$	stresses in x, y and z direction respectively, N/mm^2
σ_{xy}, σ_{xz}	stresses in the x direction on the plane whose normals are along y and z respectively, N/mm^2
σ_{yx}, σ_{yz}	stresses in the y direction on the plane whose normals are along x and z respectively, N/mm^2
σ_{zx}, σ_{zy}	stresses in the z direction on the plane whose normals are along x and y, N/mm^2
τ_0	yield stress in shear test, N/mm^2
τ_{max}	maximum shear stress, N/mm^2
$\tau_{xy}, \tau_{yz}, \tau_{zx}$	shearing stresses

θ	degree of multi-axiality and follow-up
6_p	angle of principal plane for moments
ξ	geometric scaling factor depending on configuration and boundary conditions
ς	iteration variable

Acronyms and Abbreviations

APDL	Ansys Parametric Design Language
BFGS	Broyden, Fletcher, Goldfarb and Shanno (Founders of the BFGS method)
CSA	Canadian Standards Association
ECM	Elastic Compensation Method
FEA	Finite Element Analysis
GLOSS	Generalized Local Stress and Strain
R-NODE	Redistribution Node
UDL	Uniformly Distributed Load

Chapter 1

Introduction

1.1 General Background

Most structures are currently analyzed by assuming elastic behavior. The results of this elastic analysis are used to design the structures for limit behaviour of individual components.

Elastic analysis implies that the structure is subjected to elastic stresses at specified loads. In adopting a limit design, the structure needs to be subjected to limiting stresses. Limit stresses usually involve local or global plastic zones. Therefore, there is a discrepancy between the analysis and design philosophies of structures. In case of determinate structures, the effect of this discrepancy is usually negligible. Even for other structures, the presence of residual stresses produced by repeated loading beyond elastic limit (shake down) and other beneficial effects can sometimes offset this discrepancy [Adluri, 2001b]. However in general, for indeterminate structures and complex situations, the difference could be very significant. Many practical structures are highly redundant and hence are complex and indeterminate.

One way of removing this discrepancy is by analyzing structures using limit analysis. Using limit analysis, the reserve strength which is available beyond the formation of first plastic deformations in most practical structures could be made use of, thereby achieving

considerable economy in design. However, rigorous limit analysis has several difficulties associated with it.

1.2 Need for the Proposed Work

The methods available for plastic analysis such as those based on the upper bound and lower bound theorems are tedious for structures with a high degree of redundancy. They are also impracticable for large structures. Finite element nonlinear analyses have problems including, modeling difficulties and excessive computational requirements for practical applications. Hence, a systematic, simple and robust estimation of limit loads would be a useful addition to the tools currently available.

Methods such as the Gloss R-node method and the m_α method have been developed for this purpose. These methods work well for components where very large plastic zones characterize collapse mechanism. However, these methods have some difficulties for civil engineering type structures where a large number of members interact with relatively small plastic zones at collapse. These methods are based on stress level modification and therefore make use of solid elements with discretization through the thickness. If shell elements can be adopted as in the case of the Elastic Compensation method, they require additional calculation of material and cross sectional parameters such as generalized stress resultants.

An approach involving the use of modified secant rigidity [Adluri, 1999, 2001a&b] built on top of the existing robust methods addresses many of these difficulties. This approach

has not been applied in great detail for continuous structures such as plates. The present work has been carried out to adopt and implement this method for the estimation of limit loads of plates. The effectiveness of the technique is checked for both simple as well as complex types of plate configurations.

1.3 Objectives

The present research has the following objectives:

1. Implement the robust technique for limit load estimation of plates based on modified secant rigidity using ANSYS software and it's APDL (Ansys Parametric Design Language) routines.

2. Use different yield criteria and apply the scheme to:

   a) Regular plates: Simply supported and fixed plates of various shapes and loading

   b) Irregular plates: Plates with irregular boundary conditions as well as shape

   c) Continuous plates: Continuous plates with different extreme end conditions and loading on the panels.

3. Compare the method with analytical methods for the determination of limit loads, existing robust methods or non-linear finite element analysis (wherever appropriate).

1.4 Organization of the Thesis

The thesis is organized on the following lines:

Chapter 1 briefly introduces the need for the present method and other relevant material.

Chapter 2 provides a detailed review of the available literature and appropriate theoretical background. A description of plasticity, robust methods and their origin, has been given. A brief outline of a few well-known robust methods has been presented. A section describing the theoretical aspects of plate analysis is included. Elastic analysis of plates using cartesian and cylindrical co-ordinate system has been discussed. Further, the upper bound and lower bound theorems and their applicability to plates has been highlighted.

Chapter 3 provides a simple description of the original theory for the technique used in the present work. This technique is discussed and compared with existing robust methods.

Chapters 4 and 5 present the application of the present method to regular, irregular and continuous plate structures, respectively. The description of the analyses and a discussion of the results are presented.

Chapter 6 concludes the research. It contains a brief summary, the main conclusion of the work along with recommendations for further study.

Several appendices are attached at the end of the thesis. These consist of ANSYS input file listings and the implementation for the various problems analyzed. The input files contain comments for the use of relevant information for future use.

Chapter 2

Literature review

2.1 Introduction to Plastic Analysis

The origin of plasticity as a branch of mechanics dates back to the period 1864-1872 when Tresca published a series of papers on the extrusion of metals. He proposed the first yield criterion for failure of metal structures. It states that a metal yields plastically when the maximum shear stress attains a critical value. Prior to this, criteria for yielding were applied mainly to plastic solids such as soils, for example by Coulomb [1773], Poncelet [1840] and Rankine [1853]. Tresca's yield criterion was applied by Saint Venant to determine the stresses in a partly plastic cylinder subjected to Torsion or bending [1870] and in a completely plastic tube expanded by internal pressure [1872]. Tresca's work was followed by Levy [1870] and then by von Mises [1913], who introduced the well-known pressure-insensitive yield criterion. Several studies have developed or extended the above formulations, e.g., Prandtl [1924], Melan [1938], Drucker, Greenberg and Prager [1951], and Hill [1951]. A good description of these and subsequent studies is given by Chen and Han [1987], Hill [1950] and Calladine [1969] among others.

At small loads, most structures behave elastically. A number of elastic analysis techniques have been well established, chief among them is the Finite Element Analysis (FEA). A large number of software programs have been developed and used by

practising engineers to perform elastic analysis of structures. Elastic analysis indicates linear load-deformation pattern. A design based on elastic analysis assumes that failure would occur as soon as a critical point in the structure reaches yield stress. However, once such yielding occurs in the structure, redistribution of stresses takes place. The zones that would have yielded at a particular load level would not offer further resistance to increased loads. Such increase in load will have to be resisted by the remaining portions of the structure. This redistribution continues with increase in load and would reach a stage when the structure would form a mechanism and would be on the verge of collapse. This load is termed as "limit load" of the structure.

This was initially observed during column buckling investigations during the 1880s. Subsequently in 1914, Kazinczy observed that the ultimate load-carrying capacity of clamped steel beams was considerably higher than that predicted by theory of elasticity [Szilard, 1974]. The increased load carrying capacity is due to ductility or plasticity of most structural materials such as steel, aluminum and reinforced concrete.

Although, structural analysis based on elastic theory yields results for stresses and deformations at working loads, it fails to assess the real load carrying capacity of the structure at ultimate (or factored) loads. At failure, the fundamental assumptions of elastic theory (such as Hooke's law, etc.) are no longer valid. Hence, using elastic analysis, information obtained on the basis of factor of safety against collapse is inaccurate. This is recognized by the widely established "Limit States Design" philosophy [CSA, 1994]. The discrepancy is partly offset by the use of nonlinear

component design and use of load factors. However, for a rational design, the structure must be designed using a properly developed limit analysis [Adluri, 1999, 2001a, b].

Proper estimation of limit loads involves plastic analysis considering non-linear behavior of materials and geometry. Such limit load estimates give us the amount of reserve strength available beyond the initial yield. This results in efficient use of material, leading to economy in design and improved safety.

Limit load may be estimated using upper bound or lower bound techniques depending on the equations of mechanics involved in its determination. Lower-bound techniques give consideration to equilibrium and yield conditions. Whereas, upper bound techniques consider failure modes and energy dissipation.

A complete non-linear analysis would involve complexities arising out of an incremental iterative analysis. Although commercial software programs have been developed for this purpose, they often require considerable judgement and result in high computational costs. Also, if a structure is analyzed using both linear and non-linear FEA and the results compared with corresponding classical analysis, the difference in results would be considerably more for non-linear FEA. In other words, the accuracy obtained in nonlinear FEA is not comparable to that obtained in linear analyses.

When a beam is loaded (Fig.2.1-a) such that at maximum moment location, stress is below the proportional limit, the stress distribution is as shown (Fig 2.1-d (i)). With further increase in load, the outer fibers of the beam in the vicinity of the maximum

moments reach yield stress f_y (Fig. 2.1-d (ii)). As the load is increased further, the yield stress will propagate towards the neutral axis of the section (Fig. 2.1-d (iii)) until the stress distribution is nearly rectangular (Fig. 2.1-d (iv)).

When yielding propagates throughout the depth, a plastic hinge occurs at that location. The constant moment of resistance offered by the section in this case would be the plastic moment M_p. The beam can still carry an additional load P_2 with no further increase in moment at the clamped section. Failure would occur due to formation of a second plastic hinge in the span of the beam. The deformation pattern is called as collapse mechanism and consists of rigid body motions.

By introducing an idealized stress-strain relationship, we can estimate the moment carrying capacity of the beam. The fully plastic moment or ultimate moment capacity of a rectangular beam is given by

$$M_p = \left(\frac{bh}{2}\right)(f_y)\frac{h}{2} = f_y\frac{bh^2}{4} \qquad (2.1.1)$$

where, b is the breadth, h is the depth of the beam and f_y is the yield stress.

Alternatively, ultimate moment per unit width is given by,

$$M_p = f_y\frac{h^2}{4} \qquad (2.1.2)$$

It is assumed here that the material is elastic-perfectly plastic and can undergo large strains without initiating strain-hardening effect. A comparison of this ultimate moment with the moment capacity of the section, obtained from elasticity theory gives,

$$\frac{M_p}{M_{el}} = \frac{f_y h^2/4}{f_y h^2/6} = 1.5 \qquad (2.1.3)$$

From the above relationship, it is clear that there is a 50% increase in capacity by adopting plastic analysis for the rectangular beam section instead of using elastic analysis results. These benefits will be further compounded when the overall structural behaviour is involved in estimating limit loads.

2.2 Theoretical Background

2.2.1 Plastic Behavior in Simple Tension and Compression:

Uni-axial state of stress represents the simplest type of loading condition. The simple tension test has $\sigma_1>0$ and $\sigma_2=\sigma_3=0$ and the simple compression test has $\sigma_1=\sigma_2=0$ and $\sigma_3<0$.

A plot- of the axial principal stresses (σ_1 or σ_3) against the axial strain ε_1(or ε_3) represents the well known *uniaxial stress strain diagram*. (Fig. 2.2 a)

- Point A defines the limit of proportionality.

- Point B defines the *elastic limit* of the material. It is also called as *yield point*.

- Usually, there is not much difference between proportional limit A and elastic limit B. Mild steel exhibits an *upper yield point* B and a *lower yield point* C.

- Beyond point C, there is an increase in strain at approximately constant load. The behavior in the flat region CD is termed as *plastic flow*.

Most metals exhibit neither a definite yield point nor plastic flow. For such cases, yield strength is generally defined as an offset of stress corresponding to, usually a strain of 0.1%. (Fig 2.2 b)[Chen, 1988]. This offset yield stress is defined as *initial yield stress*.

Above the yield point, the response of the material is elastic-plastic. The slope of the curve decreases steadily and monotonically leading to failure of the specimen at point E.

A ductile material like mild steel can sustain large strains without failure. On the other hand, cast iron being brittle material fails with a little strain. Failure also depends on the type of loading. For example, concrete exhibits brittle behavior under tensile loading, but under compression it may exhibit a certain degree of ductility before failure.

2.2.2 Unloading and reloading

Consider the case of a test specimen loaded monotonically to some value beyond the yield point and then completely unloaded. The behavior is as shown in Fig. 2.3.

- OB on the strain axis indicates the irrecoverable *residual strain* or *plastic strain*.

- BC is the recoverable strain and is called as *elastic strain.*

- At this stage, if the specimen is re-loaded, the stress-strain curve follows the path BA similar to the unloading path AB.

- The material behavior is elastic till it reaches the previous maximum stress at point A.

- σ_A is called as *subsequent yield stress*, beyond which further plastic deformation is induced and stress-strain curve follows the original path for monotonic loading.

2.2.3 Idealized stress-strain models

From the previous discussion, the following may be noted:

- No single relationship exists between stress and strain for different materials.

- Stress need not be a function of strain alone, but also depends on the previous loading history. Thus the material behaviour is load-path dependent.

- Residual strains of different magnitudes can be obtained by varying the loading history with the stress starting and finishing at zero.

In order to obtain a solution for a deformation problem, it is necessary to idealize stress-strain behavior of the material. A few well known idealized models are given below and are shown in Fig.2.4:

a) Elastic-Perfectly plastic model

b) Elastic-Linear work hardening model

c) Elastic-Exponential work-hardening model

d) Ramberg-Osgood-model

2.2.4 Tangent modulus, Plastic modulus and Secant modulus

As can be seen from the previous discussions, elastic-plastic stress-strain response of a material is non-linear and therefore an incremental approach is adopted to solve a deformation problem. It is assumed that a strain increment $d\varepsilon$ consists of two parts, namely the elastic strain increment $d\varepsilon^e$ and plastic strain increment $d\varepsilon^p$ (Fig.2.5)

$$d\varepsilon = d\varepsilon^e + d\varepsilon^p \qquad (2.2.1)$$

The stress increment $d\sigma$ is related to the strain increment $d\varepsilon$ by

$$d\sigma = E_t d\varepsilon \qquad (2.2.2)$$

If plastic strain is separated from total strain, the stress increment $d\sigma$ is related to the plastic strain increment $d\varepsilon^p$ by

$$d\sigma = E_P \, d\varepsilon^p \qquad (2.2.3)$$

where, E_t is the *tangent modulus* and E_P is the *plastic modulus*

For elastic strain increment,

$$d\sigma = E d\varepsilon^e \tag{2.2.4}$$

where, E is the elastic modulus.

The relationship between the three modulii E, E_t and E_P is given by,

$$(1/E_t) = (1/E) + (1/E_p) \tag{2.2.5}$$

Secant modulus is the value of Young's modulus derived from a secant drawn between the origin and any point on a nonlinear stress-strain curve (Fig. 2.5). The secant modulus is very useful in estimating the inelastic state directly without tracing the load path. It was used for well over a century to solve a variety of nonlinear problems. Many robust methods have been developed to take advantage of the secant modulus. The nonlinear FEA schemes also use the secant stiffness. The most popular of these is the BFGS (Broyden, Fletcher, Goldfarb and Shanno – named after founders of the method) scheme commonly used with quasi-Newton methods. It has been implemented in several FEA software packages.

2.2.5 Concept of Limit load

In the preceding discussions of stress-strain curves, there was a stage after "proportional limit," at which the strain increases at a constant value of load. This constant value of load is called the *limit load* or *plastic load*. Alternatively, *plastic* or *limit analysis* can be

defined as a method to predict the load at which the structure will fail through the development of excessive deflections. Therefore, limit load or plastic load can also be defined as that constant load on the structure at which the deflections can increase indefinitely.

2.2.6 Mechanism of Failure

Plastic hinges occur in the yielded regions of structures. When sufficient number of plastic hinges are developed in a structure, it forms a mechanism of free rotating links. This leads to collapse. For a determinate structure a single plastic hinge is sufficient to cause collapse. In the case of indeterminate structures, the number of plastic hinges required to form a mechanism, is given by $R+1$, where 'R' is the degree of indeterminacy. This implies that an indeterminate structure fails by shedding the indeterminacy through the formation of plastic hinges.

2.2.7 Classical Upper and Lower Bound theorems

Classical limit analysis is carried out by applying static or kinematic theorems. The following assumptions are used for their application:

1. Plane sections before bending remain plane even after bending (Kirchoff or Euler-Bernoulli)

2. Deflections are such that equilibrium equations can be formulated for the undeformed structure (Lagrangian formulation)

3. The stress-strain relation is assumed to be elastic-perfectly plastic

4. Local failure does not occur prior to the attainment of ultimate load

5. The loading is proportional, i.e., loads are increased in fixed proportions to one another.

Upper Bound Method:

The theorem states that "the critical load that is calculated based on a possible mechanism must either be equal to or greater than the actual collapse load." The application of this is also called as the "mechanism or kinematic method" as the analysis is conducted based on some assumed collapse mechanism and by equating the rate of external work with the rate of dissipation of internal energy.

Lower Bound Method:

The collapse load is obtained based on an assumed equilibrium moment diagram that is safe everywhere. The load obtained is less than or equal to the true collapse load.

2.3 Yield Criterion and Yield locus

2.3.1 Yield criterion

The previous discussions were based on uni-axial state of stress. However, these concepts can be generalized for a combined state of stress. *Yield criterion* defines elastic limit of

the material under a combined state of stress. In general, the principal stress is a function of the state of stress σ_{ij}. This can be expressed as,

$$f(\sigma_{ij}, k_1, k_2, \ldots\ldots) = 0 \qquad (2.3.1)$$

where, k_1, k_2, etc., are material constants.

For isotropic materials, values of the three principal stresses or their invariants sufficiently describe the state of stress and the corresponding yield conditions.

2.3.2 The Tresca Yield Criterion

The first yield criterion for a combined state of stress for metals was proposed by Tresca in 1864. This is also known as the maximum shearing stress theory, or simply the maximum shear theory, which results from observations that in a ductile material slipping occurs during yielding along critically oriented planes. According to this theory, yielding would occur when the maximum shear stress at a point reaches a critical value k. In terms of principal stresses, this condition is fulfilled when one-half of the greatest absolute difference between the principal stresses taken in pairs must be equal to k at yield.

$$\max\left(\frac{1}{2}|\sigma_1-\sigma_2|, \frac{1}{2}|\sigma_2-\sigma_3|, \frac{1}{2}|\sigma_3-\sigma_1|\right) = k \qquad (2.3.2)$$

The material constant k can be determined from the maximum shear stress in a simple tension test. Therefore,

$$k=\frac{f_y}{2} \tag{2.3.3}$$

A detailed explanation about this theory is provided in Section 3.2.3

2.3.3 The von Mises Yield Criterion

The octahedral shearing stress or strain energy of distortion is the basis of the von Mises criterion. It states that yielding begins when the octahedral shearing stress reaches a critical value k. In terms of principal stresses,

$$(\sigma_1-\sigma_2)^2 + (\sigma_2-\sigma_3)^2+(\sigma_3-\sigma_1)^2 = 6k^2 \tag{2.3.4}$$

where k is the yield stress in pure shear. For uniaxial case, the above equation reduces to,

$$k=\frac{f_y}{\sqrt{3}} \tag{2.3.5}$$

A detailed explanation about this theory is provided in Section 3.2.3

2.4 Robust methods for Limit Analysis

2.4.1 Need for robust methods

Limit load determination is usually based on classical upper bound and lower bound theorems. However, this method becomes highly tedious for structures with high degree of indeterminacy. It is also impracticable for complex structures. This has motivated researchers to develop simplified methods to determine limit loads. Simplified methods such as Gloss r-node method, Elastic compensation method and m_α method have been developed for a similar purpose.

Current robust methods provide a simple and quick estimate of limit loads for problems involving material non-linearity. Since the process involves successive elastic analyses, the solution is more stable and systematic and therefore has much lesser convergence difficulties. It also saves enormous computation time.

2.4.2 Origin of Robust methods

Recent robust methods initially paved their way into limit design of pressure vessels by use of reduced modulus technique. A reduced modulus technique was introduced to categorize stresses in pressure vessels [Dhalla, 1984; Dhalla, 1987; Dhalla and Jones, 1986]. This was intended to classify local clamp stresses induced in Liquid Metal Fast Breeder Reactors. However a significant observation from this technique was that clamp-induced stresses could be secondary owing to their redistribution on account of material

or geometric non-linearity. Hence, a systematic reduction of elastic modulus resulted in inelastic response of the structure. The method was then extended to study inelastic response and follow-up characteristics of piping problems and the results were found to be satisfactory [Dhalla, 1984, 1987; Dhalla and Severud, 1984].

Subsequently, Marriott [1988] proposed a reduced modulus method for determining primary stresses in pressure vessel components. The method involves performing an elastic analysis and identifying elements having stresses greater than those defined by the code. The elastic modulus of each element would then be modified using the relation:

$$E_R = E_o \frac{S_m}{SI} \tag{2.4.1}$$

where, E_o is the original value of elastic modulus, S_m is the code allowable stress and SI is the stress intensity.

The modified structure is then re-analyzed. This is followed by further re-adjustment of elastic modulii of critically stressed elements and the procedure is repeated until maximum stress intensity is less than S_m or some other convergence criteria.

Further to this, the method of robust limit load analysis has been under extensive study by Seshadri and co-workers [Seshadri, 1991; Seshadri and Fernando, 1992; Fernando, 1992; Mangalaramanan and Seshadri 1995; Seshadri, 1997] and Mackenzie and Boyle [Mackenzie, et. al., 1992; Mackenzie and Boyle 1993; Mackenzie, et. al., 1993; Boyle, et. al., 1997; Mackenzie, et. al., 2000; Nadarajah, et. al., 1993].

Studies by Seshadri and co-workers led to the development of r-node method, which predicts limit load by determining r-node stresses and subsequently modifying elastic modulus in repeated elastic analysis.

2.4.3 Gloss Method

The Gloss method is a simple technique to determine the peak inelastic strains in structures and mechanical components for a given load [Seshadri and Kizhatil 1990; Kizhatil and Seshadri, 1991; Seshadri 1991; Raghavan, 1998]. It is a robust, systematic and effective technique involving the use of two linear finite element analyses. The structure under consideration is divided into a local region and remainder region for the purpose of analysis. The local region is a portion in the structure that undergoes high plastic deformations. The remainder exhibits normal elastic stresses.

The application of this concept involves relating the inelastic multiaxial stress redistribution in the local region due to plasticity or creep, to the uniaxial stress relaxation process. This is achieved in an approximate manner using a secant modulus scheme for all the points that have yielded:

$$E_s = \frac{f_y}{\sigma_{ei}} E_o \qquad (2.4.2)$$

where, σ_{ei} is the von Mises equivalent stress from the initial elastic analysis of the i^{th} element.

After making the above modification, a second linear elastic analysis is conducted.

A typical GLOSS diagram is shown in Fig. 2.6. Here, OAF is the elastic perfectly plastic stress-strain curve and OC is the elastic line. The pseudo elastic point C ($\sigma_{e1}, \in_{e1}$), of the local element is located on this elastic line. The stress and strain of the local element ($\sigma_{e2}, \in_{e2}$) determined from the second linear analysis is represented by point E. The slope of the line OE is called as the secant modulus and that of BE as the relaxation modulus. The line BE can be extended to intersect the material stress-strain curve. This gives the inelastic strain in the local region. Some researchers used techniques similar to the GLOSS, e.g., Ralph [2000], who used the method to repeatedly increment the load to obtain a limit value.

2.4.4 R- Node Method

The salient features of the GLOSS method and the reference stress method were combined with ideas from Dhalla, Marriott, etc., by Seshadri [Seshadri and Marriott, 1992]. They proposed the r-node method as an approximate procedure for determining limit loads on the basis of two linear analyses [Seshadri and Fernando, 1991]. The r-nodes are load-controlled locations in a structure and can be described where the distribution of stress corresponds to primary stresses. The method is briefly described below:

1. The structure under consideration is discretized and a linear finite element analysis is carried out for an arbitrary proportional load factor.

2. The elastic modulii of all the elements in the structure are modified using the secant scheme (similar to GLOSS).

3. An elastic reanalysis is carried out and r-nodes are identified as points where the stress does not change between the two iterations.

Use of the modified modulii in a second linear finite element run produces a stress distribution, which tends to a limit type distribution. From the results of the two runs, it is possible to locate points in the structure where stresses remain the same between the analyses. This means the stresses at these locations are insensitive to the material constitutive relations. These stresses are thus load controlled. These load-controlled locations are called redistribution nodes (r- nodes). The effective stresses at r-nodes are linearly proportional to externally applied loads.

Thus, by knowing the effective r-node stress, the limit load on the structure can be readily evaluated. The local maxima of the stresses at the r-nodes are estimated. Each such local maxima are thought to be representing a plastic hinge location. These plastic hinges give rise to collapse mechanisms. The combined r-node effective stress, σ_n can be found using the following relation,

$$\sigma_n = \frac{\sum_{j=1}^{n} \sigma_{nj}}{n} \qquad (2.4.3)$$

where, n is the number of r-node peaks or plastic hinges. The corresponding limit load is given by,

$$P_l = \left[\frac{f_y}{\sigma_n}\right] P \qquad (2.4.4)$$

The r-node method has been successfully applied to several applications by Seshadri and associates. Of particular interest is the work by Mangalaramanan [1993] who applied the r-node method to several plate problems to obtain limit load estimates using the von Mises criterion. The present thesis uses several of his results to make comparisons.

2.4.5 m-α method

The m-α method [Mangalaramanan, 1997a; Seshadri, 2000; Seshadri and Mangalaramanan, 1997] is based on Mura's variational formulation [Mura and Lee, 1962; Mura, Rimawi and Lee, 1964]. According to Mura's formulation, the exact limit load factor is bounded by upper and lower bound multipliers namely, m' and m^0. The key to the m-α method is to identify the multipliers m' and m^0, and the m-α method achieves this on the basis of two linear elastic finite element analyses It determines an improved lower bound limit load compared to Mura's limit load estimate. The m-α method has also introduced the concept of leapfrogging to limit state based on two linear finite element analyses. From these results, the limit load multipliers and hence the limit load can be evaluated. For proper identification of these multipliers, it is necessary to identify the kinematically active portion of the structure (termed as "reference volume") that is

involved in the plastic action [Seshadri and Mangalaramanan, 1997]. An iteration variable ζ is used such that the infinitesimal changes in the elastic modulus of elements during second and subsequent analyses would reflect corresponding changes in $\Delta\zeta$. It is ascertained that repeated analysis with modified modulus results in a decrease in stress distribution. The flatter (or even) distribution of stress during subsequent analyses would result in increase of m^0 with ζ. But m^0 evaluated on the basis of total volume would decrease with increasing ζ. Referring to Fig. 2.7, for reference volume V_R, such that $\Delta V_1 < V_R \leq V_T$, the multiplier m^0 is assumed to remain invariant with successive iterations. The calculation of reference volume based on m^0 is shown in Fig.2.7. The variation of m', m^0 with ζ is shown (Fig.2.8).

The method involves a secant modulus adjustment scheme similar to the r-node method. Firstly, a linear elastic analysis is conducted and the elastic-modulus of appropriate elements are modified using:

$$(E_s)_k = \left[\frac{\sigma_{arb}}{(\sigma_e^0)_k}\right] E_0 \qquad (2.4.5)$$

where, E_0 and E_s are the Young's modulus in the first and second elastic analysis respectively. $(\sigma_e^0)_k$ is the equivalent stress for any element number k and σ_{arb} is an arbitrary stress value.

If V is the volume of the component or structure,

$$m^0 = \frac{\sigma_y \sqrt{V}}{\sqrt{\sum_{k=1}^{\alpha} (\sigma_{ek}^0)^2 \Delta V_k}} \tag{2.4.6}$$

and m_1^0 and m_2^0 can be determined for the two analyses. The average surfaces of dissipation can be expressed as

$$\begin{aligned} m_1^0 &= c_1 \\ m_2^0 &= c_2 \end{aligned} \tag{2.4.7}$$

where c_1 and c_2 are constants. In Eq. 2.4.6, $V_R \le V \le V_T$. The theorem of nesting surfaces necessitates that $m_1^0 \ge m_2^0 \ge m$, where m is the exact factor of safety.

In terms of iteration variable, Mura's lower bound multiplier is given by:

$$m' = \frac{2m^0(\zeta) f_y^2}{f_y^2 + [m^0(\zeta)]^2 [\sigma_M^0(\zeta)]^2} \tag{2.4.8}$$

where, $\sigma_M^0(\zeta) = (\sigma_e^0)_M$ is the maximum equivalent stress at iteration number i.

The quantities m', m^0 and σ_M are all functions of iteration variable ζ. With the use of repeated analysis, the multiplier m_α, which implies the use of α elements in the finite element discretization that would lead to identification of an appropriate reference volume. The idea of leapfrogging of intermediate iterations is illustrated in Fig. 2.9.

2.4.6 Reference Stress Method

The reference stress method [Sim, 1968] is a useful simplified method since it attempts to overcome some of complications of creep analysis.

By definition, reference stress can be called as a stress which is a function of stress components that must reach the value of yield stress in simple tension (or compression) for yielding to occur. The basic principle of reference stress method is that the deformation of structures subjected to multiaxial creep can be related to the results of a uniaxial creep test carried out at the reference stress, through a scaling factor.

Therefore, deflection 'δ' at a point in a structure at sometime 't' is given by:

$$\delta(t) = \xi \epsilon_c(t) \qquad (2.4.9)$$

where, ξ is the geometric scaling factor depending on configuration of structure and boundary conditions,

$\epsilon_c(t)$ is the creep strain at time 't' as obtained by uniaxial creep test performed at the reference stress (σ_{ref}).

During creep analysis of beams, it is seen that stresses are redistributed from an initial elastic distribution to the stationary state, and the stresses at particular locations in the cross-section are invariant. The r-node method is based on this concept. Deflections of rectangular beams based on this reference stress were found to be reasonably accurate.

Anderson [Anderson, Gardner, and Hodgkins, 1963] observed that reference stress is insensitive to exact creep exponent 'm' in the strain rate to stress relationship.

$$\epsilon_c = B\sigma^m \tag{2.4.10}$$

But as m $\Rightarrow \alpha$, limit solution to perfect plasticity would be approached, i.e., at limit load, the reference stress would equal the yield stress. Using this as a basis, reference stress at any other load is,

$$\sigma_{ref} = (\frac{p}{p_l}) f_y \tag{2.4.11}$$

where, p = Load on the structure and p_l= the limit load.

2.4.7 Elastic compensation method

The elastic compensation method (ECM) to evaluate limit loads methods [Mackenzie, Shi and Boyle, 1992; Shi, Mackenzie, and Boyle, 1993] is based on the secant modulus scheme similar to that of the GLOSS and r-node.

The elastic compensation method can be used to define lower or upper bound limit loads for any structure modeled by continuum finite elements. A finite element model is created and a nominal load set P_d is applied. A linear elastic finite element analysis is then performed and the linear elastic stress field is obtained. The process then involves

iteration in a series of linear elastic analysis of the model. After each iteration, the elastic modulus of each element in the model is modified according to the equation:

$$E_i = E_{(i-1)} \frac{\sigma_n}{\sigma_{(i-1)}} \tag{2.4.12}$$

where, i is the present iteration number, σ_n a nominal stress value and $\sigma_{(i-1)}$ the maximum (unaveraged) nodal equivalent stress associated with the element from the previous solution.

A typical plot of the maximum stress in the entire model against the iteration number results in a graph of the form shown in (Fig. 2.10). Modifying the elastic modulus causes redistribution of stresses between iterations. In some cases the maximum stress increases between iterations. Generally, over a number of iterations, there is a net decrease in maximum stress with respect to the initial solution.

The stress field obtained for each iteration meets the lower bound limit load theorem requirement of statical admissibility. The maximum stress may or may not violate the requirement that it should not exceed yield, depending on the magnitude of applied load set P_d. The best value for lower bound limit load possible for a given stress distribution is one in which the maximum stress equals yield. The value of the load to cause such stress can thus be calculated by using proportionality. Thus, the lower bound limit load P_L is given by:

$$P_L = P_d \frac{f_y}{\sigma_R} \qquad (2.4.13)$$

where, P_d is the applied load set, f_y is the yield stress and σ_R is the lowest value of maximum stress over successive iterations

Similarly, the results of the above procedure can be used to estimate the upper bound limit load as well. Generally, the upper bound method is considered to give a very close result when compared to the lower bound.

2.4.8 Summary of the Current Robust Methods

The methods discussed have many similarities. They involve conducting linear elastic finite element analyses and projecting the value of limit load or inelastic evaluations, using stresses at points. They all adopt secant modification schemes. The r-node method is a simple and systematic method that estimates the limit loads with ease. The plot of the r-node peaks in the structure could sometimes give a quick idea about the collapse mechanism of the structure. The reference stress method helps us to overcome difficulties faced in creep analysis and also leads to the ideas used in developing the r-node analysis. Determining reference stress by itself is a difficult task. But this difficulty can be overcome by evaluating limit loads using the r-node method and thereby evaluating the reference stress. The ECM uses schemes similar to the r-node method but does not require the identification of any special points. The m-α method has a better theoretical basis but essentially predicts limit loads with similar accuracy.

2.5 Differential equation of plates in cartesian co-ordinate system

The present thesis is concerned with robust estimates of limit loads for plate structures. The basic plate theory for elastic analysis is well established. It is briefly reviewed below.

2.5.1 General

The deflected shape of a plate is adequately defined by describing the geometry of its middle surface, which is a surface that bisects the plate thickness at each point. The small deflection plate theory, generally attributed to Kirchoff and Love is based on the following assumptions:

1. The material of the plate is elastic, homogeneous and isotropic

2. The plate is initially flat

3. The thickness of the plate is small compared to its other dimensions. The smallest lateral dimension is at least ten times larger than its thickness

4. The deflections are small compared to the plate thickness.

5. The slopes of the deflected middle surface are small compared to unity

6. The deformations are such that straight lines, initially normal to the middle surface, remain straight lines normal to the middle surface (deformations due to transverse shear will be neglected)

7. The deflection of the plate is produced by the displacement of points of the middle surface normal to its initial plane

8. The stresses normal to the middle surface are of negligible order of magnitude.

Many of these assumptions are similar to the assumptions in elementary beam theory. Small and large-scale tests have proved the validity of these assumptions. An additional simplifying assumption is also introduced often:

9. The strains in the middle surface produced by in-plane forces can usually be neglected in comparison with the strains due to bending (inextensional plate theory).

2.5.2 Co-ordinate System and Sign Conventions

For rectangular plates the Cartesian co-ordinate system is the most convenient. The external and internal forces and the deflection components u, v, and w are considered positive when they point towards the positive direction of the coordinate axes x, y, and z. In general engineering practice, positive moments produce tension in the fibers located at the bottom part of the structure. This sign convention is maintained for plates.

Consider an elemental parallelepiped cut out of the plate as shown in Fig. 2.11. Assign positive internal forces and moments to the near faces. To satisfy equilibrium of the element, negative internal forces and moments must act on its far sides. The first subscript of the internal forces indicates the direction of the surface-normal pertinent to the section on which the force or moment acts.

2.5.3 Equilibrium of the Plate Element

Assuming that the plate is subjected to lateral forces only, from six fundamental equilibrium equations, the following three can be used:

$$\sum M_x = 0, \qquad \sum M_y = 0, \quad \sum P_z = 0. \tag{2.5.1}$$

The behavior of the plate is in many respects analogous to that of a two-dimensional gridwork of beams. The external load P_z is carried by transverse shear forces Q_x and Q_y and by bending moments M_x and M_y. The significant derivation from the two-dimensional gridwork action of beams is the presence of the twisting moments M_{xy} and M_{yx}. In the theory of plates it is customary to deal with internal forces and moments per unit length of the middle surface. To distinguish these internal forces from the above mentioned resultants, the notations q_x, q_y, m_x, m_y, m_{xy} and m_{yx} are introduced.

In order to set up the differential equation of equilibrium, the following steps need to be adopted:

1. Select a convenient co-ordinate system such as the one shown in Fig. 2.12

2. Show all the external and internal forces acting on the element

3. Assign positive internal forces with increments to the near sides and negative internal forces to the far sides

4. Express the increments by a truncated Taylor's series

5. Express equilibrium of internal and external forces acting on the element. This leads to derivation of the following equation:

$$\frac{\partial^2 m_x}{\partial x^2} + 2\frac{\partial^2 m_{xy}}{\partial x \partial y} + \frac{\partial^2 m_y}{\partial y^2} = -p_z(x, y) \tag{2.5.2}$$

2.5.4 Relation between Stress, Strain and displacements

The moments m_x and m_y produce stresses σ_x and σ_y given by,

$$\sigma_x = \frac{E}{1-\nu^2}(\varepsilon_x + \nu\varepsilon_y) \tag{2.5.3}$$

$$\sigma_y = \frac{E}{1-\nu^2}(\varepsilon_y + \nu\varepsilon_x) \tag{2.5.4}$$

The twisting moments m_{xy} and m_{yx} produce shear stresses τ_{xy} and τ_{yx} which are again related to shear strain giving:

$$\tau_{xy} = G\gamma_{xy} = \frac{E}{(1-\nu^2)}\gamma_{xy} = \tau_{yx} \tag{2.5.5}$$

Strains and displacements are related by:

$$\varepsilon_x = -z\frac{\partial^2 w}{\partial y^2}. \tag{2.5.6}$$

$$\varepsilon_x = -z\frac{\partial^2 w}{\partial y^2}. \tag{2.5.7}$$

The curvature changes of the deflected middle surface are defined by:

$$\kappa_x = -\frac{\partial^2 w}{\partial x^2},\ \kappa_y = -\frac{\partial^2 w}{\partial y^2},\ \text{and}\ \chi = \frac{-\partial^2 w}{\partial x \partial y} \tag{2.5.8}$$

Where, χ represents the warping of the plate.

2.5.5 Internal Forces Expressed in Terms of 'w'

The stress components σ_x and σ_y produce bending moments in the plate element. Thus, by integration of the normal stress components, the bending moments acting on the plate elements are obtained:

$$m_x = \int_{-(h/2)}^{+(h/2)} \sigma_x z dz \quad \text{and} \quad m_y = \int_{-(h/2)}^{+(h/2)} \sigma_y z dz \tag{2.5.9}$$

Similarly, the twisting moments produced by shear stresses $\tau = \tau_{xy} = \tau_{yx}$ can be calculated from:

$$m_{xy} = \int_{-(h/2)}^{+(h/2)} \tau_{xy} z dz \quad \text{and} \quad m_{yx} = \int_{-(h/2)}^{+(h/2)} \tau_{yx} z dz \tag{2.5.10}$$

Since $\tau = \tau_{xy} = \tau_{yx}$, $m_{xy} = m_{yx}$

Substituting all the above equations and integrating finally leads to,

$$m_x = -\frac{Eh^3}{12(1-\nu^2)}\left(\frac{\partial^2 w}{\partial x^2} + \nu \frac{\partial^2 w}{\partial y^2}\right) \tag{2.5.11}$$

$$= -D\left(\frac{\partial^2 w}{\partial x^2} + \nu \frac{\partial^2 w}{\partial y^2}\right)$$

$$= D(\kappa_x + \nu \kappa_y) \tag{2.5.12}$$

$$m_y = -\frac{Eh^3}{12(1-\nu^2)}\left(\frac{\partial^2 w}{\partial y^2} + \nu \frac{\partial^2 w}{\partial x^2}\right) \tag{2.5.13}$$

$$= -D\left(\frac{\partial^2 w}{\partial x^2} + \nu \frac{\partial^2 w}{\partial y^2}\right)$$

$$= D(\kappa_y + \nu \kappa_x) \tag{2.5.14}$$

where,

$$D = -\frac{Eh^3}{12(1-\nu^2)} \tag{2.5.15}$$

represents the bending or flexural rigidity of the plate. Similarly twisting moments are given by,

$$m_{xy} = m_{yx} = \int_{-(h/2)}^{+(h/2)} \tau z dz \tag{2.5.16}$$

$$= -2G \int_{-(h/2)}^{+(h/2)} \frac{\partial^2 w}{\partial x \partial y} z^2 dz \tag{2.5.17}$$

$$= -(1-\nu) D \frac{\partial^2 w}{\partial x \partial y} \tag{2.5.18}$$

$$= D(1-\nu)\chi \tag{2.5.19}$$

2.5.6 Governing Differential Equation of the Plate Subjected to Lateral Loads

Using the above equations, we can obtain a single governing differential equation of equlibrium:

$$\frac{\partial^4 w}{\partial x^4} + 2\frac{\partial x^2 \partial y^2}{\partial^4 w} + \frac{\partial^4 w}{\partial y^4} = \frac{p_z(x,y)}{D} \tag{2.5.20}$$

Using the two-dimensional Laplacian operator:

$$D \nabla^2 \nabla^2 w = p_z \tag{2.5.21}$$

The equation is a fourth-order, non-homogeneous, partial differential equation of the elliptic type with constant coefficients, often called a non-homogeneous bi-harmonic equation. The equation is linear since the derivatives of w do not have exponents higher than one.

2.5.7 Differential Equation of Plates in Polar Co-ordinate System

Polar co-ordinate system becomes necessary when solving circular plate problems. This can be derived by using co-ordinate transformation or considering the equilibrium of a infinitesimally small element.

The co-ordinate transformation between the Cartesian and polar co-ordinates is:

$$x = r\cos\varphi\,, \qquad y = r\sin\varphi \tag{2.5.22}$$

$$r = \sqrt{x^2 + y^2}\,, \qquad \varphi = \tan^{-1}\left(\frac{y}{x}\right) \tag{2.5.23}$$

The Laplace operator on terms of polar co-ordinates becomes,

$$\nabla_r^{\,2} = \frac{\partial^2}{\partial r^2} + \frac{1}{r^2}\frac{\partial^2}{\partial \varphi^2} + \frac{1}{r}\frac{\partial}{\partial r} \tag{2.5.24}$$

The Laplacian operator ∇^2 is replaced by $\nabla_r^{\,2}$ to give:

$$\nabla_r^{\,2}\nabla_r^{\,2} w = \frac{p_z(r,\varphi)}{D} \tag{2.5.25}$$

Moment equations in polar co-ordinates:

$$m_r = -D\left[\frac{\partial^2 w}{\partial r^2} + \nu\left(\frac{1}{r^2}\frac{\partial^2 w}{\partial \varphi^2} + \frac{1}{r}\frac{\partial w}{\partial r}\right)\right], \tag{2.5.26}$$

$$m_\varphi = -D\left[\frac{1}{r}\frac{\partial w}{\partial r} + \frac{1}{r^2}\frac{\partial^2 w}{\partial \varphi^2} + \nu\frac{\partial^2 w}{\partial r^2}\right] \tag{2.5.27}$$

$$m_{r\varphi} = m_{\varphi r} = -(1-\nu)D\left[\frac{1}{r}\frac{\partial^2 w}{\partial r \partial \varphi} - \frac{1}{r^2}\frac{\partial w}{\partial \varphi}\right] \tag{2.5.28}$$

These equations are solved using a variety of classical techniques such as the double trigonometric series, etc. The results are tabulated for several cases by several authors [e.g., Timoshenko and Woinowsky-Krieger, 1989].

2.6 Yield Line Theory for Plates

During the 1950s and 60s, Johansen [1972] extended the ultimate load analysis of beam and frame structures to reinforced concrete slabs and plates by introducing the concept of yield lines, which are two-dimensional counterparts of plastic hinges. Instead of calculating the shape of elastically deformed slab, the yield line considers lowest load corresponding to a failure pattern to be the critical or ultimate load. When a laterally loaded slab is on the verge of collapse, yield lines are formed at locations of the maximum negative and positive moments. These yield lines divide the slab into plane segments. Once the correct failure pattern is known, the critical load can be obtained

either from virtual work or from equilibrium considerations. In either case, following are the assumptions:

1. At impending collapse, yield lines are developed at the location of maximum moments

2. The yield lines are straight lines (strictly speaking for distributed loads only. For point loads, yield lines may be curved)

3. Along the yield lines, constant ultimate moments are developed

4. The elastic deformations within the slab segments are negligible compared to the rigid body motions, created by the large deformations along the yield lines

5. There are many possible collapse mechanisms and only one, corresponding to the lowest failure load governs. For this case, the yield line pattern is optimum

6. When yield lines are in the optimum position, only ultimate bending moments and no twisting moments or transverse shear forces are present along yield lines

7. For one-way slabs and for smaller span lengths of two-way slabs, the location of maximum positive moment from elastic analysis gives an idea about collapse

8. Along fixed edges, negative yield lines develop

9. Yield lines pass through the intersection of the axis of rotation of adjacent slab segments

10. Lines of support generally serve as axes of rotation

11. Increased stiffness in the plate enhances development of yield lines, while flexibility counteracts their formation

12. The failure of individual points is governed by a rectangular yield criterion rather than the hexagonal criterion of Tresca or the octahedral shear stress criterion of von Mises.

It is generally assumed that the slab is isotropic. Although, initially yield lines were used to obtain ultimate loads of under-reinforced or pre-stressed slabs, the method gives accurate estimates of over-reinforced or ductile metallic plates as well [Wood, 1965]. [Szilard, 1974] has shown that in most cases, yield line analysis may be used to estimate ultimate loads of metallic plates.

Yield lines generally follow the above rules. However there may be certain cases wherein the optimum collapse mechanism follows a different yield pattern. Therefore in order to assess the optimum failure mechanism, a trial and error procedure coupled with an iterative technique is usually adopted. For the most common plate problems, yield lines are readily available.

Johansen's superposition theorem offers a simple method of finding the optimum yield line pattern. The theorem states that:

The sum of ultimate moments for a series of loads is greater than, or equal to, the ultimate moment for the sum of loads. Mathematically,

$$m_{u1} + m_{u2} + m_{u3} + m_{u4} + ... + m_{uk} + ...m_{un} \geq m_{\Sigma p} \tag{2.6.1}$$

Where m_{uk} is the ultimate moment corresponding to load p_{uk}, while $m_{\Sigma p}$, is the ultimate moment corresponding to the yield line pattern produced by the total of the loads:

$$p_{u1} + p_{u2} + p_{u3} + ...p_{un} \geq \sum_{n} P \tag{2.6.2}$$

2.7 Summary

In the present chapter, the basic concepts of plastic analysis and limit analysis of structures have been reviewed. Existing robust methods for the obtaining limit loads such as the r-node, elastic compensation, m_α, and yield line methods have been briefly explained. The classical differential equations of equilibrium for the elastic analysis of plates are introduced. The next chapter will describe a robust technique based on secant rigidity, scaled yield criteria and weighted averages of generalized forces along special regions. The method is specifically applied to obtain limit loads of plates.

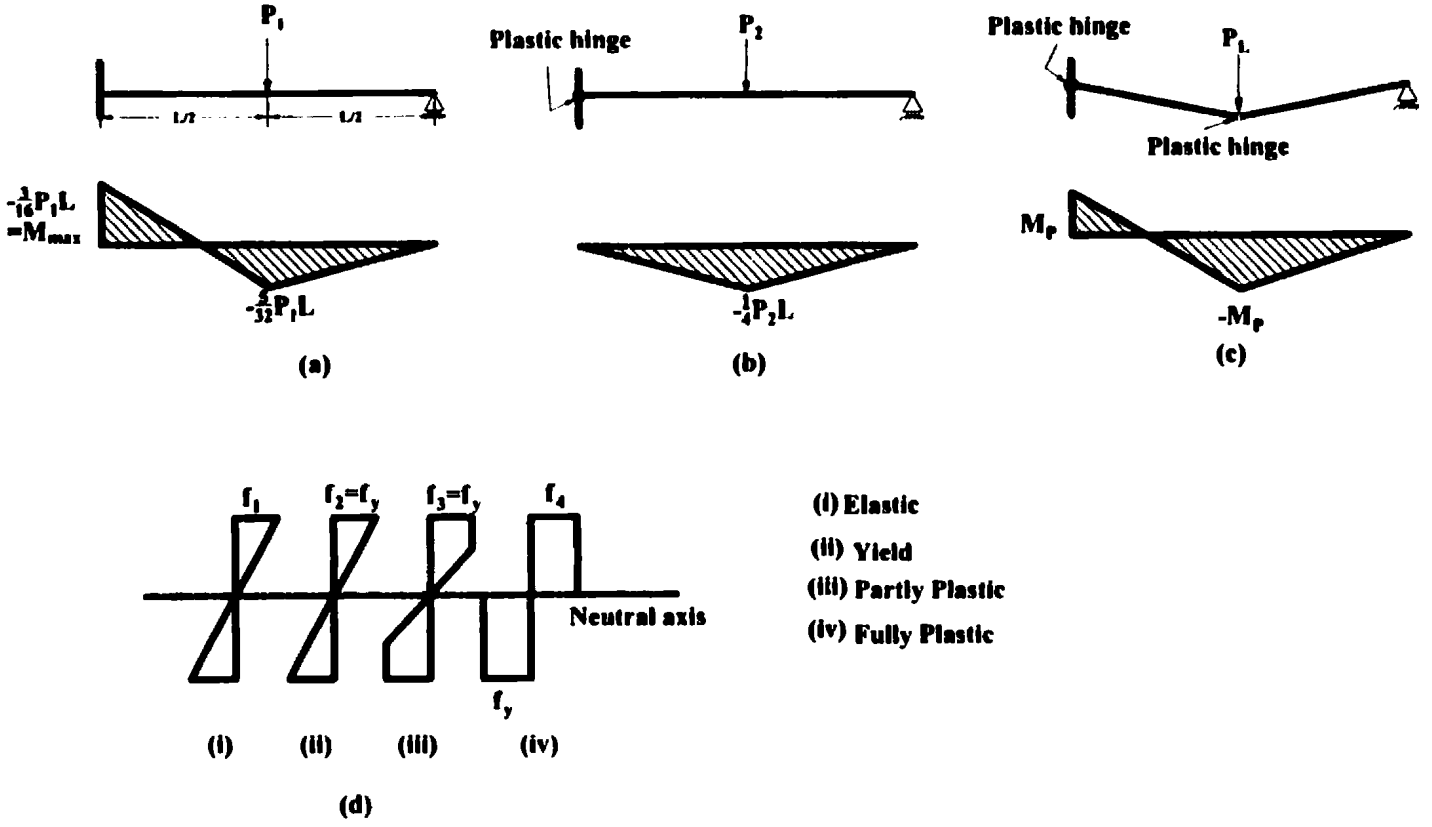

Fig. 2.1 Failure Mechanism of a Propped Cantilever [Szilard, 1974]

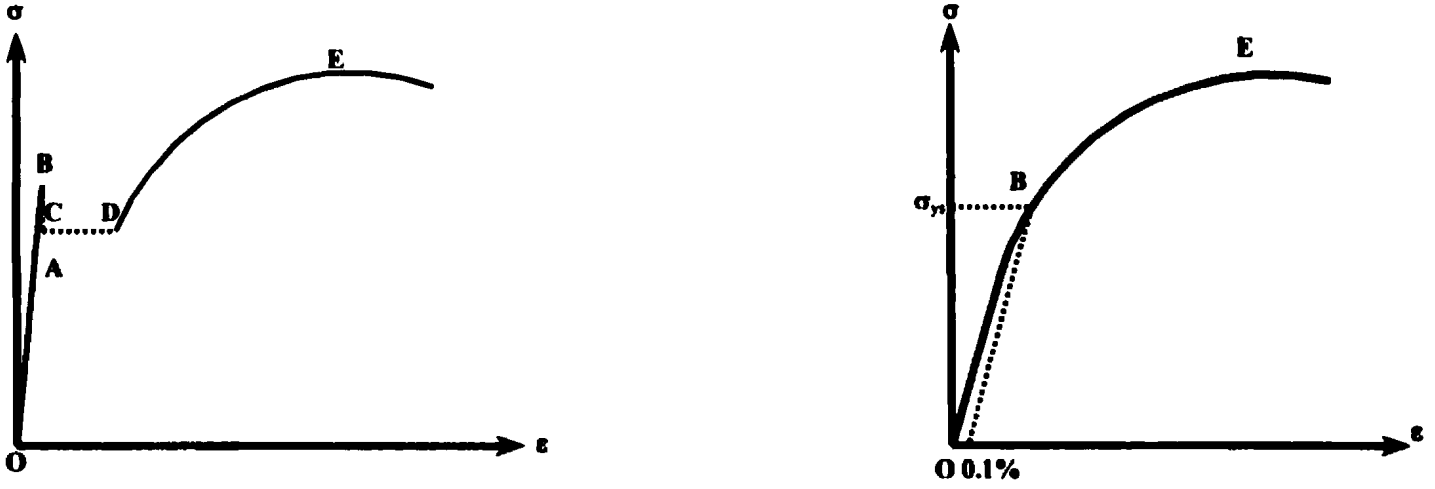

(a) (b)

Fig.2.2 Uni-axial Stress-Strain Diagram

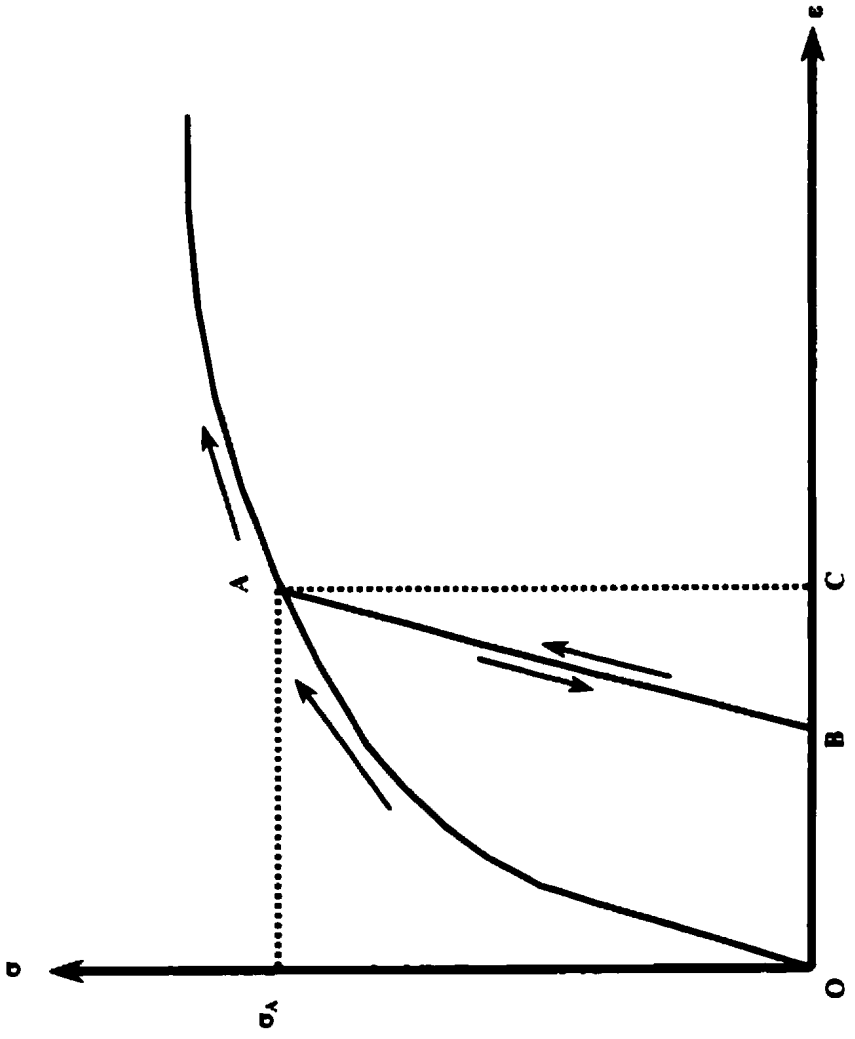

Fig. 2.3 Loading, Unloading and Re-loading of Material

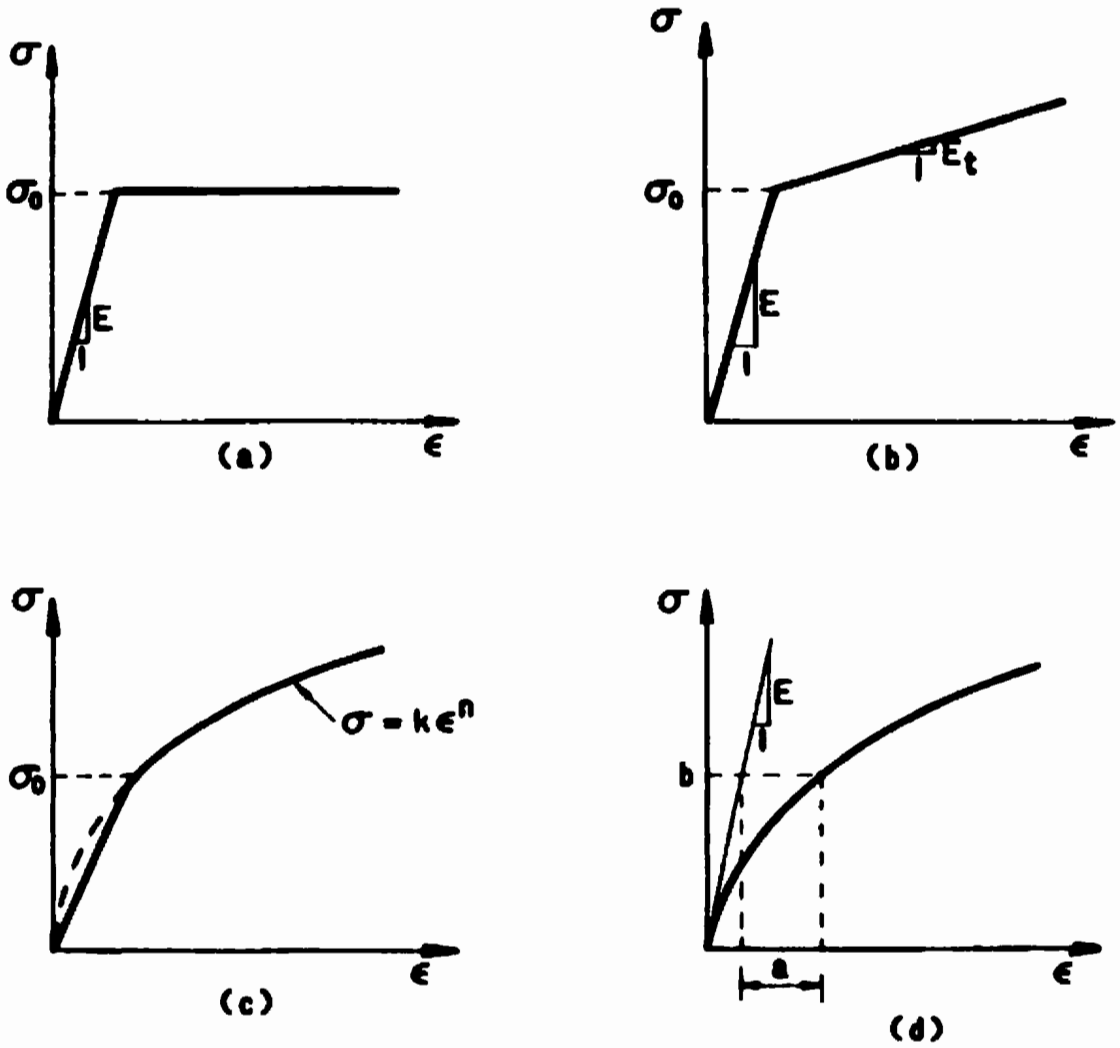

Fig. 2.4 Idealized Material Stress-Strain Models

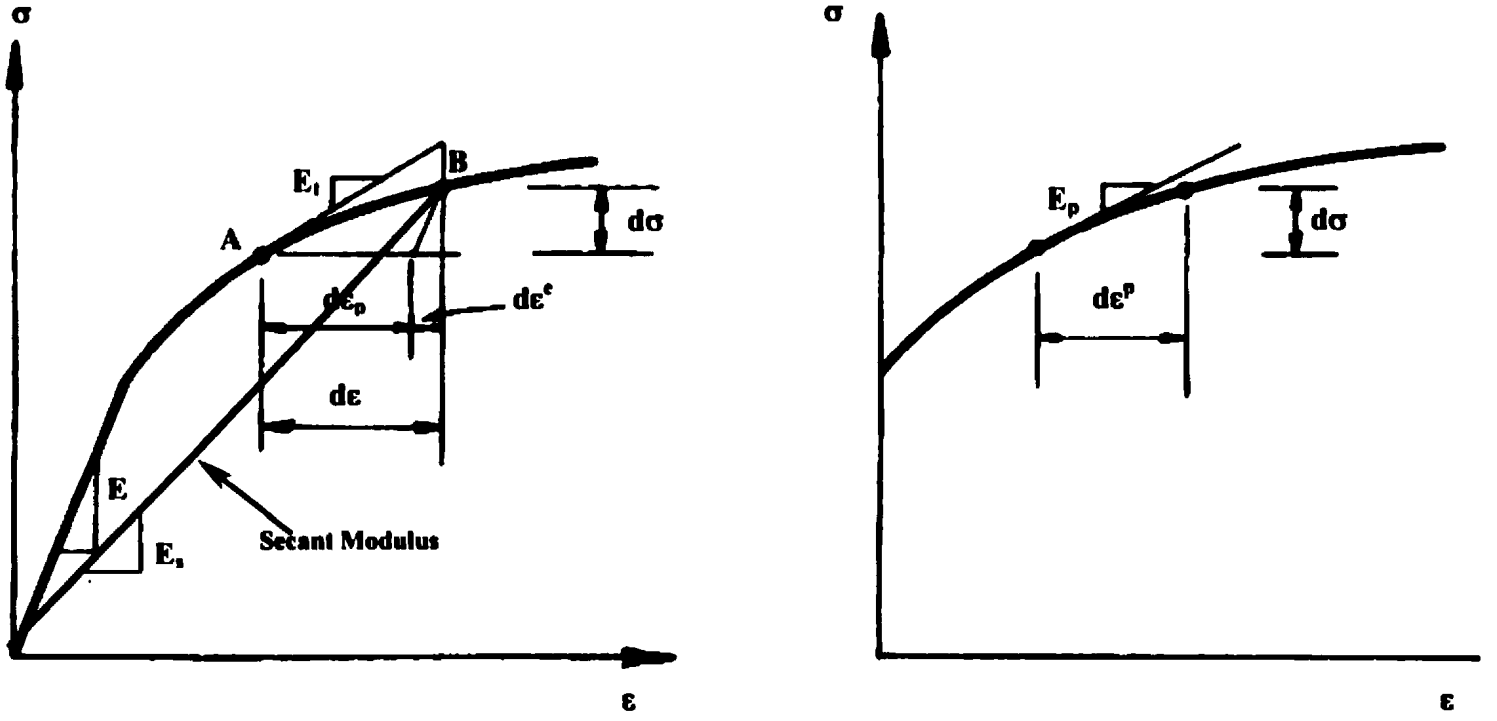

Fig. 2.5 Elastic, Tangent, and Plastic Modulii

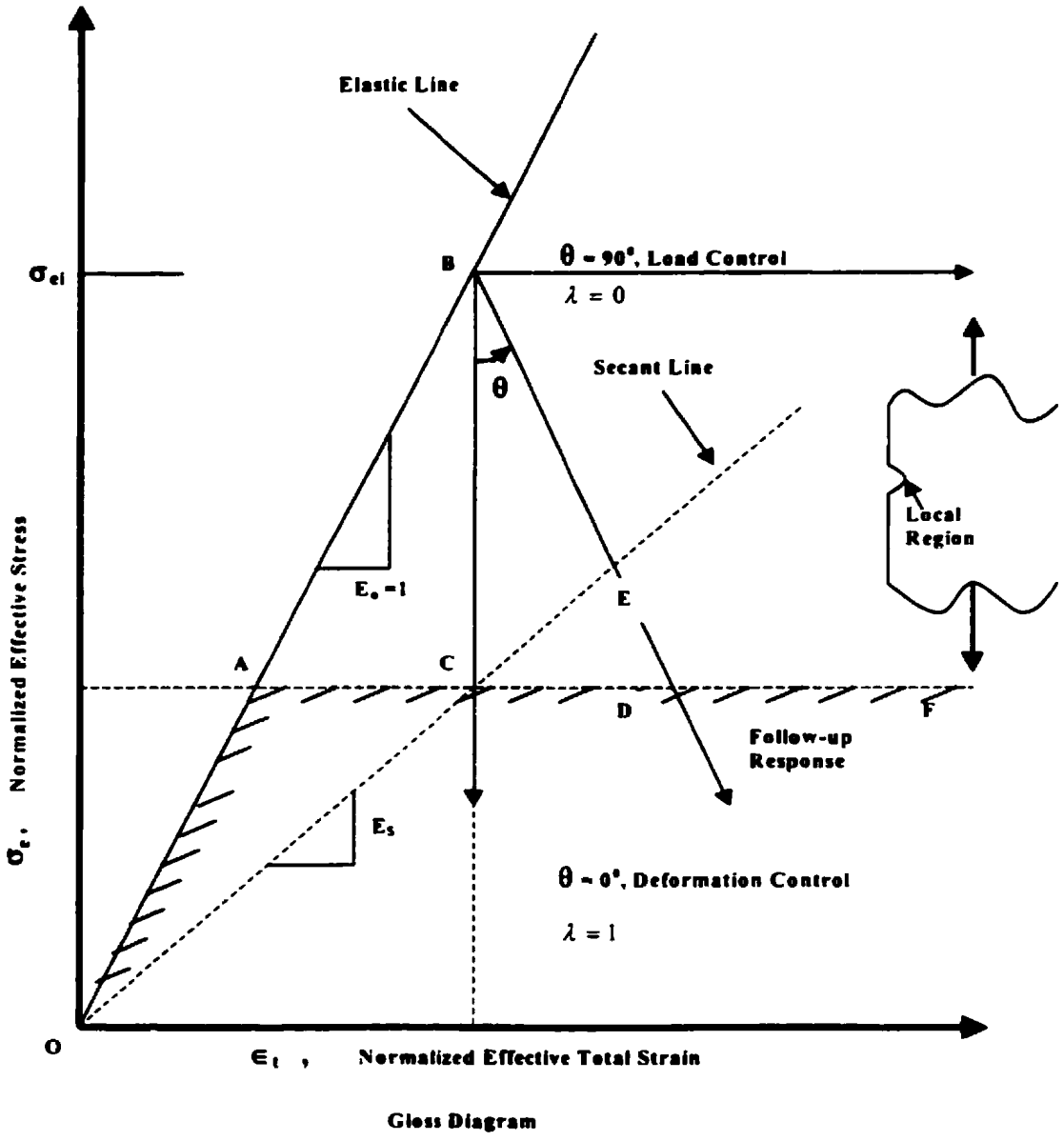

Fig. 2.6 Typical GLOSS Diagram [Seshadri and Fernando, 1992]

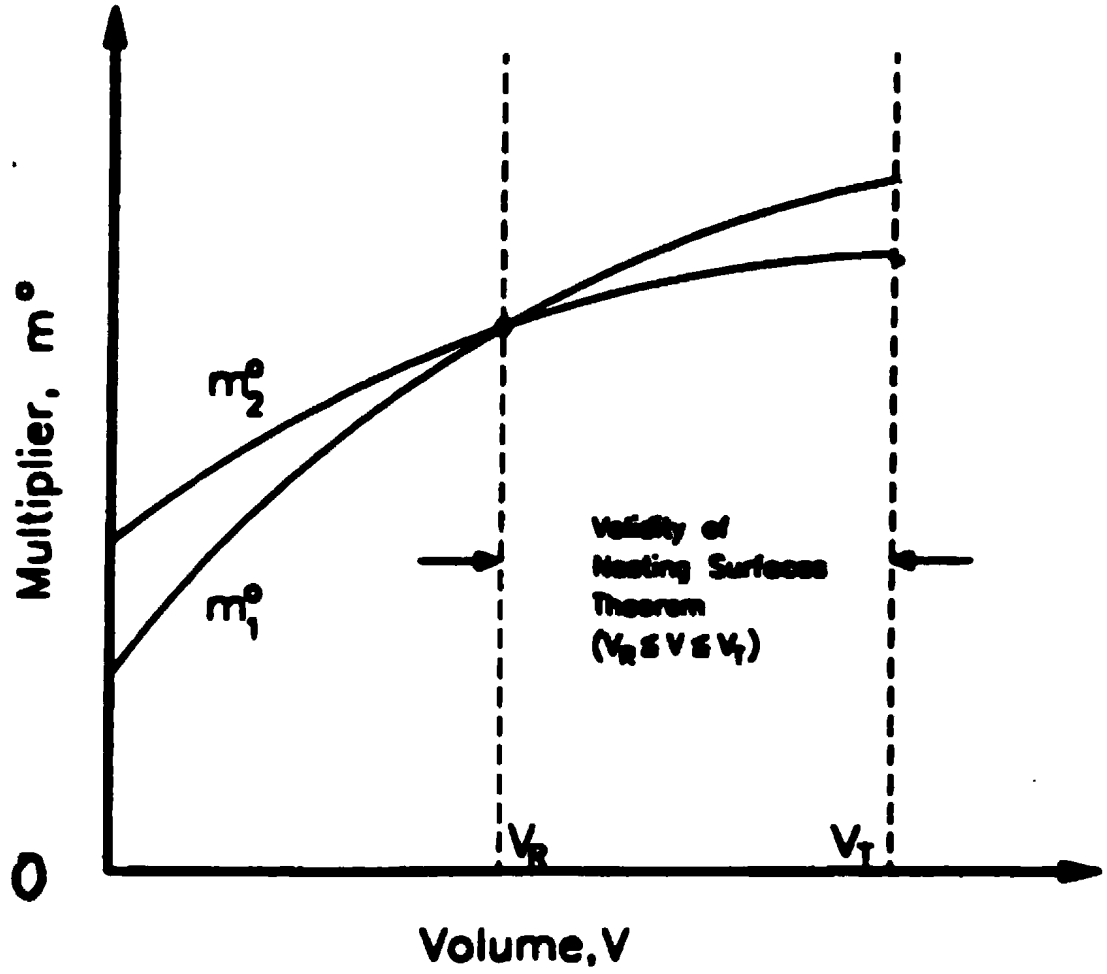

Fig. 2.7 m_α Method: Calculation of Reference Volume

[Seshadri and Mangalaramanan, 1997]

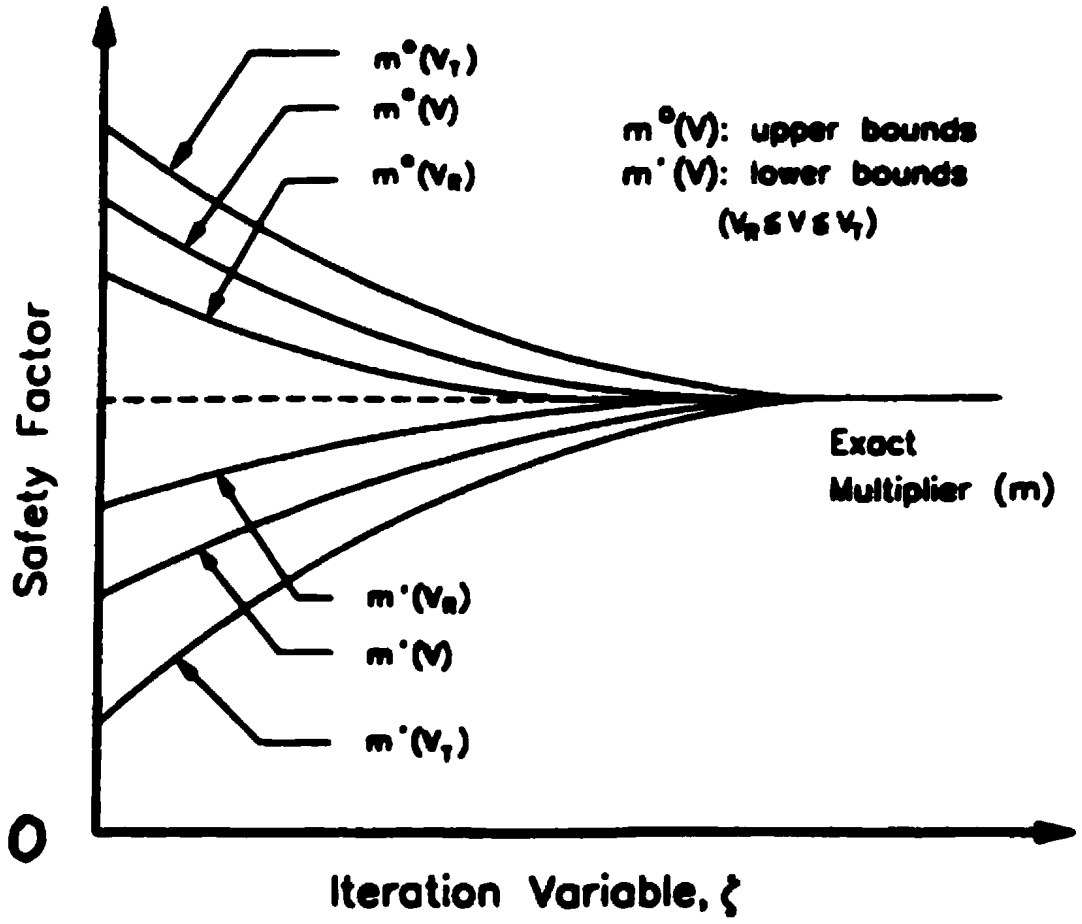

Fig. 2.8 m_α Method: Variation of $m^{\cdot}$, $m^{\bullet}$ with Iterations

[Seshadri and Mangalaramanan, 1997]

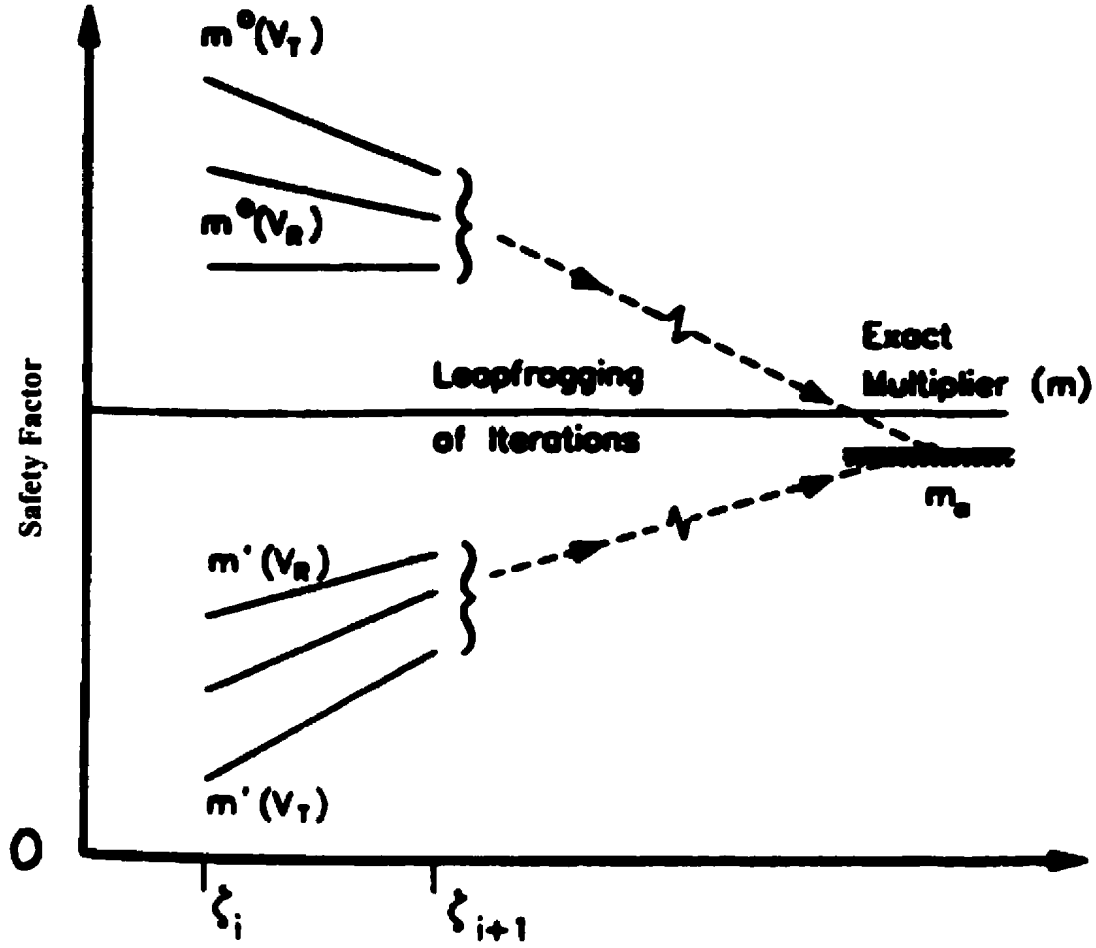

Fig. 2.9 m_α Method: Leapfrogging of iterations to near limit state

[Seshadri and Mangalaramanan, 1997]

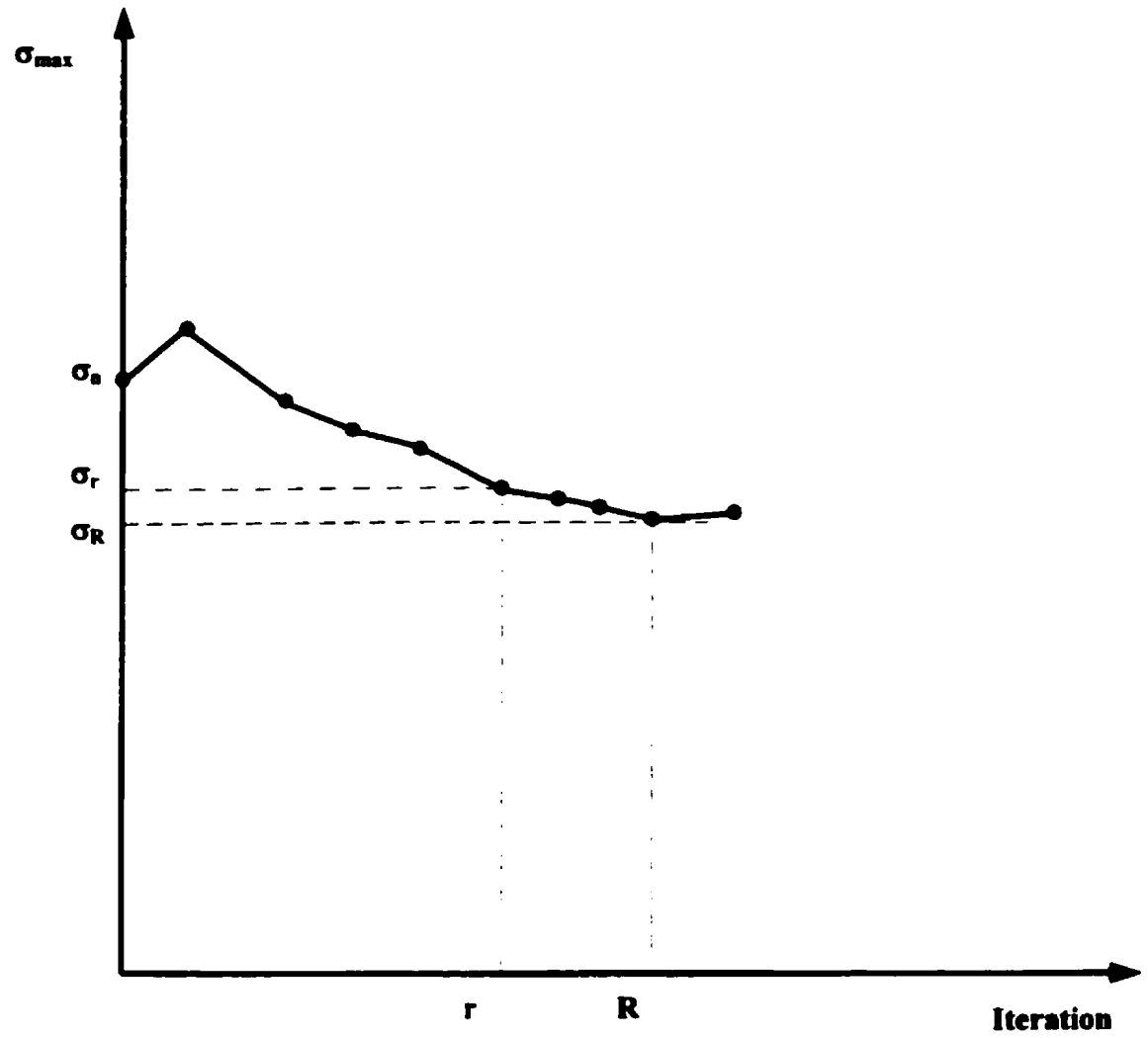

Fig.2.10 Elastic Compensation Method: Maximum Stress vs. Iteration

[Mackenzie, Shi and Boyle, 1994]

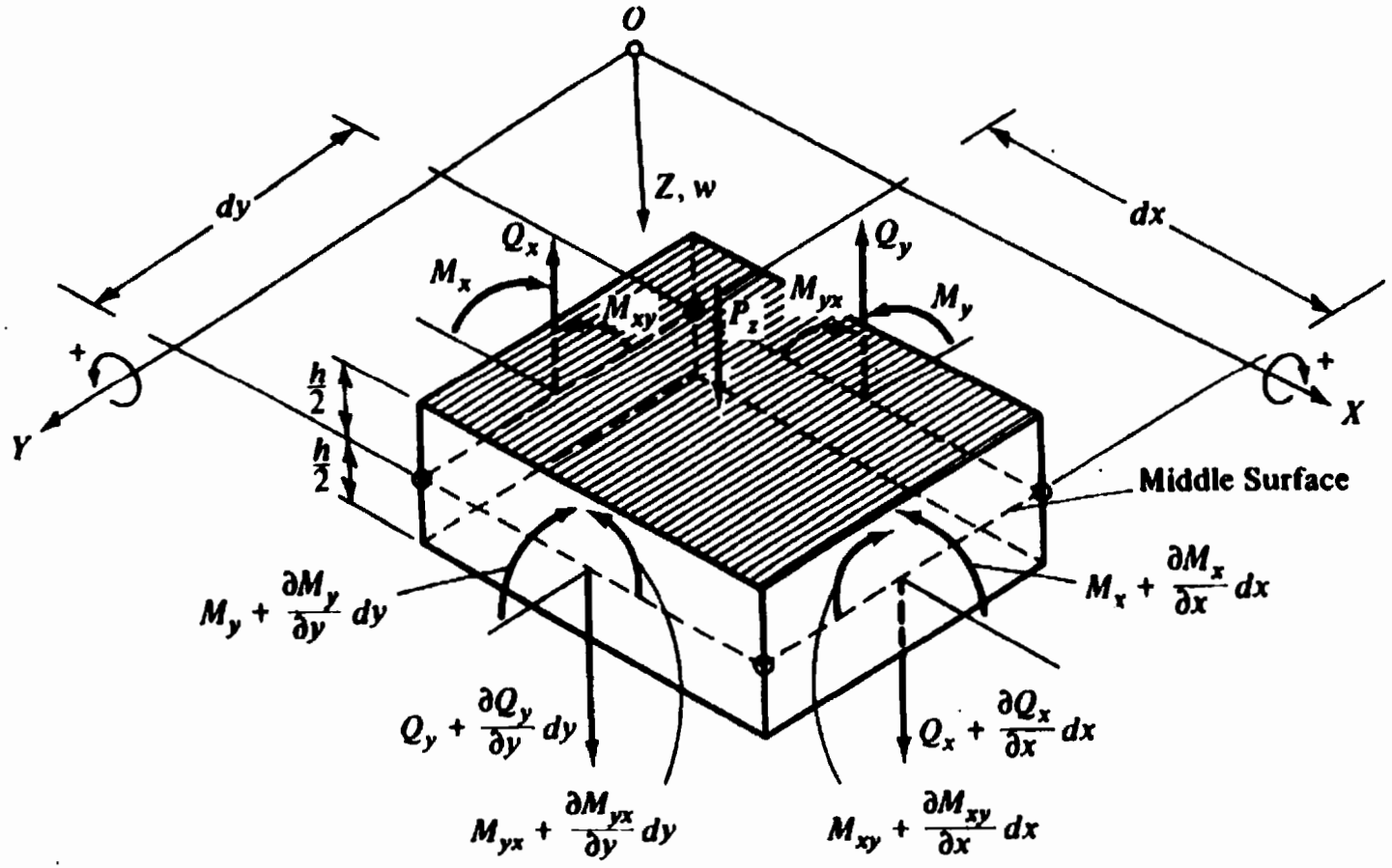

Fig 2.11 Parallelopiped Cut Out of a Plate Section

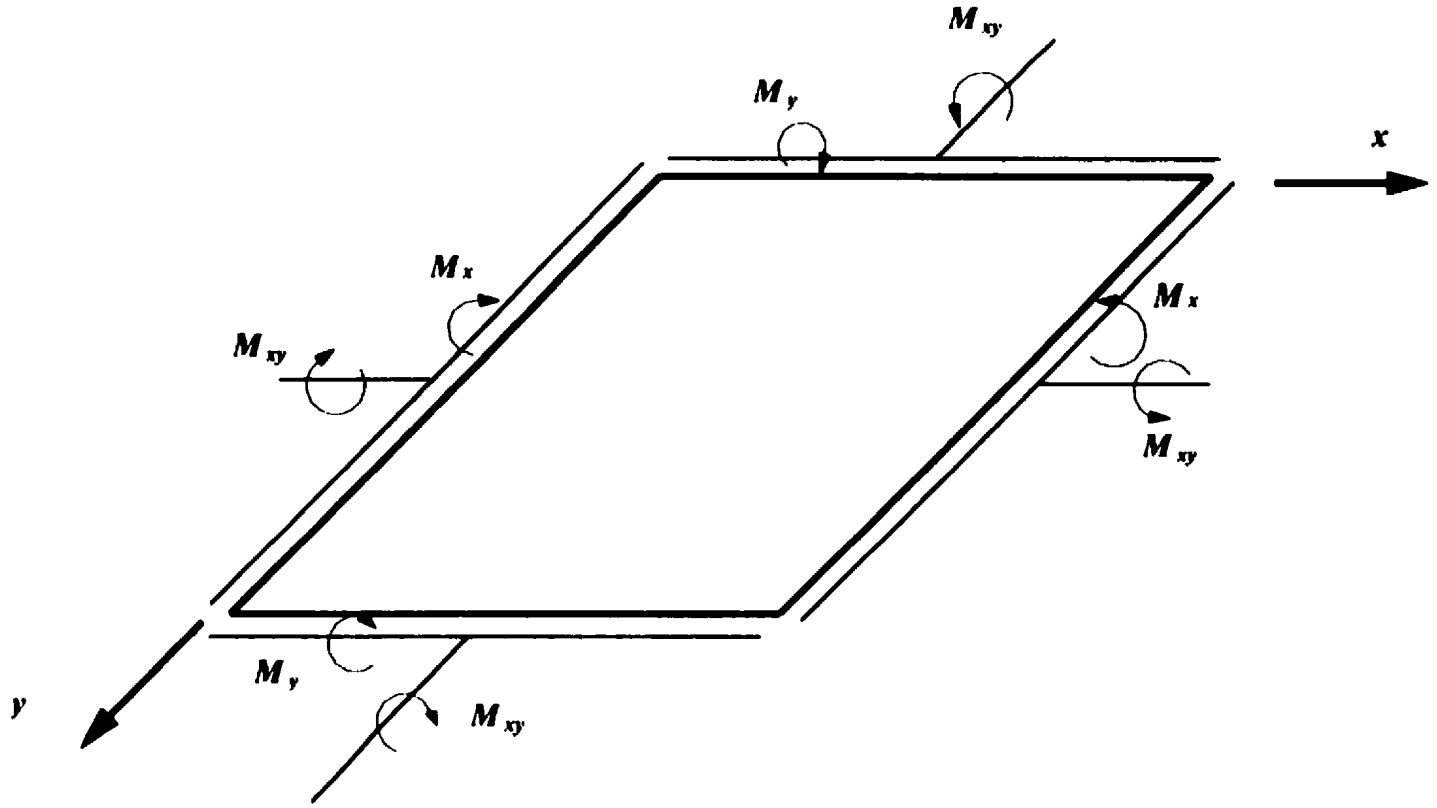

Fig. 2.12: Representation of Moments on a Plate

Chapter 3

Robust Estimation of Limit Loads using Secant Rigidity

3.1 Introduction

The previous chapter reviewed plastic analysis of structures and robust methods for limit load determination. The present chapter describes an easy and efficient analytical technique for obtaining estimates of limit loads. This technique is generally applicable to any element type in conjunction with any yield criteria. It can be used with mesh densities generally lower than those needed for other types of robust methods described in Chapter 2. The method also provides the collapse mechanism of the structure automatically. In the process, it does not make use of r-nodes (or skeletal points) in the analysis. The results given by it can be shown to be at least equal to or better than those given by the r-node method. The general procedure and the rationale are originally described by Adluri [2001a and 1999].

There are several types of non-linearity including material non-linearity, geometric non-linearity, etc. The present thesis deals with the material non-linearity aspects of limit load estimation and assumes elastic-perfectly plastic material behaviour. The procedure can be extended to any other material behaviour with ease. From the study of plastic analysis and existing robust methods, one can ascertain the following:

1. Plastic hinges or yield lines develop along yielded zones of the structure. For a very simple determinate structure, one plastic hinge is sufficient to initiate collapse. For an indeterminate structure, the degree of indeterminacy decides the number of plastic hinges. For continuous problems in 2D or 3D, yield lines and other yield patterns decide collapse mechanism.

2. When yielding occurs in a structure, the yielded region cannot sustain any additional loads. Hence, any additional load is taken by portions of structure surrounding the yielded region. In other words, redistribution of stresses is necessary to allow more loads to be carried by the structure after first yield.

3. Since the yielded region cannot carry any more loads, the secant stiffness of the yielded part of the structure is relatively lower compared to other parts of the structure.

4. Stresses may be classified into primary and secondary stresses. Primary stresses are those which are not self-limiting. In many structures, stresses at certain points will not be required to redistribute with increasing load. These points are called as equilibrium or load controlled points. For example, consider a simple bar fixed at one end, as shown in Fig 3.1a. When a load P is applied at one end, it causes stresses at various points in the structure. As long as the load is constant, the stresses in the structure remain constant. This is necessary to satisfy the equilibrium condition, i.e., the externally applied loads must be in equilibrium with the internally produced stresses. There is no redistribution or relaxation by inelastic deformation. The

structural response is equilibrium controlled or load controlled. When the stresses reach yield, collapse of the structure sets in. The stress at these points is called primary stress. Because these stresses will not be redistributed, they are called as "non-self- limiting."

5. Secondary stresses on the other hand are developed because of the influence of adjacent parts (self-constraint of the structure). These stresses are limited to a certain value, usually the yield stress. They can go beyond the yield stress in an elastic analysis. Since that violates the material law (for an elasticperfectly plastic material), these stresses redistribute themselves. For example, consider deformation applied to the free end of the bar. Let the deformation 'δ' be constant as shown in Fig. 3.1b. In this case, deformation and hence the strain remains constant. Because of the nature of the material and the constraint, the stresses calculated in an elastic analysis will not be correct for some deformations. The stresses will be "self-limited" to the yield stress. They are also called as deformation controlled stresses.

6. If the state of redistribution has to be simulated by adopting elastic analysis, the stiffness of yielded regions has to be reduced relative to that of the surrounding regions. Alternatively, stiffness of the surrounding regions can be increased, so as to cause redistribution.

7. Reducing stresses everywhere in the structure below yield provides a statically admissible stress field. Hence, modulus reduction generally yields a lower bound limit load, provided stresses are everywhere below yield.

8. In r-node method, the modified Young's modulus is inversely proportional to the von Mises equivalent stress produced in the first elastic analysis. Only two analyses are carried out.

9. In elastic compensation method, the modified modulus is inversely proportional to the maximum (unaveraged) nodal equivalent stress associated with the element from the previous solution. Several analyses might be carried out to obtain a stationary value for the maximum stress in the structure. The softening of modulus of highly stressed zones after conducting an elastic analysis followed by repeated analyses can simulate failure in a structure. This is the basic procedure adopted by all the existing robust methods.

10. There may be several peaks for the maximum equivalent stress in the structure. However, at collapse all these peaks are theoretically equal to the yield stress.

11. At collapse, structures become determinate.

This and other information was used by Adluri [1999 & 2001a, b] to propose that modified equivalent secant rigidity be used instead of equivalent material modulus. Use of material modulus implies stress level modifications. This requires modifying the

modulus whenever the stress changes across the finite element mesh. For beam and plate type structures, this would mean that the modulus needs to be changed at all relevant points through the depth or thickness. If rigidity is used instead, through the thickness modification is eliminated. It has been shown theoretically by Adluri [1999, 2001b] that this eliminates the need for the use of r-nodes. In fact, if secant rigidity is used, r-nodes cannot be identified since they depend on 'through the thickness' variation of stresses only. The analyses and softening of rigidity are repeated to achieve convergence. After convergence, a weighted average of values at yield line points is computed. This value is scaled up to obtain the limit load. It has been shown that this method is theoretically equivalent to the r-node method after the first two analyses. It is also theoretically equivalent to the elastic compensation method, if peak stress is used instead of weighted average maxima. The method is very close to the m_α method if weighted average is taken as the integral mean. The method is quite efficient in the sense that the mesh densities required are lower and special integration through the thickness is not needed. The problems associated with the use of peak stress and other numerical difficulties are avoided.

The present study applies this method for the determination of limit loads of plate structures. It will be shown that a plot of the equivalent moments after the converged analysis using modified rigidity represents the collapse mechanism for the structure. In order to implement this concept to obtain limit load, an appropriate yield criterion such as Tresca or von Mises has to be chosen.

3.2 Yield Criteria

As mentioned previously, the present chapter describes an analytical procedure for the estimation of limit loads of structures. The procedure is outlined by Adluri [2001a, 2001b] and Bolar & Adluri [2001]. In general, this procedure can be used with any yield criteria applicable for any type of element. In this thesis, this is applied to plate type problems using plate and shell elements. In order to apply the method, the yield criteria in terms of stresses need to be redefined in terms of plate (or shell) level generalized forces. This allows the direct use of the generalized force output from the particular elements chosen. In the following sections this is done for the commonly used yield criteria, namely, Tresca and von Mises.

The general state of stress at a point in a continuum is shown in Fig. 3.2. Cauchy's formula states that the eighteen components of stress, as shown in the figure are sufficient to represent traction across any surface of a continuum. In tensorial notation, this is represented as,

$$T_i^{\nu} = \sigma_{ij} \nu_j \tag{3.2.1}$$

where, T_i^{ν} is the traction along direction i,

σ_{ij} is the stress in the direction of i on the plane whose normal is along j

v_{ij} are the direction cosines of the traction forces with respect to the reference axes of the stresses.

The equilibrium of forces in each of the co-ordinate directions furnishes three differential equations of equilibrium represented as:

$$\frac{\partial \sigma_{ij}}{\partial j} + B_i = 0 \tag{3.2.2}$$

where, B_i is the body forces in the direction i

Moment equilibrium around the coordinate axes leads to the symmetry of shear stresses,

$$\sigma_{ij} = \sigma_{ji}, \qquad j \neq i \tag{3.2.3}$$

Consider an elementary tetrahedron such that the plane ABC is infinitely close to the origin O (Fig. 3.3). The direction cosines of outward normal to ABC are represented by l, m, and n. Let T_x, T_y, and T_z denote the components of the stress vector acting on this face. From equilibrium considerations (Cauchy's formula),

$$\begin{aligned} T_x &= \sigma_{xx} l + \tau_{xy} m + \tau_{xz} n \\ T_y &= \tau_{yx} l + \sigma_{yy} m + \tau_{yz} n \\ T_z &= \tau_{zx} l + \tau_{xy} m + \sigma_{zz} n \end{aligned} \tag{3.2.4}$$

For different planes considered, different sets of stress vectors are obtained. However, there are three cases wherein the shear stresses (τ) are zero. These are the principal

stresses and the directions in which they act are called the principal directions. They are denoted as, $\sigma_1, \sigma_2, and \sigma_3$ In such a case, the traction vector is collinear with the normal vector of the plane.

3.2.1 Evaluation of Principal Stresses

We can find the principal stresses $\sigma_1, \sigma_2, and \sigma_3$ by applying Cauchy's formula. This results in a cubic equation:

$$\begin{vmatrix} \sigma_x - \sigma & \tau_{xy} & \tau_{xz} \\ \tau_{xy} & \sigma_y - \sigma & \tau_{yz} \\ \tau_{xz} & \tau_{yz} & \sigma_z - \sigma \end{vmatrix} = 0 \tag{3.2.5}$$

The three roots of the equation are the principal stresses.

Consider a material subjected to direct stresses and shear stresses in 2-D. The stresses may be the result of direct forces and bending. These stresses are shown in the Fig. 3.4. The principal stresses for this case can be evaluated as,

$$\sigma_{1,2} = \frac{(\sigma_x + \sigma_y)}{2} \pm \sqrt{\left(\frac{\sigma_x - \sigma_y}{2}\right)^2 + \tau_{xy}^2} \tag{3.2.6}$$

$$\tan 2\alpha = \frac{2\tau_{xy}}{\sigma_x - \sigma_y} \tag{3.2.7}$$

The maximum and minimum shear stresses are given by:

$$\tau_{max/min} = \pm\sqrt{\left(\frac{\sigma_x - \sigma_y}{2}\right)^2 + \tau_{xy}^2} \tag{3.2.8}$$

Thus the maximum and minimum shear stress differs only in sign. And these two roots locate planes 90° apart. Hence, numerical values of shear stresses on the mutually perpendicular planes are the same. From the physical point of view, these signs have not meaning and the maximum shear stress regardless of sign is called the maximum shear stress.

3.2.2 Mohr's Circle

The state of stress for a two dimensional system shown in Fig. 3.4 can also be represented in the form of the well known Mohr's circle (Fig. 3.5). On a graph with axes σ and τ, locate points A (σ_x, $-\tau_{xy}$) and B (σ_y, τ_{yx}). Join AB and locate center of line AB as C. With C as center and radius as CA, draw a circle cutting the σ axis at D and E. Principal planes are those planes on which shear stresses are zero. Hence, the two points E and D located on the σ axis give the maximum and minimum principal stresses, respectively. The co-ordinates of the points D and E and angle α, when calculated from this plot of Mohr's circle, give Eqs. 3.2.6 and 3.2.7

3.2.3 Tresca Yield Criterion:

Tresca's failure criterion states that if the maximum shear stress at any point is equal to the shear stress at yield, the material is deemed to have failed. Thus whenever a critical value τ_{max} is reached, yielding in an element commences. For a given material, this value is set equal to the shearing stress at yield in simple compression and tension. Hence, according to Eq.3.2.8, if $\sigma_x = \pm\sigma_1 = \pm\sigma \neq 0$ and $\sigma_y = \tau_{xy} = 0$, then

$$\tau_{max} = \frac{\sigma}{2} = \frac{f_y}{2} \tag{3.2.9}$$

This conclusion also follows from the Mohr's circle of stress. To apply the maximum shear stress criterion to a biaxial state of stress, the maximum shearing stress is determined and equated to τ_{max} given by equation 3.2.9. In doing so, for the principal stresses $\sigma_1 and \sigma_2, with \sigma_3 = 0$, two cases must be considered. If $\sigma_1 > \sigma_2$, according to Equation 3.2.9, σ_1 must not exceed f_y. Similarly if $\sigma_2 > \sigma_1$, σ_2 must not be greater than σ_y. Therefore the criterion for this case becomes,

$$|\sigma_1| \leq \sigma_{yp} and |\sigma_2| \leq \sigma_{yp} \tag{3.2.10}$$

If the signs of σ_1 and σ_2 are opposite, the maximum shearing stress, $\tau_{max} = [|\sigma_1| + |\sigma_2|]/2$. The planes of these stresses correspond to possible slip planes. As before, to obtain the yield criterion, τ_{max} must not exceed the maximum shearing stress at yield in uniaxial experiment. Expressed mathematically,

$$\left|\pm\frac{\sigma_1-\sigma_2}{2}\right|\le\frac{\sigma_{yp}}{2}$$

or, for impending yield,

$$\frac{\sigma_1}{\sigma_{yp}}-\frac{\sigma_2}{\sigma_{yp}}=\pm 1 \qquad (3.2.11)$$

Eq. 3.2.11 can be plotted as shown in Fig. 3.6. Its results have relevance only in the second and fourth quadrants. In the first and third quadrants, the criterion expressed by Eq. 3.2.10 applies.

By considering σ_1 and σ_2 as the coordinates of a point, the stresses falling within the hexagon of Fig. 3.6 indicate that no yielding of the material has occurred and that the material behaves elasticaliy. The state of stress corresponding to the points falling on the hexagon shows that the material is yielding. No points can lie outside the hexagon.

For a multiaxial state of stress with principal stresses, $\sigma_1,\sigma_2,and\sigma_3$, the magnitude of the maximum shearing stress is the largest of $\frac{|\sigma_1-\sigma_2|}{2},\frac{|\sigma_2-\sigma_3|}{2},\frac{|\sigma_3-\sigma_1|}{2}$.

$$\begin{aligned}\sigma_1-\sigma_2&=\pm f_y,\\ \sigma_2-\sigma_3&=\pm f_y,\\ \sigma_3-\sigma_1&=\pm f_y\end{aligned} \qquad (3.2.12)$$

When one of the principal stress vanishes, say σ_3=0, then the yield surface is represented by a hexagon with yield condition (Fig. 3.6) as discussed before, the criterion becomes,

$$\text{Max } [|\sigma_1||\sigma_2||\sigma_1-\sigma_2|] = f_y \tag{3.2.13}$$

which represents equations 3.2.10 and 3.2.11.

3.2.4 von Mises Yield Criterion:

A more appropriate yield condition for metals considering the fact that volumetric strain does not contribute to failure is the von Mises criterion. In this approach, the total elastic energy is divided into two parts: one associated with the volumetric changes of the material and other causing shear distortions. By equating the shear distortion energy at yield point in simple tension to that under combined stress, the yield criterion for combined stress is established.

In order to derive the expression giving the yield condition for combined stress, the procedure of resolving the general state of stress must be employed. This is based on the concept of superposition. For example, it is possible to consider the stress tensor of the three principal stresses $\sigma_1, \sigma_2, and \sigma_3$ to consist of two additive component tensors. The elements of one component tensor are defined as the mean hydrostatic stress

$$\bar{\sigma} = \frac{\sigma_1 + \sigma_2 + \sigma_3}{3}. \tag{3.2.14}$$

The elements of the other tensor are $(\sigma_1 - \bar{\sigma})$, $(\sigma_2 - \bar{\sigma})$, and $(\sigma_3 - \bar{\sigma})$.

Writing this in matrix representation,

$$\begin{pmatrix} \sigma_1 & 0 & 0 \\ 0 & \sigma_2 & 0 \\ 0 & 0 & \sigma_3 \end{pmatrix} = \begin{pmatrix} \bar{\sigma} & 0 & 0 \\ 0 & \bar{\sigma} & 0 \\ 0 & 0 & \bar{\sigma} \end{pmatrix} + \begin{pmatrix} \sigma_1 - \bar{\sigma} & 0 & 0 \\ 0 & \sigma_2 - \bar{\sigma} & 0 \\ 0 & 0 & \sigma_3 - \bar{\sigma} \end{pmatrix} \tag{3.2.15}$$

The first tensor component of Eq. 3.2.15 is called spherical or dilational (hydrostatic) stress tensor (represents change in volume). The last tensor of Eq. 3.2.15 is called deviatoric or distortional stress tensor (represents change in shape).

The next step in deriving the von Mises yield criterion is to find the strain energy due to distortion. This is given by,

$$U_o = \frac{1}{2E}\left(\sigma_x^2 + \sigma_y^2 + \sigma_z^2\right) - \frac{\nu}{E}\left(\sigma_x\sigma_y + \sigma_y\sigma_z + \sigma_z\sigma_x\right) + \frac{1}{2G}\left(\tau_{xy}^2 + \tau_{yz}^2 + \tau_{zx}^2\right) \tag{3.2.16}$$

In terms of principal stresses, i.e with $\tau_{xy} = \tau_{yz} = \tau_{zx} = 0$, the strain energy per unit volume is,

$$U_{total} = \frac{1}{2E}\left(\sigma_1^2 + \sigma_2^2 + \sigma_3^2\right) - \frac{\nu}{E}\left(\sigma_1\sigma_2 + \sigma_2\sigma_3 + \sigma_3\sigma_1\right) \tag{3.2.17}$$

The strain energy per unit volume due to hydrostatic stress can be determined from the above equation by first setting $\sigma_1 = \sigma_2 = \sigma_3 = p$ and then replacing p by $(\sigma_1 + \sigma_2 + \sigma_3)/3$ Thus,

$$U_{dilatation} = \frac{3(1-2\nu)}{2E} p^2 = \frac{1-2\nu}{6E}(\sigma_1 + \sigma_2 + \sigma_3)^2 \tag{3.2.18}$$

Subtracting Eq.3.2.18 from Eq.3.2.17, simplifying and using $G = E/2(1+\nu)$, the distortion of strain energy for combined stress is given by,

$$U_{distortion} = \frac{1}{12G}\left((\sigma_1 - \sigma_2)^2 + (\sigma_2 - \sigma_3)^2 + (\sigma_3 - \sigma_1)^2\right) \tag{3.2.19}$$

According to the basic assumption of distortion energy theory, Eq. 3.2.19 must be equated to the maximum distortion energy in simple tension. The latter condition occurs when one of the principal stresses reaches the yield point f_y of the material. The distortion energy for this is $2f_y^2/12G$. Equating this to Eq.3.2.19, after minor simplifications, one obtains the basic law for ideally plastic material:

$$(\sigma_1 - \sigma_2)^2 + (\sigma_2 - \sigma_3)^2 + (\sigma_3 - \sigma_1)^2 = 2\sigma_{yp}^2 \tag{3.2.20}$$

This can be written as,

$$\sigma_1^2 + \sigma_2^2 + \sigma_3^2 - \sigma_1\sigma_2 - \sigma_2\sigma_3 - \sigma_3\sigma_1 = f_y^2 \tag{3.2.21}$$

For the case of plane stress $\sigma_3 = 0$, this reduces to equation of an ellipse (Fig. 3.7) with the equation,

$$\sigma_1^2 + \sigma_2^2 - \sigma_1\sigma_2 = f_y^2 \qquad (3.2.22)$$

Any stress falling within the ellipse indicates that the material behaves elastically. Points on the ellipse indicate that the material is yielding. It is important to note that this theory does not predict changes in material response, when hydrostatic tensile or compressive stresses are added. This can be seen from Eq.3.2.20, adding a constant stress to each of the stresses does not alter the yield condition. For this reason, in a three dimensional stress space, the yield surface becomes a cylinder with an axis having all three direction cosines equal to $1/\sqrt{3}$.

For a uniaxial state of stress with $\sigma_x=\sigma$, $\sigma_y=0$, and $\sigma_z=0$. Eq. 3.2.11 becomes,

$$\sigma^2 + 3\tau^2 = f_y^2 \qquad (3.2.23)$$

Therefore, in pure shear, yield stress is,

$$\tau_y = \frac{f_y}{\sqrt{3}} \qquad (3.2.24)$$

In terms of actual stresses, the von Mises yield surface is given by,

$$\sigma_x^2 + \sigma_y^2 + \sigma_z^2 - \sigma_x\sigma_y - \sigma_y\sigma_z - \sigma_z\sigma_x + 3\tau_{xy}^2 + 3\tau_{yz}^2 + 3\tau_{zx}^2 = f_y^2 \qquad (3.2.25)$$

3.2.5 Principal Moments:

Consider a plate under bending. The state of general bending in a plate element is shown in Fig. 2.4 (Ch.2). Stresses are produced as a result of applied loads. They vary through the thickness at any given location. These can be integrated over the thickness of the plate to obtain the bending moments about different directions.

$$M_x = \int_{-(h/2)}^{+(h/2)} \sigma_x z dz \quad \text{and} \quad M_y = \int_{-(h/2)}^{+(h/2)} \sigma_y z dz \tag{3.2.26}$$

Similarly, the twisting moments produced by shear stresses $\tau = \tau_{xy} = \tau_{yx}$ can be calculated from:

$$M_{xy} = \int_{-(h/2)}^{+(h/2)} \tau_{xy} z dz \quad \text{and} \quad M_{yx} = \int_{-(h/2)}^{+(h/2)} \tau_{yx} z dz \tag{3.2.27}$$

Since $\tau = \tau_{xy} = \tau_{yx}$, $\quad M_{xy} = M_{yx}$

Similar to principal stresses, principal moments can be defined as, moments M_x and M_y on those planes where M_{xy}=0. As in the case of principal stresses, Mohr's circle can be used as shown in Fig. 3.8. These are given by [Jaeger, 1964],

$$m_{1,2} = \frac{(M_x + M_y)}{2} \pm \sqrt{\left(\frac{M_x + M_y}{2}\right)^2 + M_{xy}^{\ 2}} \tag{3.2.28a}$$

where, M_x, M_y and M_{xy} are the plate bending moments as shown in Fig. 2.4

m_1 and m_2 are the maximum and minimum principal moments respectively

The inclination of the principal plane is given by,

$$\tan 2\theta_p = \frac{2M_{xy}}{M_x - M_y} \qquad (3.2.28b)$$

where, θ_p is the angle of the principal plane on the element.

3.2.6 Yield Criteria in Terms of Moments:

In bending of plates, the combined effect of all forces is collectively represented as 'generalized' stresses and the corresponding strains as 'generalized' strains. These generalized stresses are usually the moment resultant M_x, M_y and M_{xy} (for rectangular coordinates) or M_θ, M_r, and $M_{r\theta}$ (in polar coordinates). Since plane sections remain plane, the simplest case occurs when there is no resultant axial strain. For this case, the stresses at failure of the plate section reach the constant value σ_y on either side of the neutral axis as shown in Fig. 3.9.

If a single moment is present in the plate, the state of stress when yielding has propagated through the entire thickness is similar to that for a beam as shown in Fig. 2.1 (Ch.2) and Fig. 3.9. The moment per unit length of the plate for this state of stress can be computed by integration through the thickness. This moment is called as the plastic moment capacity M_p.

$$M_p = f_y \frac{t^2}{4} \tag{3.2.29}$$

where, f_y is the yield stress and t is the thickness of the plate.

If more than one moment component is present in the plate section, we need to use a compound yield criterion. When the fiber yield is governed by a failure criterion such as Tresca or von Mises, the failure of the overall section can be computed in terms of generalized stress moments. By integration, we can express any such stress level yield criterion in terms of resultant generalized forces. For example, the Tresca criterion (Eq. 3.2.10) can be integrated through the thickness as,

$$\int_{-t/2}^{t/2} \{\max(|\sigma_1|, |\sigma_2|, |\sigma_1 - \sigma_2|)\} z dz = \int_{-t/2}^{0} (-f_y) z dz + \int_{0}^{t/2} (f_y) z dz \tag{3.2.30}$$

or,

$$\max\left\{ \int_{-t/2}^{t/2} |\sigma_1| z dz, \int_{-t/2}^{t/2} |\sigma_2| z dz, \int_{-t/2}^{t/2} |\sigma_1 - \sigma_2| z dz \right\} = \int_{-t/2}^{0} (-f_y) z dz + \int_{0}^{t/2} (f_y) z dz$$

Using, $m_1 = \int_{-\frac{t}{2}}^{\frac{t}{2}} \sigma_1 z dz$, $m_2 = \int_{-\frac{t}{2}}^{\frac{t}{2}} \sigma_2 z dz$ and $M_p = \int_{-t/2}^{0} (-f_y) z dz + \int_{0}^{t/2} (f_y) z dz = 2 \int_{0}^{\frac{t}{2}} f_y z dz = f_y \frac{t^2}{4}$,

$$\max\{|m_1|, |m_2|, |m_1 - m_2|\} = M_p \tag{3.2.31a}$$

Letting $M_{eq} = \max\{|m_1|, |m_2|, |m_1 - m_2|\}$, (3.2.31b)

$$M_{eq} = M_p \tag{3.2.32}$$

where, t is the thickness of the plate

z is the distance on the stress diagram at which a small strip dz is considered (Fig.3.9)

M_{eq} is the equivalent moment for Tresca yield criterion,

m_1 and m_2 are the principal moments, and

M_p is the plastic moment capacity.

Similarly, for von Mises criterion,

Using $m_1 = \int_{-\frac{t}{2}}^{\frac{t}{2}} \sigma_1 z dz = \sigma_1 t^2/4$, $m_2 = \int_{-\frac{t}{2}}^{\frac{t}{2}} \sigma_2 z dz = \sigma_2 t^2/4$ and $M_p = f_y t^2/4$

in Eq.3.2.22, we get

$$M_{eq} = \sqrt{m_1^2 + m_2^2 - m_1 m_2} \quad \leq \quad M_p \tag{3.2.33}$$

where, M_{eq} is the equivalent moment from von Mises yield criterion

m_1 and m_2 are the principal moments

M_p is the plastic moment capacity

The yield locus is shown by an ellipse for von Mises in Fig. 3.10. Tresca yield locus is shown as the inscribed hexagon. The parallel flat portions AB, AF represent sagging moments and DC, DE are for hogging moments. The difference $|m_1 - m_2|$ is represented by the line EF, assuming m_1 to be positive and m_2 to be negative. A similar case of $|m_2 - m_1|$ occurs for line BC.

The yield criterion in Eq.3.2.31 or 3.2.33 are scaled versions of true M_{eq} for the respective yield criterions.

3.3 Secant Rigidity

Secant rigidity may be defined as the value of flexural rigidity obtained from a secant drawn between the origin and any point of the moment-curvature diagram (Fig.3.11).

A pseudo-elastic analysis would be represented by line OA with initial flexural rigidity D_o. If the cross-section under consideration is fully load controlled (determinate), initial elastic analysis would exhibit subsequent behavior shown by the horizontal line through point A. If the cross-section is displacement controlled, then subsequent behavior is shown by the downward line AC. A true secant line joins the origin to the actual moment-rotation point. In the absence of accurate determination of that point, we can make an approximate guess and iteratively improve the guess. The simplest guess would be to use the slope of line OC. This is also the safest. This will require the maximum amount of iterations to converge. This is the secant slope used by the r-node, ECM and m_α methods. For stress level criteria, using elastic-perfectly plastic material,

$$E_s = \frac{f_y}{\sigma_e} E_o \tag{3.3.1}$$

For moment level criteria,

$$D_s = \frac{M_p}{M_{eq}} D_o \tag{3.3.2}$$

Subject to certain conditions, other slopes are possible [Adluri, 2001b], for example,

$$D_s = \left(\frac{M_p}{M_{eq}}\right)^2 D_o \text{ or } D_s = \frac{2M_p^2}{M_{eq}^2 + M_p^2} D_o \tag{3.3.3}$$

Since the actual yield curve (or moment-curvature relationship) will not be applicable for an arbitrary load on the structure, we scale the yield criteria [Adluri, 2001a, b] to induce failure at any given load level. This can be done by replacing the M_p in Eqs. 3.3.2 and 3.3.3 by any other suitable value. In the present work, it is chosen as the absolute maximum equivalent moment in the entire field. Using this value will ensure that the secant rigidity estimate will not be too small and cause numerical problems.

Using this process, we modify the secant rigidity of all points whether they lie above or below the scaled yield criterion. This gives us an image of the relative stiffness of all the elements in the plate with respect to each other. Also, the collapse mechanism is dependent on the relative stiffness and not on the absolute values of the stiffness. This is because whatever is the value of stiffness at a given part of a structure, the formation of collapse is dictated by the stiffness of the surrounding parts as well since these contribute

to the formation of collapse. Hence the relative values of stiffness plays a role in reaching a collapse mechanism.

3.4 Limit load estimation

When the plate structure is loaded with a small amount of load, it bends elastically. When the load is increased gradually in a proportional manner, the maximum stress in the plate reaches yield. Any further increase in the load results in plasticity and local loss of rigidity. This could be simulated by a reduction of secant rigidity in the plastic zones or an increase in the elastic zone. A combination of these two can also be used. Various schemes for such an adjustment are possible. The simplest scheme is proportionate adjustment. As mentioned above, this is a most conservative adjustment for structures that do not exhibit "sudden stiffening" [Adluri, 2001b]. The proportionate adjustment is applied uniformly across the structure and hence does not need to identify the demarcation between plastic and elastic zones.

$$D_{new} \propto \frac{1}{M_{eq}} D_{old} \tag{3.4.1}$$

where, D is the rigidity and M_{eq} is the equivalent generalized force.

The proportionality constant can be taken arbitrarily. This scheme adjusts the relative rigidities across the plate structure. Regions that are prone to yield will attract more forces in an elastic analysis. These will be made softer (i.e., provide lesser rigidity) using the procedure. Similarly, the regions that will remain elastic need to attract the

redistributed forces away from the highly stressed zones. These regions will be made stiffer (i.e., provide more rigidity) by the procedure. Although it is possible that in a complicated structure the redistribution does not happen proportionally to initial rigidities, this procedure comes close to reality by adopting rigidity modification during repeat analyses.

When the rigidity is adjusted iteratively using the above scheme, the redistribution of forces is simulated. When the iteration converges, the locations that contribute to the collapse mechanism of the structure emerge clearly. In a plate, this results in the clear identification of yield lines. The equivalent moments at all the points on these simulated yield lines will be equal to each other at collapse. Due to numerical and other difficulties, the equivalent moment at these points may not be equal [Adluri, 2001a, b]. However, using this data, we can obtain a representative equivalent moment for all the yield lines. Again, several schemes are possible for obtaining this value. In case of simple structures, selection of even the maximum equivalent moment can be adopted if complete yielding has taken place and provided it is not a point of numerical error. Another method would be to use a weighted average. The simplest weighted average is to assign equal weights to all the points and obtain a simple average of all the equivalent moments on the identified yield lines. It must be noted, that the r-node method does not obtain the average of all the equivalent stresses along the yield lines. In contrast, the elastic compensation method uses only the maximum stress in the entire plate for further calculations. Using the weighted average along the yield lines is quite similar to using the integral mean in the m_α method.

The representative equivalent moment for all the yield lines obtained as a weighted average M_{eq-av} is used to obtain the collapse load. Since the analysis has been elastic (with the use of secant stiffness), the load can be changed proportionately without the need for reanalysis. The load at which the collapse occurs is the load that raises the value of M_{eq-av} to that of the plastic moment capacity M_P.

$$P_L = P\frac{M_P}{M_{eq-av}} \tag{3.4.2}$$

where, P_L is the limit load of the structure and

P is the load applied during the analysis.

The above discussion is summarized in the following procedure for limit load estimation as outlined in Adluri [1999, 2001a, b] and Bolar and Adluri [2001]:

1. Choose an appropriate failure criterion for the plate problem. For example, Tresca type moment level yield criterion is routinely used for concrete plates. For normal bending of plates, as per Tresca, the plate section is considered to have failed when the maximum principal moment is equal to plastic moment capacity (or moment of resistance).

2. Create a finite element mesh with plate or shell elements (no need for solid elements).

3. Apply a loading, $w(x,y)$ to the plate such that w is proportional to the intended loading pattern. The load intensity can be arbitrary. The objective of the analysis is to obtain the proportionality factor for this pattern that would result in collapse of the plate structure.

4. Perform a linear elastic analysis of the plate with the original properties and rigidities using the finite element mesh.

5. Compute the principal moments M_1 and M_2 using Eq. 3.2.18a for each element (or node). Find equivalent moment M_{eq} using Eqs. 3.2.31 or 3.2.33 as appropriate. At collapse,

$$M_{eq} = M_P \tag{3.4.3}$$

6. Use the results to modify the local rigidity $D(x,y)$ in the inverse proportion of equivalent moment at the point using,

$$D_{new}(x,y) = \left|\frac{M_a}{M_{eq}}\right|^{\alpha} D_{old}(x,y) \tag{3.4.4}$$

where, M_a is an arbitrarily chosen scaling factor for local failure through hinge formation (as well as for non-dimensionalization). It is recommended that this be the global maximum for the entire plate. Choosing the global maximum would avoid certain numerical difficulties. The factor α is kept as 1.0 for linear or proportional modification of rigidity. It can be chosen as less than 1.0 if slower convergence is

required in order to better represent the redistribution mechanism. If the problem behaviour is well understood, the value of α can be taken as greater than 1.0 to speed up the convergence greatly [Adluri, 1999, 2001b]. The rigidity can be changed by modifying Young's modulus, thickness or any other material or geometric property or combination of properties.

7. Repeat steps 4 to 6 above with modified properties till convergence is achieved. Usually, it takes between 4 and 15 iterations. Note that the r-node method uses only two analyses to project the limit load. However, for complex geometry including plates with fixed corners, etc., identifying the r-nodes involves considerable judgement. It can be theoretically shown that the present method predicts exactly the same results as the r-node method at the end of two analyses -provided that the average maxima for the yield lines is estimated instead of the weighted average of all the values along all yield lines.

8. For convergence, the percentage change between successive iterations is calculated for each element as:

$$\text{Percentage Change} = \left| 100 \times \left(1 - \frac{Meq_{iteration\,i}}{Meq_{iteration\,i+1}}\right) \right| \qquad (3.4.5)$$

The mean of the percentage change of values for all the elements is then calculated. This is repeated for successive iterations and the values obtained are compared.

Convergence of these values of mean percentage change would indicate convergence of limit load values.

9. A plot of the equivalent moment after converged analysis will show the scaled moment distribution similar to yield lines at collapse. The yield lines are obtained as ridge lines in this plot. They can also be obtained using optimization techniques to find local maxima in one direction (as opposed to a local peak that is obtained as a stationary point by searching in two perpendicular directions). Find a simple or weighted average of equivalent moments along these 'yield' or ridge lines ($M_{eq\text{-}average}$). This average is used to scale the applied load and obtain limit load using,

$$w_{lim} = w\frac{M_p}{M_{eq-average}} \tag{3.4.6}$$

10. If the weighted average is difficult to compute, a simple maximum of M_{eq} across the plate can also be used. However, it must be ensured that the search for maximum does not pick up a localized numerical spike as a result of FEA discretization.

3.5 Modified Secant Rigidity Method vs. R-Node & Elastic Compensation Methods

There are several similarities and differences between the present method and the well established r-node method and the elastic compensation method. Some of these are briefly outlined in the Table below:

Table 3.1: Comparison of Secant Rigidity, R-none and Elastic Compensation methods

Secant rigidity method	R-node & Elastic compensation methods
Redistribution is caused by modifying secant rigidity which effectively means modification of any geometric or material property at local level.	Redistribution is caused by modifying Elastic modulus.
Any element type can be easily adopted for the analysis. Shell/plate elements are used for the present analyses. There is no need for discretization along thickness.	For r-node method, solid elements are needed to effect stress level modifications to modulii. Number of elements required is high. ECM can use higher level elements but needs more computation in estimating equivalent properties through integration.
Any yield criterion can be adopted.	Use of r-node method has not been shown for different yield criteria. It can perhaps be extended.
A plot of equivalent moments after converged analysis clearly shows the collapse mechanism for the structure. It is necessary to obtain the collapse load.	Collapse mechanism is not used for limit load.
Limit load is calculated by determining average value of equivalent moment along all yield lines.	The global maximum stress value is used in ECM. Average of stationary values of stress is used for r-node.

3.6 Plate Problems

The thickness of the plates analyzed in this thesis is small when compared to the lateral dimensions. The normal stress in the plate through the thickness is negligible depending on whether it is a thick or a thin plate. For a thin plate, the shear stress developed through the thickness can also be neglected. However in case of thick plates, the effect of shear deformation is important and needs to be considered in the analysis (e.g., Mindlin's theory). The present thesis deals only with the analysis of thin plates and hence assumes that shear is neglected. If the shear stresses need to be accounted for, an appropriate

failure criteria can be used in lieu of the Tresca or von Mises criteria that have been used in the thesis.

As already mentioned, the analysis is for material nonlinearity only. Large deflections caused by geometric nonlinearity are not included in the study. The effect of deformations will not be significant for the collapse of plates analyzed here. It could however, be considerable for other types of problems. The method could potentially be extended to include these effects.

3.7 Finite Element Analysis Scheme

Details of finite element mesh for individual problems are discussed in Chapter 4. General details of the analysis are given below:

For all the analyses in this thesis, ANSYS FEA software has been used [ANSYS, 1997a, b, c]. Adluri [2001b] has used ABAQUS software to carry out a couple of plate problems to see the effectiveness of this method. ANSYS Shell element was chosen for the analysis. Depending on the type of analysis and accuracy required, four node (Shell 63) or eight node elements (Shell 93) were used. They have been chosen since they are well suited for linear analysis of thin to moderately thick shell structures. In the case of non-linear analysis, Shell 143 element with additional capabilities to do non-linear analysis was chosen. The elements have six degrees of freedom at each node.

The procedure outlined in 3.4 above was implemented for plates using ANSYS finite element software. A subroutine was developed for automatic processing of the data after each iteration. The analysis consisted of the following steps:

1) Conduct a linear elastic finite element analysis and output the moments M_x, M_y, and M_{xy} using the ETABLE option of ANSYS.

2) Compute equivalent moments and new rigidity for each element using the APDL (Ansys parametric design language) macro of ANSYS (see Appendix I for listings).

3) The rigidity of each element is input via a separate file named 'MODVAL1' created by the macro.

4) The problem is analyzed iteratively till convergence.

5) The values of equivalent moments for all the repeated analysis were stored in a separate file called 'results' for plotting and calculation of limit load and convergence, using a spread sheet ('Excel' or 'Surfer32').

6) Details of individual analyses are discussed in the next chapter.

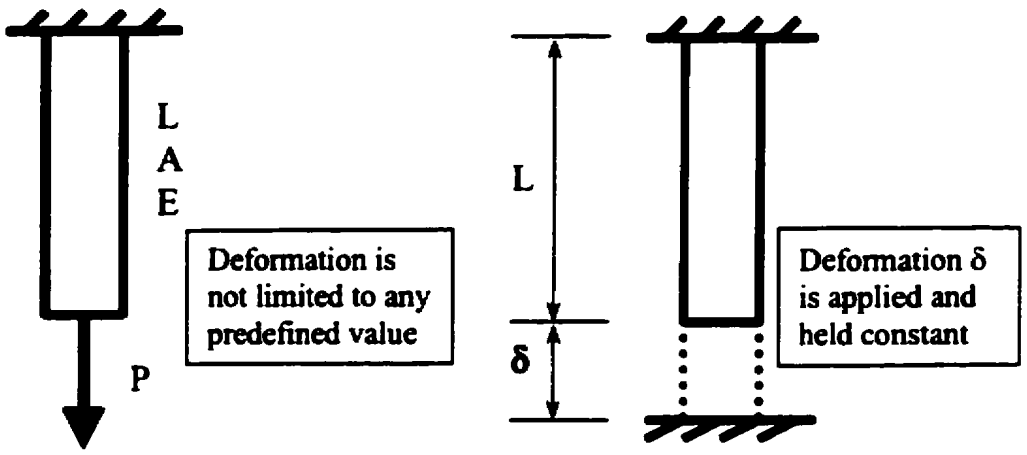

a) Load Control **b) Displacement Control**

Fig. 3.1 Simple Load and Deformation Controlled Structures

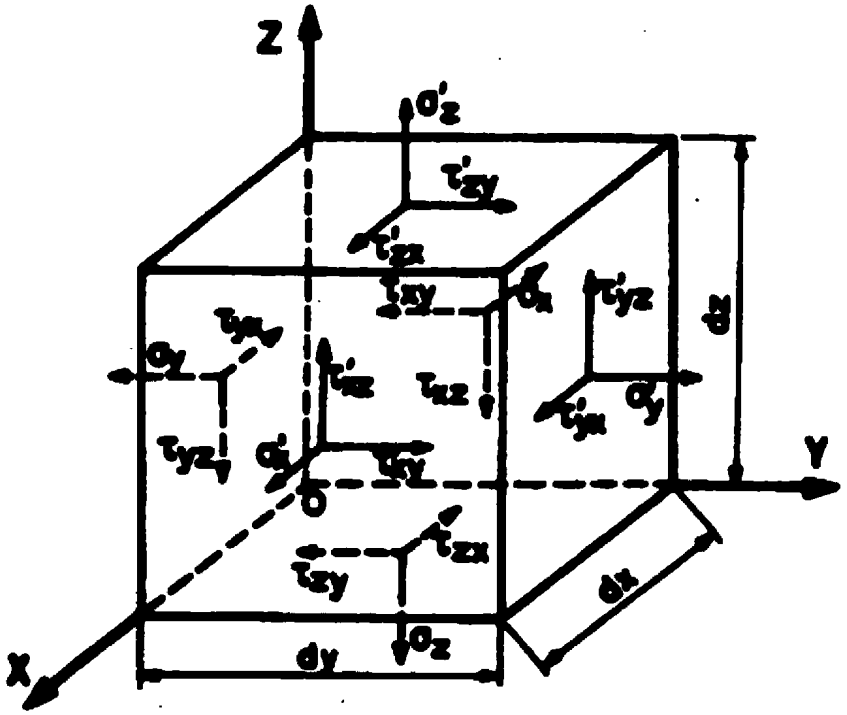

Fig. 3.2 General State of Stress in an Elemental Volume (Stress Parallelepiped) [Save and Massonet, 1972]

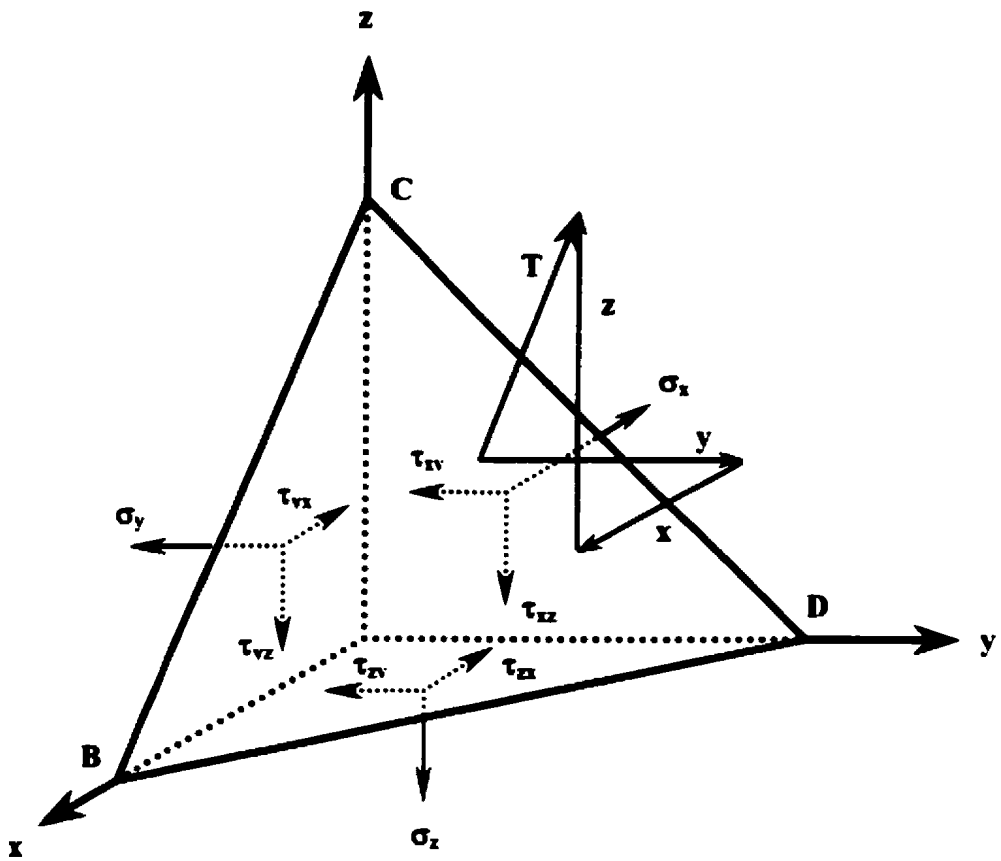

Fig. 3.3 Stress Tetrahedron

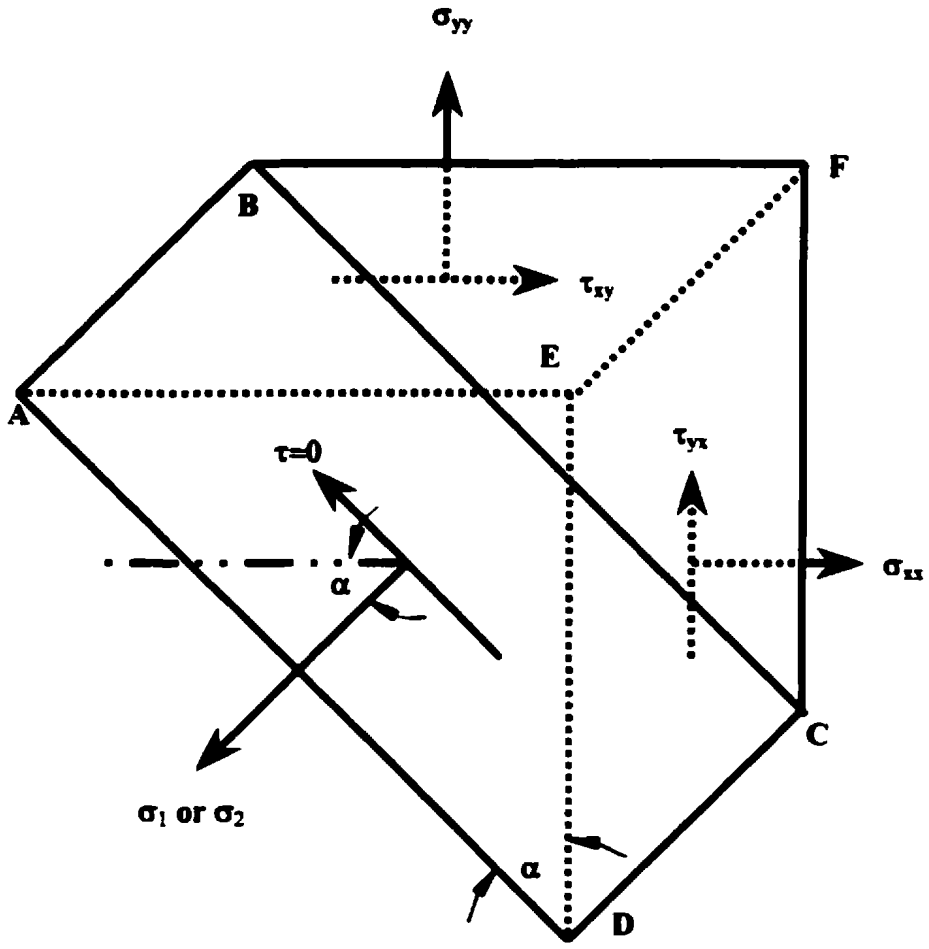

Fig. 3.4 Stress Block Showing Principal Plane (ABCD) and Principal Stresses σ_1 (or σ_2)

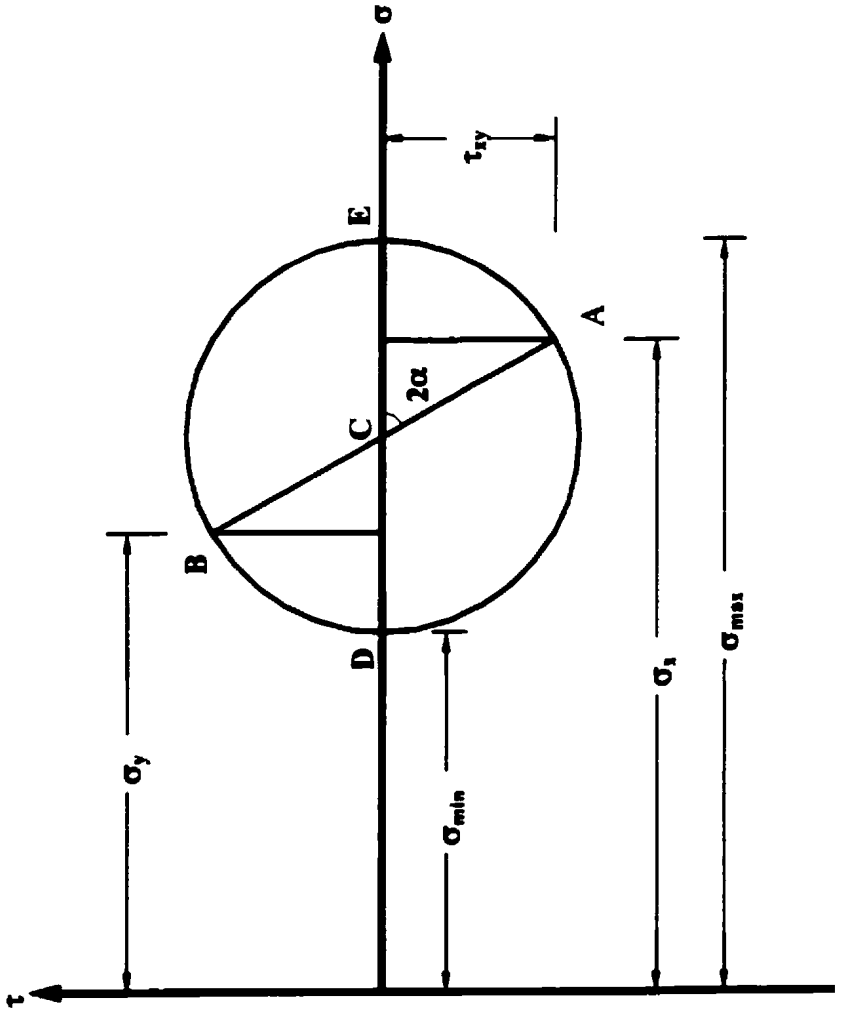

Fig. 3.5 Mohr's Circle for a 2-Dimensional State of Stress

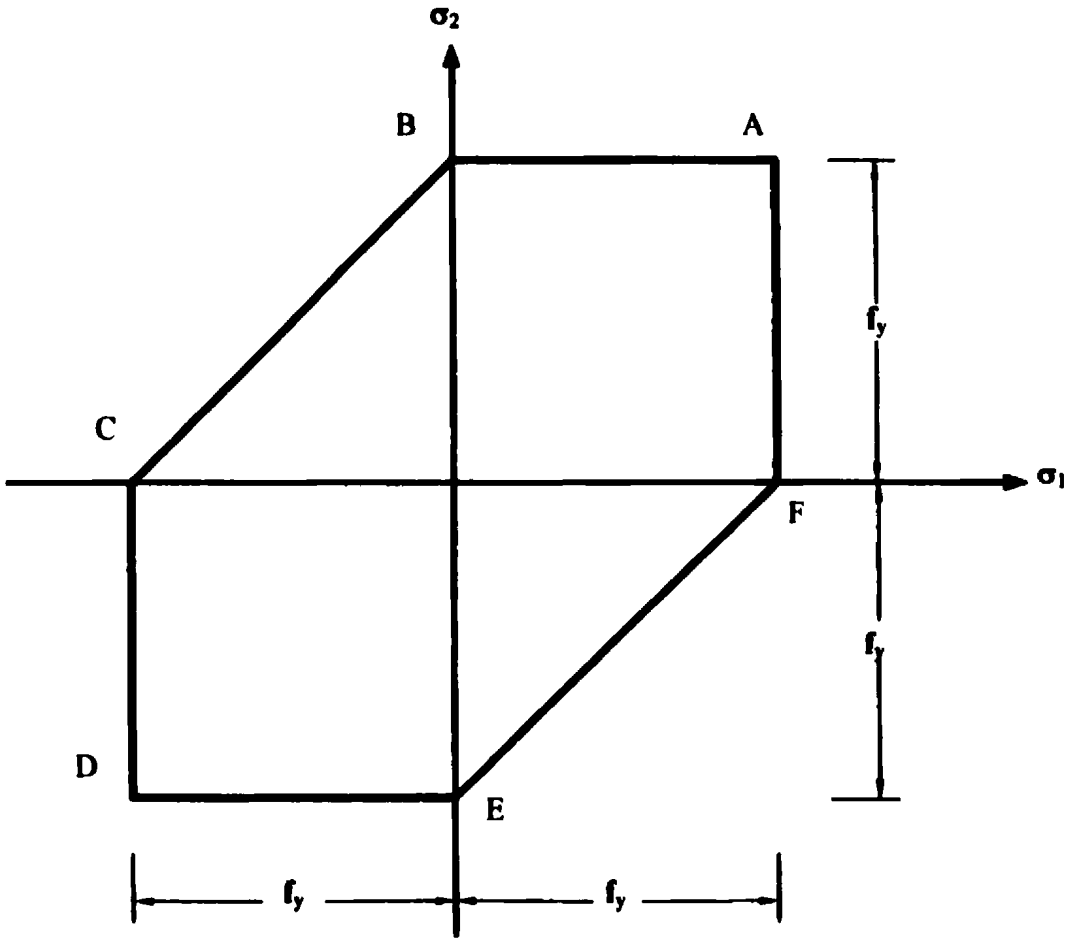

3.6 Tresca Yield Criterion for a 2-Dimensional State of Stress

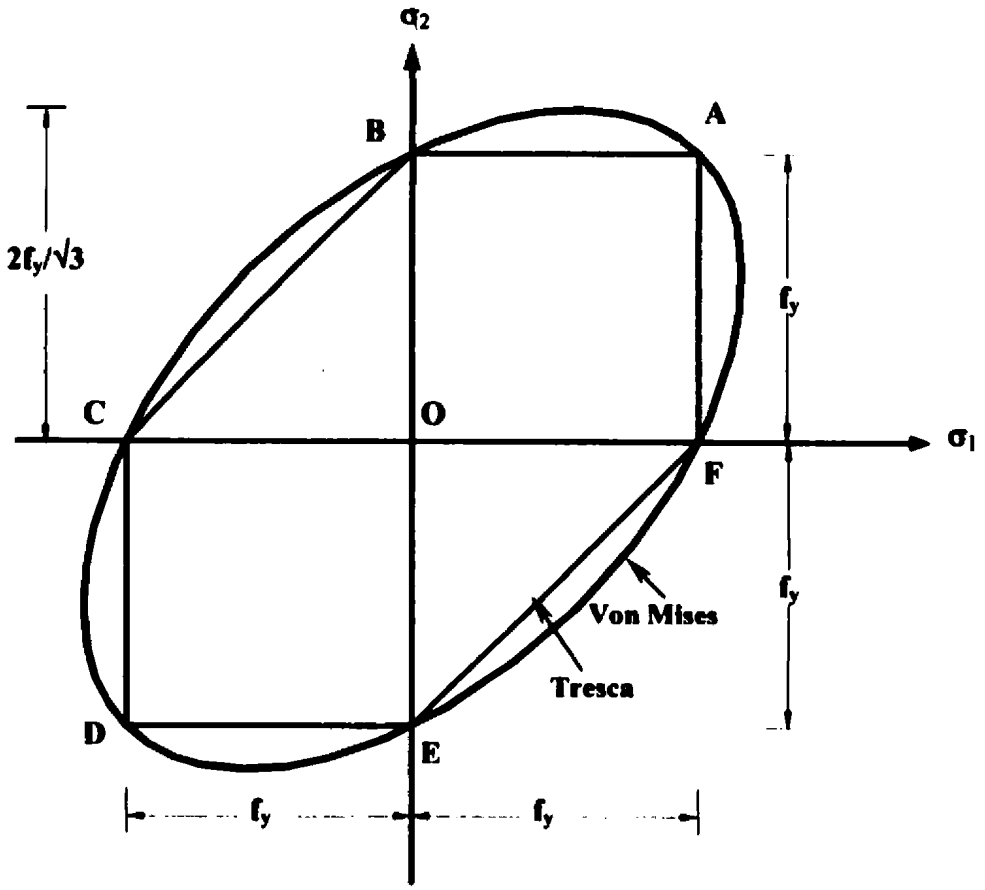

3.7 Von Mises Yield Criterion for a 2-Dimensional State of Stress

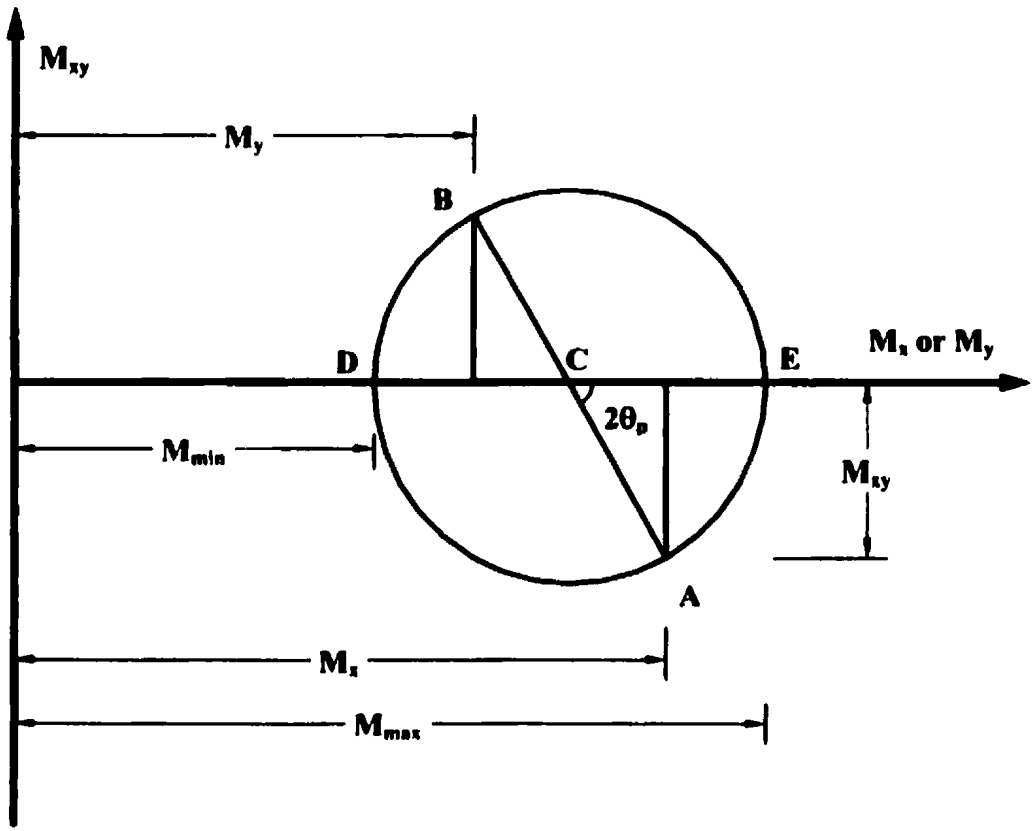

Fig. 3.8 Mohr's Circle for Bending Moments in a Plate

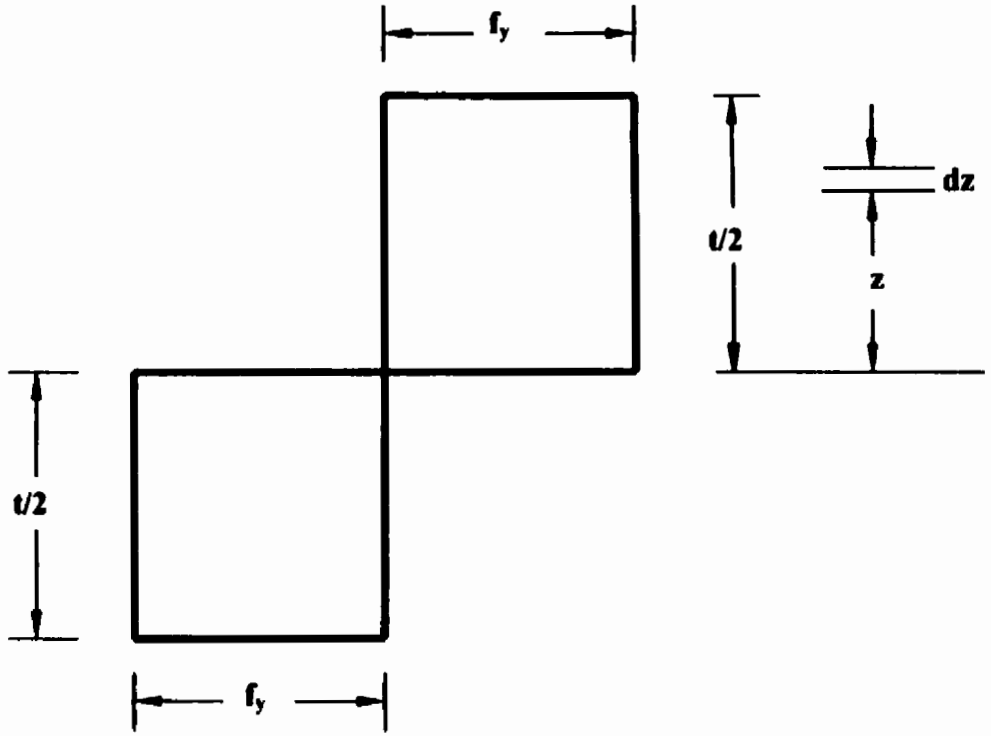

Fig. 3.9 Stress Conditions at Full Plastic Moment in a Plate Section

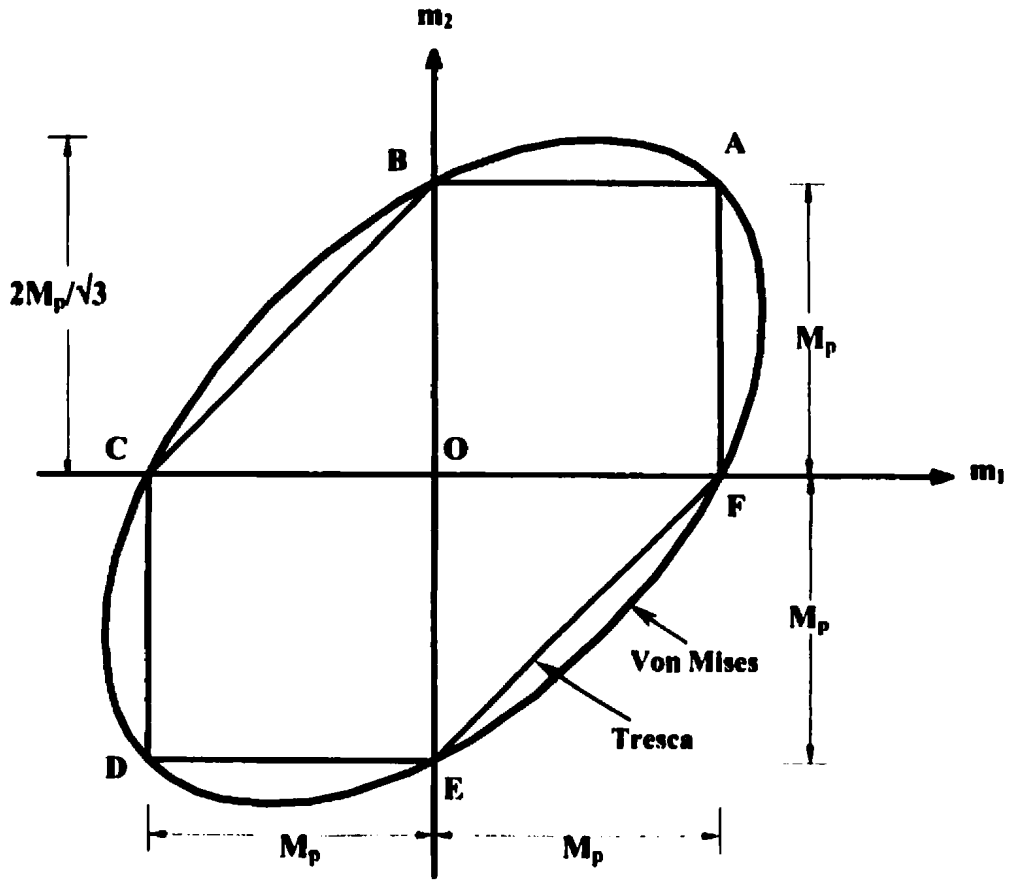

Fig. 3.10 Von Mises and Tresca Conditions for Moments in a Plate

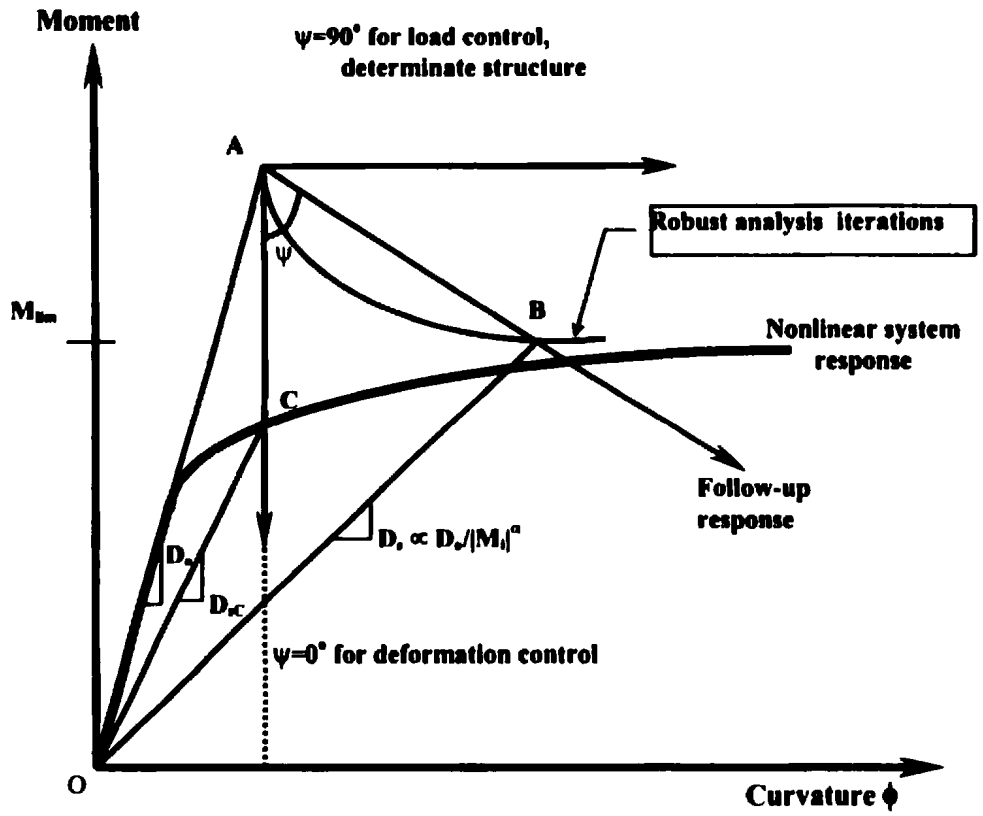

Fig.3.11 Use of Secant Rigidity in Estimating Limit Loads [Adluri, 99]

Chapter 4

Limit Analysis of Plates with Regular Shapes

4.1 Introduction

A robust method for the estimation of limit loads has been described in Chapter 3. The method uses secant rigidity modifications using a scaled version of appropriate yield criteria [Adluri, 2001a, b]. In this chapter, this method is employed to obtain limit load estimates for plates with simple geometry and loading.

For each of the cases analyzed, the initial elastic analysis results have been compared with the theoretical results available in standard references [e.g., Timoshenko & Woyinowsky-Kreiger, 1989, Szilard, 1974]. All the cases showed very good correlation indicating thereby that the finite element mesh used is acceptable. Details of subsequent analyses and calculation of limit loads are described in the following sections.

4.2 Simply Supported Square Plate with UDL

A 1000×1000×10mm plate was chosen for the analysis. A uniform pressure (UDL) of 10 N/mm^2 is applied on the plate. The load intensity is arbitrary. The material has a yield stress of 350 MPa and Young's modulus of 200,000 MPa.

ANSYS Shell 63 element, which is suitable for linear elastic finite element analysis, was chosen. The thickness of the plate is such that it can be categorized as a thin shell problem [Young, 1989]. The FEA model for the analysis consists of a mesh grid of 40×40 forming 1600 elements and 1681 nodes (Fig. 4.1). Since shell elements are being used, there is no need for discretization along the thickness. The pressure load is applied in the z-direction, i.e., perpendicular to the surface of the plate. Full model was chosen for the plate in order to demonstrate the formation of yield lines clearly. A quarter model can be used with equal effectiveness. For the present problem, the quarter model would need 400 elements to give the same accuracy as that for the full model.

4.2.1 Yield Criteria in Flexure

As per the Tresca yield criteria of bending moments, when the numerically greater of the principal moments reaches M_p, failure is considered to have occurred (see Chapter 3). The directions of the principal curvature rates are considered to coincide with the curvatures of principal moments. The idealized moment-curvature relationship is shown in Fig. 4.2.

If we consider the simplest case of a square slab on four supports with a uniformly distributed load, with degree of fixity varying from i=0 for simply supported to i=1.0 for fully restrained on all four sides, the failure mechanisms are as shown in Fig. 4.3 [Nawy, 2000; Sobotka, 1989; Wood, 1965]. In case of the simply supported plate (Fig. 4.3a), the twisting moments are zero along the diagonal lines. Hence, the moments along these

lines are principal moments. For simple bending under UDL, both the principal moments have the same sign and hence, the $|m_1 - m_2|$ condition will not govern. Therefore, the Tresca hexagon and the square yield criterion of Johansen [1972] are identical. It can be shown theoretically that for this case the yield lines occur along the diagonals alone. In case of a slab fully fixed along edges, failure occurs not only along diagonals, but also along the fixed edges (Fig. 4.3c). The failure mechanism involves the formation of yield fans near the corners [MacGregor, and Bartlett, 2000; Nawy, 2000]. For a partially restrained slab, the failure mechanism is as shown in Fig. 4.3b.

In all the plate cases solved in the present thesis, the governing parameters have been $|m_1|$ and $|m_2|$. This is because both these moments happen to be of the same sense, i.e., either hogging or sagging in respective directions. Hence, for Tresca criterion $|m_1|$ or $|m_2|$ would always be greater than. $|m_1 - m_2|$

However, in case of problems where opposite sense of moments occur (such as m_1 being sagging and m_2 being hogging), the governing parameter would be $|m_1 - (-m_2)|$ and should therefore be included in the analysis.

4.2.2 Limit Load

For the problem under consideration, a check on the first elastic analysis was initially carried out. At the center of the square plate, $M_x = M_y = 477699$ N-mm. The

theoretical value is given by [Table 6 & 7 in ., Timoshenko & Woyinowsky-Kreiger, 1989,]:

$$M_{max} = 0.0479qa^2 \tag{4.2.1}$$

The error of the FEA result as compared to the above theoretical value was 0.27%. The equivalent moment distribution after first analysis (Figs. 4.4and 4.6) calculated using Eqs. 3.2.21 or 3.2.23 shows regions of low and high magnitudes of moments along the potential yield lines as well as in other regions. However, at the state of collapse, moments all along the yield lines must be equal to each other. In order to simulate this uniformity, a modification of rigidity is carried out using Eq. 3.4.4. The modification of rigidity causes a redistribution of moments in such a way that regions with initially high magnitude of moment are assigned low rigidity and vice-versa. This causes the state of peak moments to even out with each successive iteration. In Fig. 4.4, the peak moment is at the center. As analysis progressed, it was noticed that the peaks develop a ridgeline from corners to the center. These ridgelines eventually match the yield lines. At the end of iterations, the moments at these lines are approximately equal to each other. Fig. 4.5 shows the converged analysis for Tresca yield criterion. As can be seen, the yield lines are right along the peak ridge lines. Figs. 4.6 and 4.7 show the results for the same plate using von Mises yield criteria as specified in Eq. 3.2.23 For this criteria too, the yield line pattern is similar to that obtained for Tresca criterion. This matches exactly with that predicted theoretically (Fig. 4.8). The input file listing along with the macro, which performs the post-analysis is given in Appendix A.1.1.

The difference between Fig. 4.4 and Fig. 4.6 is because of the assumption of Tresca and Von-Mises yield criterion. However, after convergence it can be seen that in both cases the moment distribution is very flat, indicating that the peaks of moments have been forced to attain a nearly uniform value.

After the convergence, the average moment along the yield lines is computed. This average moment is generated for an arbitrary load. The limit load is then calculated using Eq. 3.4.2. Fig. 4.9 shows a plot of limit load vs. iteration number for both Tresca and Von Mises criteria.

The limit load values obtained above were compared with closed form results from classical theory. The value of limit pressure by using Tresca criterion and applying kinematic theorem is given by [Save, 1995; Save and Massonet, 1972]:

$$P_L = 24\frac{M_p}{a^2} \tag{4.2.2}$$

where, M_p is the plastic moment capacity of the section

a is the width of the square plate

The same result is obtained by using both upper and lower bound theorems. Limit pressure for Von Mises criterion has been treated by Iliouchine [Save, 1995; Save and Massonet, 1972] and is given by:

$$P_L = 26.4\frac{M_p}{a^2} \tag{4.2.3}$$

Table 4.1 shows the comparison of results of theory and the present method.

The percentage errors as compared to theoretical results are 0.57 % and 0.43 % using Tresca and Von-mises criterion, respectively. In comparison, a full nonlinear analysis using ANSYS for the same mesh gave an error of 10.5% (Table 4.1). The present problem is the same as that solved by Adluri [2001b] using ABAQUS software. The ANSYS results from the present work for the modified secant rigidity method matched the results by Adluri [2001b] perfectly. The nonlinear analysis results obtained from the ABAQUS showed a limit load of 0.2208 N/mm^2. This gives an error of 4.4%. While the ABAQUS nonlinear analysis predicted better results than those by ANSYS, it can be seen that the modified secant rigidity method used in this thesis outperformed the nonlinear analysis of both software packages.

The present method used 1600 shell elements for the entire plate. The reason for choosing a full model in the present case (as mentioned previously) is to facilitate the surface plotting of equivalent moments, describing the behavior of the plate structure. The same result can be obtained using quarter model as well. As mentioned in Chapter 3, the present method avoids discretization along the thickness. As can be seen, there is a significant improvement in results using the present method. These results have been obtained after 8 iterations. It can be seen from Fig. 4.9 that limit load values even after 3rd iteration have a very good accuracy in comparison with theoretical results. Moreover,

the value of equivalent moments plotted after the converged analysis clearly shows the collapse mechanism of the structure. The method improves the results with each successive iteration where as the r-node method is restricted to two analyses only. There is however, no theoretical bar on why the r-node method cannot be used with more than two iterations although Seshadri and associates restricted it to two analyses only.

4.2.3 Comparison with the R-Node Method

Another square plate of size 609.6×609.6×38.1 was solved by Mangalaramanan [1993] using the r-node method. The mesh was 17x17x5 (total 1445) solid elements for quarter model. The corresponding limit load was 4.66 N/mm^2. The analytical limit load was 5.334 N/mm^2 using Eq. 4.2.3. This gives an error of 12.6%. However, Managalaramanan used $1.155*24M_p/L^2$ = 5.6013 N/mm^2 as the theoretical value. Compared to this, the r-node result showed an error of 16.8%. Using the present method, the same problem was solved with a shell element grid of 17x17 (total 289) for quarter model. The limit load after convergence was 5.32 N/mm^2 giving an error of 0.26% as compared to that given by Eq. 4.2.3. For comparison, the limit load using the secant rigidity method was computed after just two iterations as is the case with the r-node method. The resulting value was 5.164 N/mm^2 with an error of 3.2%. As can be seen, the present method is much closer to the theoretical results than the r-node method even after two iterations. This improvement can be attributed, among other things, to the use of shell elements instead of solid elements and the fact that the average of the values along yield lines is used instead of maxima.

4.3 Simply Supported Circular Plate with UDL

A simply supported circular plate with uniformly distributed load has been analyzed using the robust method discussed above. The plate has a radius of 250mm and a thickness of 10 mm. An arbitrary uniform pressure of 0.5 N/mm^2 is applied perpendicular to the surface of the plate. The plate material has a yield stress of 350 MPa and Young's modulus of 200,000 MPa.

As in the case of the square plate, ANSYS Shell 63 element was chosen for the analysis. The plate is analyzed as a thin shell problem. The model for the analysis consists of 30 line divisions along the circumference and 24 line divisions along the radius forming 720 elements and 721 nodes (Fig. 4.10). This was generated, by revolving a line of length equal to radius, to form a circular surface. This resulted in triangular shaped elements at the center. Shell 63 is capable of generating solutions using triangular elements as well as quadrilateral elements. Cylindrical co-ordinate system has been used for modeling as well as the output. Symmetry has not been used in order to obtain a good surface plot representation of the equivalent moments for demonstration purposes. In a practical analysis, however, there is no difficulty in making use of symmetry.

The yield criteria adopted for this problem are similar to those explained in Chapter 3 and used for the square plate in section 4.2. Since cylindrical co-ordinate system is being used, the principal moments are given by:

$$m_{1,2} = \frac{(M_r + M_\theta)}{2} \pm \sqrt{\left(\frac{M_r + M_\theta}{2}\right)^2 + M_{r\theta}^{\,2}} \qquad (4.3.4)$$

The computations using ANSYS involve conducting a linear analysis and generating the equivalent moments using Eqs. 3.2.22 and 3.2.23. The rigidity of each element is then modified using Eq. 3.4.4. The next analysis is conducted on the modified structure keeping all other conditions the same. The analysis is repeated till satisfactory convergence is achieved. The input file listing along with the macro, which performs the post-analysis is given in Appendix A.1.2.

4.3.1 Failure Criteria

In case of an isotropic circular plate with uniform loading, a great number of yield lines start from the center. These radiating lines are shown in Fig. 4.11. Since this is an axisymmetric problem, the principal moments become M_r and M_θ. Hence the mathematical form of Tresca criterion [Save and Massonet, 1972] is (Fig. 4.12),

$$\text{Max}\left(|M_r|, |M_\theta|, |M_r - M_\theta|\right) = M_{eq} \qquad (4.3.5)$$

The strain rate vector in polar co-ordinates has the form,

$$K_r = -\frac{d^2 W}{dR^2} \qquad K_\theta = -\left(\frac{1}{R}\right)\left(\frac{dW}{dR}\right) \qquad (4.3.6)$$

where, K_r and K_θ are the curvatures in the radial and tangential direction, respectively and W is the velocity field which is a function of distance r along the radius R.

Stress points located on or inside the yield curve will represent the state of stress at various points on the plate. The locus of these stress points will be called the "stress profile." The stress profile must start from point A (r=0) because axial symmetry requires that $M_r = M_\theta$ at the center. The stress profile must end at point B for r=R since M_r=0 at the edges. In the case of line AF, K_θ =0 and hence W is constant. On the other hand, for line AB, K_r =0, which would result in a linear function. Hence, lines AF is not considered for plastic flow. Similar condition applies for other direction too.

The corresponding figure for Von Mises condition is shown in Fig. 4.13.

4.3.2 Limit Load

For the problem under consideration, a check on the first elastic analysis was initially carried out. This was achieved by checking the moments at the center and two arbitrary points on the plate. The moment at any arbitrary point r_o is given by [Table 5-11, Baker, Kovalesky and Rish, 1972].

$$\rho^2 = \left(\frac{r}{R}\right)^2 \tag{4.3.7}$$

$$M_r = \left(\frac{pR^2}{16}\right)(3+\mu)(1-\rho^2) \tag{4.3.8}$$

$$M_\theta = \left(\frac{pR^2}{16}\right)\left[(3+\mu)-(1+3\mu)\rho^2\right] \tag{4.3.9}$$

At center, r=0. Therefore,

$$M_r = M_\theta = \left(\frac{pR^2}{16}\right)(3+\mu) \tag{4.3.10}$$

where, R is the radius of the plate, r is the distance along the radius of the plate, p is the applied UDL, μ is the Poisson's ratio, M_r is the moment along the radial direction, and M_θ is the moment along the tangential direction.

The elastic analysis moments at the center as well as two other arbitrary points compared very well with the above theoretical values. Subsequently, re-analysis was performed and 6 iterations led to convergence of values.

Hopkins and Wang [1954] solved the problem with Tresca criterion to obtain the limiting value for a uniformly distributed load. They considered a velocity field and used equilibrium considerations to show that,

$$P_L = \frac{6M_p}{R^2} \tag{4.3.11}$$

Hopkins and Wang [1954] have also solved the same problem for Von Mises yield criterion as well. The curved stress profile AB (Fig. 4.13) is used. From the very nature of Von Mises condition, the resulting differential equilibrium equation is non-linear and has to be integrated numerically. The resulting limit load for Von Mises condition is given by:

$$P_L = \frac{6.51M_p}{R^2} \tag{4.3.12}$$

Limit load was calculated using Eq. 3.4.2. Fig. 4.14 shows a plot of the percentage change vs. number of iterations. Table 4.2 shows the comparison of results from theory and the present method.

The percentage errors as compared to theoretical results are -0.05 % and 0.46 % for Treca and Von Mises criteria, respectively. These errors are very small and within the convergence deviations thus pointing to a near perfect set of results. A similar problem solved using r-node method as a two-dimensional axi-symmetric model with 100 elements along the radius and 10 elements through thickness, had an error of 1.8 % [Mangalaramanan, 1993]. In the present problem, the number of elements used along the radius is 24 only. The present results have been obtained using 6 iterations. However, after the third iteration, the results are very close with analytical values as can be seen from Fig. 4.14.

From classical analysis, the collapse mechanism is similar to that of an inverted cone (Fig. 4.11). The initial analysis produces a moment distribution as shown in Fig. 4.15 for Tresca criterion and Fig. 4.17 for Von Mises criterion. It must be noted that the plotting software used for obtaining the surface plot could only handle rectangular regions. Hence, for the sake of plotting, the circular plate is extended to look like a square with dummy areas to fill the extra material. The extra space does not affect the results in any way and is not part of the analysis. Fig. 4.16 and Fig. 4.18 show equivalent moment distribution after converged analysis. It must be pointed out that Figs. 4.15 and 4.16 plotted for initial and final analyses look very similar. But the scales for moment values are different. In Fig. 4.16 for final iteration, the difference between the maximum and minimum moment is around 1%. Corresponding difference in Fig. 4.15 is more than 20%.

4.4 Fixed Square Plate with UDL

A 1000x1000x10 mm fixed square plate with uniformly distributed load is analyzed using the procedure described earlier. An arbitrary uniform pressure of 6 N/mm^2 is applied on the plate. The plate material has a yield stress of 350 MPa and young's modulus of 200,000 MPa.

ANSYS Shell 93 element was chosen for the analysis. It is suitable for linear and non-linear finite element analysis. The element has eight nodes with six degrees of freedom at each node. The finite element model for the analysis consists of a mesh grid of 80x80

forming 6400 elements and 19521 nodes (the element is 8-noded). As before, since shell elements are being used, there is no need for discretization along the thickness. Symmetry has not been utilized. However, it can be used in a practical analysis without any restriction. The plate model is as shown in Fig. 4.19. The input file listing along with the macro, which performs the post-analysis is given in Appendix A.1.3.

4.4.1 Limit Load

For the problem under consideration, a check on the first elastic analysis was initially carried out. The moment M_x (=M_y) at the center is given by [Table 35, ., Timoshenko & Woyinowsky-Kreiger, 1989],

$$M_x = 0.0230qa^2 \tag{4.4.1}$$

The Finite Element result compared very well with the theoretical value (Table 4.3). Subsequent re-analysis was done and 10 Iterations led to convergence of values. Limit load was calculated using Eq. 3.4.2.

The equivalent moment distribution after first analysis shows regions of high moments at the center and fixed edges (Figs. 4.20 and 4.22). But at the state of collapse, moment at all former peaks even out. It can be seen from Fig. 4.21 and 4.23 that the yielded zones are found along the diagonals and also the fixed edges. Hence an average value of the equivalent moment along diagonal yield lines and those along fixed edges is adopted for calculation of limit load.

Fig. 4.24 shows a plot of the percentage change between iterations for Tresca and Von Mises criteria:

The value of equivalent moment after the 10th iteration has been considered for calculations after checking for convergence.

The theoretical value of limit pressure by using Tresca criterion is given by Sobotka [1989]:

$$P_u = \frac{43.85 M_p}{a^2} \tag{4.4.2}$$

The upper bound limit load is given by [Szilard, 1974]:

$$P_u = \frac{48 M_p}{a^2} \tag{4.4.3}$$

This value has been used in lieu of Von Mises criterion limit load. Table 4.3 shows the comparison of results. The percentage errors as compared to theoretical results are 2.00% and 1.95%, respectively. A similar problem solved as a quarter model using r-node method with a grid of 17x17x5 was reported to have an error of -13.4 % with the corresponding theoretical value [Mangalaramanan, 1993].

It can be seen from Fig. 4.24 that the 10^{th} iteration has resulted in a good accuracy of analysis. Limit load values even after 4^{th} iteration have considerably small error.

From classical analysis, the collapse mechanism is as shown in Fig. 4.25. The initial analysis produces a moment distribution as shown in Fig. 4.20 for Tresca and in Fig. 4.22 for Von Mises. The difference between the two figures is because of the assumption of Tresca and Von-mises yield criterion. However, it can be seen that in both cases the moment distribution after converged analysis (Fig. 4.21 for Tresca and Fig. 4.23 for Von Mises) is much flatter, indicating that the peaks of moments have been forced to attain a uniform value, which is equal to M_p at collapse. It must be noted that Fig. 4.23 shows a sudden increase in the moment at the four corners of the plate. This spike is unlikely to be part of the collapse mechanism as indicated by the radial fans shown in Fig. 4.25. It is possibly just a numerical local error. Such spikes must obviously not accounted for in the calculation of limit loads. The elastic compensation method, if followed, would use such spikes rather than the average of the moments along the yield lines to obtain limit loads. Using this spike would give a larger error than would otherwise be the case.

4.5 Circular Plate with Central Concentrated Load

A circular plate with central concentrated load is analyzed using the robust method described earlier. The plate has a radius of 250 mm and a thickness of 10 mm (Fig. 4.26). A central concentrated load of 1 kN is applied on the plate. The plate material has a yield stress of 350 MPa and young's modulus of 200,000 MPa.

The description of the model and other data is similar to that adopted in section 4.3. The failure mechanism is similar to that shown in Fig. 4.11. The input file listing along with the macro, which performs the post-analysis is given in Appendix A.1.4

4.5.1 Limit Load

The elastic moment at any arbitrary point r is given by [Appendix A, Szilard, 1974]:

$$\rho = \left(\frac{r}{R}\right) \tag{4.5.1}$$

$$M_r = \left(\frac{-P}{4\pi}\right)(1+\mu)(\ln \rho) \tag{4.5.2}$$

$$M_\theta = \left(\frac{P}{4\pi}\right)[(1-\mu)-(1+\mu)\ln \rho] \tag{4.5.3}$$

The moments from the initial FEA compared very well with the above theoretical values. Subsequently, re-analysis was performed and 20 iterations led to convergence of values. Fig. 4.31 shows a plot of the limit load vs. iteration for both Tresca and von Mises criteria. The convergence is slower in this problem because of the presence of a large concentrated force instead of a distributed pressure.

The equivalent moment distribution from initial analysis is shown is Fig. 4.27 (for Tresca) and Fig. 4.29 (for Von Mises). The Final results are shown in Fig. 4.30 for Tresca and Fig. 4.31 for Von Mises. It can be seen that in both cases the moment

distribution after converged analysis is much flatter, indicating that the peaks of moments have been forced to attain a uniform value along ridgelines. Note that in the converged analyses representation (Figs. 4.28 and 4.30) the moment axis difference is very small.

Hopkins and Wang [1954] have solved the same problem for both Tresca and Von mises criterion and have shown that both the limit load values coincide at limit state for a simply supported circular plate with central concentrated load. It is given by,

$$P_L = 2\pi M_p \qquad (4.5.4)$$

Table 4.4 shows the comparison of results from theory and the present method.

4.6 Rectangular Plate Simply Supported on Shorter Edges

A uniformly loaded 1500x1000x10 mm rectangular plate simply supported on the shorter edges (Fig. 4.32) is analyzed using the secant rigidity method described earlier. An arbitrary uniform pressure of 5 N/mm^2 is applied on the plate. The plate material has a yield stress of 350 MPa and Young's modulus of 200,000 MPa. ANSYS Shell 63 element was chosen for the analysis. The model for the analysis consists of a mesh grid of 60×40 forming 2400 elements and 2501 nodes. The analysis procedure is similar to that described in section 4.1. The input file listing along with the macro, which performs the post-analysis is given in Appendix A.1.5.

4.6.1 Limit Load

The theoretical maximum moment is given by [Appendix A, Szilard, 1974]:

$$M_{x,max} = 0.12787 pL^2 \tag{4.6.1}$$

where, p is the UDL on the plate, L is the length of the plate.

This compared well with value obtained from the initial elastic analysis using FEA. Subsequently, a re-analysis was performed and 9 iterations led to convergence of values.

The equivalent moment distribution after first analysis shows the mid plate region with a high magnitude of moment (Fig. 4.33). A plot of equivalent moment after converged analysis clearly shows one yield line as is expected at the center (Fig.4.34). Fig. 4.35 shows a plot of limit load vs. iteration.

The limit load value obtained above was compared with theoretical results. The value of limit pressure by using Tresca criterion [Sobotka, 1989]:

$$P_L = \frac{8M_p}{L^2} \tag{4.6.2}$$

Table 4.5 shows the comparison of results from theory and the present method.

The percentage errors as compared to theoretical results is 0.1% by assuming Tresca's yield criterion. A similar problem solved as a half model using r-node method with a grid

of 18×12×6 was reported to have an error of -16.4% [Mangalaramanan, 1993] in comparison with the corresponding theory.

4.7 Rectangular Plate Simply Supported on Three Edges with UDL

A uniformly loaded 1500×900×10mm rectangular plate simply supported on three edges (longer edge free) is analyzed (Fig. 4.36). An arbitrary uniform pressure of 5 N/mm^2 is applied on the plate. The plate material has a yield stress of 350 MPa and Young's modulus of 200,000 MPa.

ANSYS Shell 63 element was chosen for the analysis. The finite element model for the analysis consists of a mesh grid of 60×40 forming 2400 elements and 2501 nodes as shown in Fig. 4.36. The input file listing along with the macro, which performs the post-analysis is given in Appendix A.1.6.

4.7.1 Limit Load

For the problem under consideration, the maximum moment obtained in the first elastic analysis compared very well with the theoretical value given by [Table 42, Timoshenko & Woyinowsky-Kreiger, 1989]:

$$M_{x,max} = 0.0738qb^2 \qquad (4.7.1)$$

where, q is the UDL on the plate and b is the free length of the plate

NOTE TO USERS

Page(s) not included in the original manuscript are unavailable from the author or university. The manuscript was microfilmed as received.

115-121

This reproduction is the best copy available.

UMI

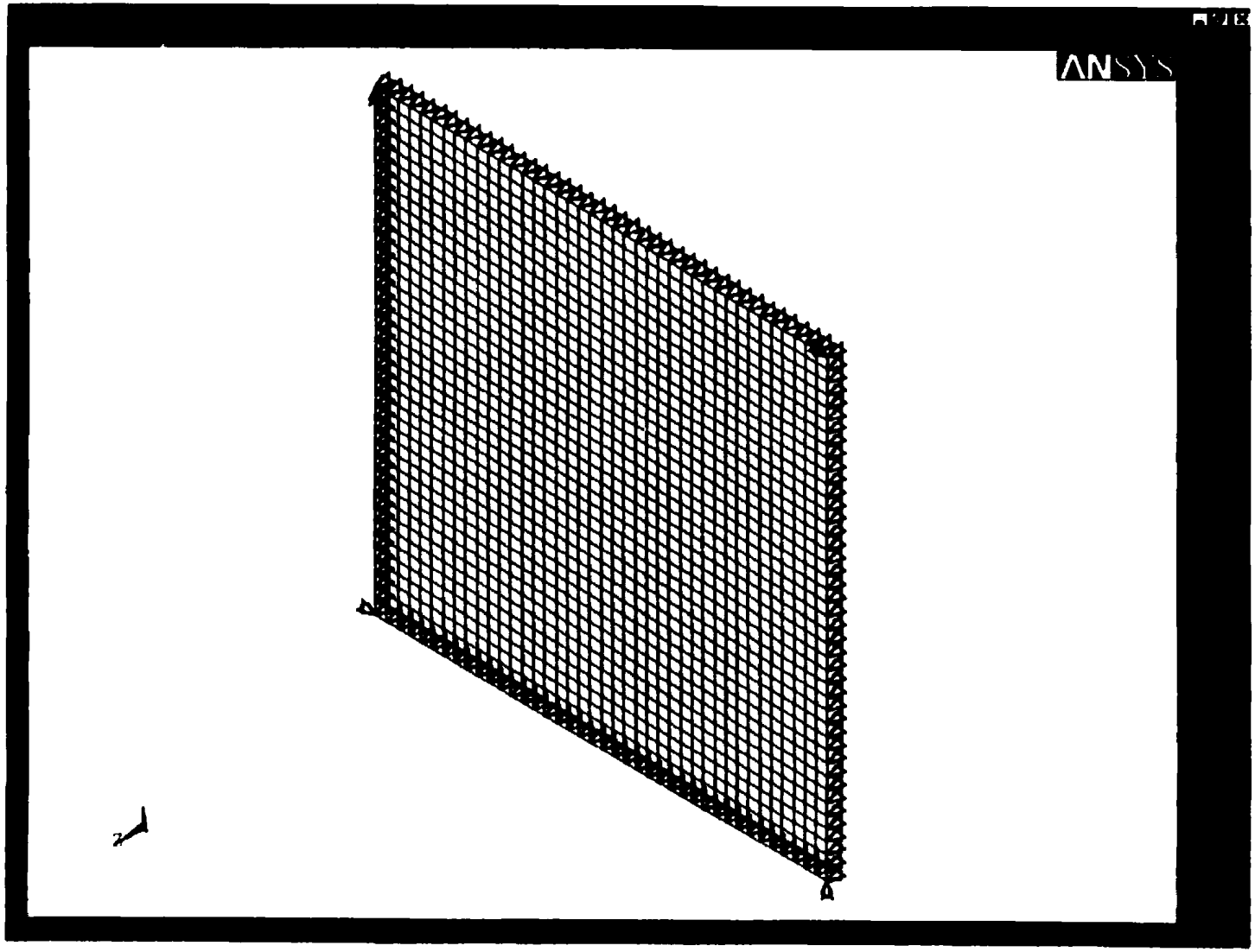

Fig. 4.1 Finite Element Model of a Square Plate with UDL

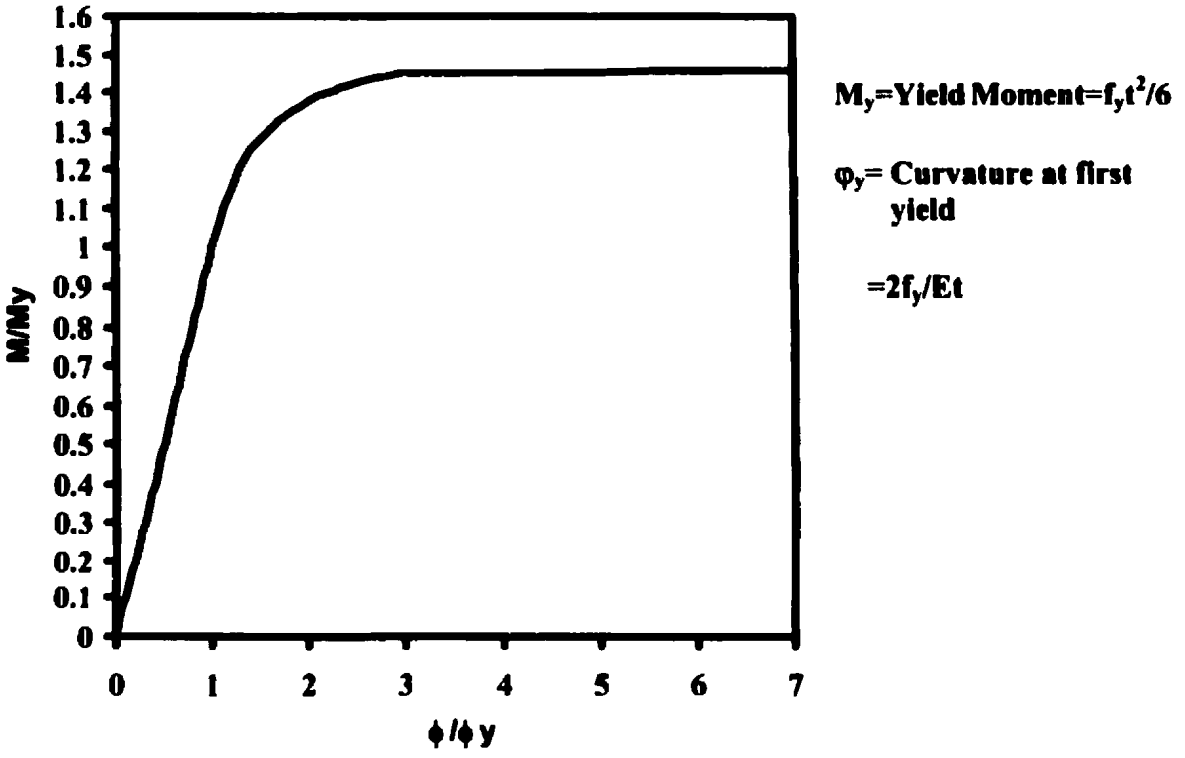

Fig. 4.2 Moment-Curvature Relationship for a Plate Section

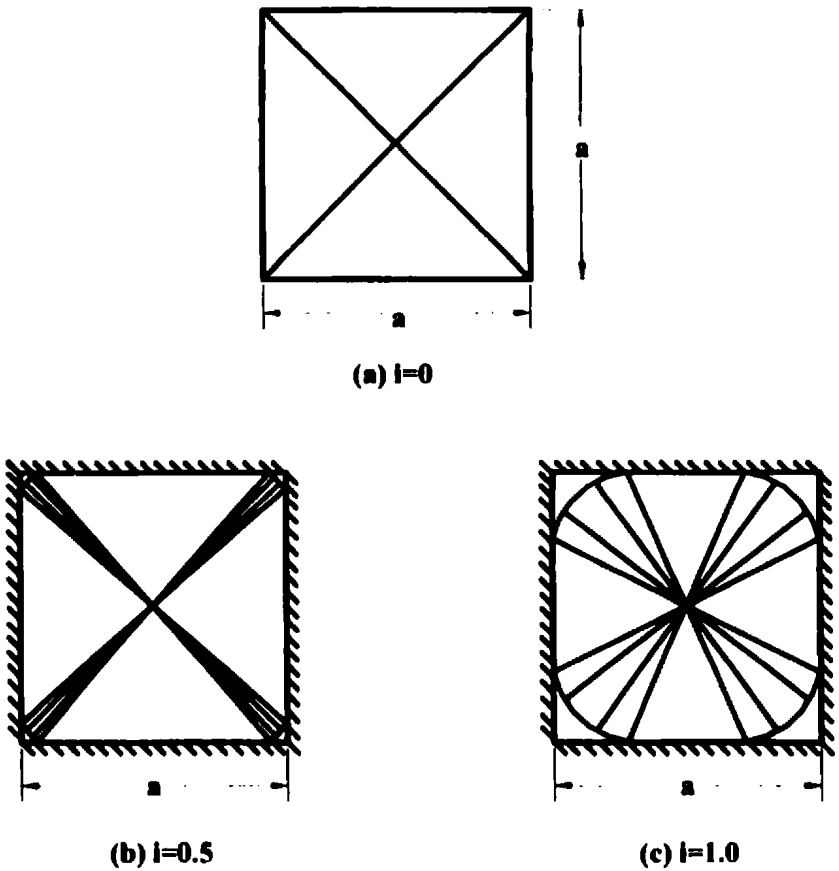

(a) i=0

(b) i=0.5

(c) i=1.0

Fig. 4.3 Failure Mechanism of a Square Slab with Different End Fixities

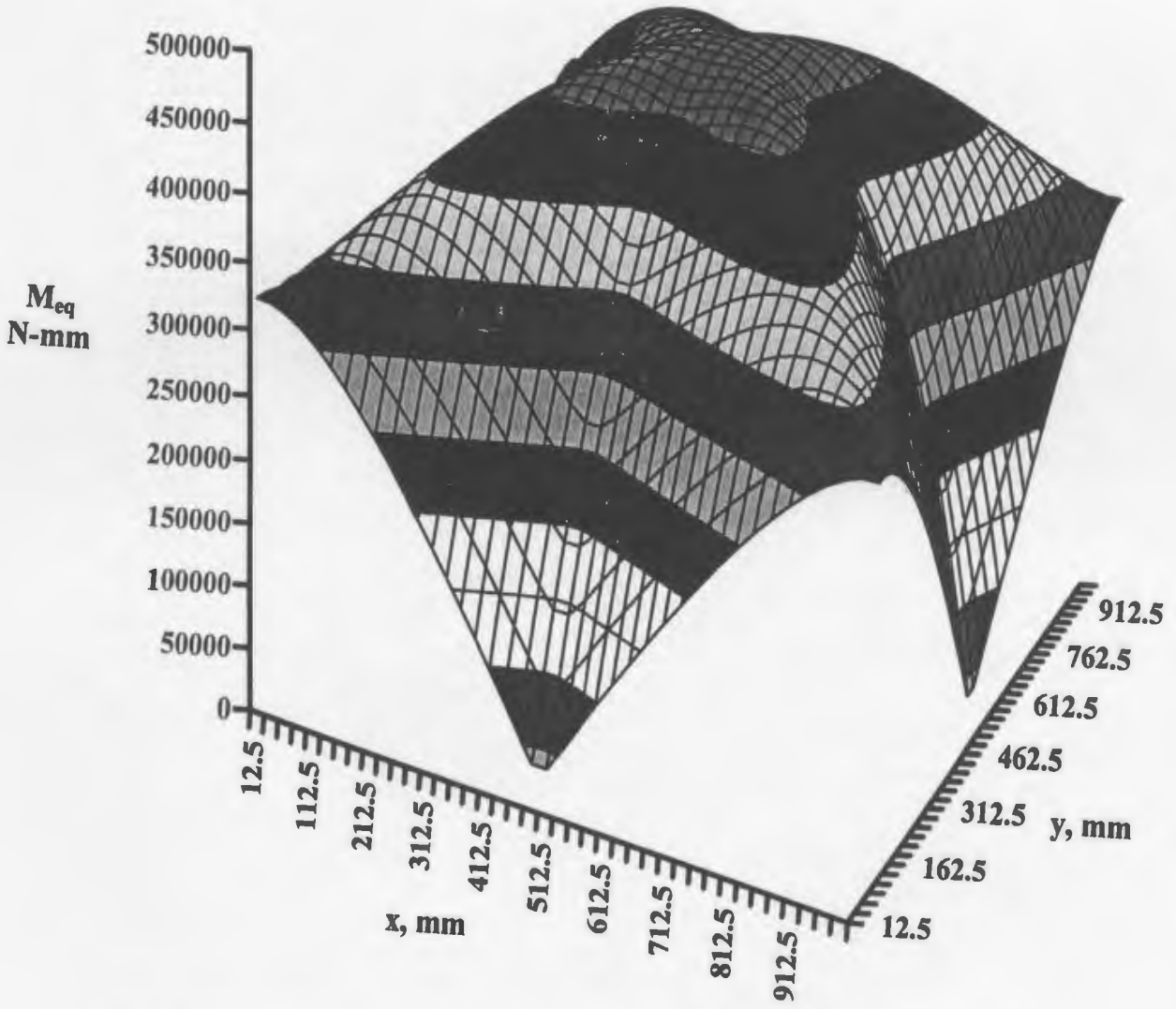

Fig. 4.4 Simply Supported Square Plate –UDL, Tresca, First Analysis

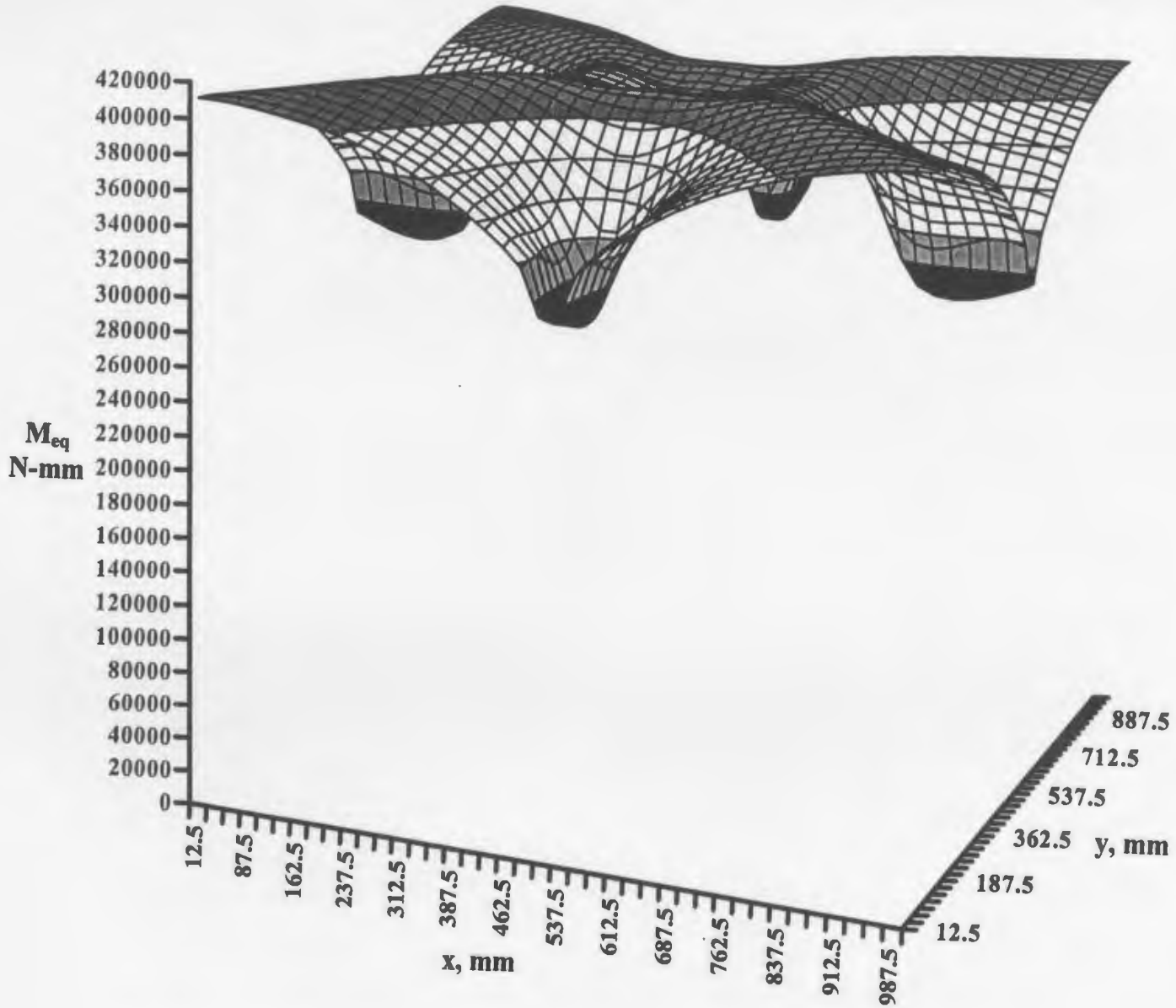

Fig. 4.5 Simply Supported Square Plate- UDL, Tresca, Converged Analysis

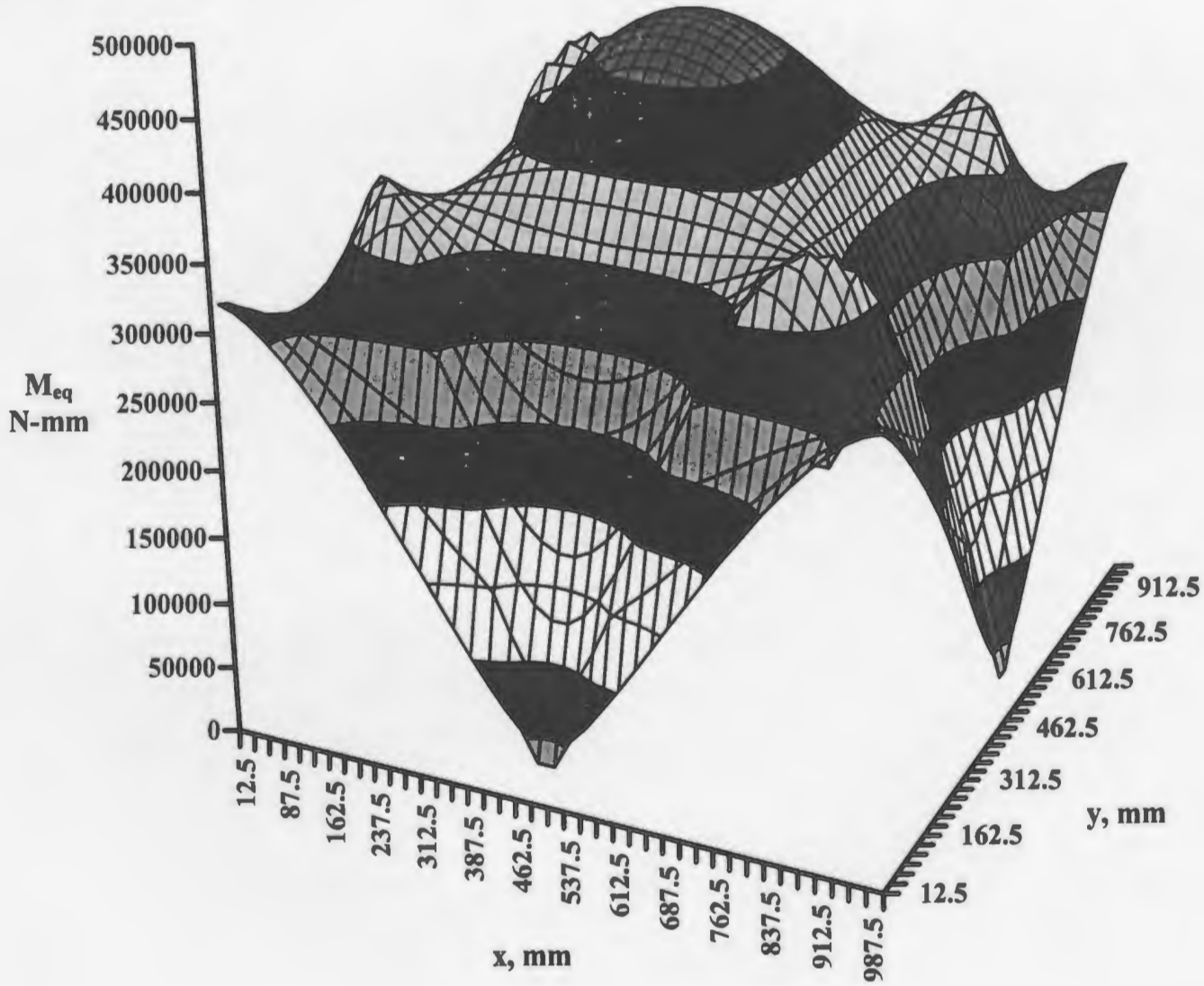

Fig. 4.6 Simply Supported Square Plate- UDL, Von Mises, First Analysis

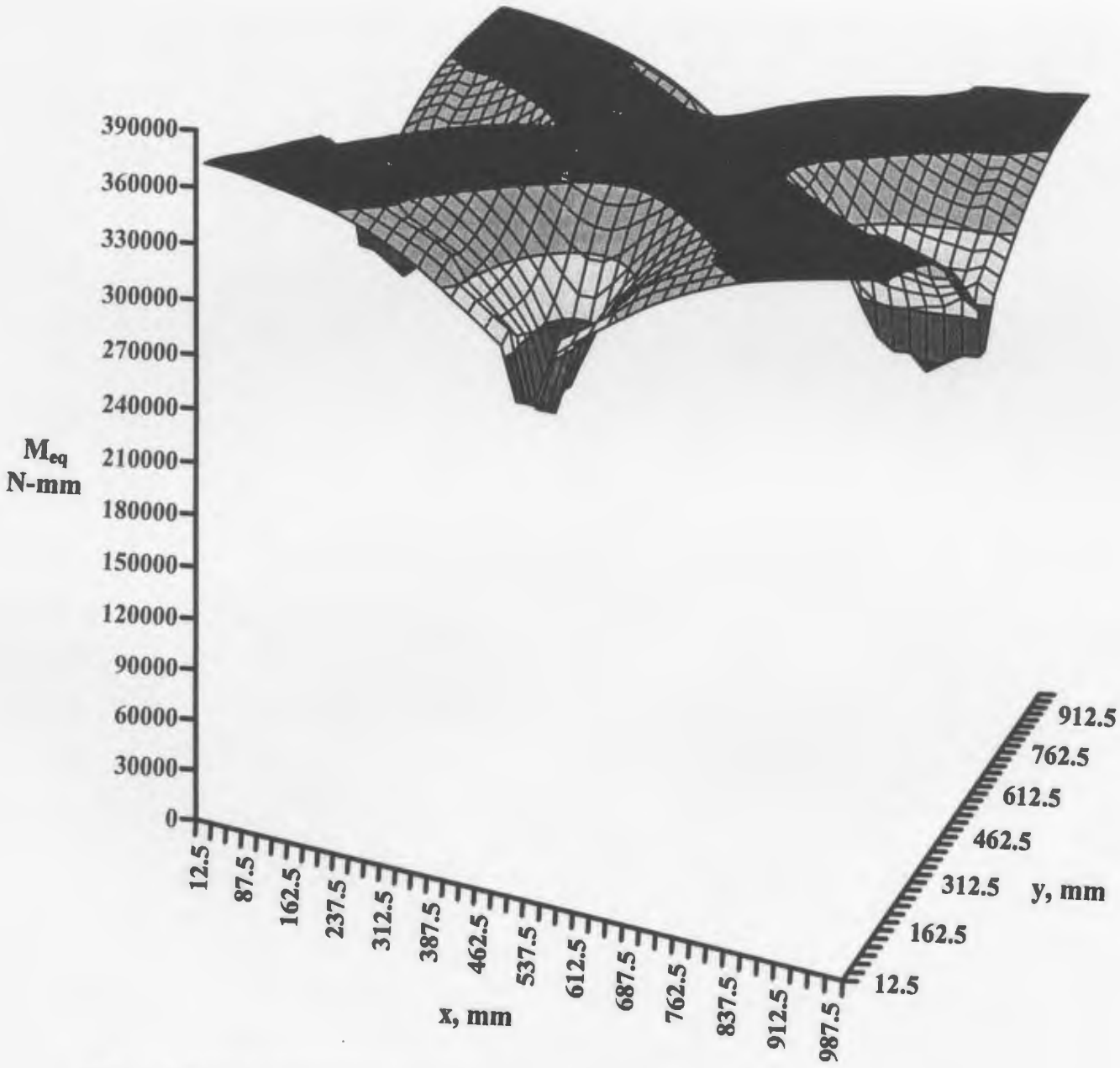

Fig. 4.7 Simply Supported Square Plate- UDL, Von Mises, Converged Analysis

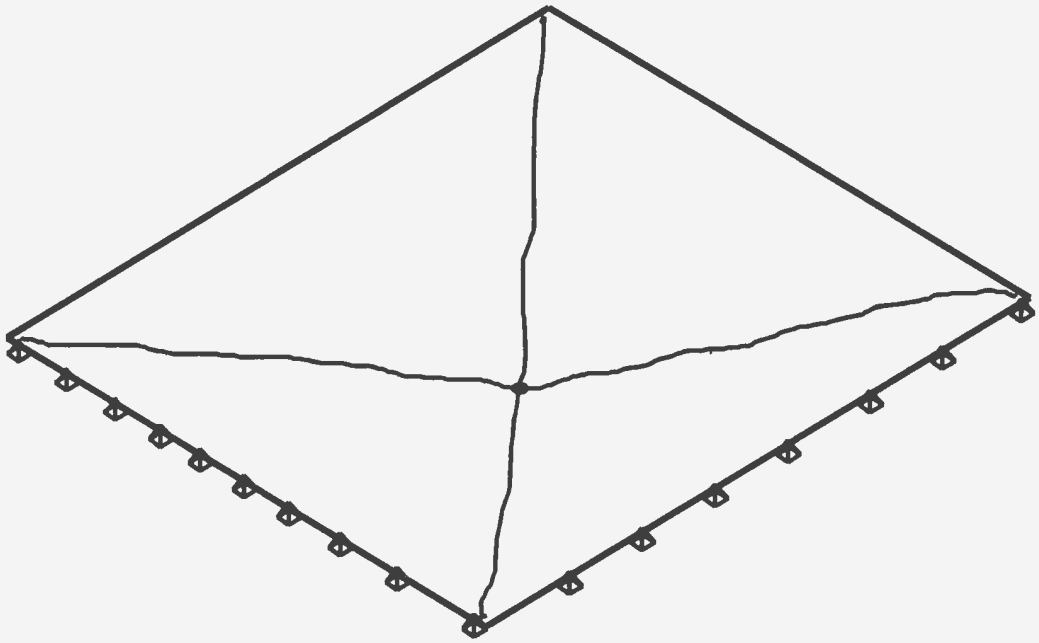

Fig. 4.8 Expected Collapse Mechanism for a Square Plate with Uniform Pressure

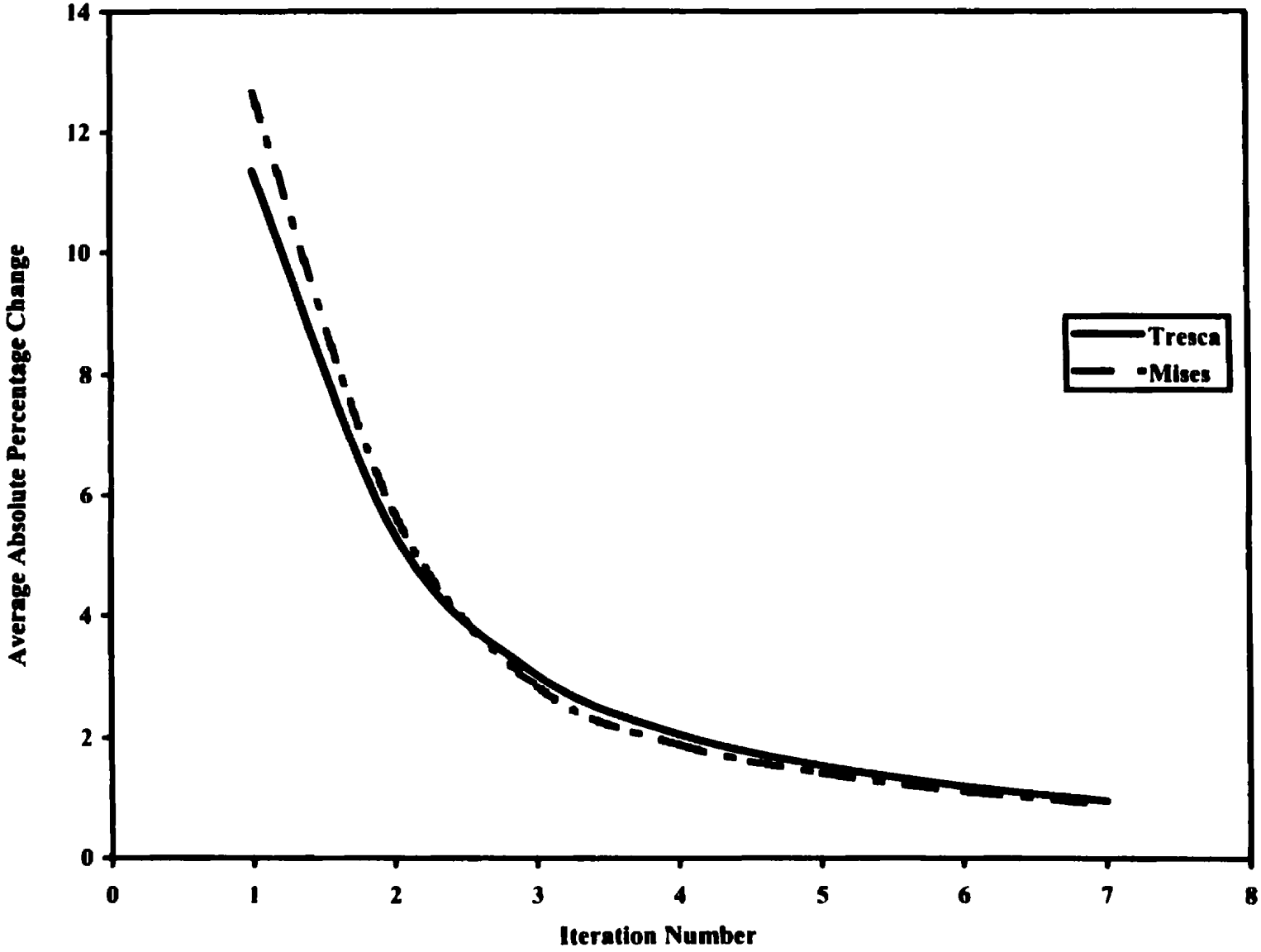

Fig. 4.9 Convergence of Analysis for a Simply Supported Square Plate with UDL

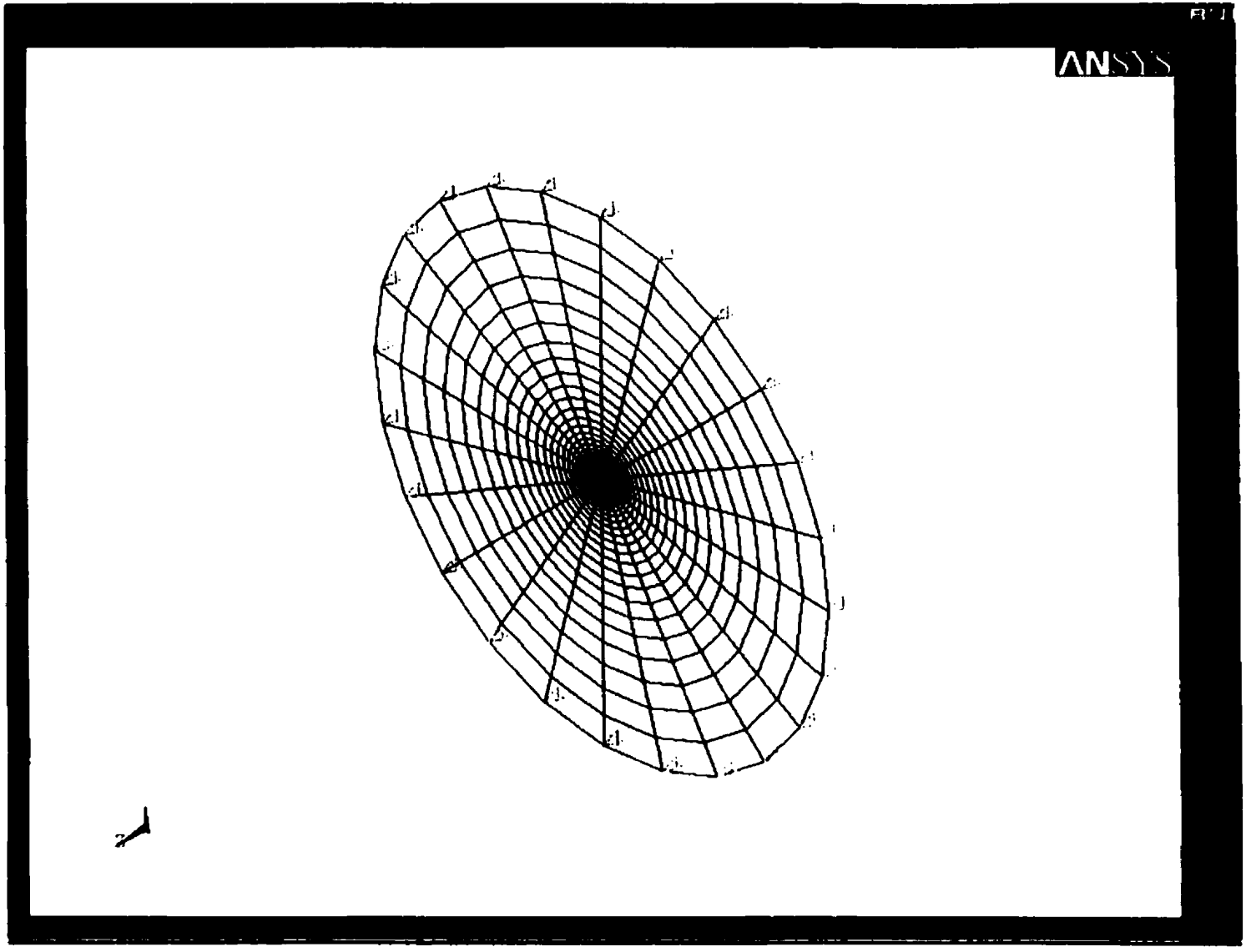

Fig. 4.10 Finite Element Model of a Circular Plate with UDL

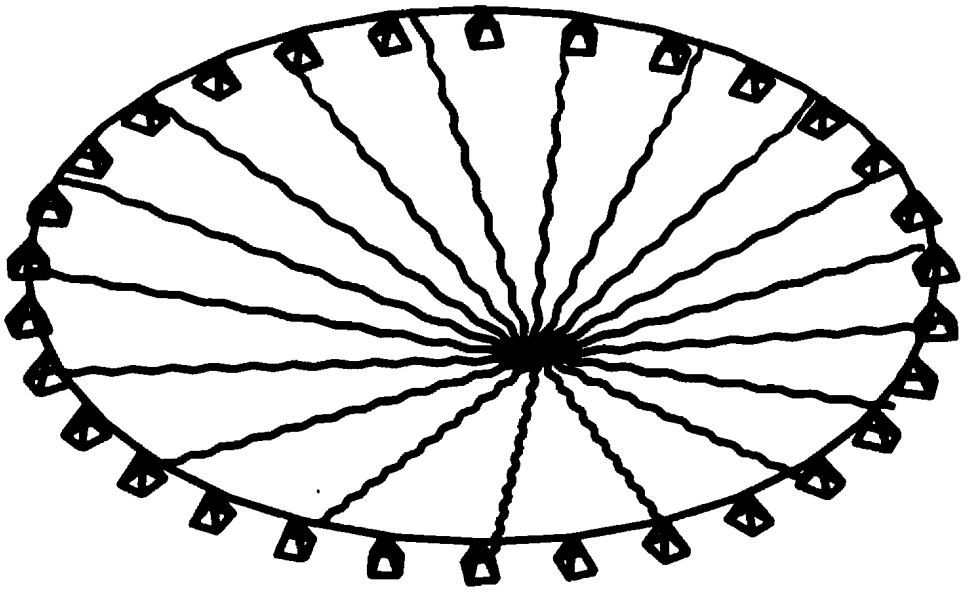

Fig. 4.11 Expected Collapse Mechanism for a Circular Plate with Uniformly Distributed Load

NOTE TO USERS

Page(s) not included in the original manuscript are unavailable from the author or university. The manuscript was microfilmed as received.

133-140

This reproduction is the best copy available.

UMI

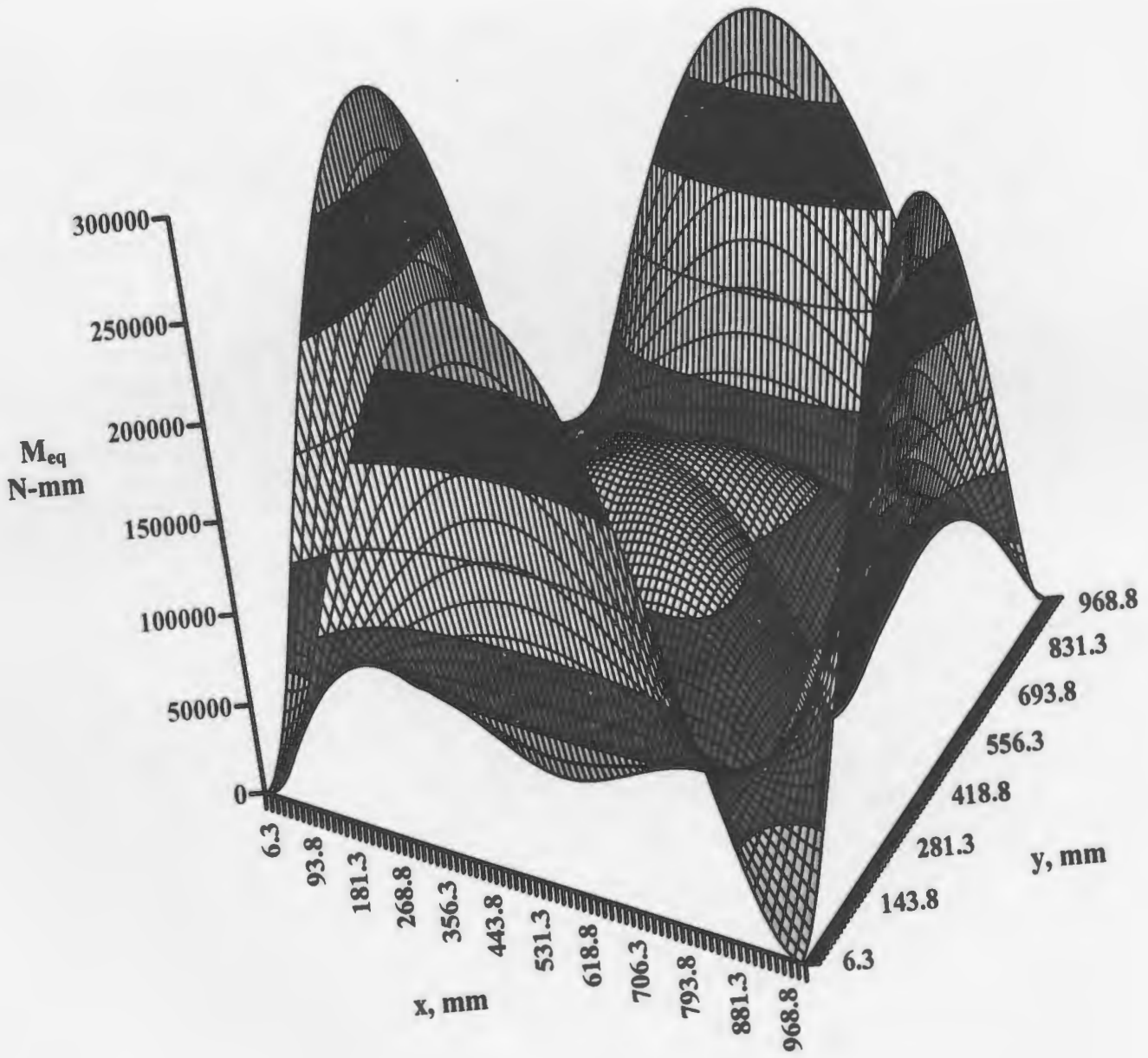

Fig. 4.20 Fixed Square Plate -UDL, Tresca, First Analysis

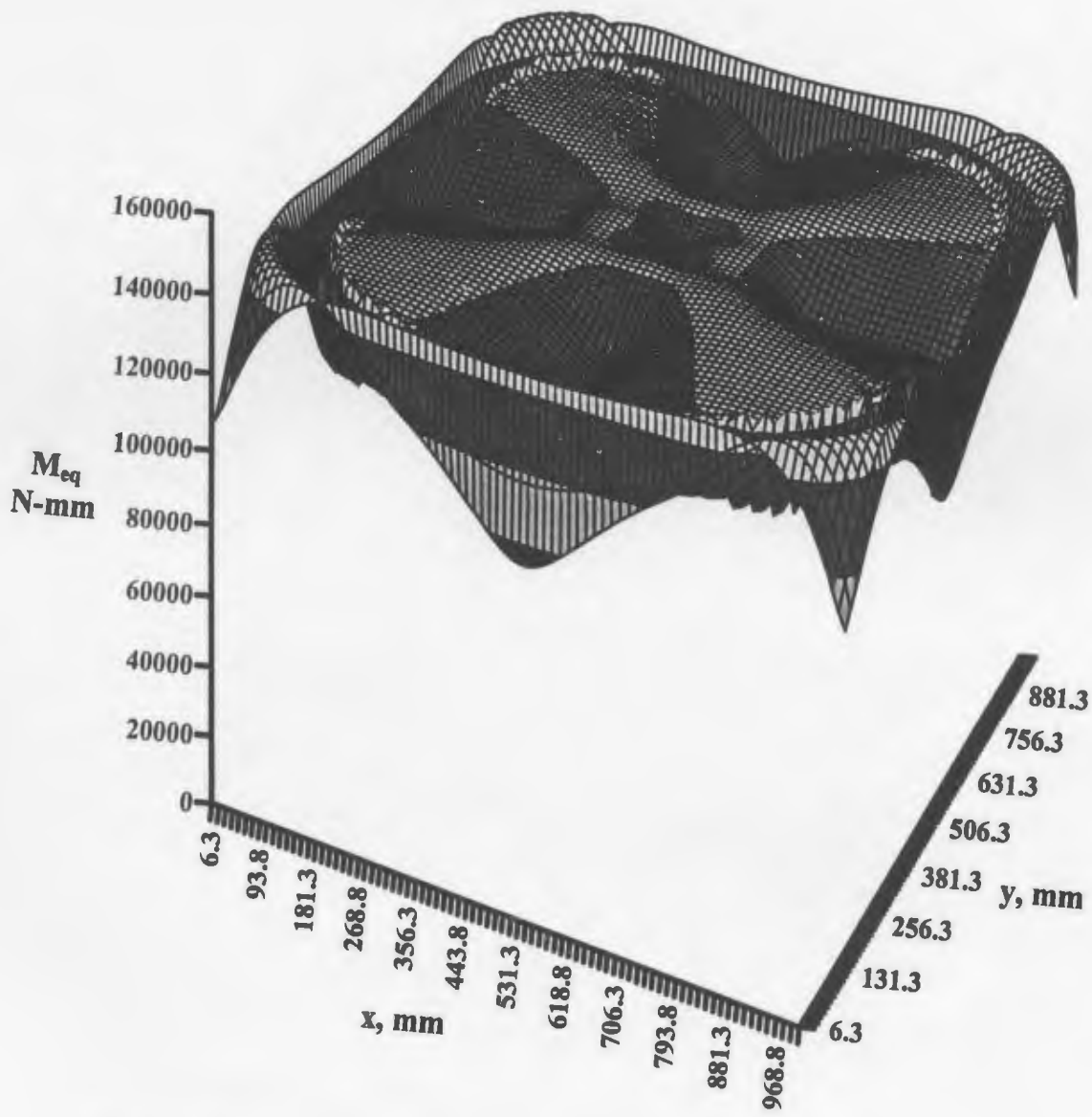

Fig. 4.21 Fixed Square Plate -UDL, Tresca, Converged Analysis

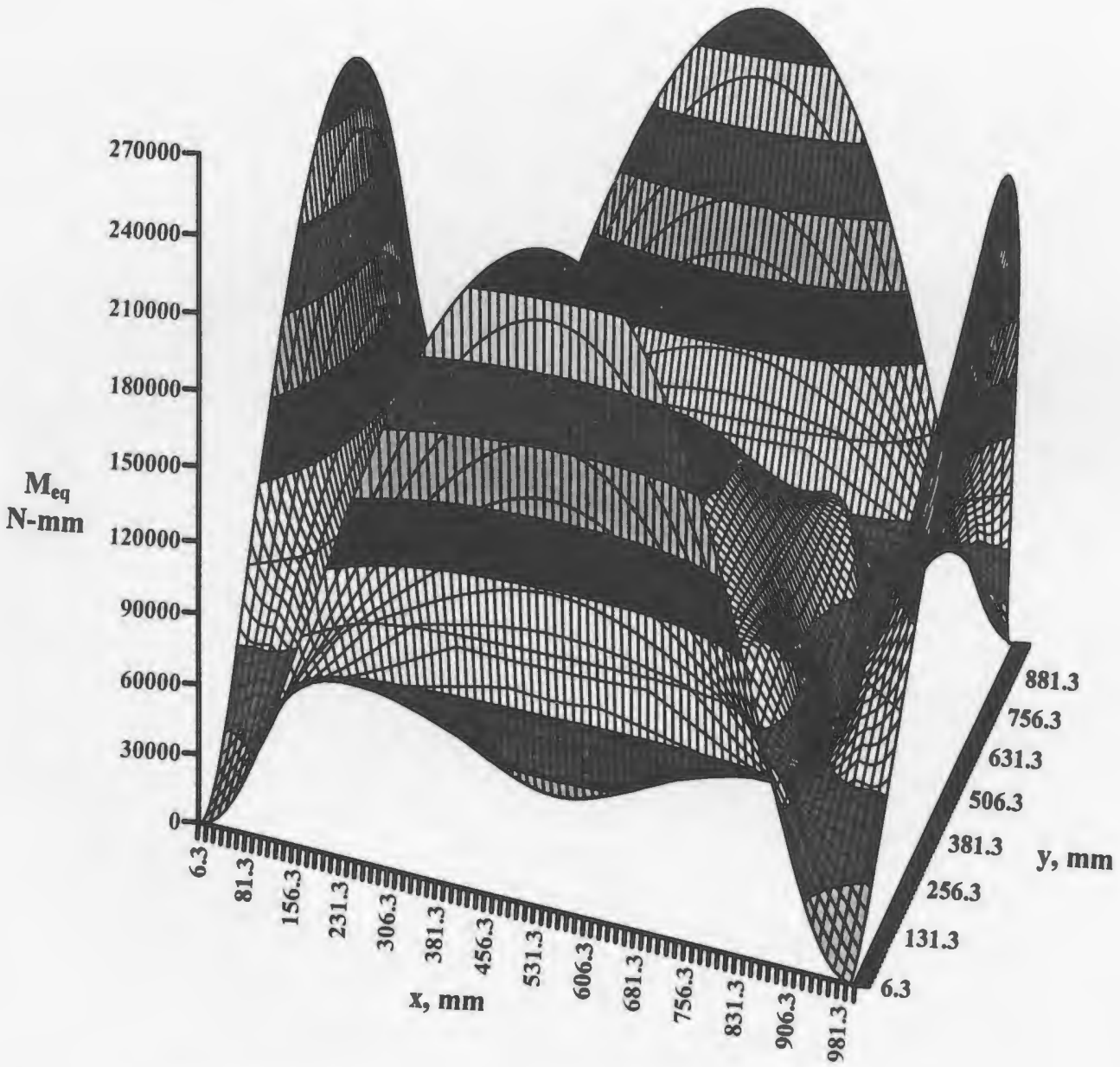

Fig. 4.22 Fixed Square Plate -UDL, Von Mises, First Analysis

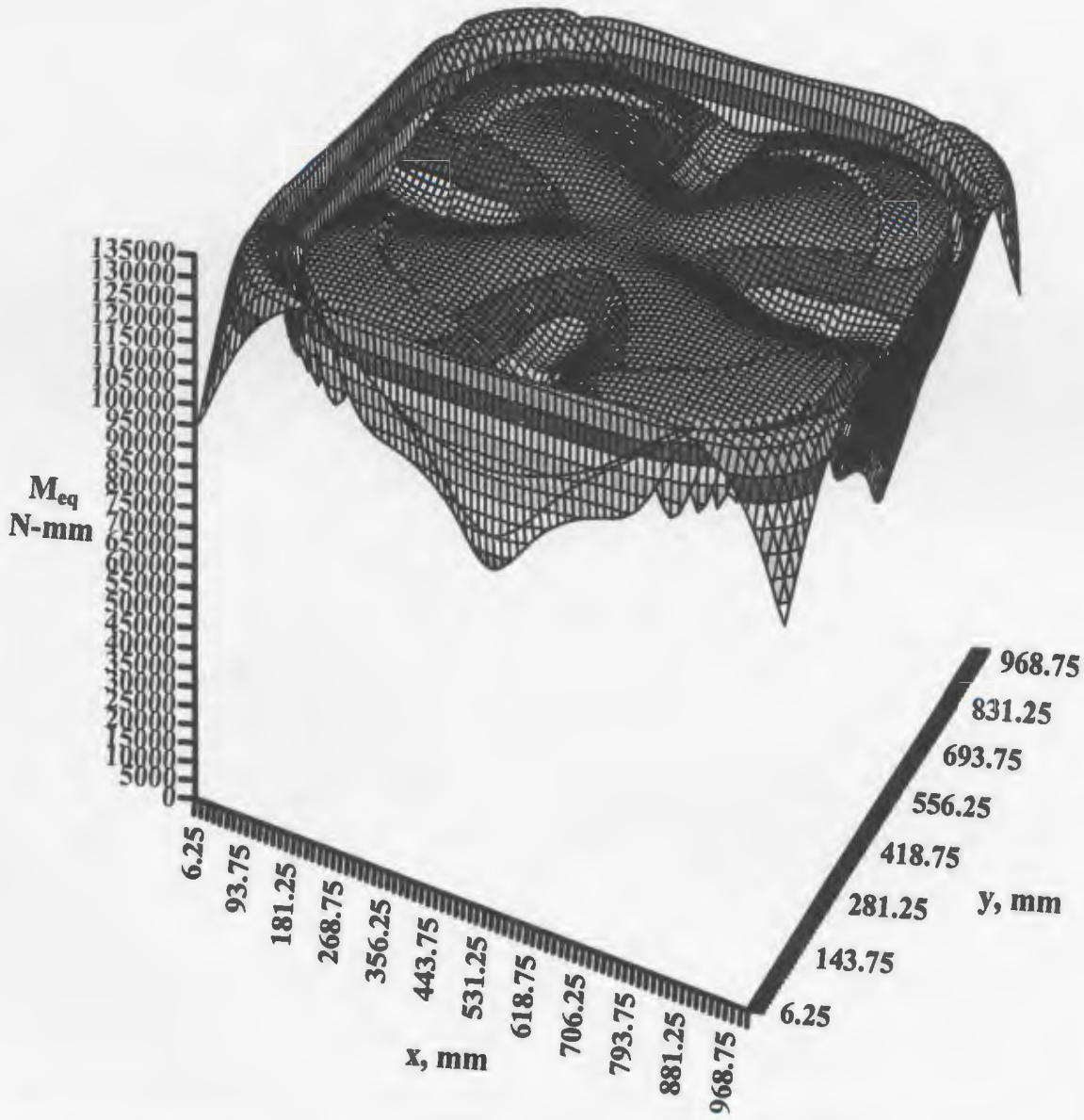

Fig. 4.23 Fixed Square Plate -UDL, Von Mises, Converged Analysis

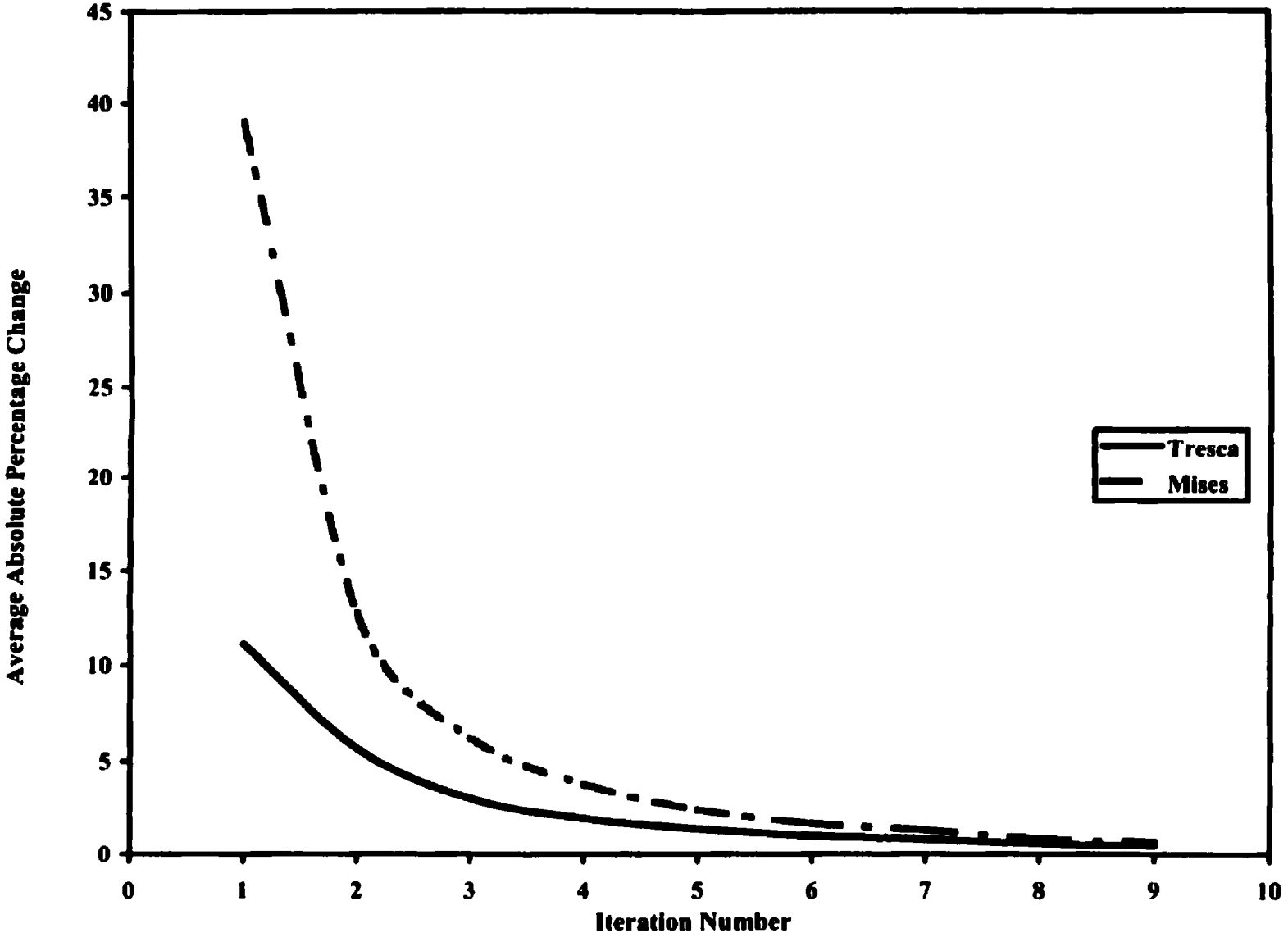

Fig. 4.24 Convergence of Analysis for a Fixed Square Plate with UDL

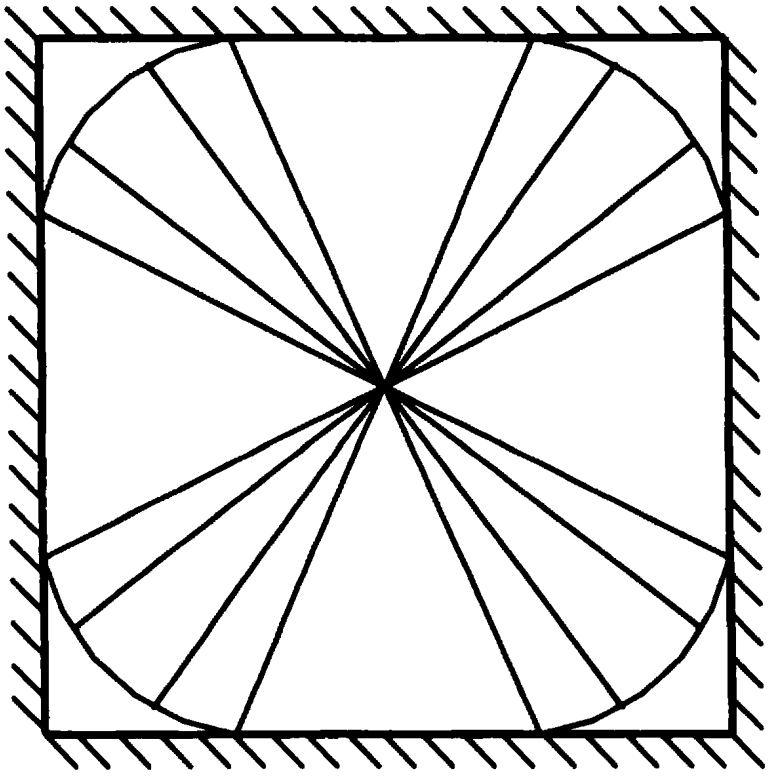

Fig. 4.25 Expected Collapse Mechanism for a Fixed Square Plate with Uniform Pressure

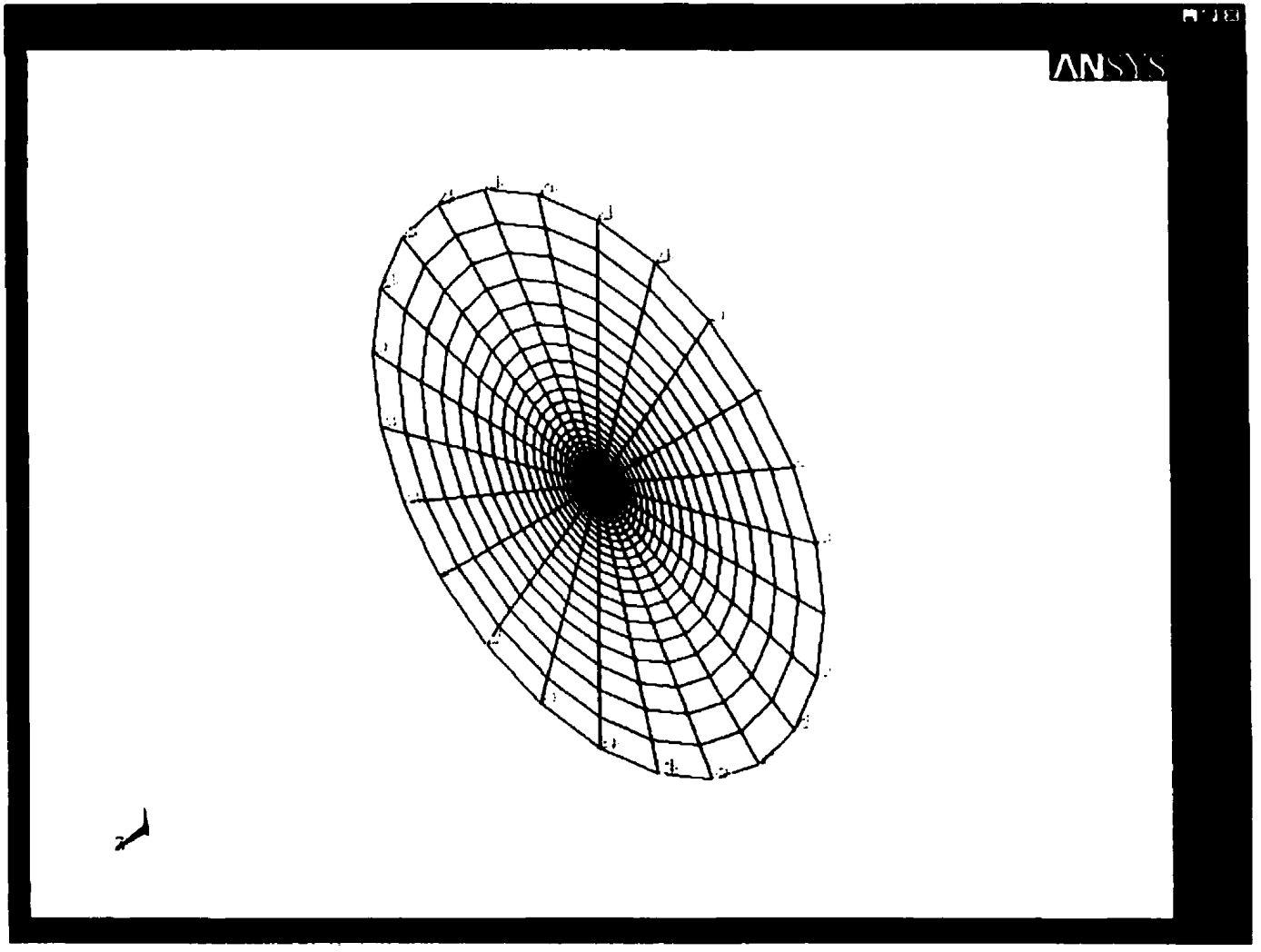

Fig.4.26 Finite Element Model of a Circular Plate with Central Concentrated Load

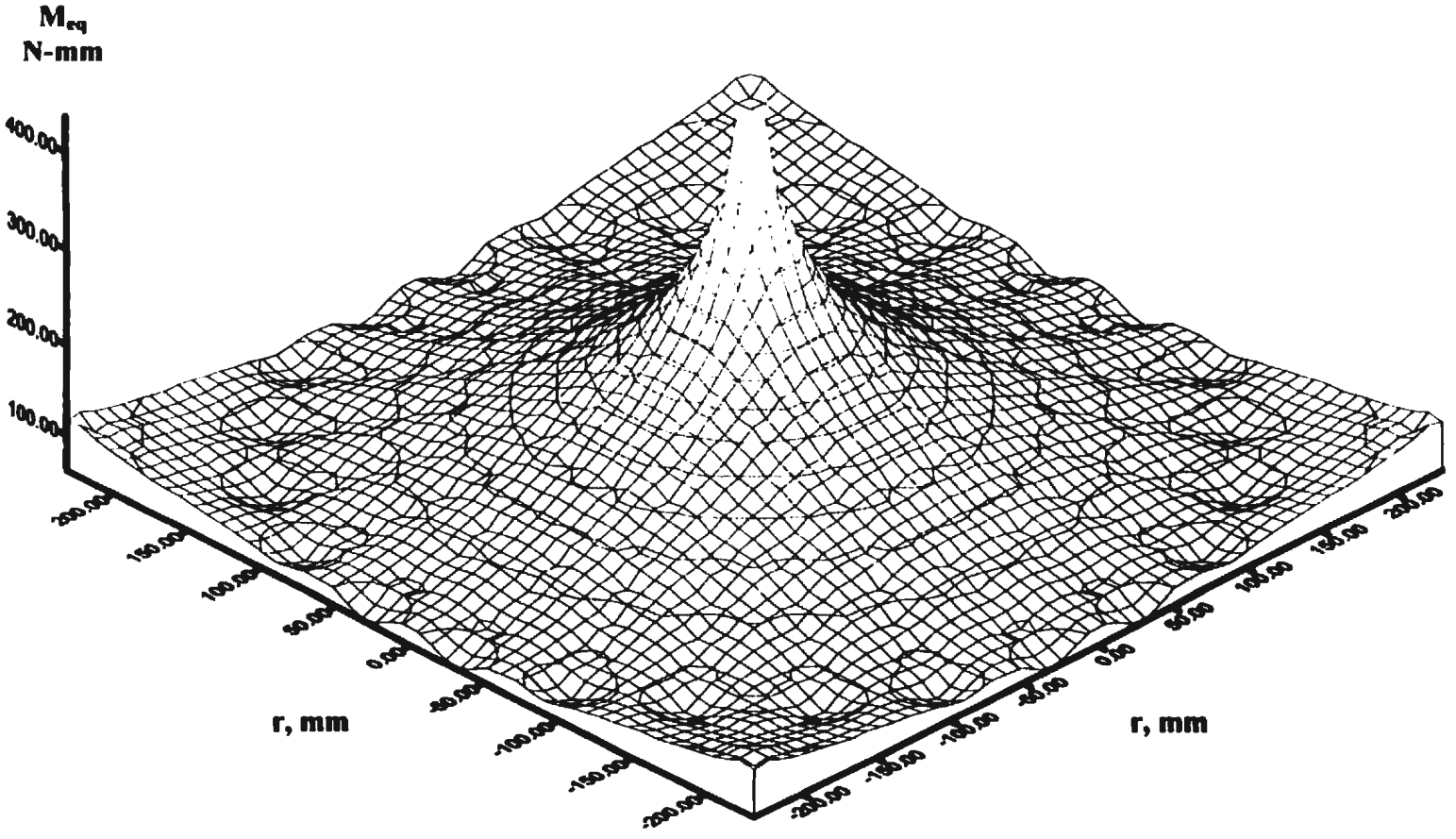

Fig. 4.27 Simply Supported Circular Plate -Central Concentrated Load, Tresca, First Analysis

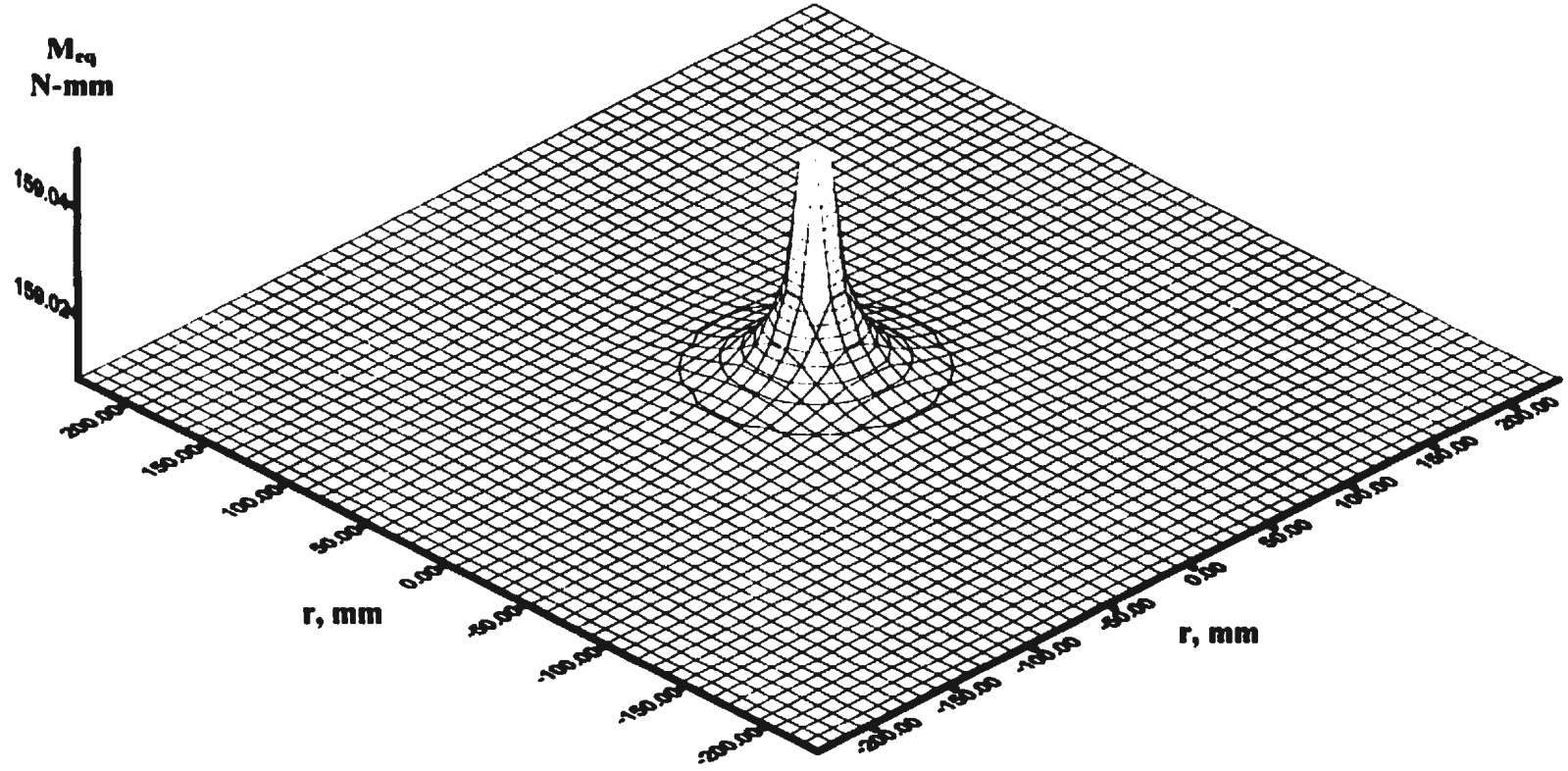

Fig. 4.28 Simply Supported Circular Plate -Central Concentrated Load, Tresca, Converged Analysis

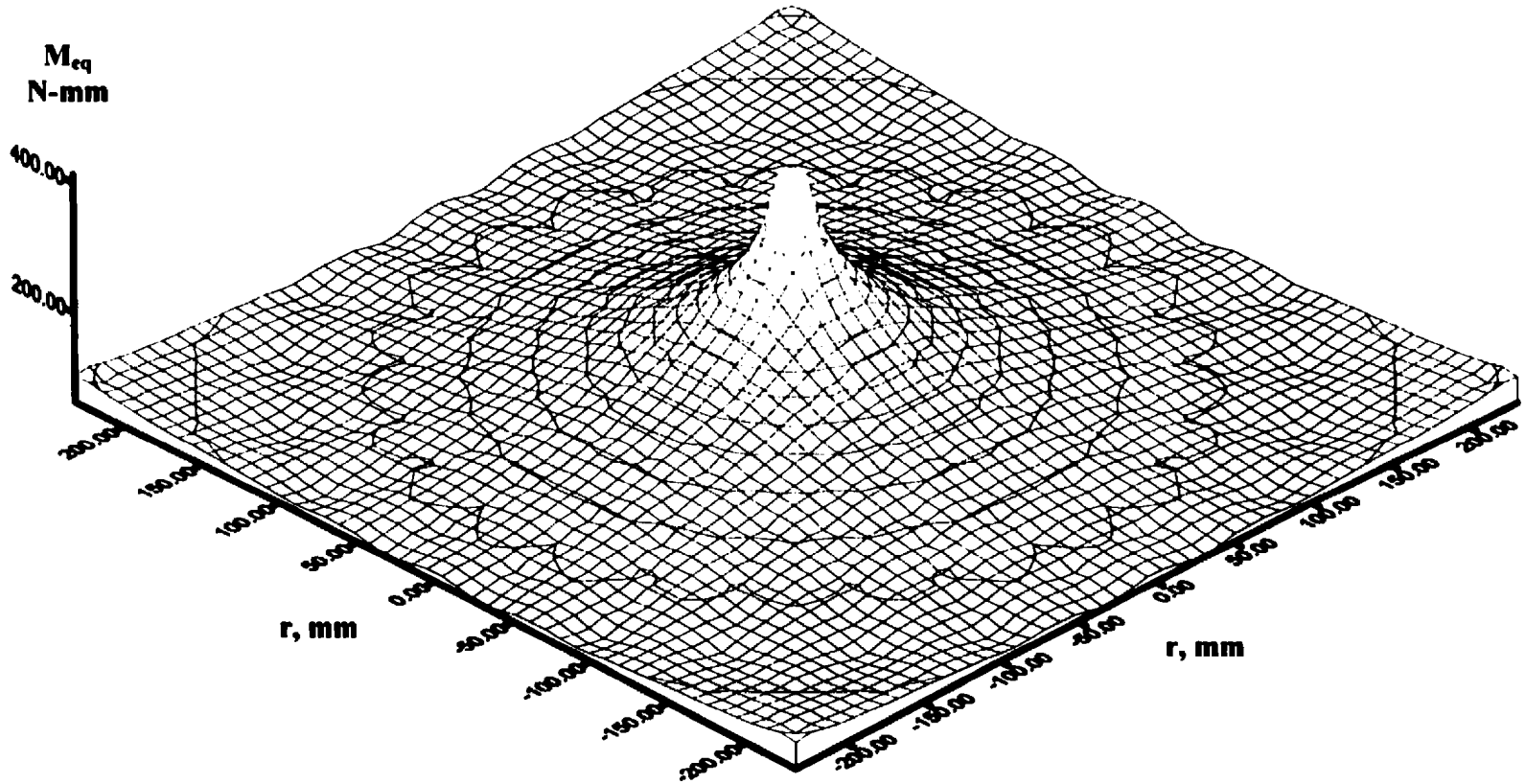

Fig. 4.29 Simply Supported Circular Plate -Central Concentrated Load, Von Mises, First Analysis

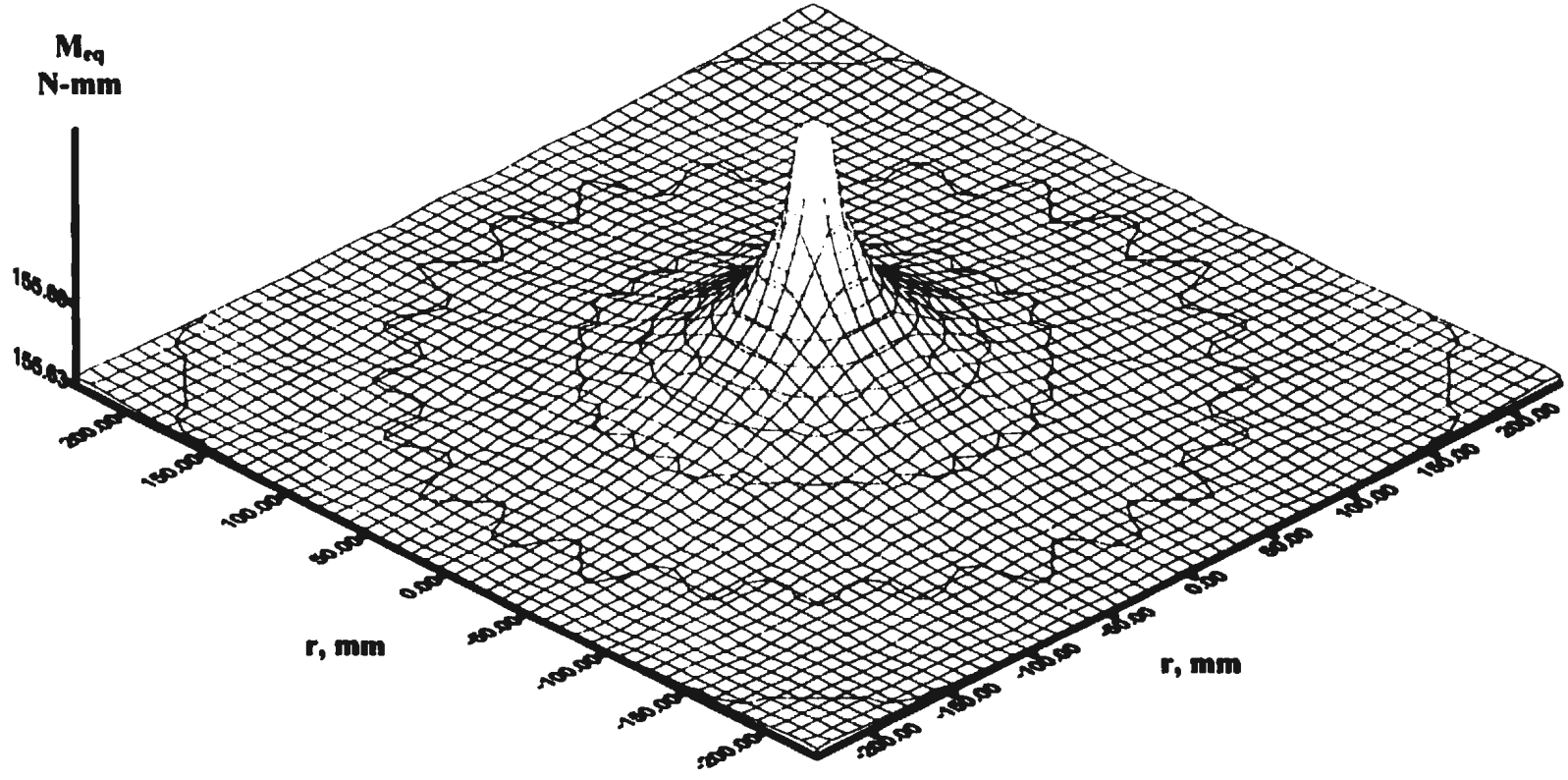

Fig. 4.30 Simply Supported Circular Plate -Central Concentrated Load, Von Mises, Converged Analysis

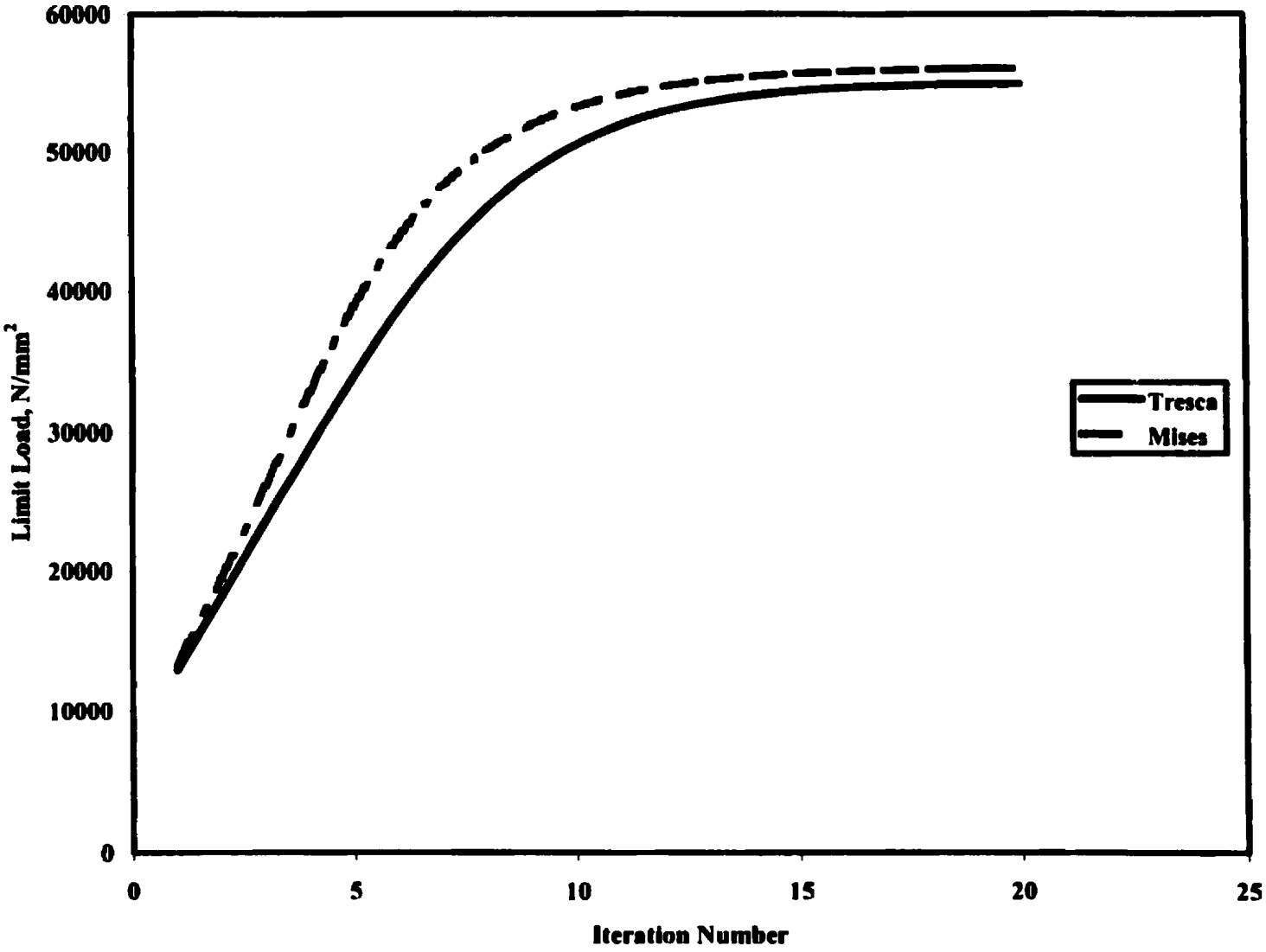

Fig. 4.31 Convergence of Analysis for a Simply Supported Circular Plate with Central Concentrated Load.

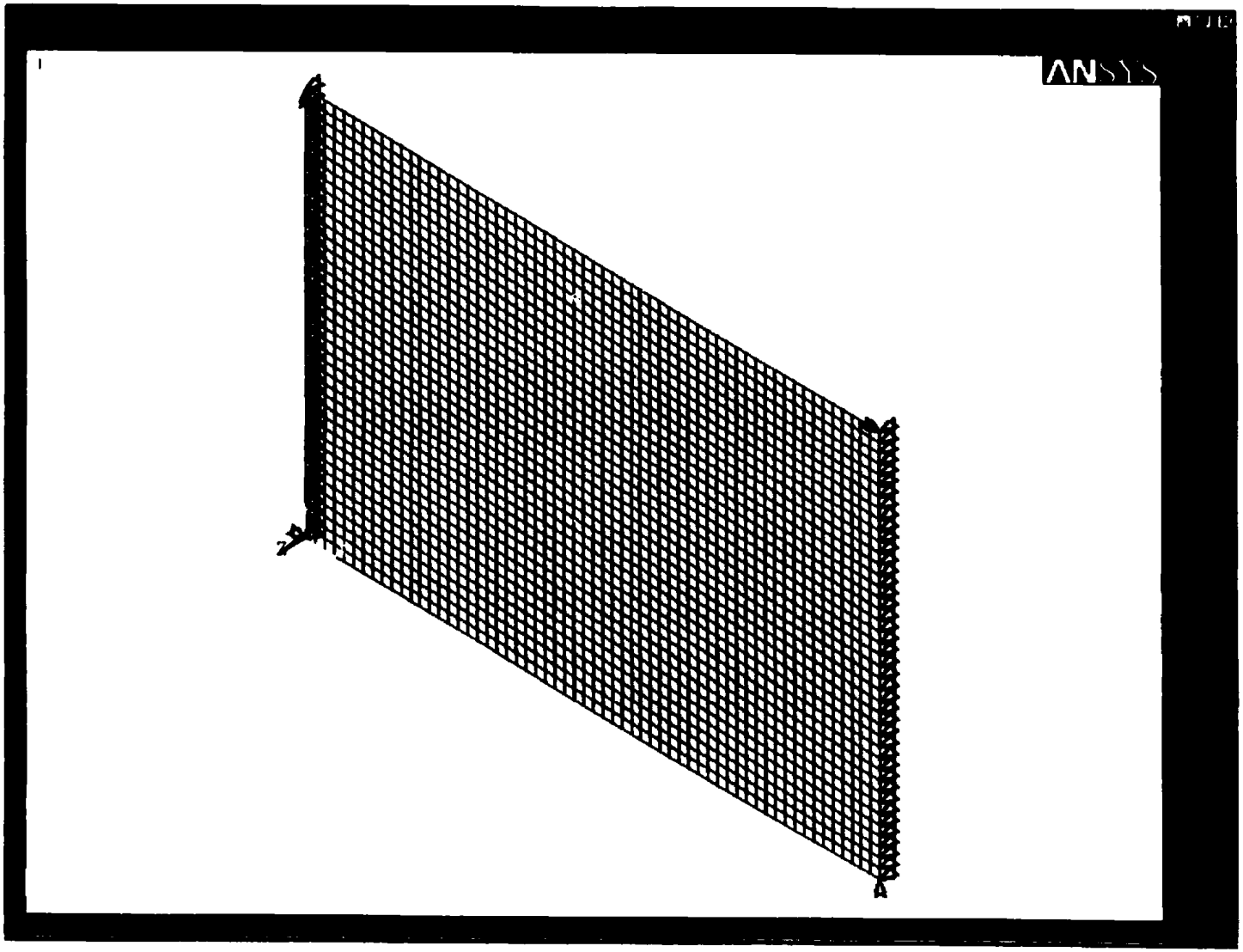

Figure 4.32 Finite Element Model of a Rectangular Plate Simply Supported on Opposite Sides with UDL

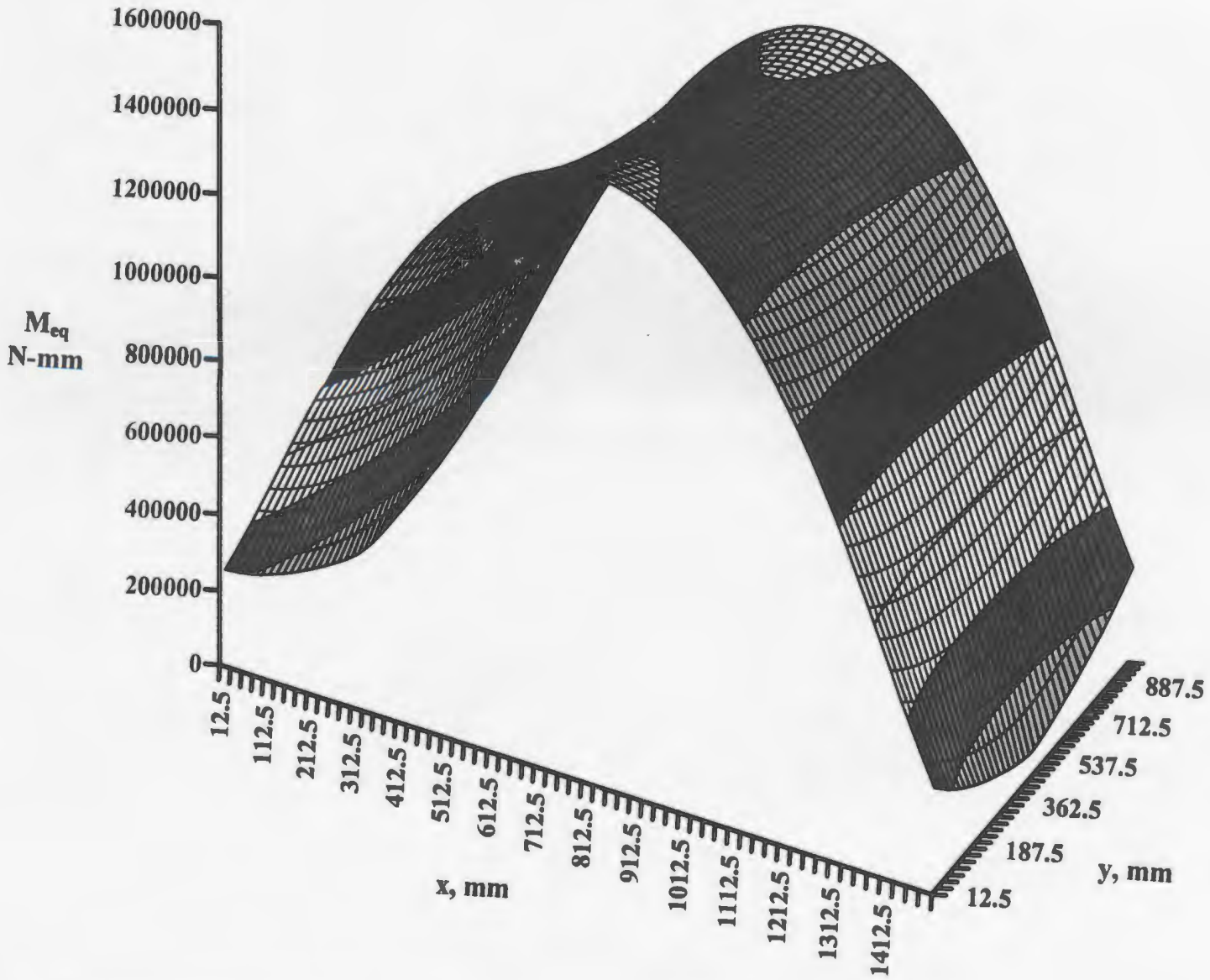

Figure 4.33 Rectangular Plate Simply Supported on Opposite Sides -UDL, Tresca, First Analysis

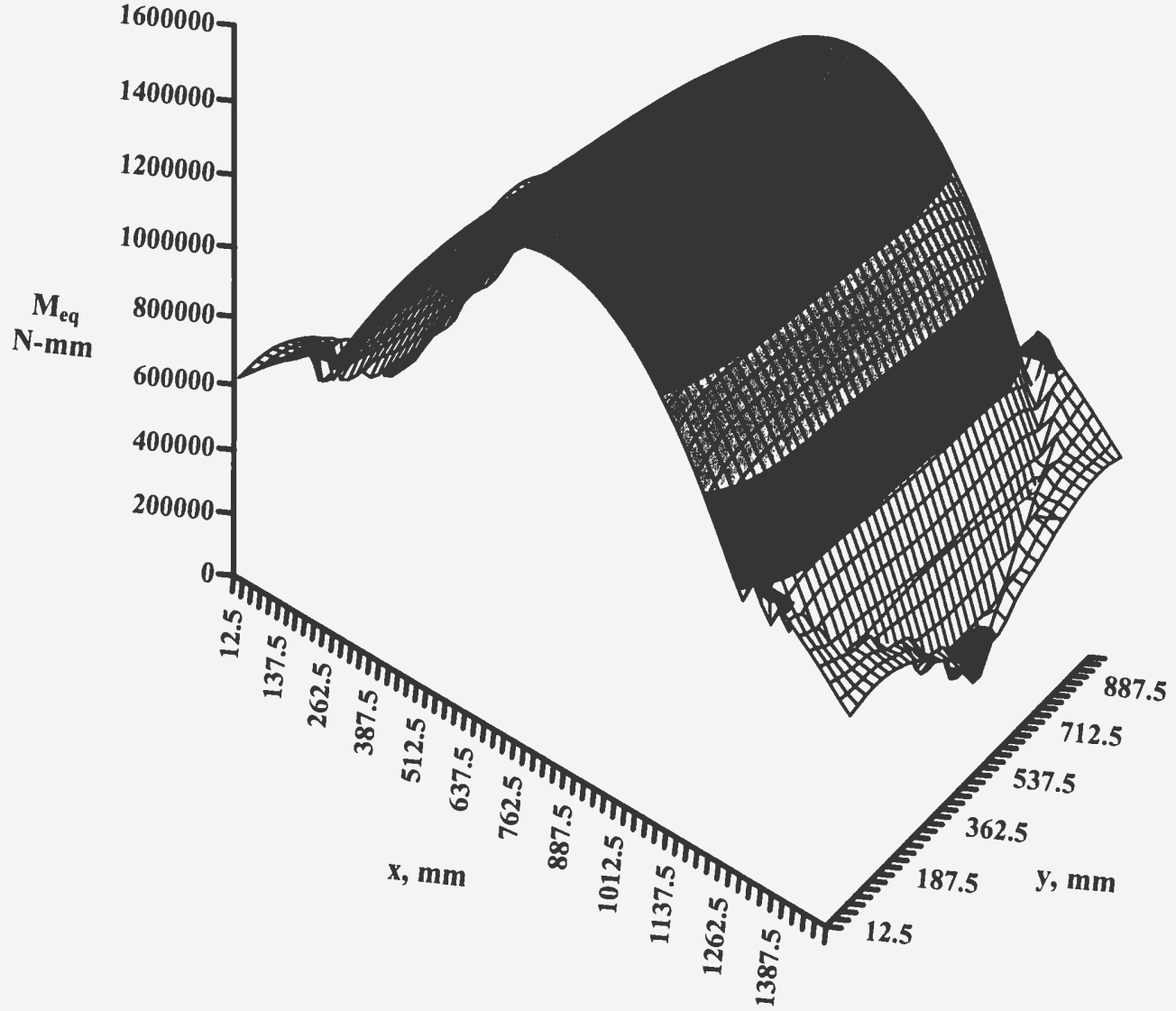

Figure 4.34 Rectangular Plate Simply Supported on Opposite Sides – UDL, Tresca, Converged Analysis

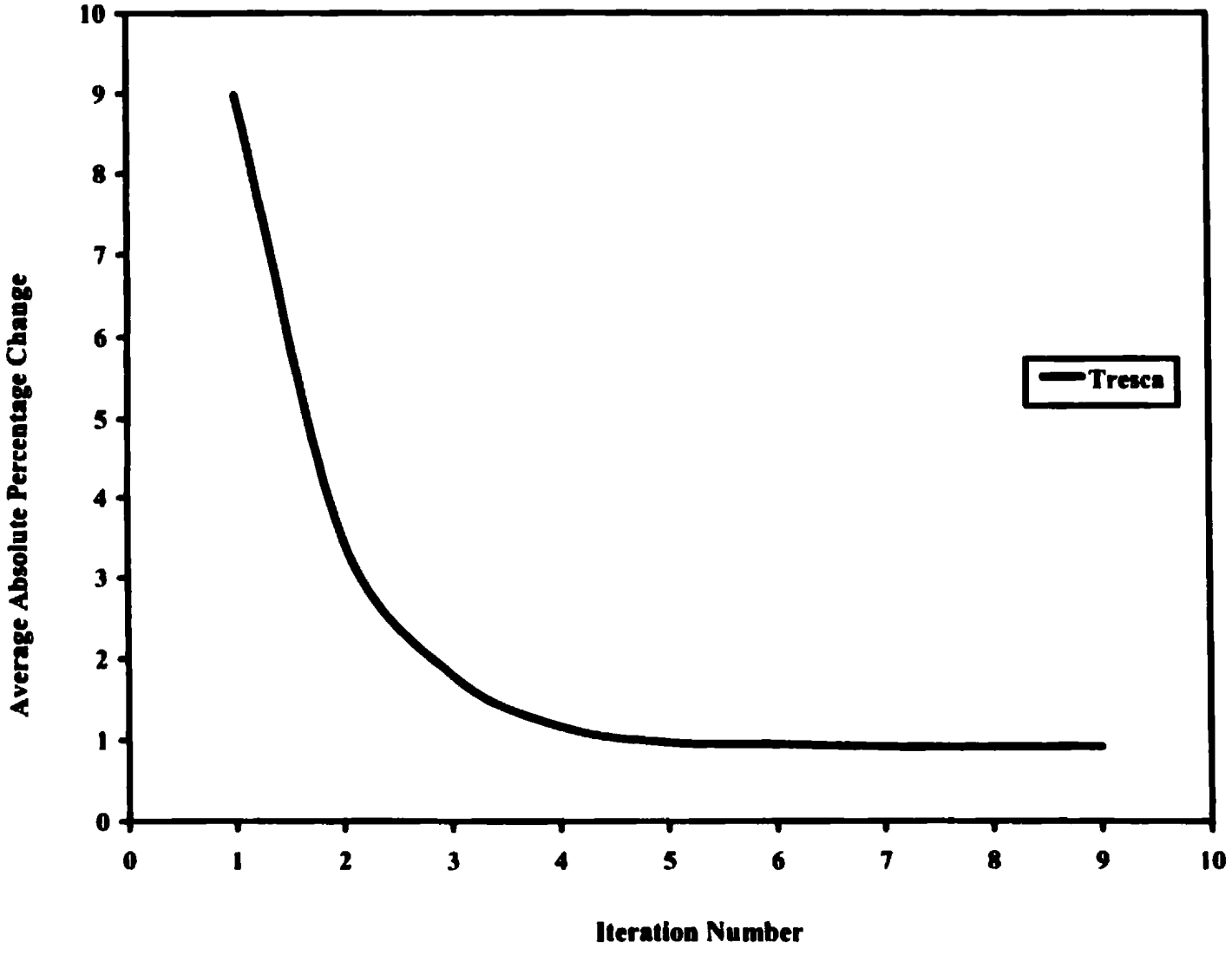

Figure 4.35 Convergence of Analysis for a Rectangular Plate Simply Supported on Opposite Sides

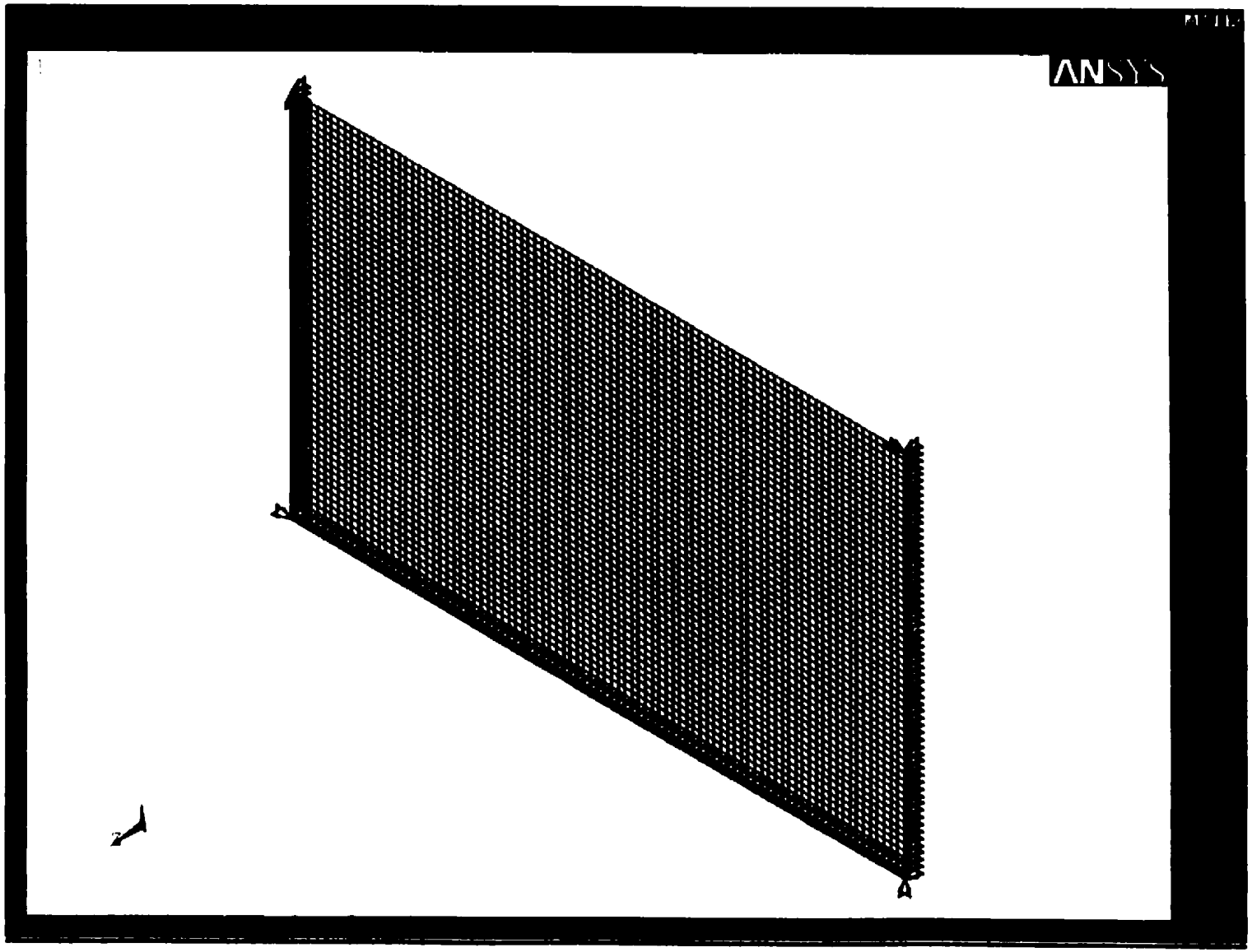

Figure 4.36 Finite Element Model of a Rectangular Plate Simply Supported on Three Sides with UDL

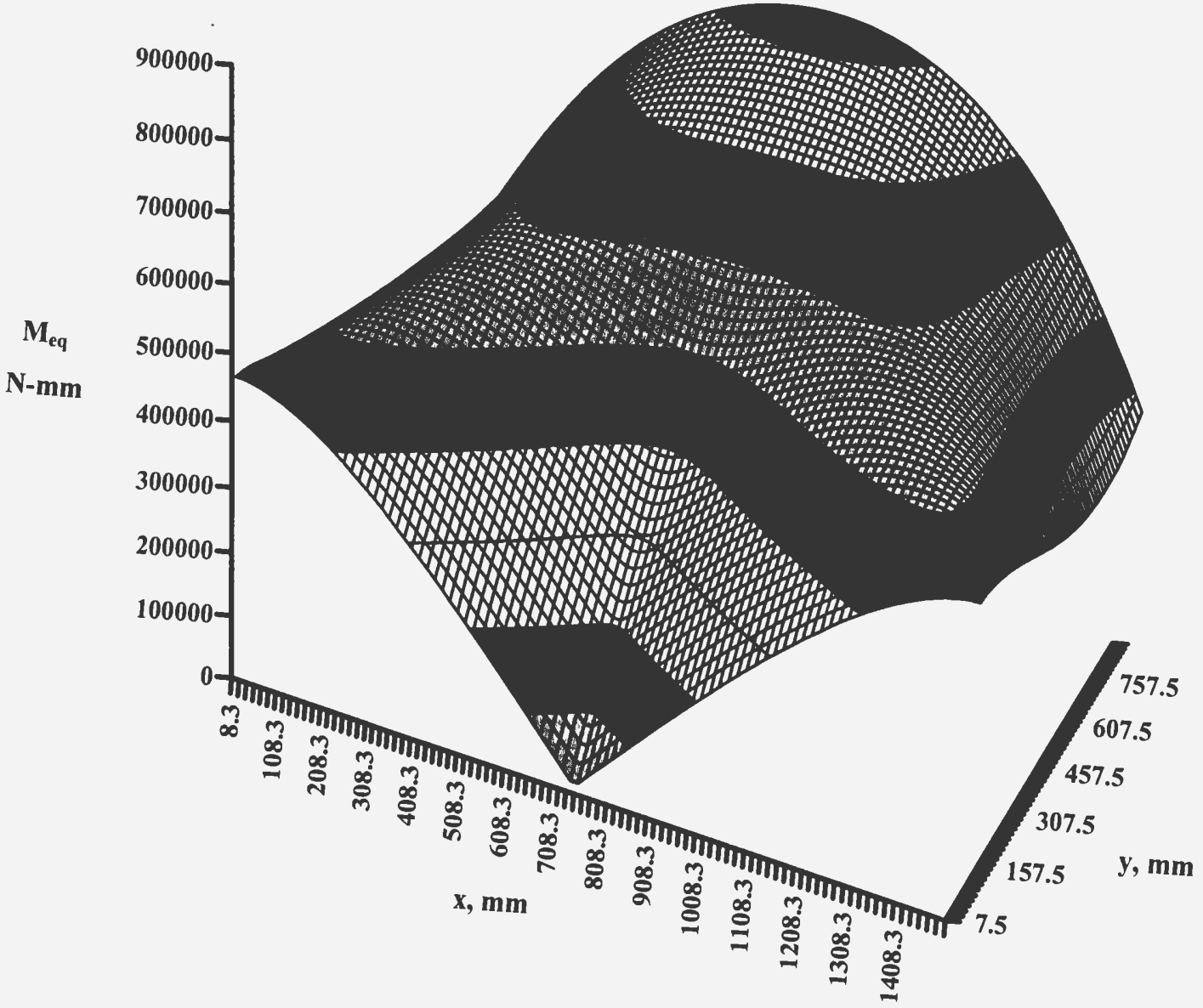

Figure 4.37 Rectangular Plate Simply Supported on Three Sides -UDL, Tresca, First Analysis

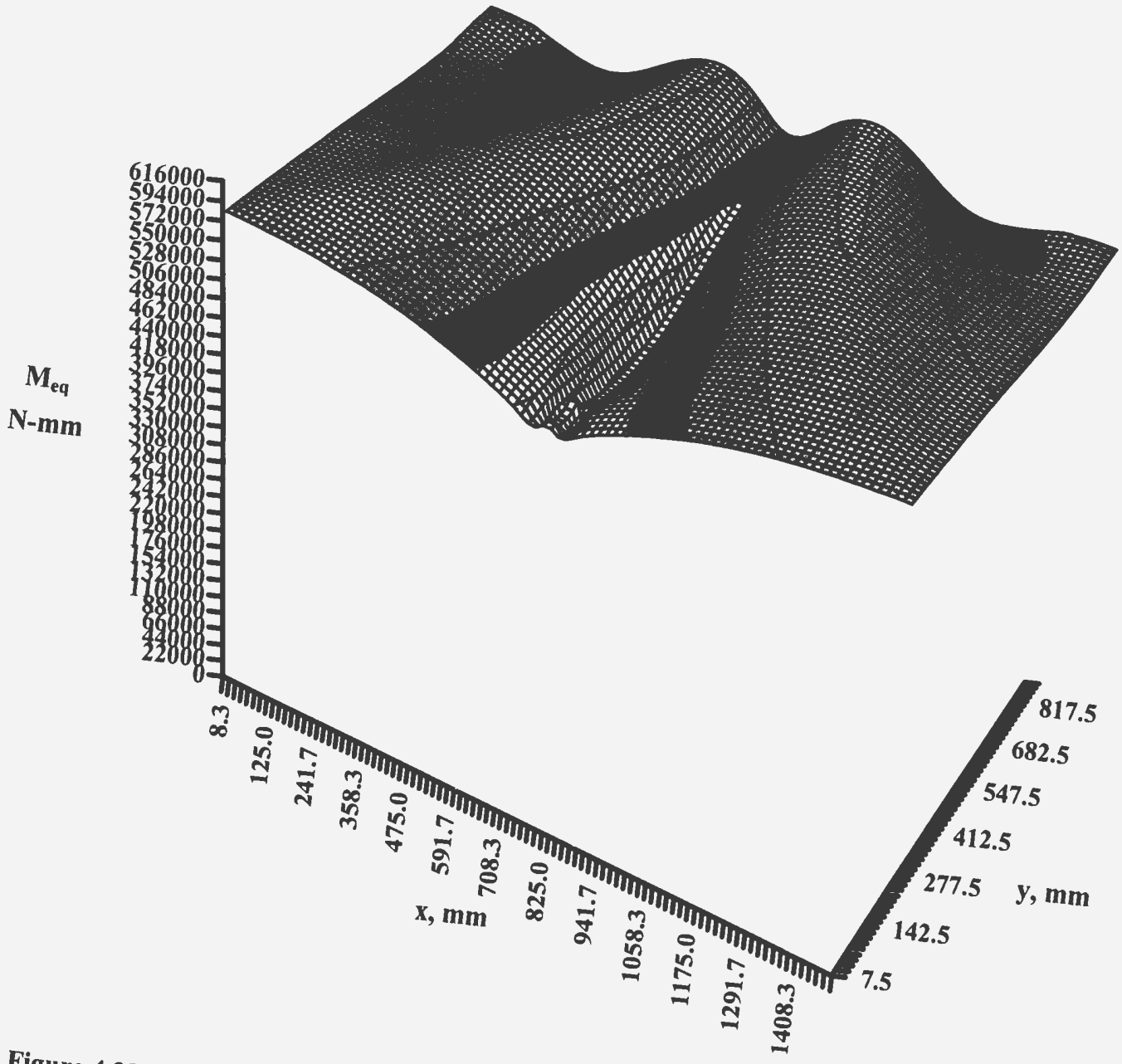

Figure 4.38 Rectangular Plate Supported on Three Sides – UDL, Tresca, Converged Analysis

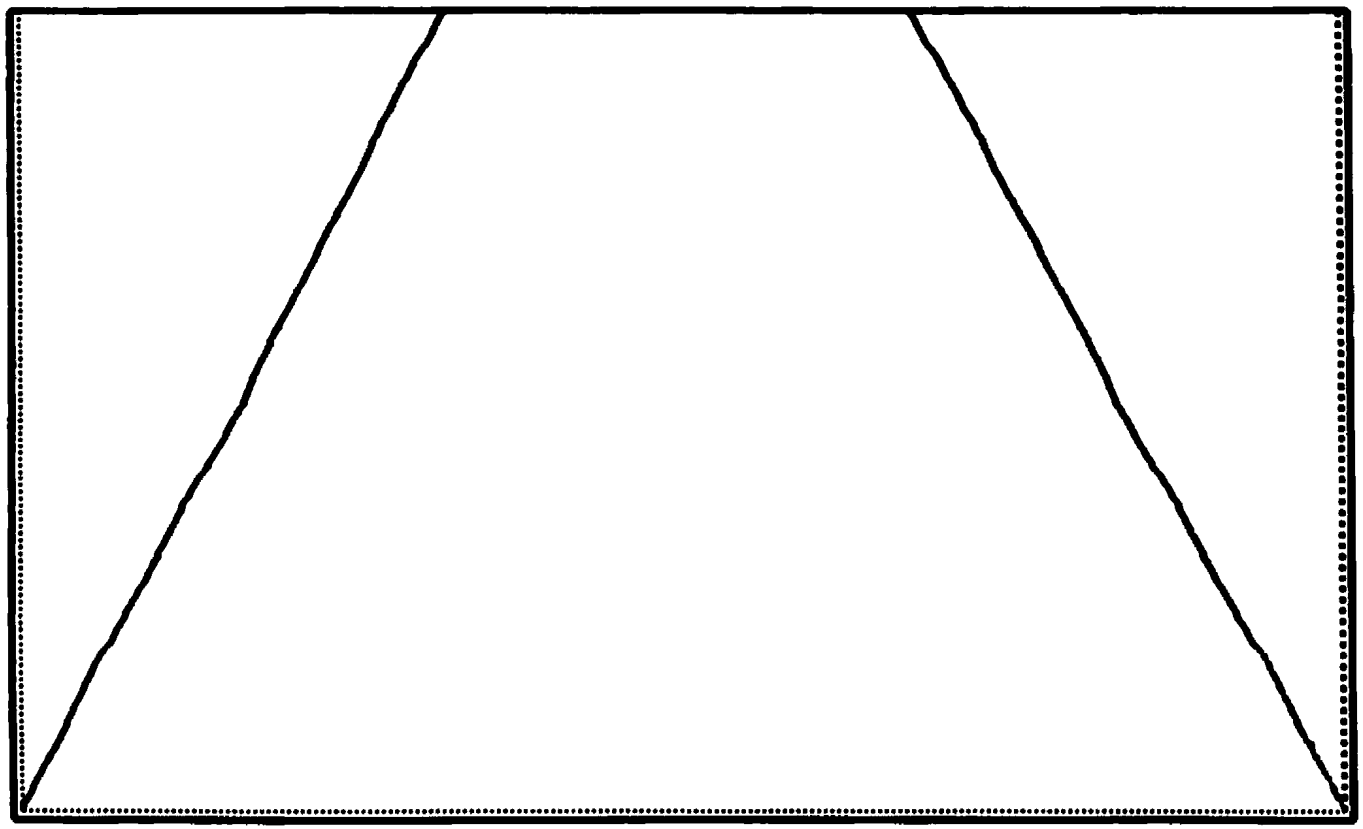

Fig. 4.39 Expected Collapse Mechanism for a Rectangular Plate Supported on Three sides under UDL

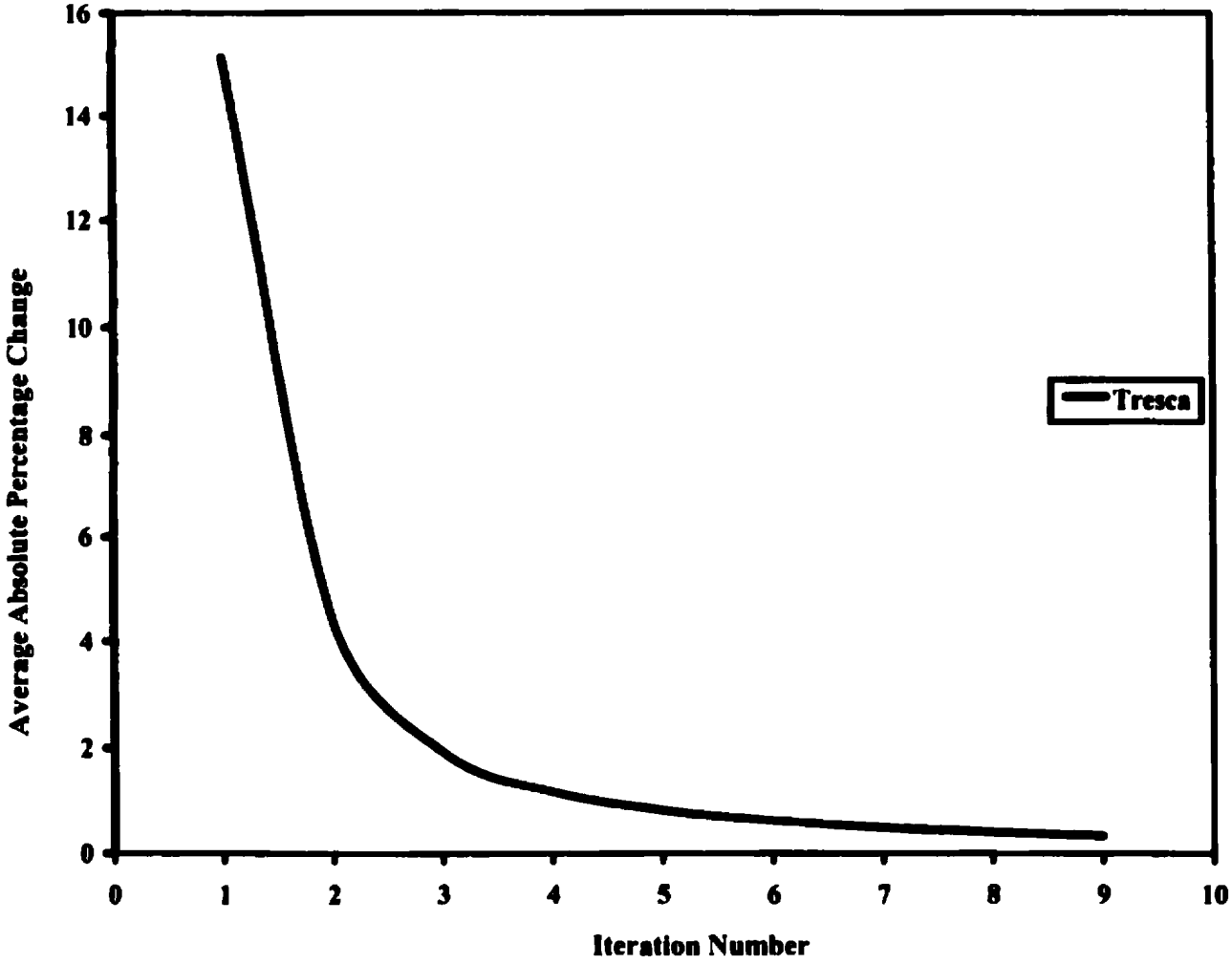

Figure 4.40 Convergence of Analysis for a Rectangular Plate Simply Supported on Three Sides

Chapter 5

Limit Analysis of Irregular Plate Structures

5.1 Introduction

The previous chapter dealt with plates of regular shape such as square, circle and rectangle with different boundary and loading conditions. The present chapter deals with a rectangular plate with partial boundary conditions, an irregularly shaped plate and a continuous plate. Since theoretical results are not readily available to compare with, a non-linear finite element analysis was conducted for some of the problems.

5.2 Rectangular Plate with Partial Boundary Conditions

A 254×381×12.7 mm plate was chosen with non uniform boundary conditions as shown in Fig. 5.1 (a). The problem is similar to that used by Mangalaramanan [1993, Sec. 5.11]. An arbitrary uniform pressure of 5 N/mm^2 is applied on the plate. The plate material has a yield stress of 207 MPa and Young's modulus of 207,000 MPa.

ANSYS element Shell 63 was chosen for the analysis. The analysis was initially conducted for a mesh grid of 18×12 and then increased to 42×27 and 84×54. The finite element model for the 84×54 mesh is shown in Fig. 5.1 (b). The Von Mises yield criterion for moments as defined in Chapter 3 was used. The rigidity modification and

re-analysis was conducted till satisfactory convergence was achieved. The input file listing along with the macro, which performs the post-analysis is given in Appendix A.2.1.

5.2.1 Limit Load

The equivalent moment distribution after the first analysis is shown in Fig 5.2. It shows relatively high magnitudes of moments at the fixed edges and discontinuity points. A spike can be seen in the lower left side of the plot, which is a possible numerical error because of local numerical error. The region between the clamped edge to simply supported edge has a parabolic variation of equivalent moment. However, after re-analysis and convergence, moment at all former peaks is flattened and is nearly equal as shown in Fig 5.3. Fourteen iterations led to convergence. The yield lines were identified in a manner similar to that for a fixed square plate described in Chapter 4. The value of average equivalent moment along yield lines was considered. The average absolute percentage change at the end of each iteration is noted and this is plotted in Fig. 5.4.

5.2.2 Comparison of Results

The limit load value obtained above was compared with that from non-linear finite element analysis as obtained by Mangalaramanan [1993]. The limit load for various mesh sizes was calculated and this is tabulated in Table 5.1. The input file for the analysis is given in Appendix C.1.1.

From Table 5.1, it can be seen that the difference between the present result and nonlinear FEA is 8.9%. This is quite high compared to the very low errors obtained for all the previous cases when compared to the closed form theoretical results. Part of the reason must be the fact that nonlinear FEA gives inaccurate results. This can be seen from the comparison made in Table 4.1. The nonlinear FEA for the simply supported square plate under UDL gave an error of 10.5%. If a similar error is present in the nonlinear FEA analysis reported in Table 5.1, it would explain the discrepancy between the secant rigidity method and the nonlinear FEA for the present problem. The same problem solved as a full model using solid elements with r-node method was reported to have an error of -6.6% [Mangalaramanan, 1993] compared to non-linear Finite element analysis. This needs to be contrasted with the more than 10% errors that he obtained for other regular plates problems.

5.3 Irregular Plate

A plate that is irregular in shape and boundary conditions shown in Fig. 5.5 (a) is analyzed in this section. Since theoretical results are not readily available to compare with, a non-linear finite element analysis was carried out. The thickness of the plate is 10 mm. An arbitrary uniform pressure of 5 N/mm^2 is applied on the plate. The plate material has a yield stress of 350 MPa and Young's modulus of 200,000 MPa.

ANSYS Shell 93 element was chosen for the analysis. The finite element model for the analysis consists of 5962 elements and 18261 nodes (Fig. 5.5 (b))

The Tresca yield criterion was chosen for the analysis. The input file listing along with the macro, which performs the post-analysis is given in Appendix A.2.2.

5.3.1 Limit Load

The equivalent moment distribution for the first to fourth analyses is shown in Figs. 5.7 (a) to (d). Subsequent re-analysis was performed for 30 iterations in order to see the possible trends (see Fig. 5.6(a) for 30 iterations and Fig. 5.6(b) for the first 12 iterations). It was noted that after 12 iterations the apparent convergence was reversed and that there was an increase in the values of average absolute percentage change. These results showed trends of convergence again after 30 iterations. For the present analysis, the 12th iteration was considered as converged and the corresponding limit load was calculated from yield lines as before. The equivalent moment distribution after converged analysis (iteration 12) is shown in Fig. 5.8.

The limit load value obtained above was compared with the results from a non-linear finite element analysis. The same model with ANSYS Shell 143 element was chosen for the analysis. The material property assumed was bi-linear isotropic hardening with the assumption of true stress-strain behavior. An arbitrary pressure of 0.5 N/mm^2 was applied. The input file for the analysis is given in Appendix.C.1.2. Table 5.2 shows the comparison of results from non-linear finite element analysis and the present method. The difference as compared to non-linear finite element analysis is 3.4%.

5.4 Continuous Plates

A continuous plate system was analyzed using the modified rigidity method. If the supporting beams are sufficiently strong to carry the imposed loads without developing plastic hinges, the case involves merely the study of individual slab failures. This is also valid if the plate is uniformly loaded on all panels. However, by superimposing on the dead load a checkerboard type live loading, a different yield line pattern may be obtained as shown in Fig. 5.9.

Details of the continuous plate are given in Table 5.3. The plates are also shown in Figs. 5.10 (a) to (d). An arbitrary uniform pressure of 10 MPa is applied on all the plates. The plate material has a yield stress of 350 MPa and Young's modulus of 200,000 MPa.

As before, ANSYS Shell 63 element was chosen for the analysis. For Cases 1 and 2, the overall size of the system is 9m×4.5m. Supports have been provided at every 1.5m and 3m for shorter and longer direction, respectively. For cases 3 and 4, the total dimension of the system is 10.5×21m. The boundary conditions for the plate along with loading are shown in Fig 5.10. A macro was written for modeling the continuous plate. It can easily generate the model for any panel size and divisions. This is given in Appendix A.3.1 for the simply supported case and Appendix A. 3.2 for the fixed case.

5.4.1 Limit pressure

The analysis procedure is similar to that described for the previous analyses. The average of absolute percentage changes of equivalent moment between iterations is plotted in Fig. 5.11. Twelve to fourteen iterations led to convergence. After checking for convergence, the equivalent moments across the plate were plotted as a surface plot. The equivalent moment distributions for the first elastic analysis and for converged analysis are shown in Figs. 5.12-15. The limit load of the central interior panel was calculated using equivalent moment identified along yield lines.

5.4.2 Analytical Limit Loads

The critical load for an interior panel of a continuous slab can be calculated from an equivalent simply supported slab having reduced span lengths. This can be calculated from Johansen's formula given by [Szilard, 1974]:

$$p_{crit} \approx \frac{8m_u\left[1+\left(\frac{a_r}{b_r}\right)+\left(\frac{b_r}{a_r}\right)\right]}{a_r b_r} \qquad (5.4.1)$$

where, a is the longer span of the individual panel,

b is the shorter span of the individual panel,

$$a_r = \frac{2a}{\sqrt{1+\mu_2}+\sqrt{1+\mu_4}}, \quad \text{and} \quad b_r = \frac{2b}{\sqrt{1+\mu_1}+\sqrt{1+\mu_3}}$$

μ_i for an edge, is the ratio of the negative moment of resistance to the positive moment of resistance of the slab.

In this case, the moment capacity of the plate was considered for obtaining the ratios μ_1, μ_2, μ_3, μ_4.

Initially, Case 1 and Case 2 were solved and compared with Johansen's formula. From Figs. 5.12 (b) to 5.15 (b), it may be seen that, the effect of outer edges being fixed or simply supported has a bearing on the behavior of the interior panels. This is also evident from the corresponding limit load values. Keeping the mesh size and panel size the same, the number of panels were increased to 7×7 (Cases 3 and 4) and the analysis was repeated. The behavior of the plate in this case can be seen from the plot of the equivalent moments after converged analysis. The limit load values for the interior panel have not been affected by the outer edges of the plate being simply supported or fixed. The interior panel behaves more like a fixed plate, since yield lines have formed in the span and along the supports. For a different loading pattern, the yield pattern might be different. If a dead load is present in addition to the live load as used in this problem, the yield lines may not form at the support lines. Instead, a set of negative bending yield lines might form in the panels where there is no live load.

Using the present analysis, two approaches were adopted for the calculation of limit load. Firstly, the average equivalent moment of yield lines along edges and diagonals of

the central panel was considered. Next, the average equivalent moment of yield lines all over the plate was used to calculate limit load.

For Cases 3 and 4, the mesh density used was only 12×7 for each panel. Since there were forty-nine panels in total, this coarse mesh was chosen to save time and computational effort. An increase in mesh size would certainly improve results with the comparisons mentioned in Table 5.4.

Also, for Case 3, since the extreme edges were simply supported, a non-linear finite element analysis did not produce relevant results. The limit loads obtained were due to failure of the corner four panels, which behave like a plate with two edges simply supported and two edges fixed. Hence, a difference of 21 % was produced when the failure load for the central panel using modified secant rigidity method was compared with the non-linear finite element analysis. On the other hand, Case 4 which has extreme edges fixed has produced good results in comparison with non-linear finite element analysis.

As can be seen, the modified rigidity approach for limit load estimation can handle simple or continuous plates with a variety of boundary conditions and shapes. Although it has not been illustrated here, other types of loading patterns which produce non-standard yield patterns in continuous plates can be handled with the same ease.

Table 5.1: Rectangular Plate with Partial Boundary Conditions under UDL

Analysis	Secant rigidity (Mises)			Non-linear FEA [Mangalaramanan, 1993]
Mesh size	18 x 12	42 x 27	84 x 54	18 x 12
Limit Load N/mm^2	3.79	3.20	3.05	3.48

Table 5.2: Irregular Plate with Partial Boundary Conditions under UDL

Analysis	SRM (Tresca)	Non-linear FEA	Difference
Limit Load N/mm^2	0.137	0.132	3.65%

Table 5.3: Details of Continuous Plates Analyzed

Case No.	No. of panels	Overall size (m)	t (mm)	Mesh (/panel)	Total elements	Boundary cond. @ edges
1	3 × 3	9.0 × 4.5	10	28 × 18	4536	S.S.
2	3 × 3	9.0 × 4.5	10	28 × 18	4536	Fixed
3	7 × 7	21.0 × 10.5	10	12 × 8	4704	S.S.
4	7 × 7	21.0 × 10.5	10	12 × 8	4704	Fixed

Table 5.4: Limit Loads of Continuous Plates with Loading on Alternate Panels

3x3 panels	Secant rigidity interior panel	%Difference (*)
Case 1 N/mm^2	0.0833	23.5
Case 2 N/mm^2	0.1023	6.05

7x7 panels	Interior panel	% Diff. (*)	All panels	% Diff. (*)	Non-linear	% Diff. (*)
Case 3 N/mm^2	0.1059	2.74	0.0975	10.5	0.0805	26.1
Case 4 N/mm^2	0.1068	1.92	0.1082	0.63	0.1022	6.14

(*) NOTE: Johansen's result is 0.10888 N/mm^2. All results are compared with the theoretical values as per Johansen [Szilard, 1974]

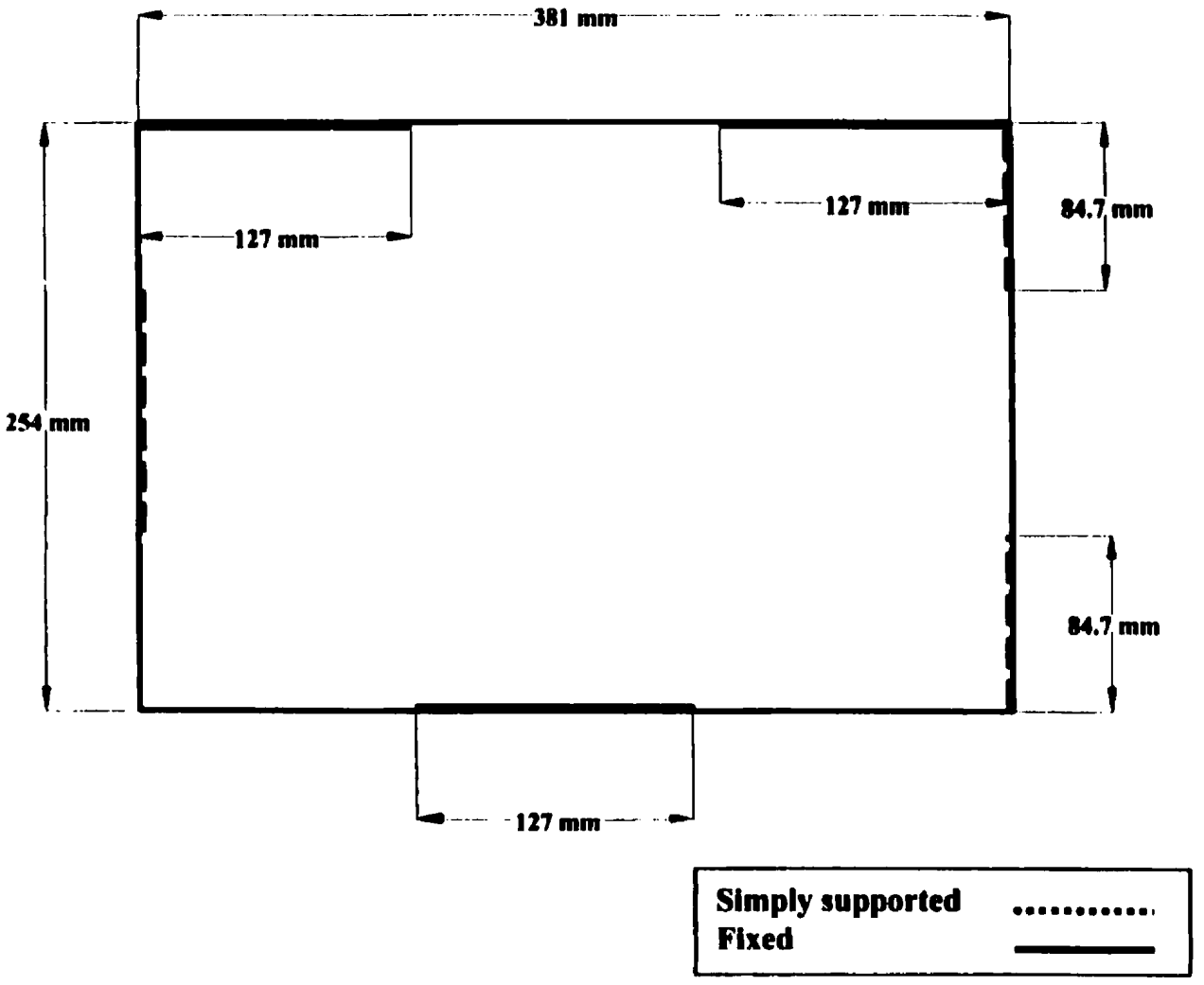

Fig. 5.1 (a) Rectangular Plate with Partial Boundary Conditions under UDL

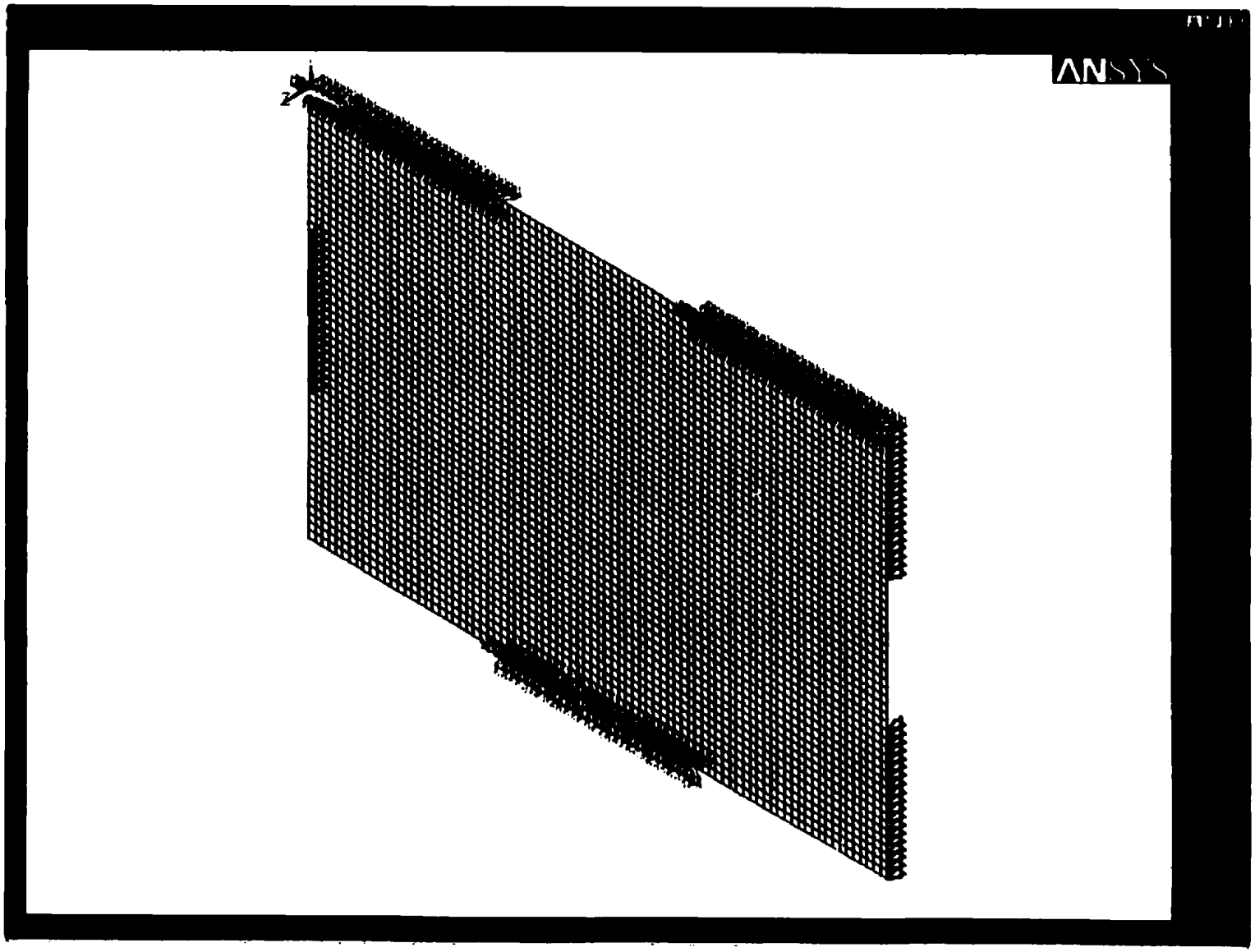

Fig. 5.1 (b) Finite Element Model of a Irregular Plate with Partial Boundary Conditions under UDL

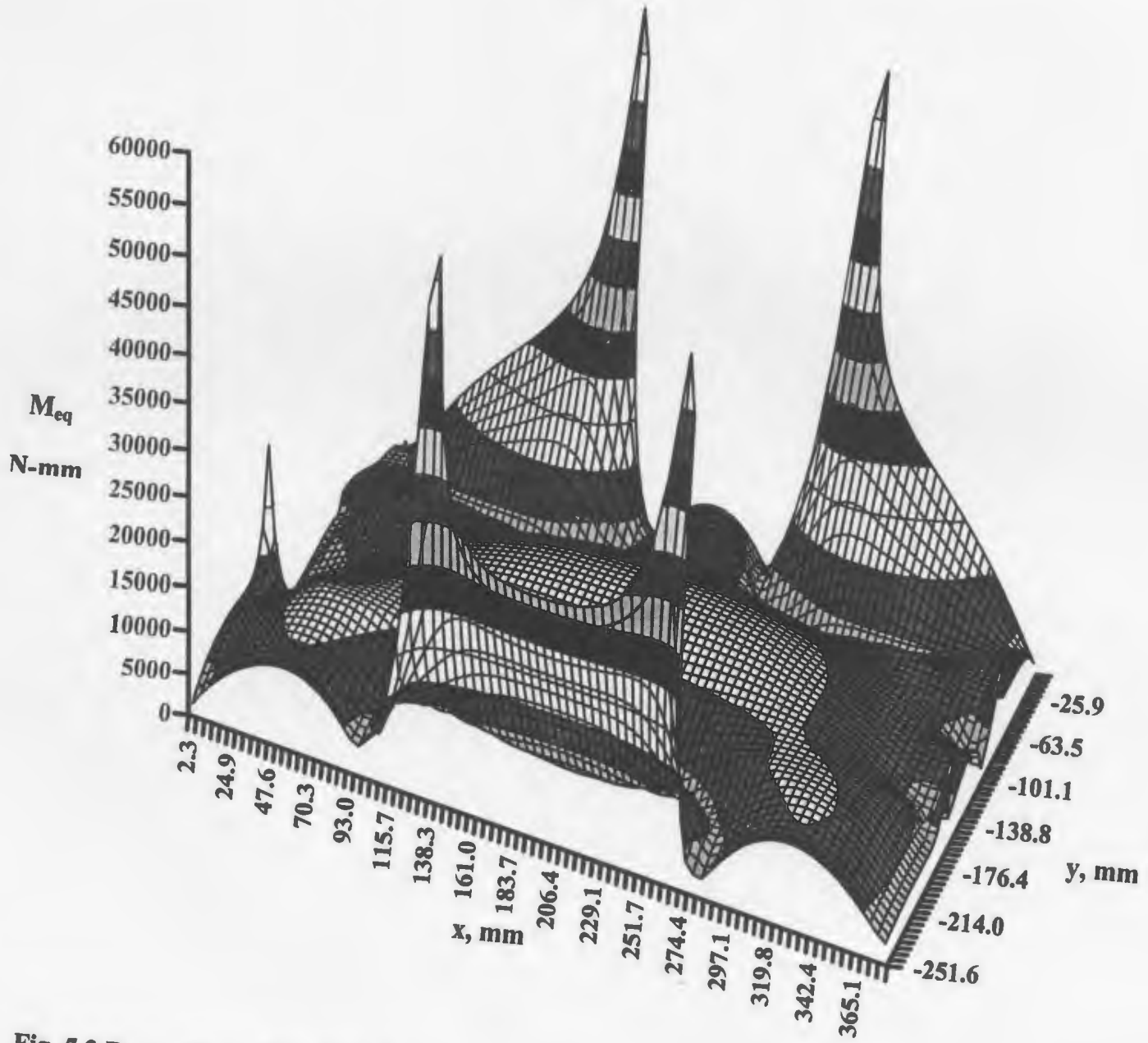

Fig. 5.2 Rectangular Plate with Partial Boundary Conditions –UDL, Mises, First Analysis

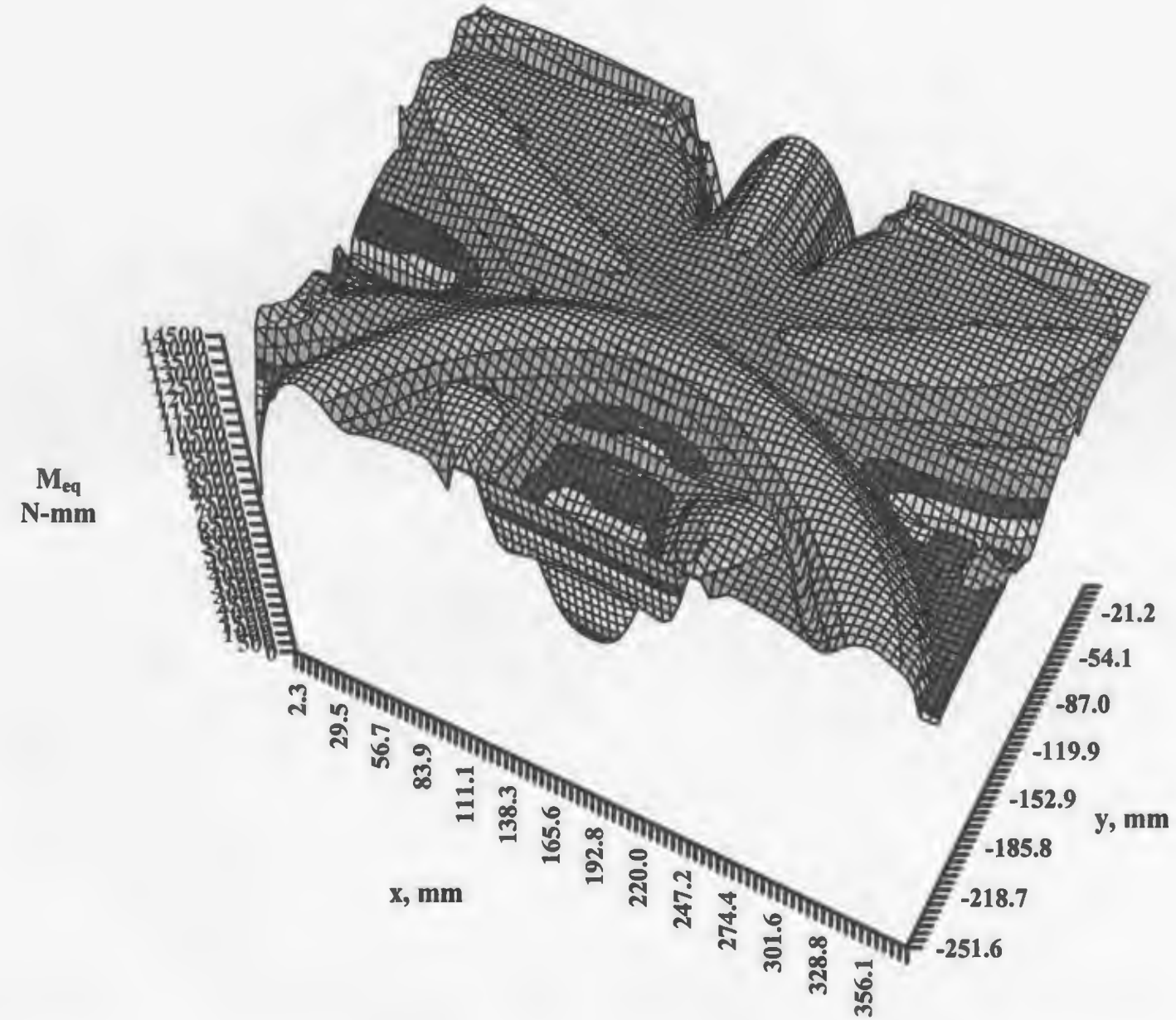

Fig. 5.3-1 Rectangular Plate with Partial Boundary Conditions –UDL, Mises, Converged Analysis

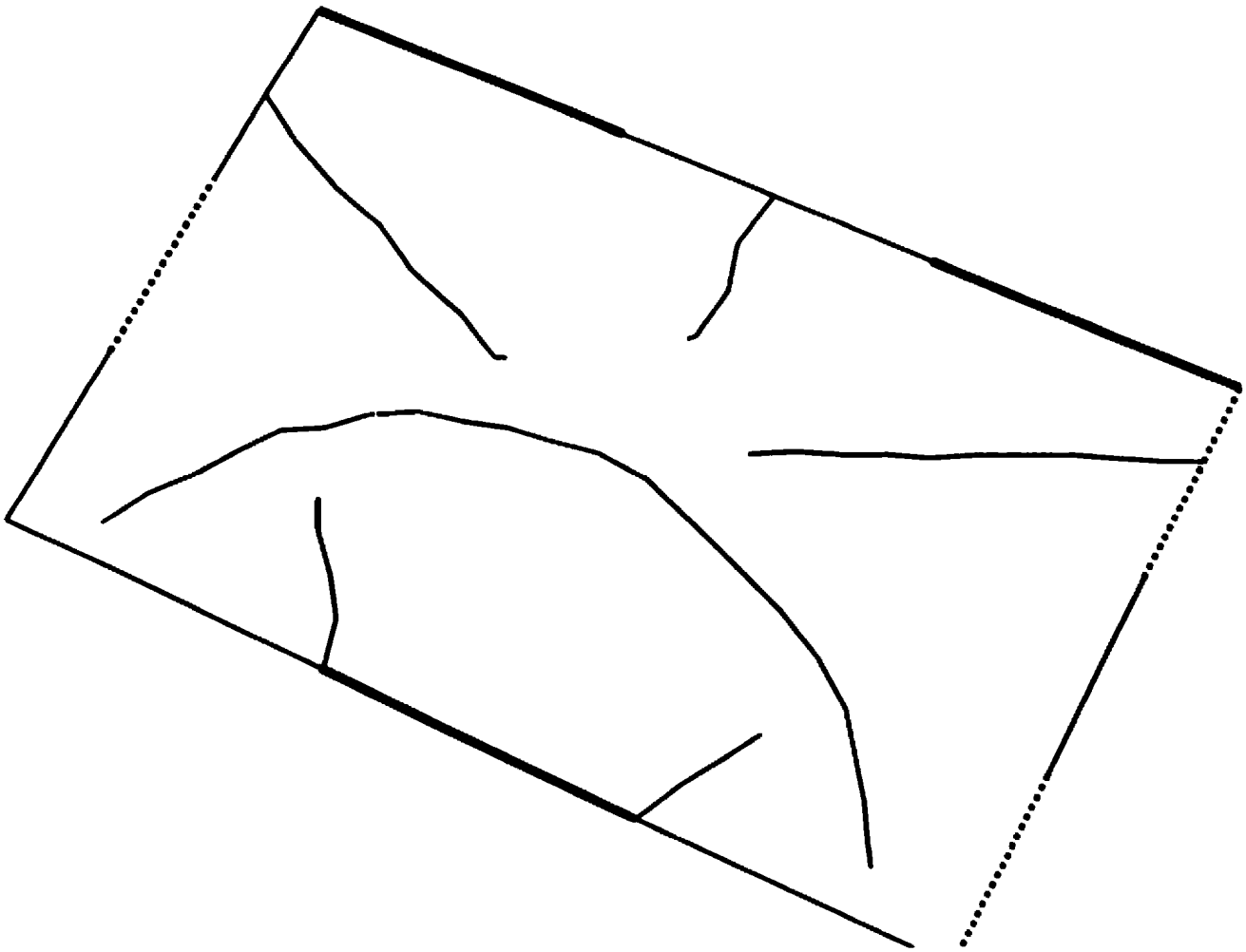

Fig.5.3-2 Yield Line Pattern as obtained from the Converged Analysis

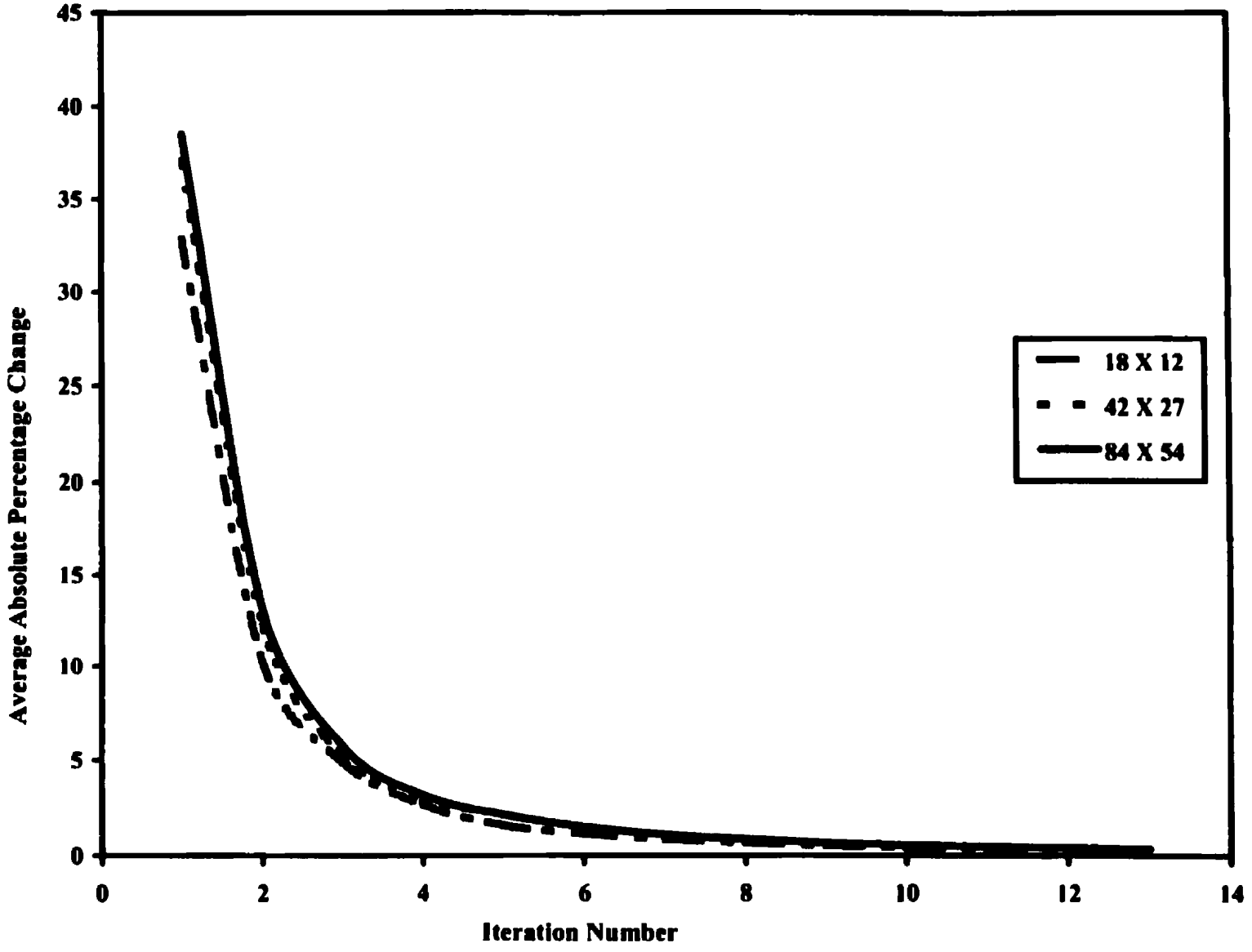

Fig. 5.4 Rectangular Plate with Partial Boundary Conditions under UDL

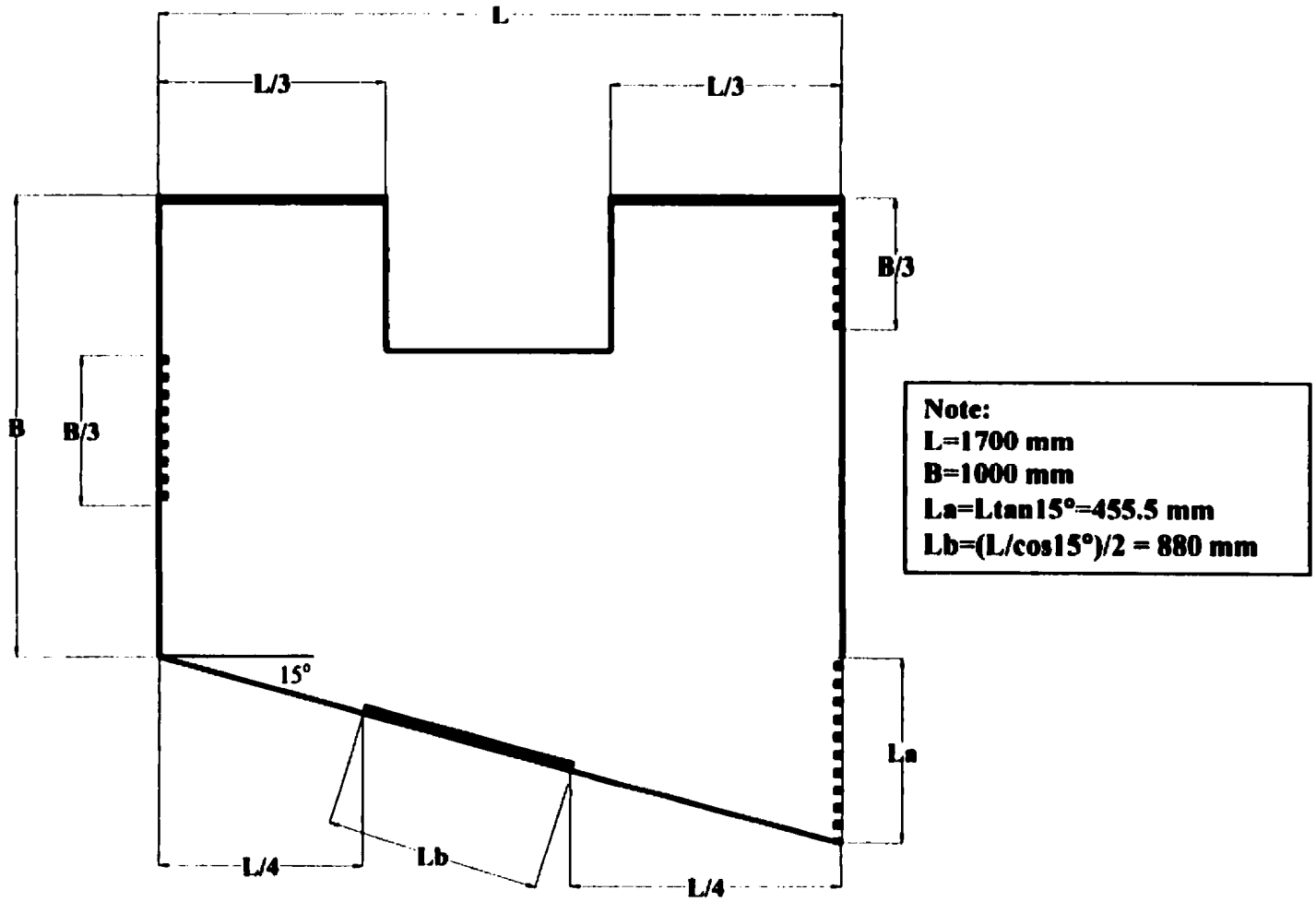

Fig. 5.5 (a) Irregular Plate with Partial Boundary Conditions under UDL

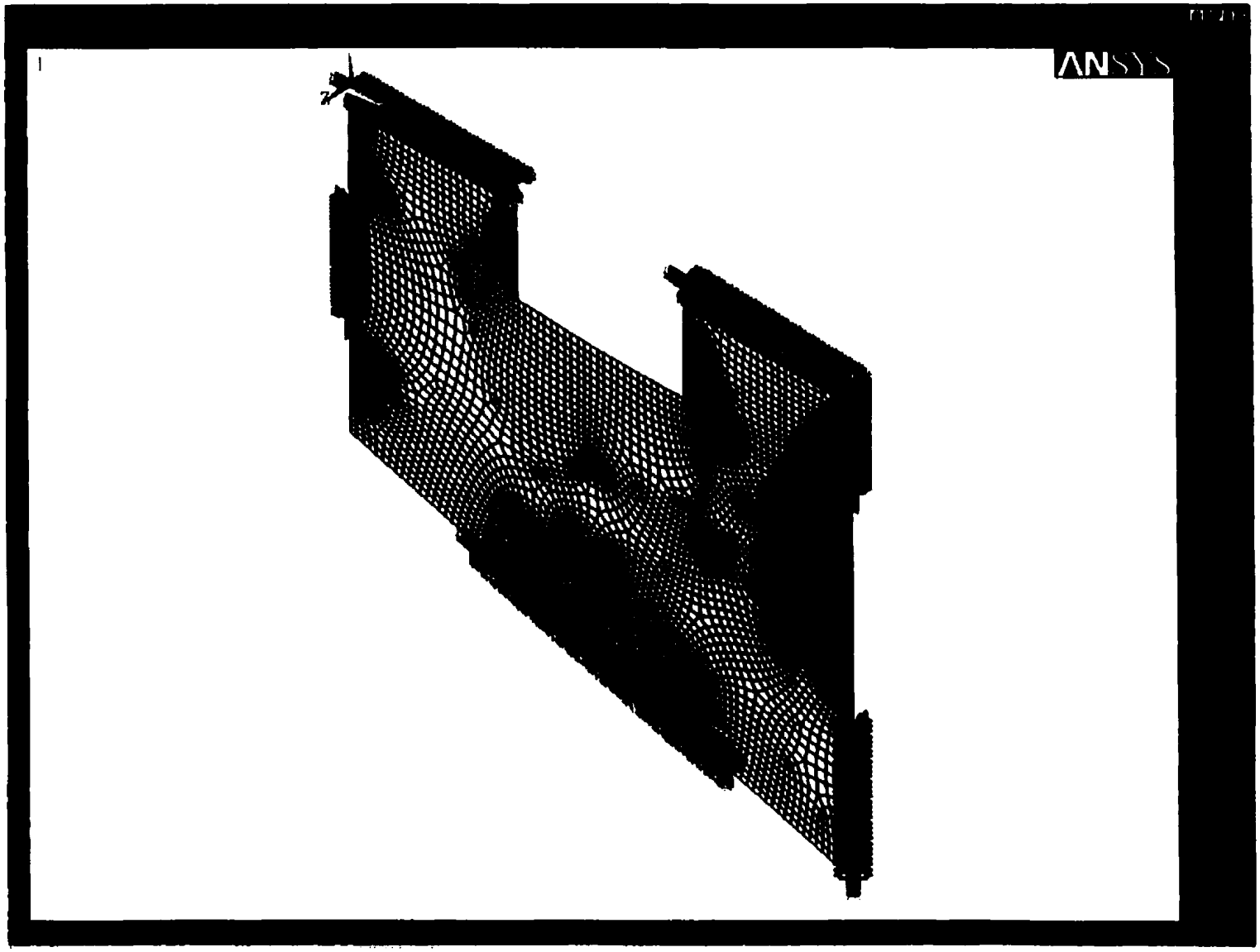

Fig. 5.5 (b) Finite Element Model of a Irregular Plate with Partial Boundary Conditions under UDL

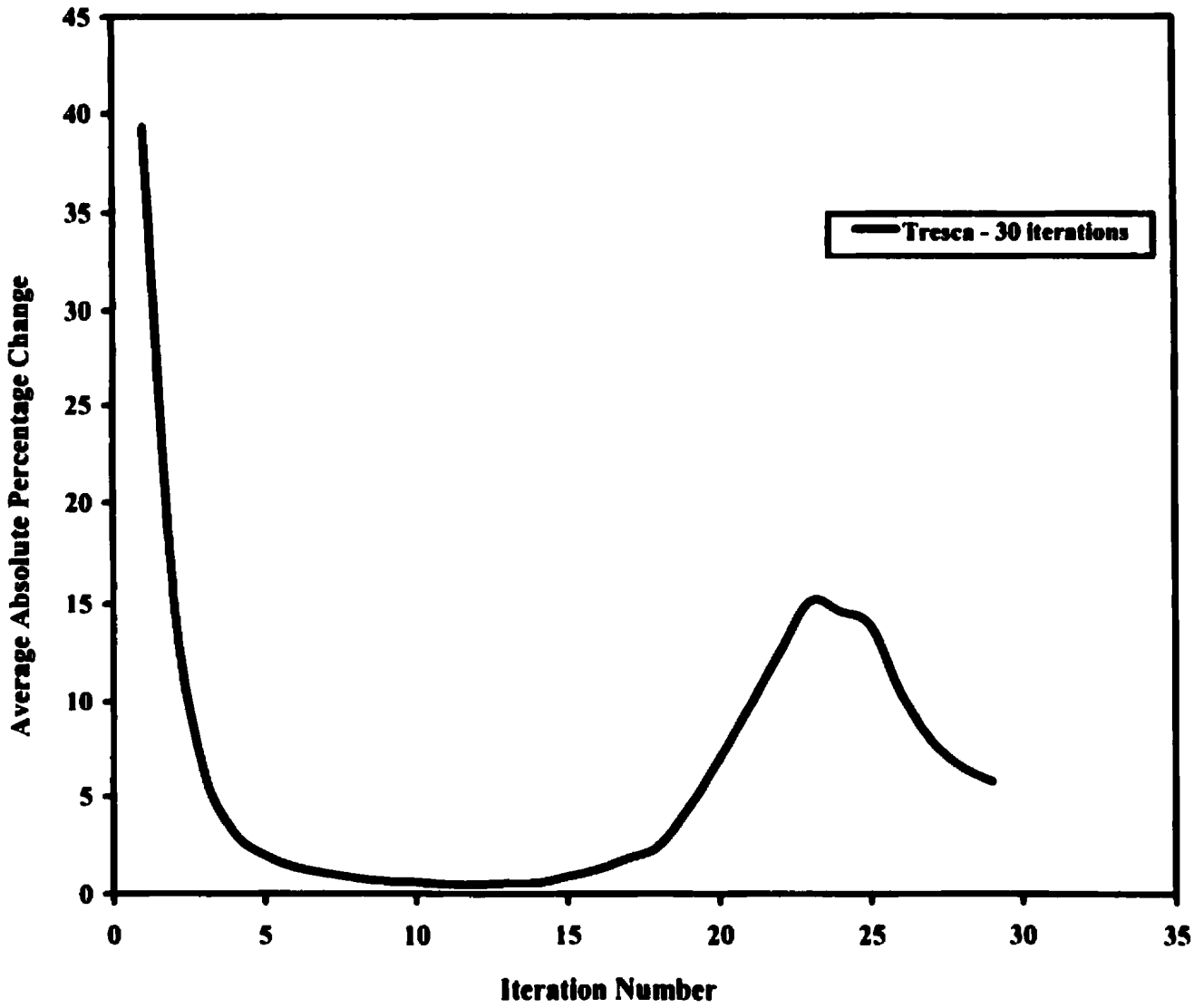

Fig. 5.6(a) Irregular Plate with Partial Boundary Conditions under UDL - 30 Iterations

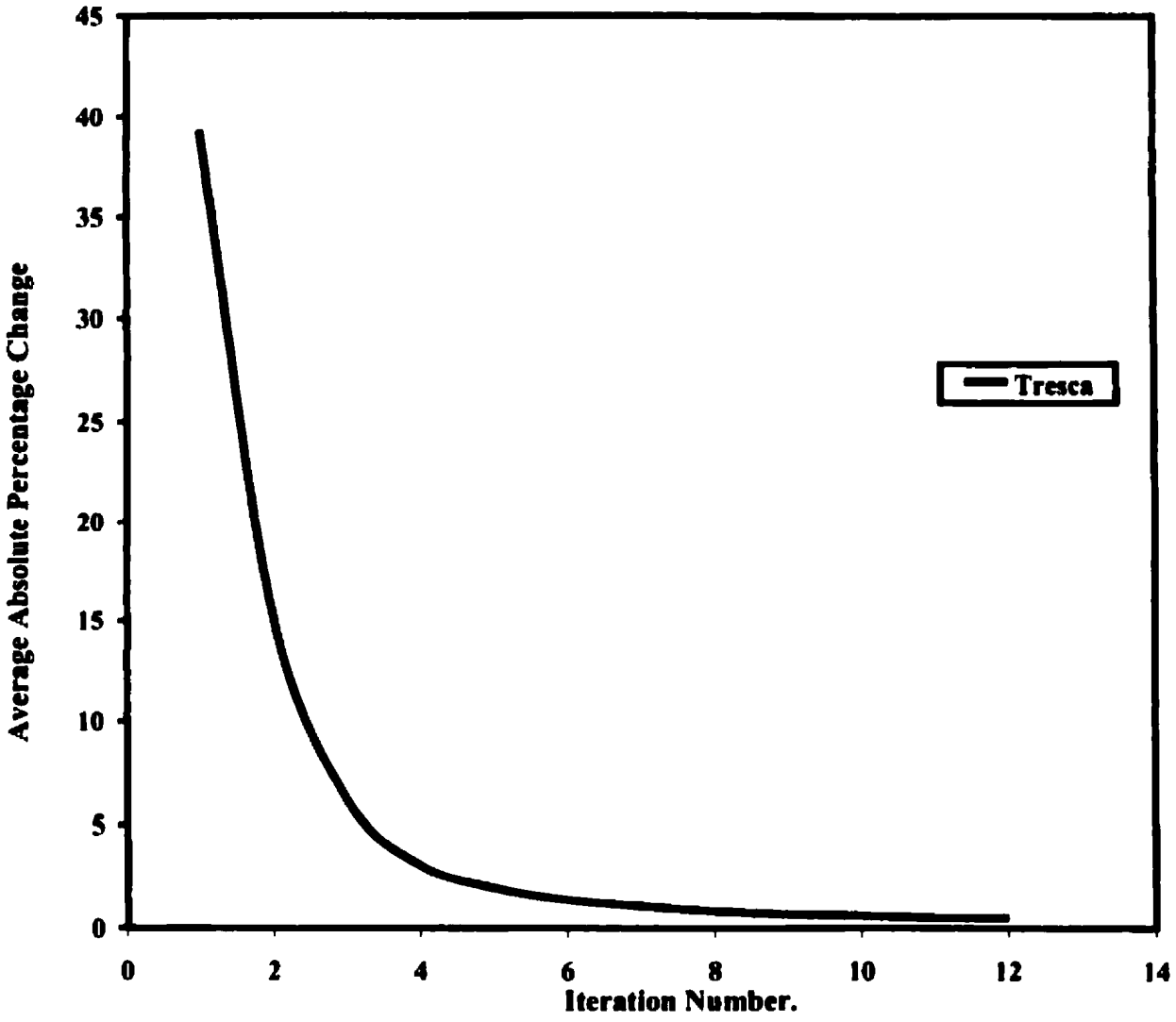

Fig. 5.6 (b) Irregular Plate with Partial Boundary Conditions under UDL –First 12 iterations

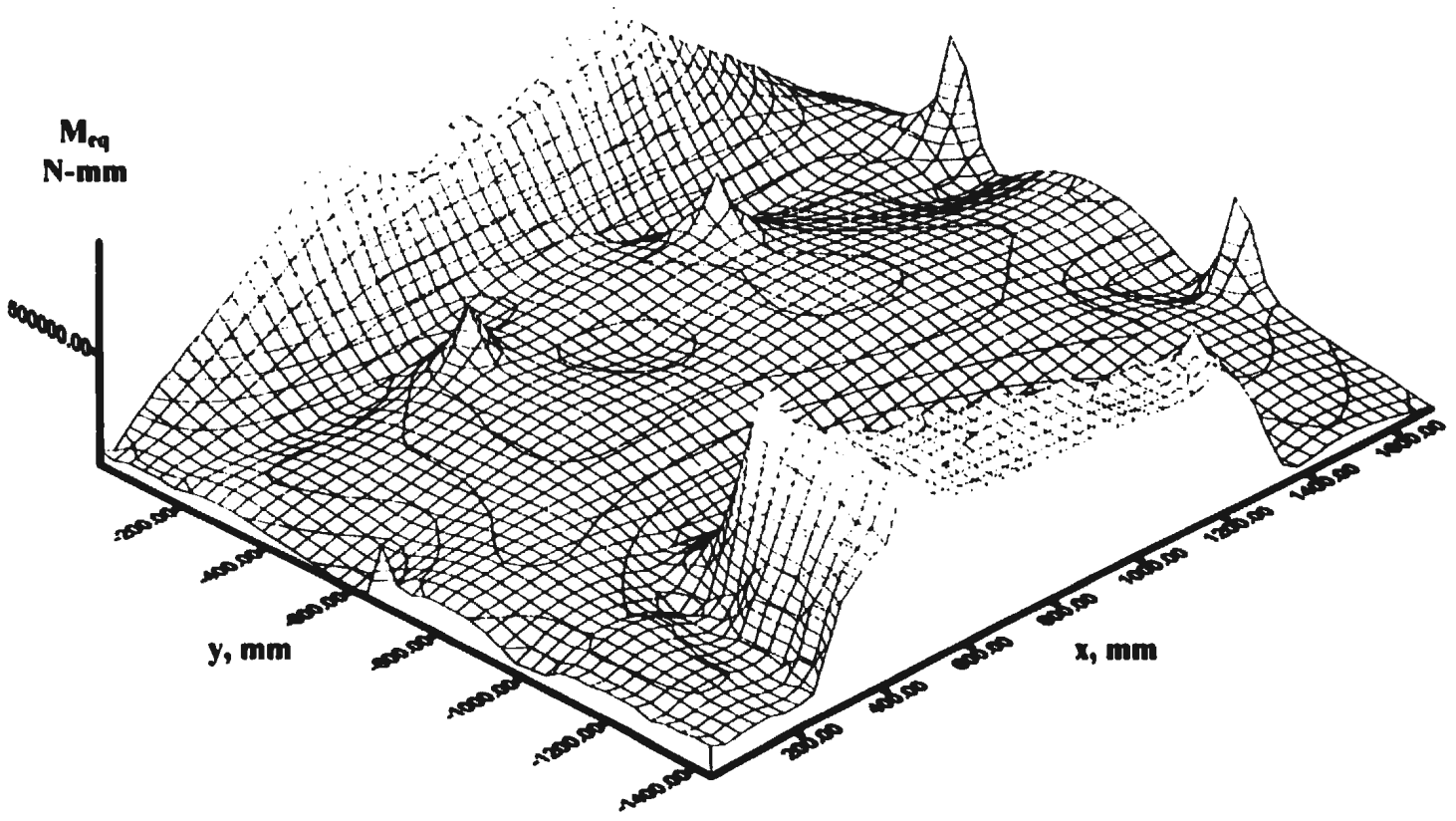

Fig. 5.7 (a) Irregular Plate with Partial Boundary Conditions –UDL, Tresca, First Analysis

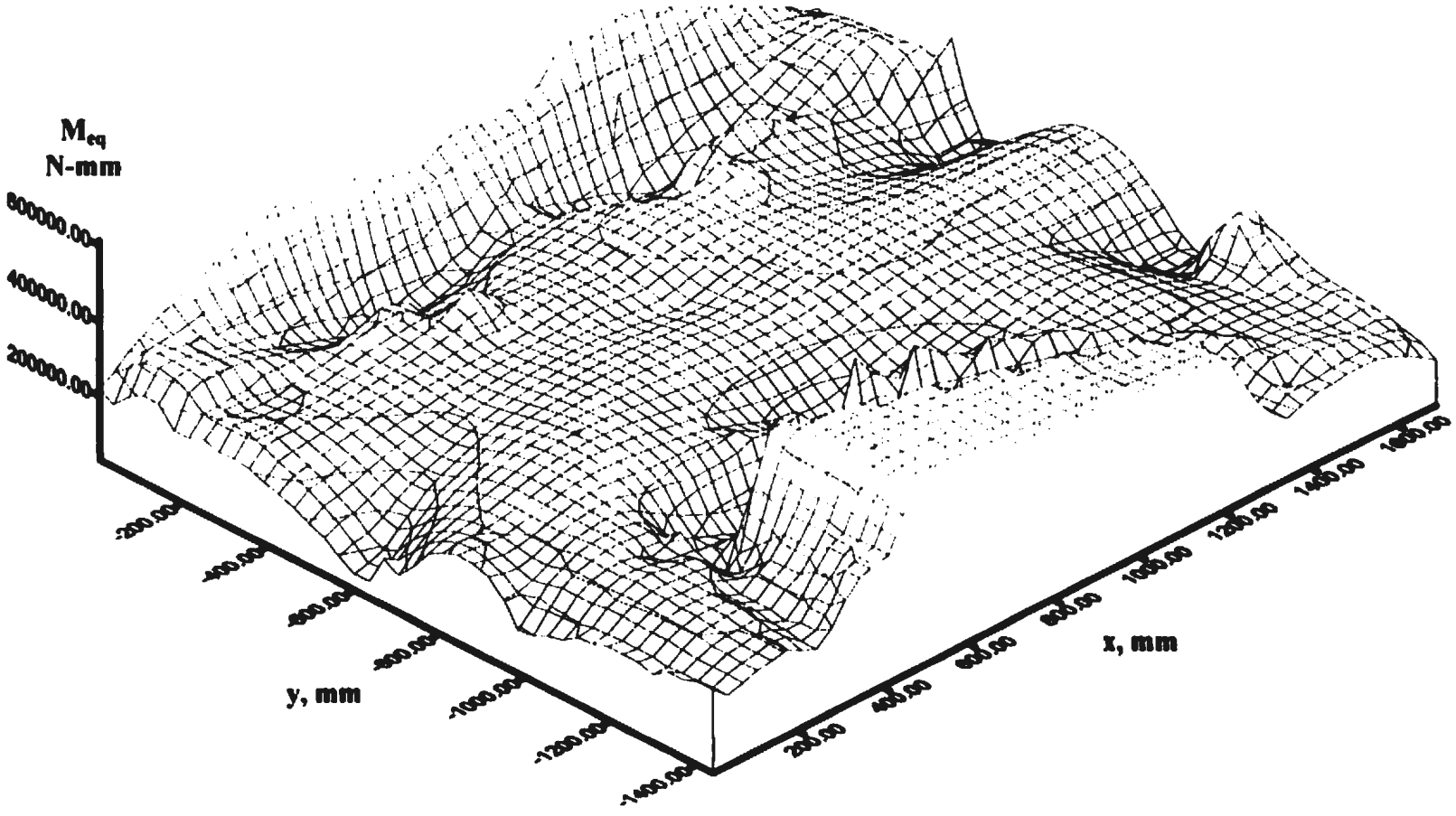

Fig. 5.7 (b) Irregular Plate with Partial Boundary Conditions –UDL, Tresca, Second Analysis

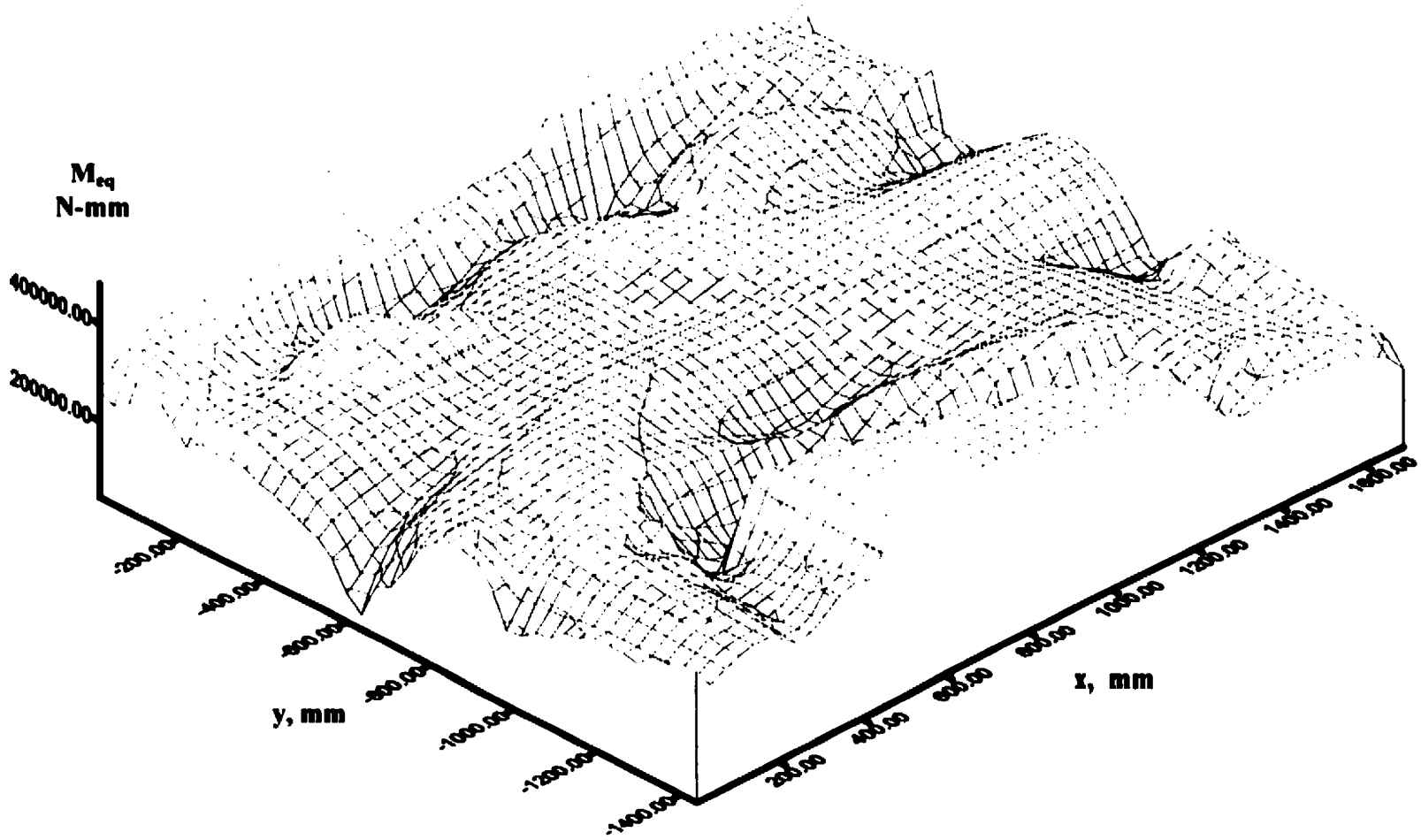

Fig. 5.7 (c) Irregular Plate with Partial Boundary Conditions –UDL, Tresca, Third Analysis

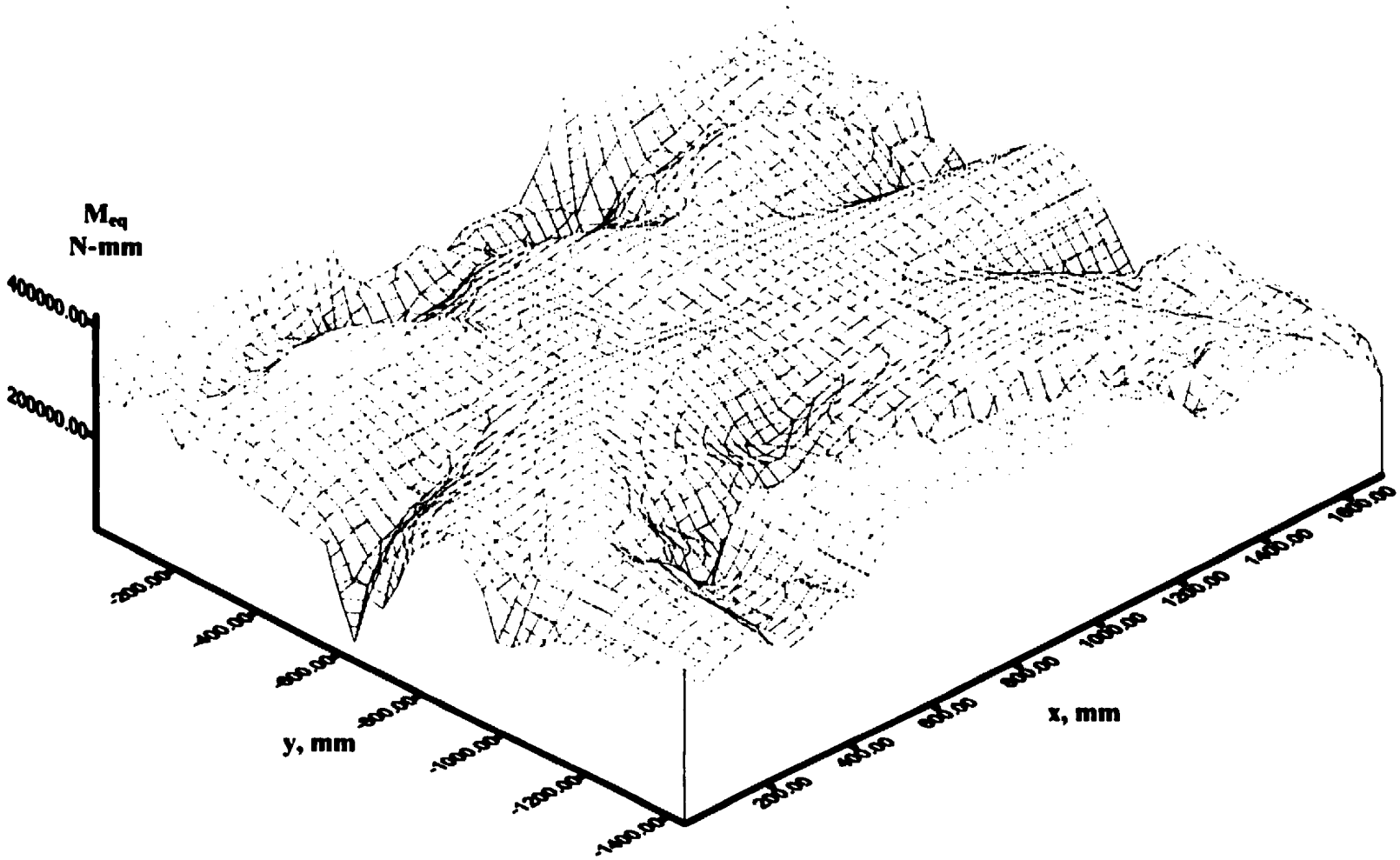

Fig. 5.7 (d) Irregular Plate with Partial Boundary Conditions –UDL, Tresca, Fourth Analysis

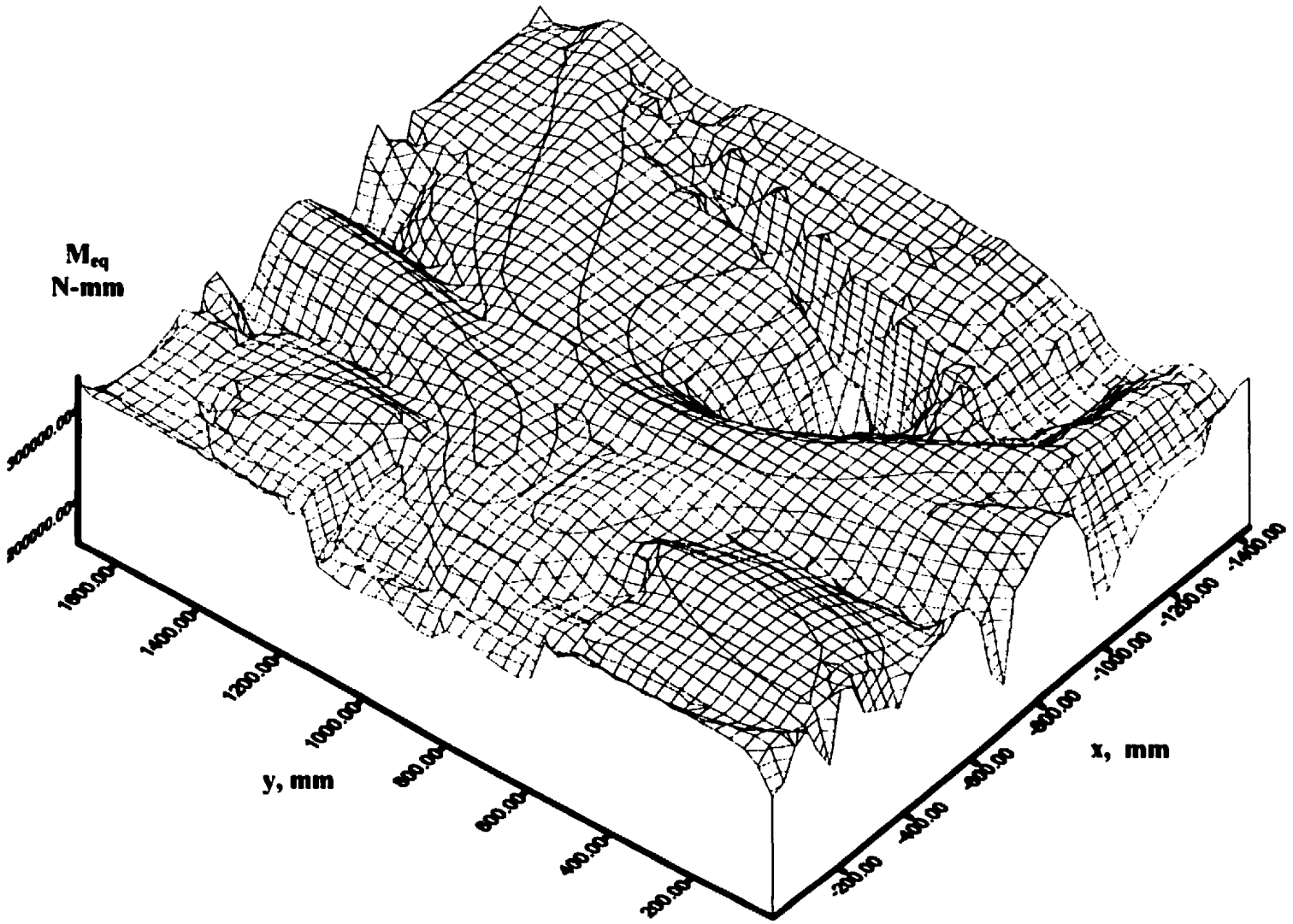

Fig. 5.8-1 Irregular Plate with Partial Boundary Conditions –UDL, Tresca, Converged Analysis

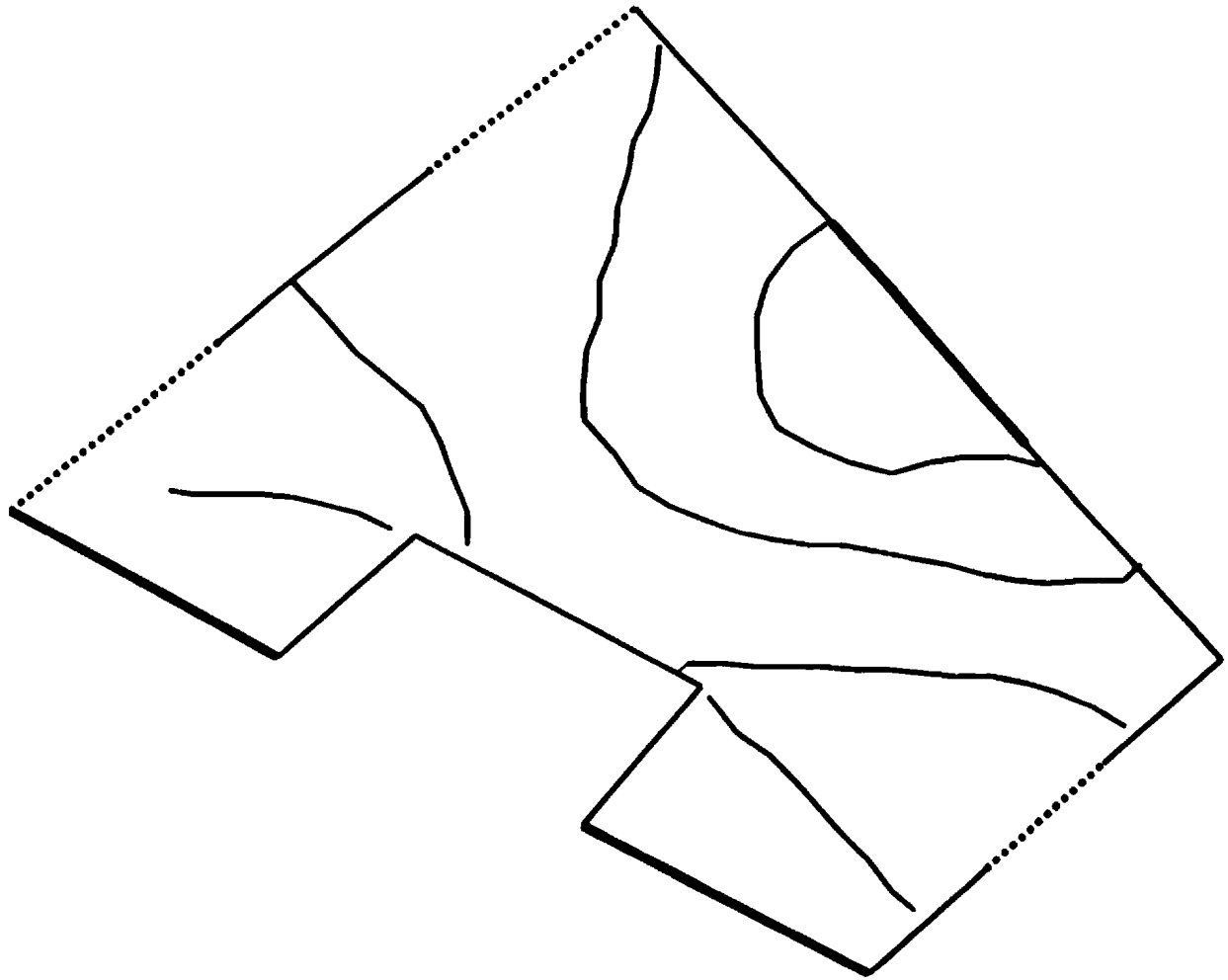

Fig.5.8-2 Yield Line Pattern as obtained from Converged Analysis

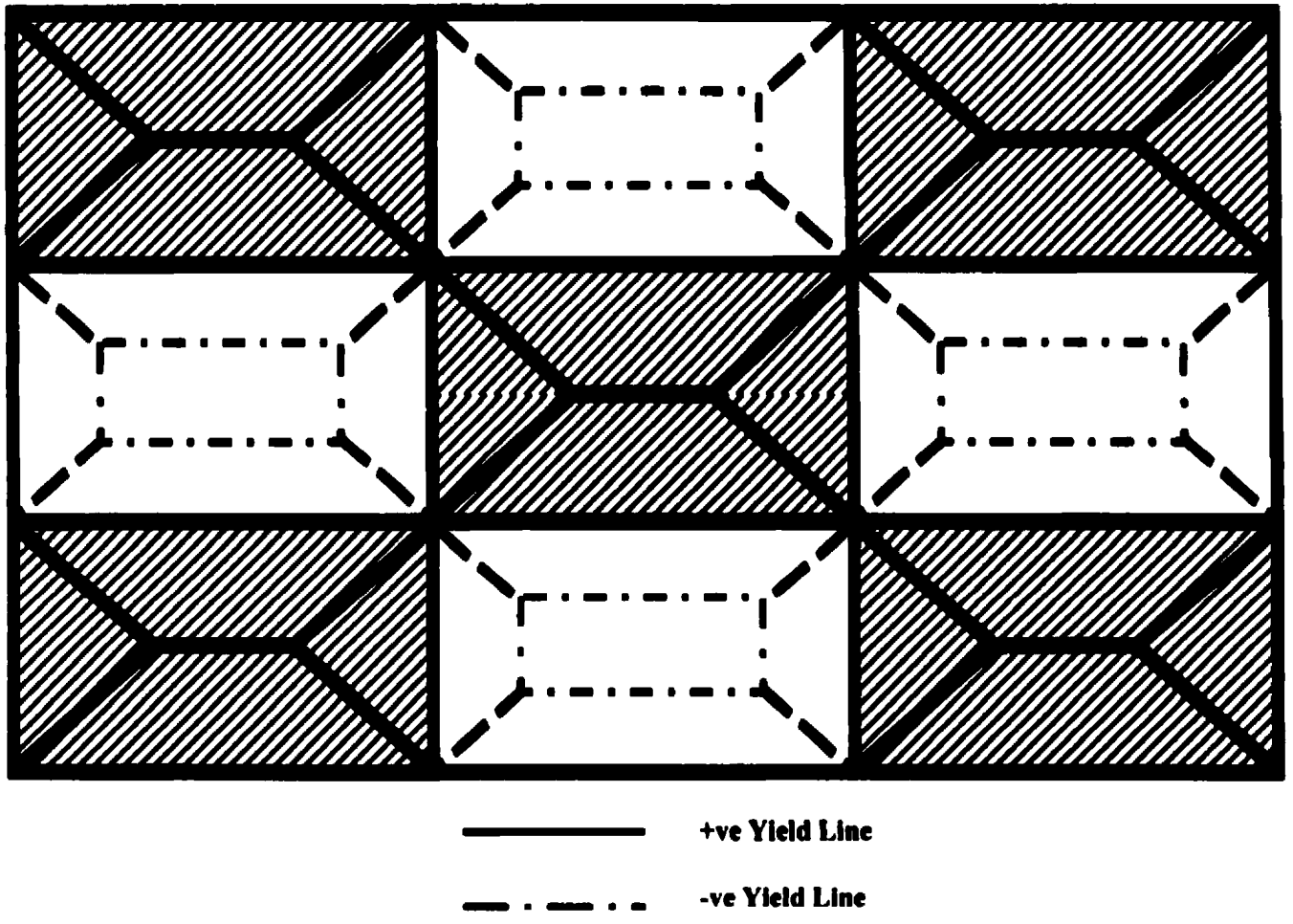

Fig. 5.9 Expected Yield Line Pattern for a Continuous Plate System [Szilard, 1974]

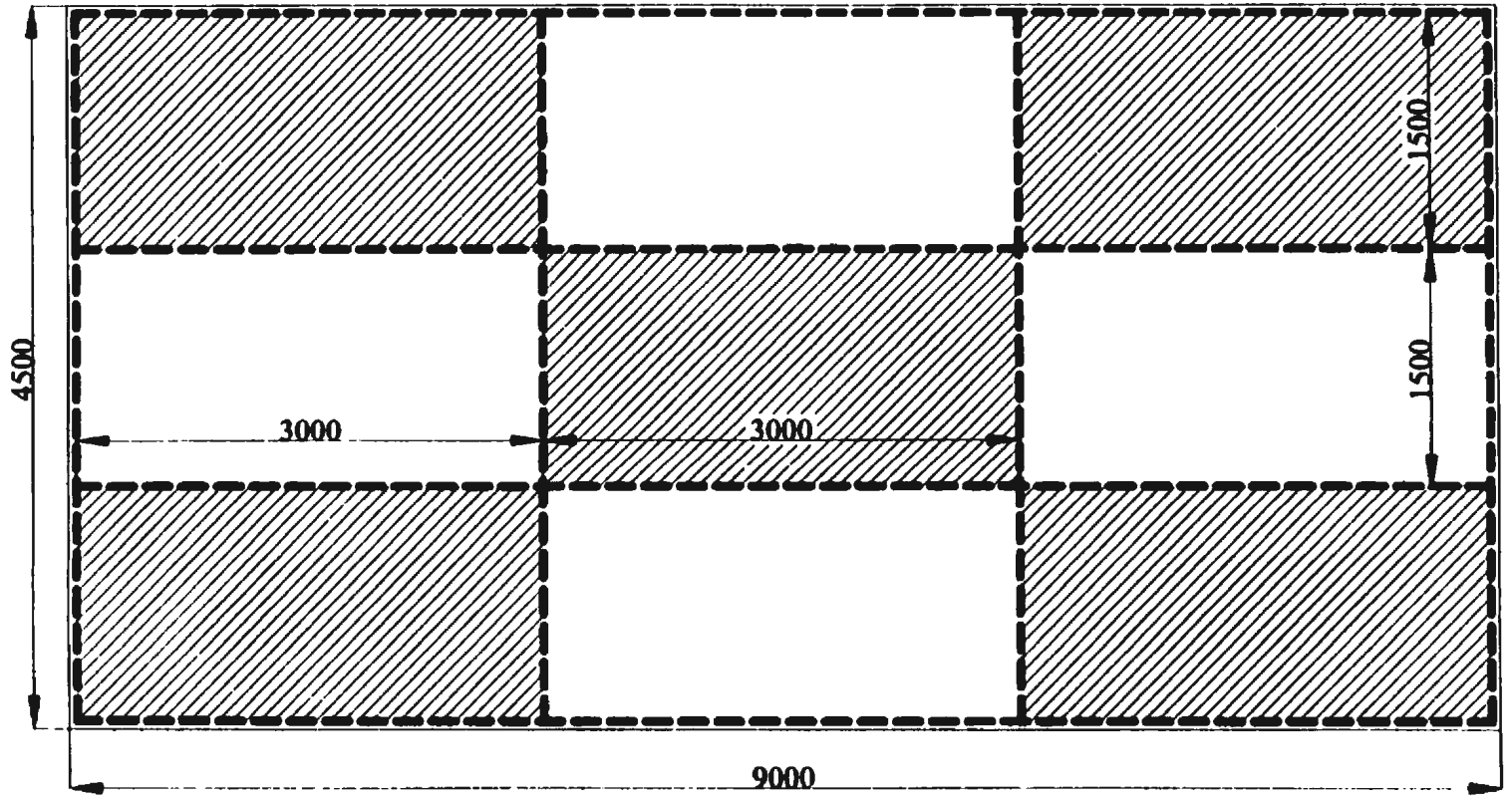

Fig.5.10 (a) 3×3 Panel Continuous Plate with Outer Edges Simply Supported

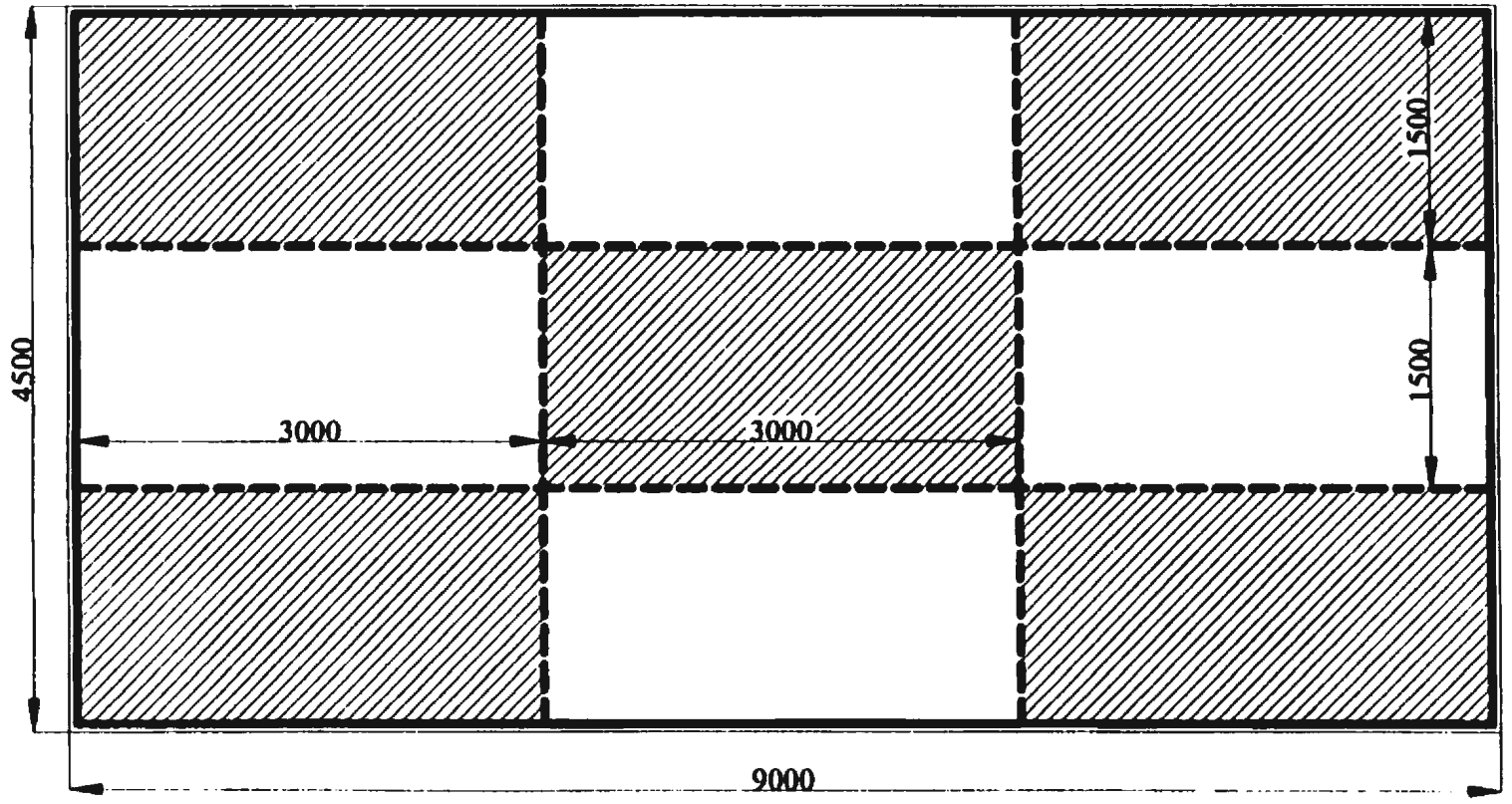

Fig.5.10 (b) 3×3 Panel Continuous Plate with Outer Edges Fixed

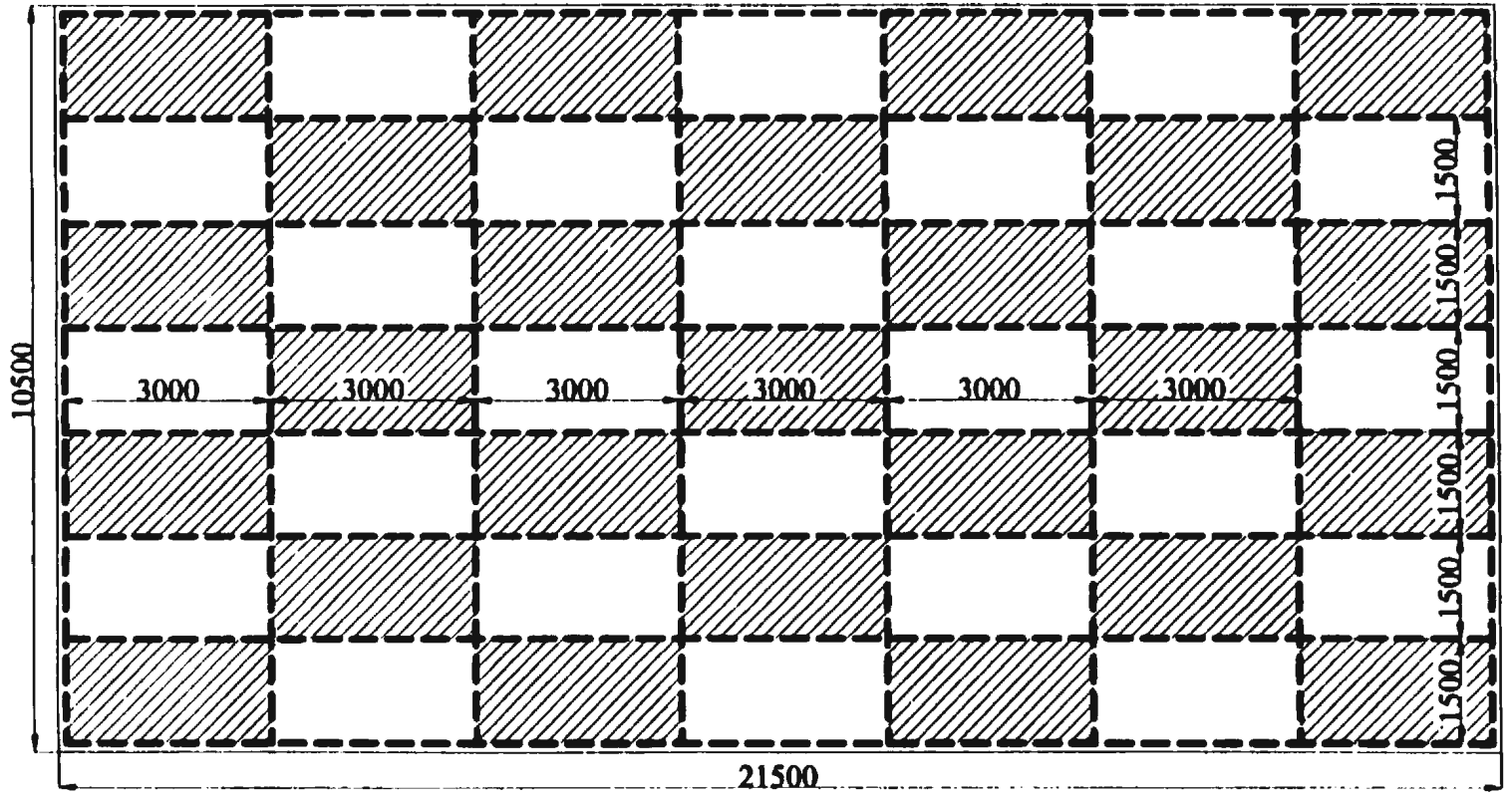

Fig.5.10 (c) 7×7 Panel Continuous Plate with Outer Edges Simply Supported

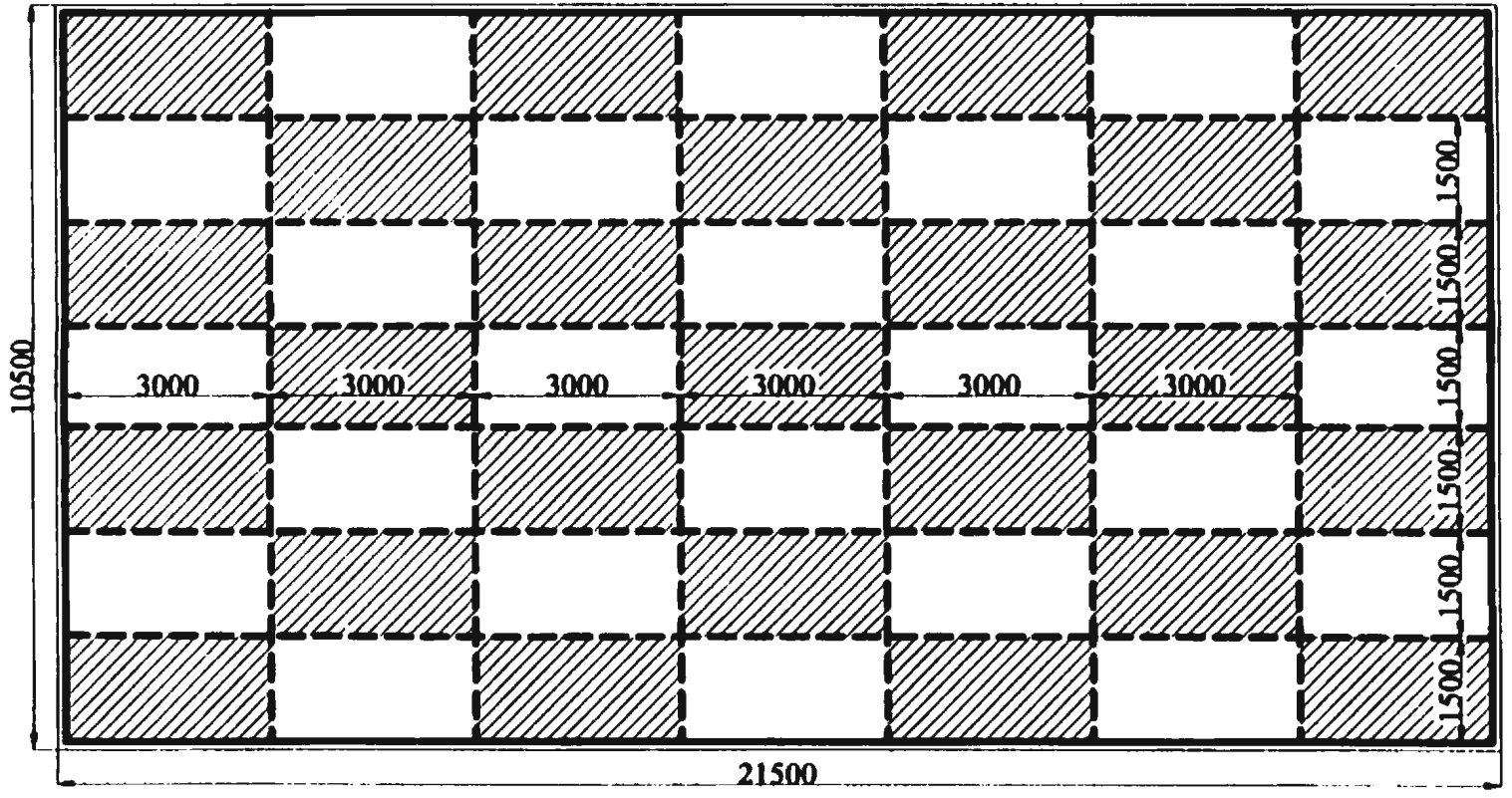

Fig.5.10 (d) 7×7 Panel Continuous Plate with Outer Edges Fixed

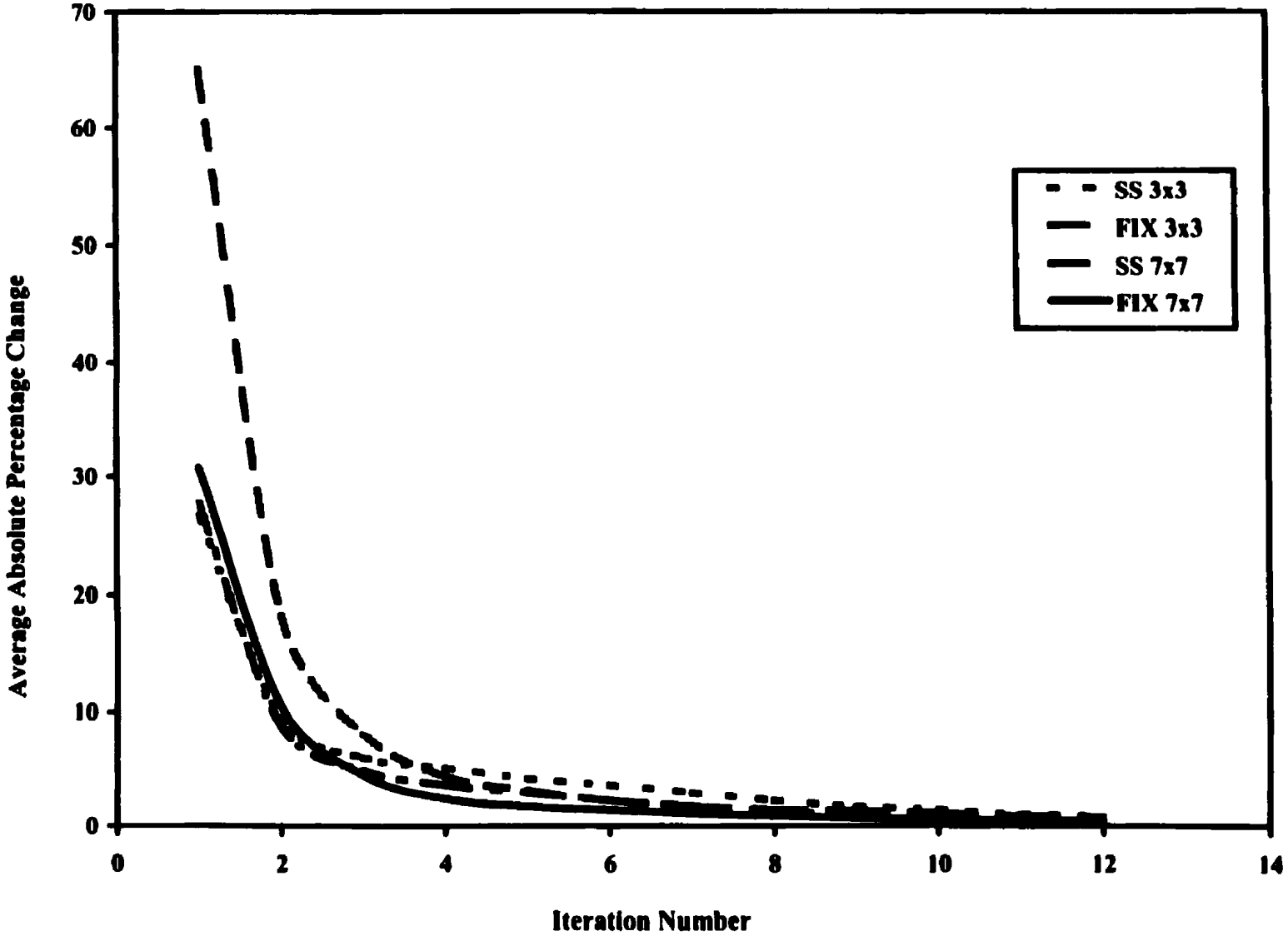

Fig. 5.11 Average Absolute Percentage change vs. Iteration Number

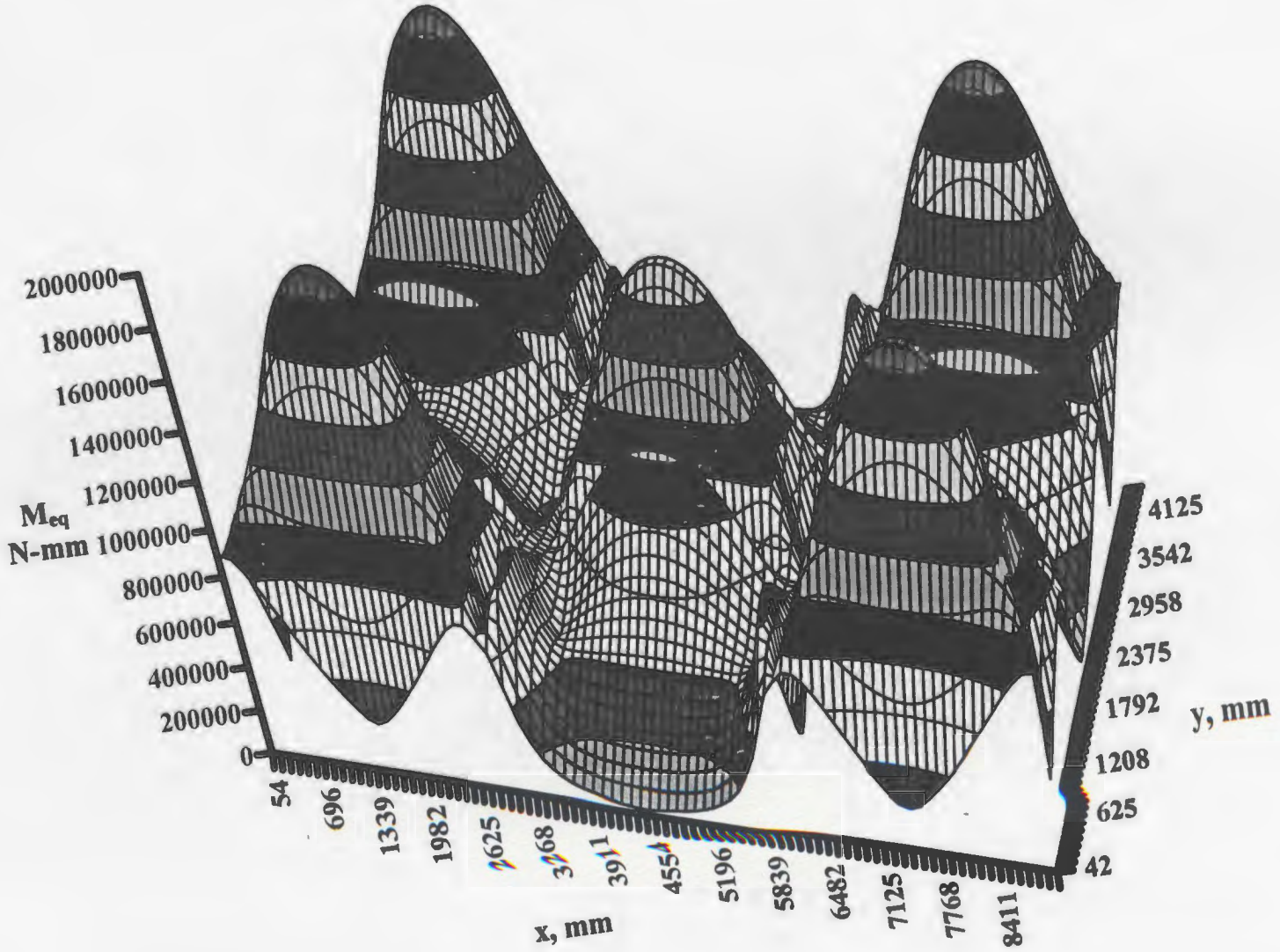

Fig.5.12 (a) 3×3 Simply Supported Continuous Plate –Alternate Loading, Tresca, First Analysis

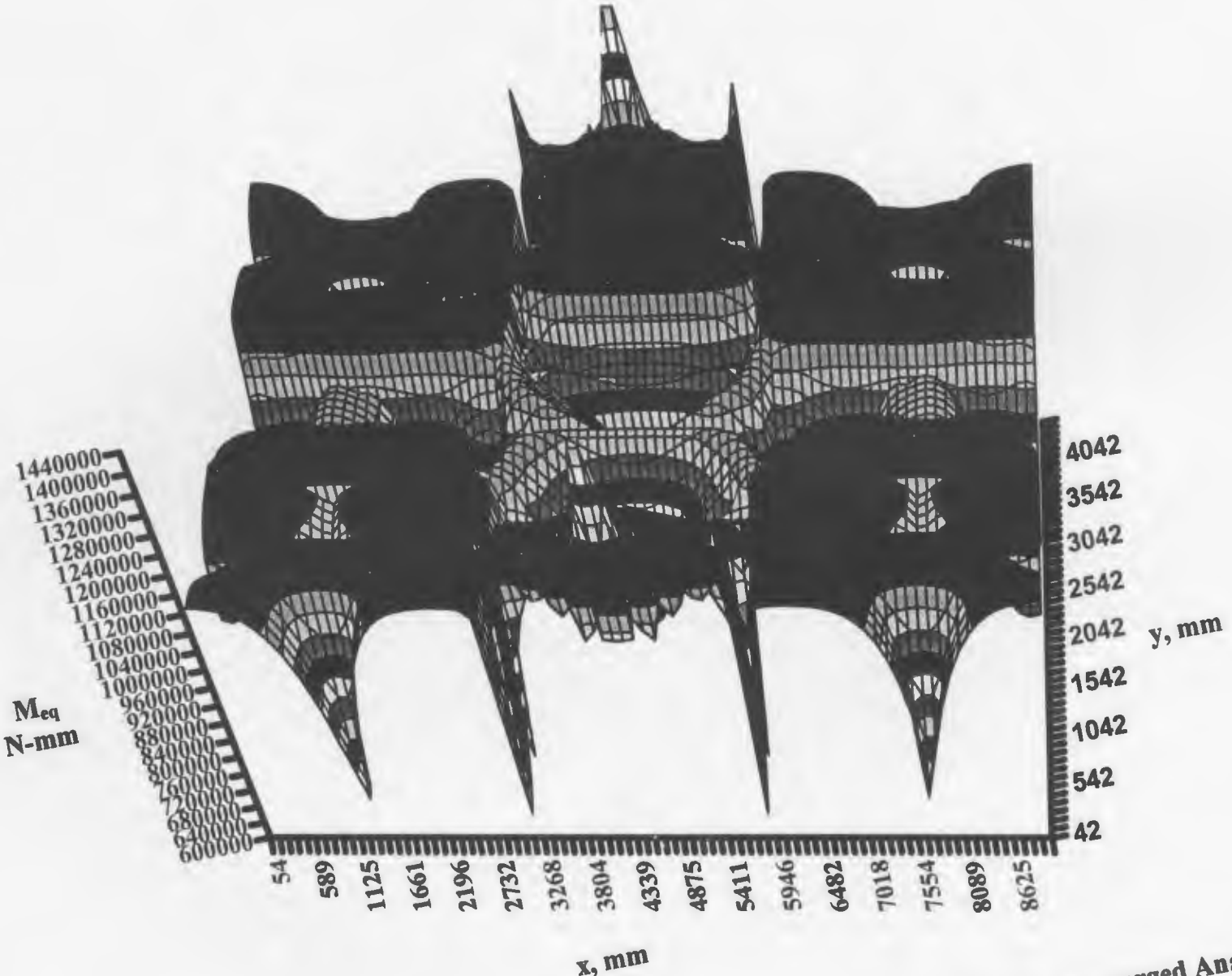

Fig 5.12 (b) 3×3 Simply Supported Continuous Plate -Alternate Loading, Tresca, Converged Analysis

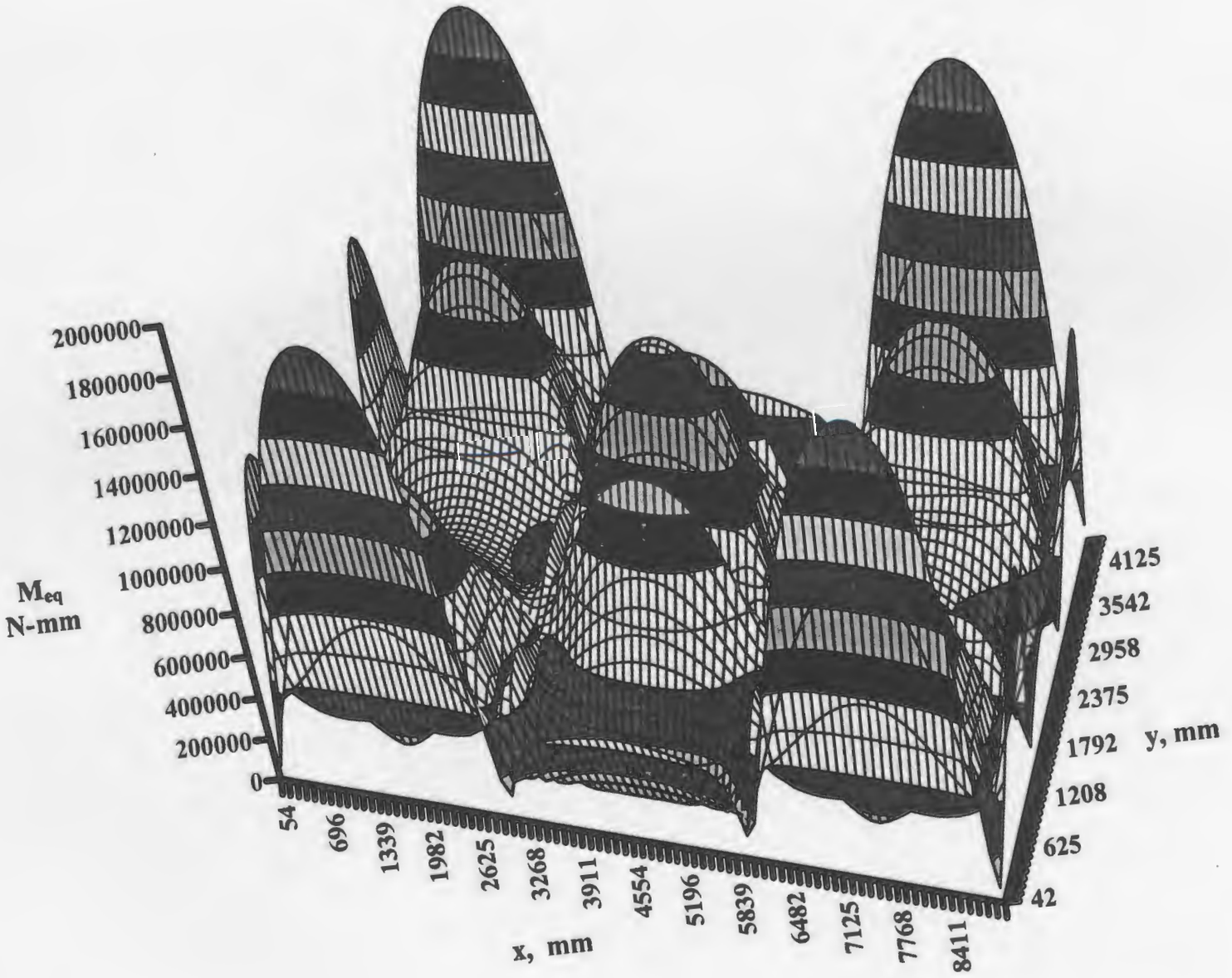

Fig.5.13 (a) 3×3 Fixed Continuous Plate –Alternate Loading, Tresca, First Analysis

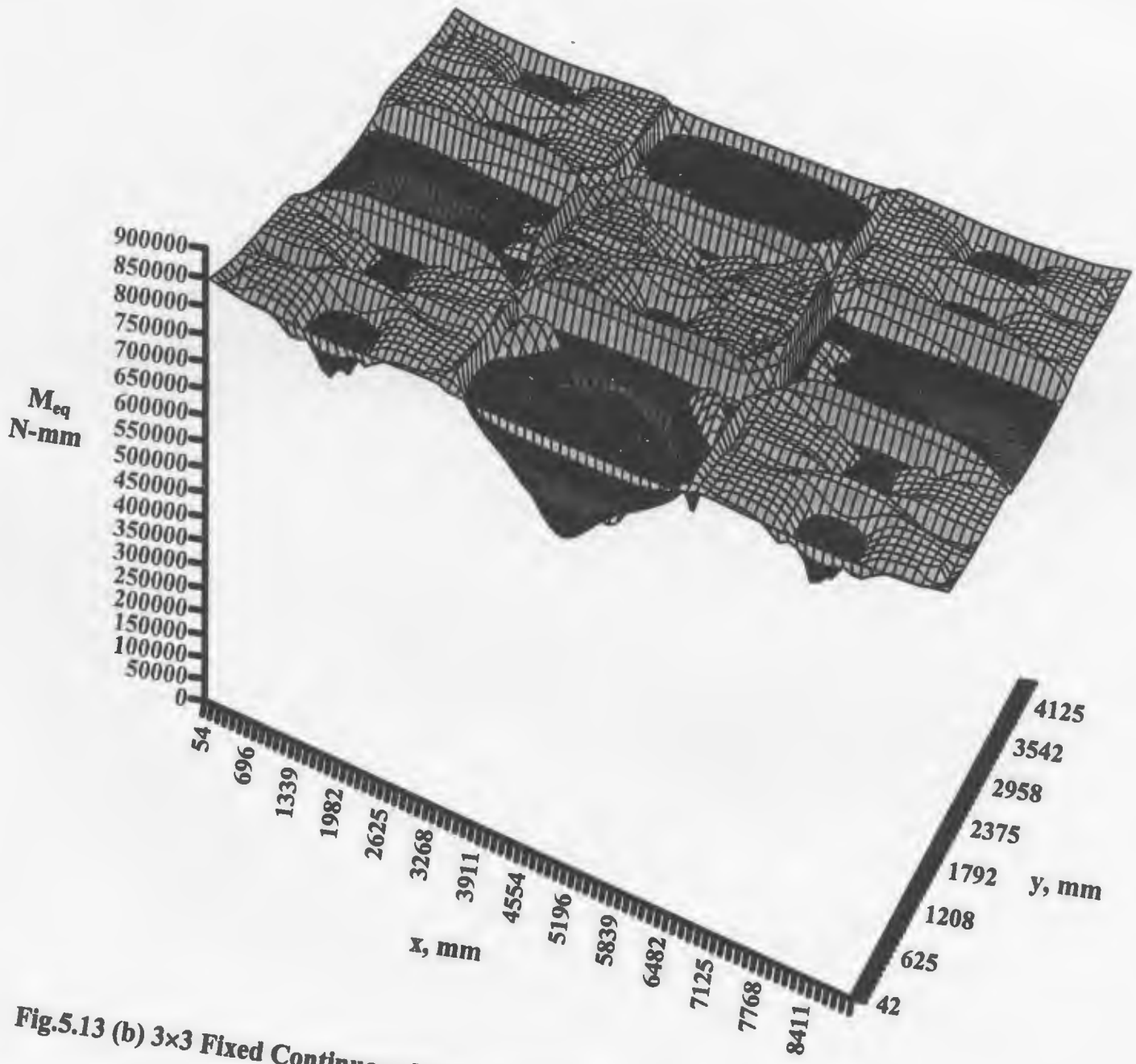

Fig.5.13 (b) 3×3 Fixed Continuous Plate –Alternate Loading, Tresca, Converged Analysis

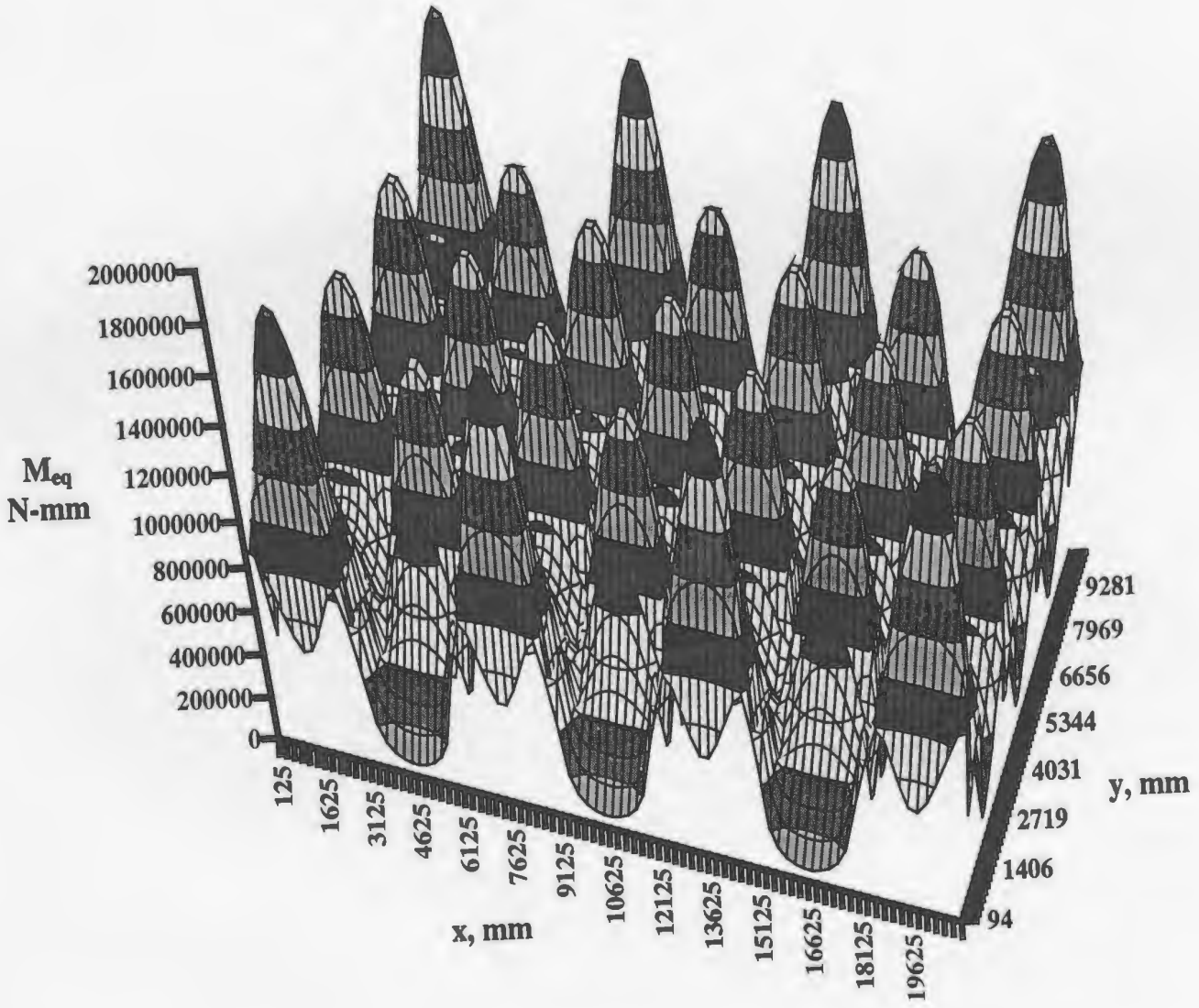

Fig. 5.14 (a) 7×7 Simply Supported Continuous Plate –Alternate Loading, Tresca, First Analysis

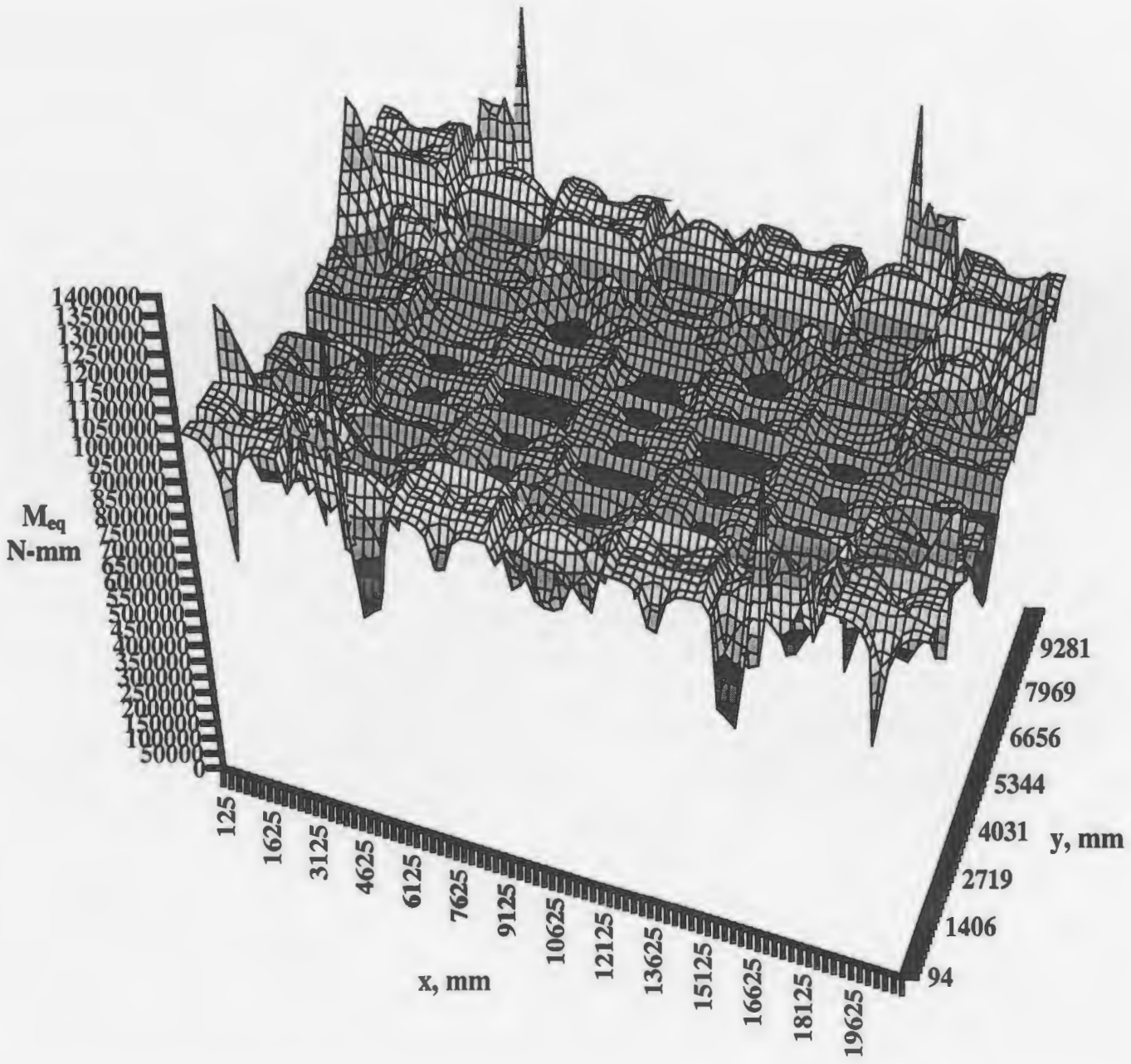

Fig. 5.14 (b) 7×7 Simply Supported Continuous Plate –Alternate Loading, Tresca, Converged Analysis

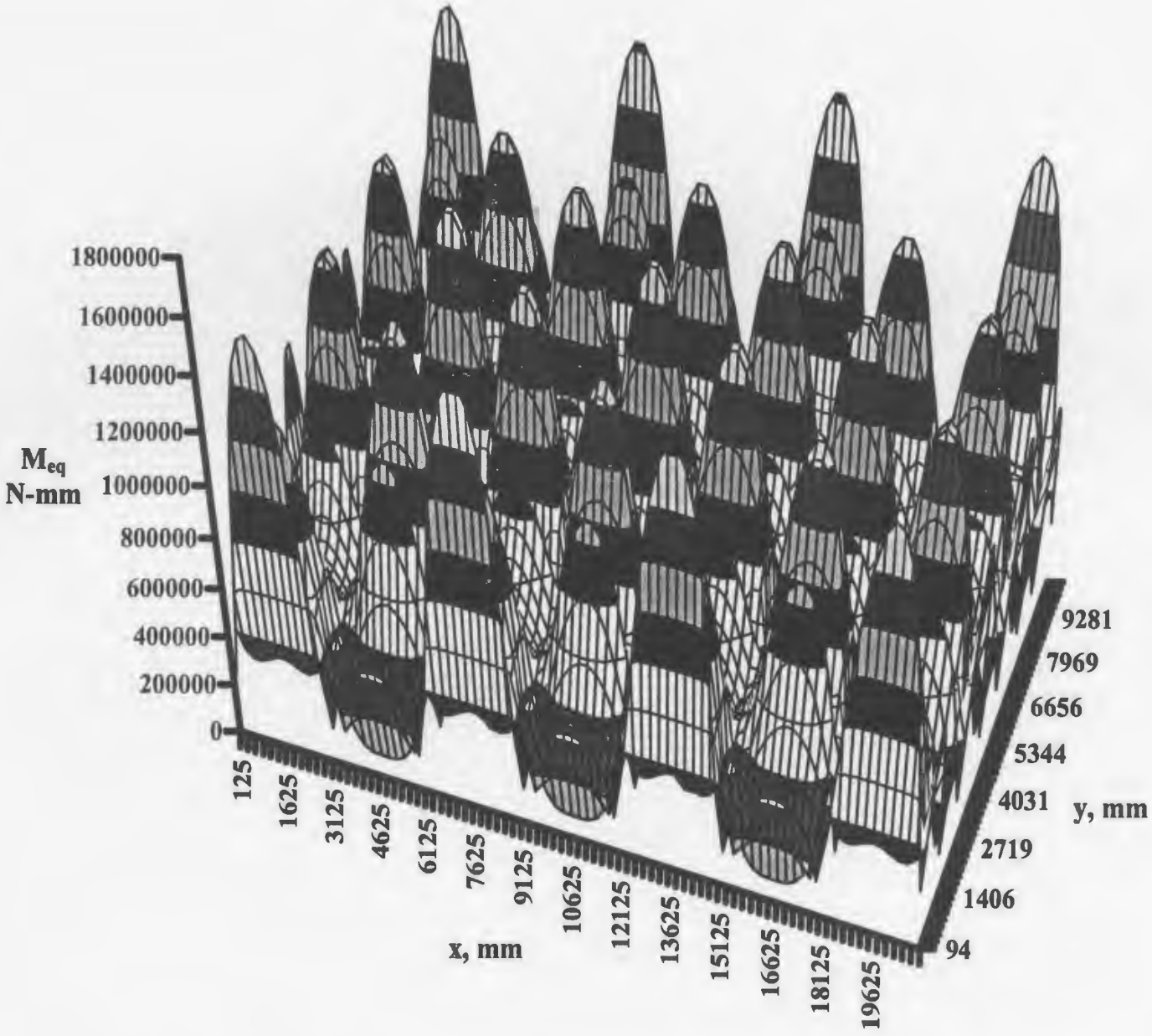

Fig. 5.15 (a) 7×7 Fixed Continuous Plate –Alternate Loading, Tresca, First Analysis

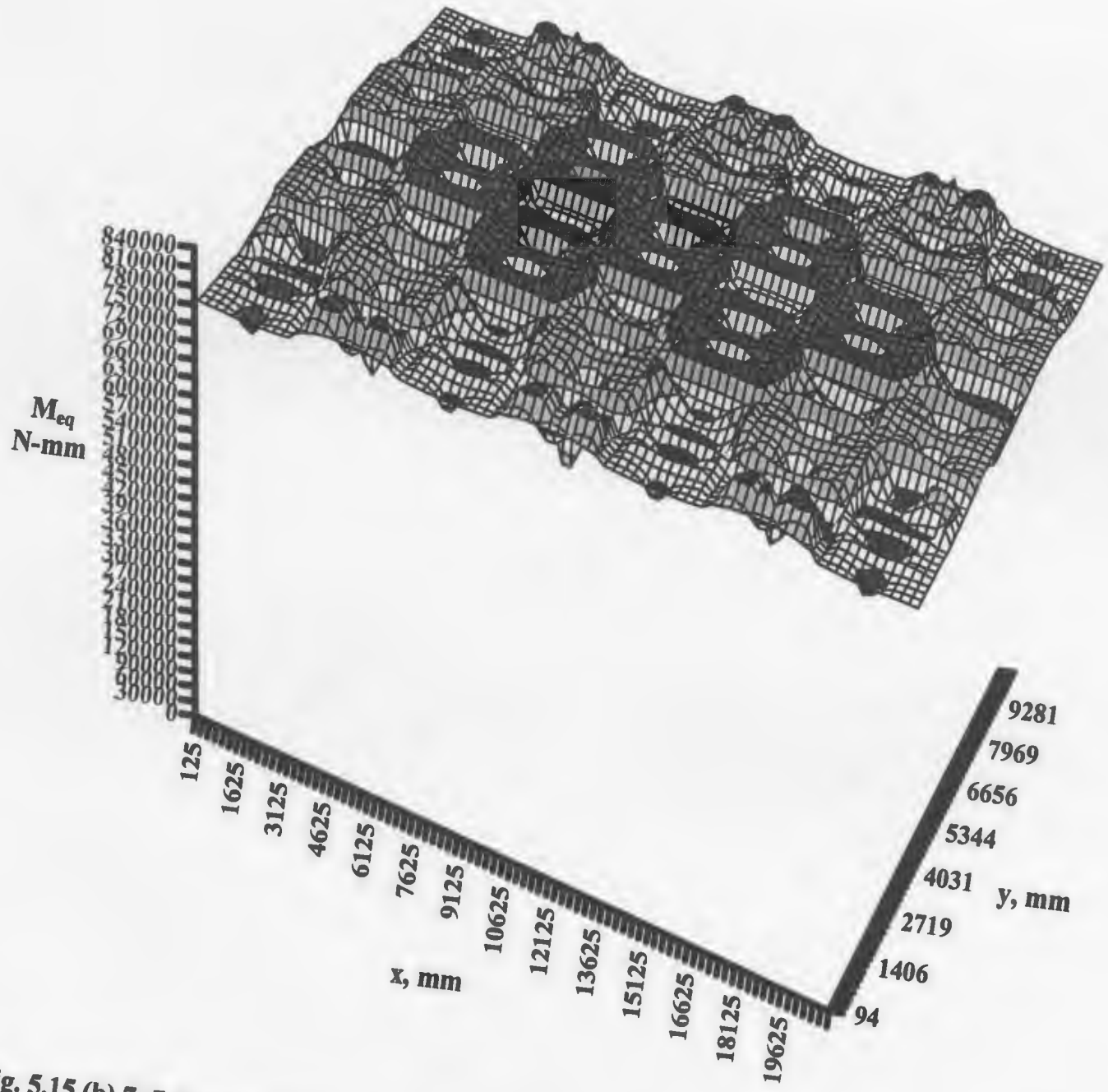

Fig. 5.15 (b) 7×7 Fixed Continuous Plate –Alternate Loading, Tresca, Converged Analysis

Chapter 6

Conclusions and Recommendations

6.1 Introduction

Limit load estimates are very useful for many engineering applications -both in design and analysis type problems. There has always been a need for robust methods for limit load analysis from the point of view of numerical stability and effort. Robust limit load analysis has gained considerable attention over the past several years. Available robust methods adopt secant modulus modification as a means to cause redistribution in an elastic structure thereby producing limit behavior. The most significant among these methods are the r-node method, elastic compensation method and the m_α method. All of these use the Von Mises yield criterion to define an effective stress. This effective stress is used to obtain an estimate of secant modulus. The r-node method involves identification of r-node peaks to obtain limit loads. Such identification might require considerable judgement in some cases. The elastic compensation method is based on a maximum stress value. Because of numerical local errors, it can sometimes be difficult to properly identify the failure mechanism and the consequent limit load. The m_α method has a better theoretical basis but is more involved than the other methods. All of these modulus modification methods need stress level modifications and consequent discretization requirements. The present thesis made use of a robust method which has

several features of the above mentioned robust techniques for the estimation of limit loads along with additional advantages. The method generalizes the advantages of the existing robust methods so that it can be applied for any yield criterion and any finite element type [Adluri, 1999, 2001a, b]. The criteria can be in terms of stresses or generalized forces such as moments and shears. The elements can be solid or plate/shell or other types. The generalization uses scaled yield criteria and is at least as accurate or better than the existing methods. It is easier (and cheaper) to apply since any type of finite element can be used. The use of this technique has been demonstrated in the present work for a variety of plate type problems.

6.2 Summary

The robust method used in the present thesis [Adluri, 2001b] is briefly summarized below:

For the plate to be analyzed, apply a loading that is proportional to the intended loading pattern. The load intensity can be arbitrary. The objective of the analysis is to obtain the proportionality load factor for this pattern that would result in the collapse of the plate structure. Choose an appropriate pattern for failure criterion such as Tresca or von Mises patterns. The actual values of the patterns are not relevant. The form of the criterion must conform to the element output variables, e.g., if plate or shell elements are used, the failure criterion must be in terms of generalized forces and moments. The objective of the analysis is to produce the relative secant stiffness field at or near collapse. Such

simulation will automatically result in the identification of the failure mechanism of the structure.

Perform a linear elastic analysis of the plate with the original properties and rigidities. Compute the principal moments and find equivalent moment as appropriate to the yield criterion chosen. Use the results to modify the local secant rigidity.

Repeat the iterative process with modified properties until convergence is achieved. A plot of the equivalent moment after converged analysis will show the scaled moment distribution similar to yield lines at collapse. Find a simple or weighted average of the equivalent moments along these 'yield' lines. The ratio between this average and the yield moment capacity of the plate section gives the required limit load factor.

This modified secant rigidity method has been implemented using plate/shell elements and ANSYS software. The implementation used fairly standard methods and was easy. Several plate problems have been analyzed using this technique. The post analysis consisted of surface plotting of equivalent moments after converged analysis. The average equivalent moment along yield lines was identified and used for limit load calculations.

6.3 Conclusions

The following are general conclusions of the present research:

1. Detailed implementation schemes have been developed for the robust method using ANSYS software and APDL routines. These routines have been automated to take any mesh and plate sizes as well as loading, material, etc. The implementation is very simple and was achieved with relative ease. If desired, it can be fully automated for any general problem thus freeing the user from any effort other than choosing the finite element mesh for initial elastic analysis.

2. The robust method using modified secant rigidity has been shown to work very well for plates of different shapes, sizes, boundary conditions, loading and yield criteria. All mesh densities are considerably smaller than those employed for the other robust techniques.

   a) For simply supported square and circular plates with UDL the error was within 0.5% compared to theoretical values.

   b) For fixed plates of regular shapes and plates with concentrated loads, the method gives limit load estimates that are very close to the classical solutions (within 0.5% to 2.5%).

   c) A rectangular plate with partial boundary condition was solved using the Von Mises criterion. This gave a difference of nearly 9% for a very coarse mesh when compared to the corresponding nonlinear FEA result. Further increase in mesh density led to better results.

d) An irregularly shaped plate with partial boundary conditions has produced an error of 3.5 % in comparison to non-linear finite element analysis. Hence the method is effective in solving irregular plate problems as well.

e) In case of continuous plates, limit load for 3×3 panel had a difference of 6 % when compared with Johansen's formula [Szilard, 1974]. The Johansen result was derived assuming that the plate had unlimited number of panels on either side. When the number of panels were increased to 7×7, the error fell to about 0.6% (even with a very coarse mesh).

f) For all problems dealt with in this thesis, eight to fourteen iterations have led to convergence. By convergence, it is meant that the average absolute percentage change was between 0.25% to 0.9%. In some problems (such as square and circular plates with UDL), limit load values computed even after the third iteration have produced very good results (within 2%) and a clear plot of collapse mechanism. In case of irregular plates, the convergence leads to divergence and again convergence.

3. In all cases where classical solutions are available, the method used here significantly out performed the nonlinear finite element analysis.

4. The method used does not require any discretization through the thickness of the plates. Hence, much less number of elements is needed compared to those for other robust methods that generally require solid elements.

5. The method can be shown to predict better limit load estimates in comparison to other methods. For example, after two analyses, the method is theoretically guaranteed to give at least as good an accuracy (or better) when compared to the r-node method.

6. The surface plot of the converged equivalent moment clearly shows the yield lines and hence the collapse mechanism of the structure.

7. The study conducted in this thesis involved the use of both Tresca and Von Mises yield criteria and has produced very good results for various types of plates. The present method works with any other yield criterion. Other methods such as r-node have not been implemented for general yield criteria such as Tresca.

8. The modification of secant rigidity can be performed by using any material or geometric parameter, such as Young's modulus, area, thickness, etc. There is no need for calculation of additional parameters (such as yield functions based on Ilyushin's model as in the case of ECM).

9. Some of the disadvantages of the existing modified modulus methods could be avoided by using the present technique.

10. In some cases, the method suggested yield line patterns that slightly deviated from the traditionally assumed yield line set. With further research, this might result in the improvement of classical results.

6.4 Recommendations for Further Research

The research presented in this thesis is applicable for thin plate structures with bending capabilities. The present study was limited to material non-linearity and isotropic material behavior. Further work is recommended for the following areas:

1. Thick plate structures, deep beams and shells that involve significant shear forces in addition to bending moments.

2. Extending the method to large deformation or geometrically non-linear problems.

3. The effectiveness of the method needs to be checked on complicated areas such as stress concentration, fracture, etc.

4. The selection of average equivalent moment along yield lines requires a bit of judgement. Hence, research may be directed towards developing an automated process, which can select the yield line pattern with ease.

5. Materials such as reinforced concrete are generally orthotropic in behavior. Hence, it would be relevant to extend this technique for orthotropic material behavior.

References

Adluri, Seshu Madhava Rao, 1999. "Robust estimates of limit loads of steel structures using modified geometric properties of members," *MUN EAST Report No: 99-1, Engineering & Applied Science Research Report Series*, Faculty of Engineering & Applied Science, Memorial University of Newfoundland, St. John's, NF, Canada.

Adluri, Seshu Madhava Rao, 2001a. "Direct Estimation of Limit Loads Using Secant Rigidity and Scaled Yield Criteria," *CANCAM 2001*, Canadian Conf. App. Mech., St. John's, NF.

Adluri, Seshu Madhava Rao, 2001b. "Robust Estimates of Limit Loads using Secant Rigidity and Scaled Yield Criteria," (Under Review).

Anderson, R.G., Gardner, L.R.T., and Hodgkins, W.R., 1963. "Deformation of uniformly loaded beams obeying complex creep laws," *Journal of Mechanical Engineering Science*, Vol. 5, pp.238.

ANSYS, 1997a. *User manuals for Theory, Commands, Elements and Procedures*, Ninth ed. ANSYS Inc., PA, USA.

ANSYS, 1997b. *Structural analysis guide*, Third ed. ANSYS Inc., PA, USA.

ANSYS, 1997c. *Basic analysis procedures guide*, Second ed. ANSYS Inc., PA, USA.

Baker, E.H., Kovalevsky, L., and Rish, F.L., 1972. *Structural analysis of shells*, McGraw Hill Inc., USA.

Bolar, A.A., and Adluri, S.M.R., 2001. "Limit Load Estimation for Plates using Secant Rigidity," *CANCAM 2001*, Canadian Conf. App. Mech., St John's, NF

Boyle, J.T., Hamilton, R., Shi, J., and Mackenzie, D., 1997. "A simple method of calculating lower-bound limit loads for axisymmetric thin shells," *Transactions of the ASME*, Vol. 119 pp.236-242.

Calladine, C.R., 1969. *Engineering Plasticity*, First ed. Pergamon press, London.

Chen, W.F., and Han, D.J. 1987. *Plasticity for Structural Engineers*, Springer-Verlag New York Inc., USA.

CSA, 1994. *CAN/CSA-S16.1-94 -- Limit States Design of Steel Structures*, Canadian Standards Association, Rexdale, Ontario.

Dhalla, A.K., and Jones, G.L. 1986. "ASME code classification of pipe stresses: A simplified elastic procedure," *International Journal of Pressure Vessels and Piping*, Vol. 26 pp. 145-166.

Dhalla, A.K., 1984. "Verification of an elastic procedure to estimate elastic follow-up," *Design of Elevated Temperature Piping, Pressure Vessels and Piping Division, ASME, New York* Vol. 86 pp. 81-96.

Dhalla, A.K., 1987. "A simplified procedure to classify stresses for elevated temperature service," *Design and Analysis of Piping, Pressure Vessels and Components: Pressure Vessesls and Piping Division, ASME, New York* Vol. 120 pp. 177-188.

Fernando, C.P.D., 1992. *Limit loads of mechanical components and structures using the Gloss r-node method*, M.Eng thesis, University of Regina, Saskatchewan.

Florin G.P.E., 1980. *Theory and Design of surface structures and slabs and plates*, Series on Structural Engineering, Vol.2,, Trans Tech Publications, Germany.

Hopkins, H.G., and Wang, A J., 1954. "Load carrying capacities of circular plates of perfectly plastic material with arbitrary yield condition," *Journal of Mechanics and Physics of Solids*, Vol. 3, pp.117-129.

Johansen, K.W., 1972. *Yield line formulae for slabs*, Cement and Concrete Association, London.

Jaeger, L.G., 1964. *Elementary theory of elastic plates*, Pergamon press Ltd.

Kizhatil, R.K., and Seshadri, R., 1991. "Inelastic strain concentration factors and low cycle fatigue of pressure components using GLOSS Analysis," *Proceedings of the ASME-PVP Conference*, San Diego, Vol. 210, pp 149-154.

Lopez, L A., and Ang, A H-S, 1966. *Flexural analysis of elastic plastic rectangular plates*, Technical report, University of Illinois, Urbana, Illinois.

MacGregor, J.G. and Bartlett, F.M., 2000. *Reinforced Concrete- Mechanics and Design*, Prentice Hall Canada Inc., Ontario, Canada.

Mackenzie, D., and Boyle, J.T., 1993. "A method of estimating limit loads by iterative elastic analysis. I-simple examples," *Journal of Pressure Vessel Technology*, Vol. 53 pp. 77-95.

Mackenzie, D., Boyle, J.T., and Hamilton, R., 2000. "The elastic compensation method for limit and shakedown analysis: a review," *Journal of Strain Analysis*, Vol. 35 No. 3, pp. 171-188.

Mackenzie, D., Nadarajah, C., Shi, J., Boyle, J.T., 1993. "Simple bounds on limit loads by elastic finite element analysis," Journal of Pressure vessel technology Vol. 115 pp. 27-31.

Mackenzie, D., Shi, J., and Boyle, J.T., 1992. "Finite element modeling for limit analysis by the elastic compensation method," *Computers and Structures, Elsevier Science Limited*, Vol. 51 No.4 pp. 403-410.

Mangalaramanan, S.P., 1993. *Robust limit loads for plate structures*, M.Sc. Thesis, Faculty of Engineering, University of Regina, Regina, Saskatchewan, Canada.

Mangalaramanan, S.P., 1997a. *Robust limit loads using elastic modulus adjustment techniques*, Ph.D. Dissertation, Faculty of Engineering, Memorial University, St John's, Newfoundland, Canada.

Mangalaramanan, S.P., 1997b. "Conceptual models for understanding the role of r-nodes in plastic collapse," *Journal of Pressure Vessel Technology*, Vol. 119 pp. 374-378.

Mangalaramanan, S.P., and Seshadri, R., 1995. "Robust limit loads of symmetric and non-symmetric plate structures," *Transactions of the CSME*, Vol.19, No.3, pp.227-246.

Marriott, D.L., 1988. "Evaluation of deformation or load control of stresses under inelastic conditions using elastic finite element stress analysis," *Proceedings of the ASME-PVP Conference*, Pittsburgh, Vol. 136.

Mura, T., and Lee, S.L., 1962. "Application of variational principles to limit analysis," *Quarterely of Applied Mathematics*, Vol.21, No. 3, pp.243-248.

Mura, T., Rimawi, W.H., Lee, S.L., 1964. "Extended theorems of limit analysis," *Quarterely of Applied Mathematics*, Vol.23, No. 2, pp.171-179.

Nadarajah, C., Mackenzie, D., and Boyle, J.T., 1993. "A method of estimating limit loads by iterative elastic analysis. II-nozzle sphere intersections with internal pressure and radial load," *International Journal of Pressure Vessels and Piping*, Vol. 53 pp. 97-119.

Nawy, E.G., 2000. *Reinforced Concrete -A fundamental approach*, Fourth ed., Prentice Hall, Upper Saddle River, New Jersey

Popov, Egor, 1968. *Introduction to Mechanics of Solids*, Prentice Hall Inc., Englewood Cliffs, N.J.

Raghavan, P., 1998. *Simplified inelastic analysis of notched components subjected to mechanical and thermal loads*, M.Eng thesis, Faculty of Engineering, Memorial University, St John's, Newfoundland, Canada.

Ralph, F., 2000. *Robust methods of finite element analysis: Evaluation of non-linear, lower bound limit loads of plated structures and stiffening members*, M.Eng. thesis, Faculty of Engineering, Memorial University, St John's, Newfoundland, Canada.

Save, M., 1995. *Atlas of limit loads of metal plates, shells and disks*, Elsevier, Amsterdam, Netherlands.

Save, M.A., and Massonet, C.E., 1972. *Plastic analysis and design of plates, shells and disks*, North-Holland publishing company, Amsterdam, Netherlands

Seshadri, R., 1991. "The generalized local stress strain (GLOSS) analysis - Theory and applications," *Journal of pressure vessel technology*, Vol. 113 pp. 219-227.

Seshadri, R., 1997. "In search of redistribution nodes," *International Journal of Pressure Vessels and Piping* Vol. 73 pp. 69-76.

Seshadri, R., 2000. "Limit loads using extended variational concepts in plasticity," *Journal of pressure vessel technology*, Vol. 122 pp. 379-385.

Seshadri, R., and Fernando, C.P.D., 1992. "Limit loads of mechanical components and structures using the GLOSS r-node method," *ASME Journal of pressure vessel technology*, Vol. 114, pp. 201-208.

Seshadri, R., and Kizhatil, R.K., 1990. "Inelastic analyses of pressure components using the GLOSS diagram," *Proceedings of the ASME-PVP Conference*, Nashville, Vol. 186, pp. 105-113.

Seshadri, R., and Mangalaramanan, S.P., 1997. "Lower bound limit loads using variational concepts: the m_α method," *International Journal of Pressure Vessels and Piping*, Vol. 71 pp.93-106.

Seshadri, R., and Marriott, D.L., 1992. "On relating to the reference stress, limit load and the ASME stress classification concepts," *Journal of Pressure vessels and piping* Vol.230 pp.135-149.

Shi, J., Mackenzie, D., and Boyle, J.T., 1993. "A method of estimating limit loads by iterative elastic analysis. III-torospherical heads under internal pressure," *International Journal of Pressure Vessels and Piping*, Vol. 53 pp. 121-142.

Sim, R.G., 1968. *Creep of Structures*, Ph.D. Dissertation, University of Cambridge.

Sobotka, Z., 1989. *Theory and Limit design of plates*, Elsevier, Amsterdam, Netherlands.

Szilard, R., 1974. *Theory and analysis of plates -classical and numerical methods*, Prentice-hall, Inc., Englewood Cliffs, New Jersey.

Timonshonko, S.P., and Woinowsky-Krieger, S., 1989. *Theory of Plates and Shells*, Second ed., McGraw-Hill book company, Singapore

Ugural, A. 1999. *Stresses in plates and shells*, Second ed., McGraw-Hill companies Inc., USA.

Wood, R.H., 1965. *Plastic and elastic design of slabs and plates*, First ed. The Ronald Press Company, New York.

Young, W.C., 1989. *Roark's Formulas for stress and strain*, Sixth ed., McGraw-Hill Book Company, USA.

Appendices

The macros presented in Appendix A are for elastic analysis of the plate structures analysed in this thesis. Appendix B has the macro for modifying secant rigidity, calculating equivalent moments and repeated analysis. These have to work in conjunction with the problems of Appendix A. The appropriate macro, Tresca (Appendix B.1.1) or Von Mises (Appendix B.1.2) can be placed in the current working directory of the operating system along with a plate model macro of Appendix A.. The results after the analysis will be stored in a file named "results"

Appendix C consist of macros for non-linear analysis implemented in this thesis

The dimensions and mesh sizes for all these problems can easily be changed at places mentioned in the comments of the macro. As for the continuous plates (A.3.1 and A.3.2), the macro can permit different sizes of mesh, panel as well as number of panels.

APPENDIX A

A.1. ANALYSIS OF REGULAR PLATES USING MODIFIED SECANT RIGIDITY.

A.1.1 Simply supported square plate subjected to uniform pressure.

```
!
! ###### ANALYSIS OF A PLATE USING MODIFIED SECANT RIGIDITY ######
!

/TITLE, ANALYSIS OF A SQUARE PLATE USING MODIFIED SECANT RIGIDITY
/GRA,POWER
/GST,ON
/PREP7                          ! ENTER PRE PROCESSOR

ET,1,SHELL63                    ! USE SHELL 63 ELEMENT

*SET,THK,10                     ! THICKNESS IN MM
*SET,EM,200000                  ! YOUNG'S MODULUS IN N/SQ MM
*SET,L1,1000                    ! LENGTH IN MM
*SET,B1,1000                    ! BREADTH IN MM
*SET,LZ,40                      ! LINE DIVISIONS ALONG LENGTH
*SET,BZ,40                      ! LINE DIVISIONS ALONG BREADTH
*SET,P,10                       ! PRESSURE LOAD IN NEWTONS/SQ.MM

R,1,THK, , , , , ,              ! INPUT THICKNESS
RMORE, , , , , ,
UIMP,1,EX, , ,EM,               ! INPUT YOUNG'S MODULUS

k,1,0,0,0,,,,
k,2,L1,0,0,,,,                  ! DEFINE KEYPOINTS
k,3,L1,B1,0,,,,
k,4,0,B1,0,,,,
L,    1,    2
L,    2,    3                   ! DEFINE LINES
L,    3,    4
L,    4,    1

LESIZE,1, , ,LZ,1,
LESIZE,2, , ,BZ,1,              ! DEFINE DIVISIONS ON LINES
LESIZE,3, , ,LZ,1,
```

```
LESIZE,4, , ,BZ,1,
AL,1,2,3,4                    ! DEFINE AREAS
ASEL,ALL,
AMESH,ALL                     ! MESH AREAS
FINISH

/gopr

/SOLU,

nsel,s,loc,x,0
D,all, , , , , , , ,uz
nsel,all

nsel,s,loc,x,L1
d,all, , , , , , , ,uz
nsel,all

nsel,s,loc,y,0
d,all, , , , , , , ,uz
nsel,all

nsel,s,loc,y,B1,
d,all, , , , , , , ,uz        ! CONSTRAINTS UZ
nsel,all

nsel,s,loc,x,0
nsel,r,loc,y,0
D,all, , , , , , ,ux          ! CONSTRAINTS UX
nsel,all

nsel,s,loc,x,L1
nsel,r,loc,y,0
d,all, , , , , , ,uy
nsel,all

nsel,s,loc,x,L1
nsel,r,loc,y,B1
d,all, , , , , , ,ux
nsel,all

nsel,s,loc,x,0
nsel,r,loc,y,B1,
d,all, , , , , , ,uy          ! CONSTRAINTS UY
```

```
nsel,all

SFA,ALL,1,PRES,-P
SFTRAN
ANTYPE,0                    ! DEFINE STATIC ANALYSIS
OUTRES,ALL,ALL
SAVE
SOLVE
FINISH
/INP,macro1                 ! ## INPUT MACRO FOR ANALYSIS ###
```

A.1.2 Circular plate subjected to uniform pressure.

```
! # ANALYSIS OF A CIRCULAR PLATE USING MODIFIED SECANT RIGIDITY #
!

/TITLE, ANALYSIS OF A CIRCULAR PLATE USING MODIFIED SECANT
RIGIDITY
/GRA,POWER
/GST,ON
/PREP7                      ! ENTER PRE PROCESSOR

ET,1,SHELL63                ! USE SHELL 63 ELEMENT
*SET,THK,10                 ! THICKNESS IN MM
*SET,EM,200000              ! YOUNG'S MODULUS IN N/SQ MM
*SET,RAD,250                ! RADIUS IN MM
*SET,LZ,30                  ! LINE DIVISIONS ALONG CIRCUMFERENCE
*SET,P,0.5                  ! PRESSURE LOAD IN NEWTONS
*SET,BZ,24                  ! LINE DIVISIONS ALONG RADIUS

R,1,THK, , , , , ,          ! INPUT THICKNESS
RMORE, , , , , , ,
UIMP,1,EX, , ,EM,           ! INPUT YOUNG'S MODULUS

K,1,0,0,,
K,50,0,RAD,0,,
L,1,50
LSEL,ALL
LESIZE,1, , ,LZ,LZ,
K,51,0,0,20,
LSEL,ALL

AROTAT,1,,,,,,1,51,,BZ
```

```
LSEL,S,RADIUS,,RAD
LESIZE,all, , ,1,1,
LSEL,ALL

ASEL,ALL

AMESH,ALL

FINISH

/GOPR

/SOLU,

CSYS,1                          ! CYLINDRICAL CO-ORDINATES
NSEL,S,LOC,X,RAD,360
D,ALL,UZ, , , , , ,
NSEL,ALL

CSYS,0                          ! CARTESIAN CO-ORDINATES

NSEL,S,LOC,X,0
NSEL,R,LOC,Y,0
D,ALL,UX
D,ALL,UY
D,ALL,ROTZ
NSEL,ALL

SFA,ALL,1,PRES,-P               ! APPLY PRESSURE LOAD

ANTYPE,0                        ! DEFINE STATIC ANALYSIS
OUTRES,ALL,ALL
SAVE
SOLVE
FINISH

/POST1

RSYS,1                          ! OUTPUT RESULTS IN CYLINDRICAL
                                ! CO-ORDIANTES


/INP,macro1                     ! ## INPUT MACRO FOR ANALYSIS ###
```

A.1.3 Fixed square plate subjected to uniform pressure.

```
!
! # ANALYSIS OF A FIXED PLATE USING MODIFIED SECANT RIGIDITY #
!

/TITLE, ANALYSIS OF A FIXED PLATE USING MODIFIED SECANT RIGIDITY
/GRA,POWER
/GST,ON

/PREP7                          ! ENTER PRE PROCESSOR

ET,1,SHELL93                    ! USE SHELL 93 ELEMENT
*SET,THK,10                     ! THICKNESS IN MM
*SET,EM,200000                  ! YOUNG'S MODULUS IN N/SQ MM
*SET,L1,1000                    ! LENGTH IN MM
*SET,B1,1000                    ! BREADTH IN MM
*SET,LZ,80                      ! LINE DIVISIONS ALONG LENGTH
*SET,BZ,80                      ! LINE DIVISIONS ALONG BREADTH
*SET,P,6                        ! UNIFORM LOAD IN NEWTONS PER NODE

R,1,THK, , , , , ,              ! INPUT THICKNESS
RMORE, , , , , , ,
UIMP,1,EX, , ,EM,               ! INPUT YOUNG'S MODULUS

k,1,0,0,0,,,,
k,2,L1,0,0,,,,                  ! DEFINE KEYPOINTS
k,3,L1,B1,0,,,,
k,4,0,B1,0,,,,
L,1,2                           ! DEFINE LINES
L,2,3
L,3,4
L,4,1

LESIZE,1, , ,LZ,1,
LESIZE,2, , ,BZ,1,              ! DEFINE DIVISIONS ON LINES
LESIZE,3, , ,LZ,1,
LESIZE,4, , ,BZ,1,
AL,1,2,3,4                      ! DEFINE AREAS
ASEL,ALL,
AMESH,ALL                       ! MESH AREAS
finish
```

```
/gopr

/SOLU,

nsel,s,loc,x,0
D,all, , , , , , ,uz,roty
nsel,all

nsel,s,loc,x,L1
d,all, , , , , , ,uz,roty
nsel,all

nsel,s,loc,y,0
d,all, , , , , , ,uz,rotx
nsel,all

nsel,s,loc,y,B1,
d,all, , , , , , ,uz,rotx
nsel,all

nsel,s,loc,x,0
nsel,r,loc,y,0
D,all, , , , , ,ux,rotz                ! CONSTRAINTS
nsel,all

nsel,s,loc,x,L1
nsel,r,loc,y,0
d,all, , , , , ,uy,rotz
nsel,all

nsel,s,loc,x,L1
nsel,r,loc,y,B1
d,all, , , , , ,ux,rotz
nsel,all

nsel,s,loc,x,0
nsel,r,loc,y,B1,
d,all, , , , , ,uy,rotz
nsel,all

SFA,ALL,1,PRES,-P                      ! APPLY PRESSURE LOAD
ANTYPE,0                               ! DEFINE STATIC ANALYSIS
OUTRES,ALL,ALL
```

```
SAVE
SOLVE
FINISH
/INP,macro1                    ! ## INPUT MACRO FOR ANALYSIS ###
```

A.1.4 Simply supported circular plate subjected to central concentrated load.

```
!
! #### ANALYSIS OF A CIRCULAR PLATE USING MODIFIED SECANT
!RIGIDITY ######
!

/TITLE, ANALYSIS OF A CIRCULAR PLATE USING MODIFIED SECANT
RIGIDITY
/GRA,POWER
/GST,ON
/PREP7                         ! ENTER PRE PROCESSOR

ET,1,SHELL63                   ! USE SHELL 63 ELEMENT

*SET,THK,10                    ! THICKNESS IN MM
*SET,EM,200000                 ! YOUNG'S MODULUS IN N/SQ MM
*SET,RAD,250                   ! RADIUS IN MM
*SET,LZ,30                     ! LINE DIVISIONS ALONG CIRCUMFERENCE
*SET,P,1000                    ! CENTRAL CONC. LOAD IN NEWTONS
*SET,BZ,24                     ! LINE DIVISIONS ALONG RADIUS

R,1,THK, , , , , ,             ! INPUT THICKNESS
RMORE, , , , , , ,
UIMP,1,EX, , ,EM,              ! INPUT YOUNG'S MODULUS

K,1,0,0,,
K,50,0,RAD,0,,
L,1,50
LSEL,ALL
LESIZE,1, , ,LZ,LZ,
K,51,0,0,20,
LSEL,ALL

AROTAT,1,,,,,,1,51,,BZ
```

```
LSEL,S,RADIUS,,RAD
LESIZE,all, , ,1,1,
LSEL,ALL

ASEL,ALL
AMESH,ALL
FINISH

/GOPR

/SOLU,

CSYS,1                          ! CHANGE TO CYLINDRICAL CO-ORDINATES
NSEL,S,LOC,X,RAD,360
D,ALL,UZ, , , , , ,
NSEL,ALL

CSYS,0                          ! CHANGE TO CARTESIAN CO-ORDINATES

NSEL,S,LOC,X,0
NSEL,R,LOC,Y,0
D,ALL,UX
D,ALL,UY
D,ALL,ROTZ
NSEL,ALL

F,1,FZ,-P                       ! APPLY CONCENTRATED LOAD AT CENTRE
NODE

ANTYPE,0                        ! DEFINE STATIC ANALYSIS
OUTRES,ALL,ALL
SAVE
SOLVE
FINISH

/POST1
RSYS,1                          ! OUTPUT RESULTS IN CYLINDRICAL
                                ! CO-ORDIANTES

/INP,macro1                          ! ## INPUT MACRO FOR ANALYSIS ###
```

A.1.5 Rectangular plate supported on opposite sides and subjected to uniform pressure.

```
!
! # ANALYSIS OF A PLATE FIXED ON OPPOSITE SIDES USING MODIFIED
!SECANT RIGIDITY METHOD #
!

/TITLE, ANALYSIS OF A PLATE USING MODIFIED SECANT RIGIDITY
/GRA,POWER
/GST,ON
/PREP7                          ! ENTER PRE PROCESSOR

ET,1,SHELL63                    ! USE SHELL 63 ELEMENT
*SET,THK,10                     ! THICKNESS IN MM
*SET,EM,200000                  ! YOUNG'S MODULUS IN N/SQ MM
*SET,L1,1500                    ! LENGTH IN MM
*SET,B1,1000                    ! BREADTH IN MM
*SET,LZ,60                      ! LINE DIVISIONS ALONG LENGTH
*SET,BZ,40                      ! LINE DIVISIONS ALONG BREADTH
*SET,P,5                        ! PRESSURE LOAD IN NEWTONS

R,1,THK, , , , , ,              ! INPUT THICKNESS
RMORE, , , , , , ,
UIMP,1,EX, , ,EM,               ! INPUT YOUNG'S MODULUS

k,1,0,0,0,,,,
k,2,L1,0,0,,,,                  ! DEFINE KEYPOINTS
k,3,L1,B1,0,,,,
k,4,0,B1,0,,,,

L,1,2
L,2,3                           ! DEFINE LINES
L,3,4
L,4,1

LESIZE,1, , ,LZ,1,
LESIZE,2, , ,BZ,1,              ! DEFINE DIVISIONS ON LINES
LESIZE,3, , ,LZ,1,
LESIZE,4, , ,BZ,1,
AL,1,2,3,4                      ! DEFINE AREAS
```

```
ASEL,ALL,
AMESH,ALL                    ! MESH AREAS
finish

/gopr

/SOLU,

nsel,s,loc,x,0
D,all, , , , , , , ,uz
nsel,all

nsel,s,loc,x,L1
d,all, , , , , , , ,uz
nsel,all

nsel,s,loc,x,0
nsel,r,loc,y,0
D,all, , , , , , ,ux         ! CONSTRAINTS
nsel,all

nsel,s,loc,x,L1
nsel,r,loc,y,0
d,all, , , , , , ,uy
nsel,all

nsel,s,loc,x,L1
nsel,r,loc,y,B1
d,all, , , , , , ,ux
nsel,all

nsel,s,loc,x,0
nsel,r,loc,y,B1,
d,all, , , , , , ,uy
nsel,all

SFA,all,1,pres,-P            ! APPLY UNIFORMLY DISTRIBUTEDLOAD
SFTRAN
nsel,all

ANTYPE,0                     ! DEFINE STATIC ANALYSIS
OUTRES,ALL,ALL
SAVE
SOLVE
```

```
FINISH

INP,macmises                    ! ## INPUT MACRO FOR ANALYSIS ###
```

A.1.6 Rectangular plate simply supported on three sides (longer edge free) and subjected to uniform pressure.

```
!
! ## ANALYSIS OF A PLATE SUPPORTED ON THREE SIDES USING MODIFIED
! SECANT RIGIDITY ##
!

/TITLE, ANALYSIS OF A PLATE USING MODIFIED SECANT RIGIDITY
/GRA,POWER
/GST,ON
/PREP7                          ! ENTER PRE PROCESSOR

ET,1,SHELL63                    ! USE SHELL 63 ELEMENT
*SET,THK,10                     ! THICKNESS IN MM
*SET,EM,200000                  ! YOUNG'S MODULUS IN N/SQ MM
*SET,L1,1500                    ! LENGTH IN MM
*SET,B1,900                     ! BREADTH IN MM
*SET,LZ,90                      ! LINE DIVISIONS ALONG LENGTH
*SET,BZ,60                      ! LINE DIVISIONS ALONG BREADTH
*SET,P,5                        ! PRESSURE  IN NEWTON PER SQ.MM

R,1,THK, , , , , ,              ! INPUT THICKNESS
RMORE, , , , , , ,
UIMP,1,EX, , ,EM,               ! INPUT YOUNG'S MODULUS

k,1,0,0,0,,,,
k,2,L1,0,0,,,,                  ! DEFINE KEYPOINTS
k,3,L1,B1,0,,,,
k,4,0,B1,0,,,,
L,1,2
L,2,3                           ! DEFINE LINES
L,3,4
L,4,1

LESIZE,1, , ,LZ,1,
LESIZE,2, , ,BZ,1,              ! DEFINE DIVISIONS ON LINES
LESIZE,3, , ,LZ,1,
LESIZE,4, , ,BZ,1,
AL,1,2,3,4                      ! DEFINE AREAS
```

```
ASEL,ALL,
AMESH,ALL                    ! MESH AREAS
finish

/gopr

/SOLU,

nsel,s,loc,x,0
D,all, , , , , , , ,uz
nsel,all

nsel,s,loc,x,L1
d,all, , , , , , , ,uz
nsel,all

nsel,s,loc,y,0
d,all, , , , , , , ,uz
nsel,all

nsel,s,loc,x,0
nsel,r,loc,y,0
D,all, , , , , , ,ux         ! CONSTRAINTS UX
nsel,all

nsel,s,loc,x,L1
nsel,r,loc,y,0
d,all, , , , , , ,uy
nsel,all

nsel,s,loc,x,L1
nsel,r,loc,y,B1
d,all, , , , , , ,ux
nsel,all

nsel,s,loc,x,0
nsel,r,loc,y,B1,
d,all, , , , , , ,uy
nsel,all

SFA,all,1,pres,-P            ! APPLY UNIFORMLY DISTRIBUTEDLOAD
SFTRAN
nsel,all
ANTYPE,0                     ! DEFINE STATIC ANALYSIS
```

```
OUTRES,ALL,ALL
SAVE
SOLVE
FINISH
/INP,macro1                    ! ## INPUT MACRO FOR ANALYSIS ###
```

A.2. ANALYSIS OF IRRREGULAR PLATES USING SECANT RIGIDITY

A.2.1 Rectangular plate partially fixed and partially simply supported.

```
!
! ## ANALYSIS OF A RECTANGULAR PLATE PARTIALLY FIXED AND
!  PARTIALLY SIMPLY SUPPORTED USING MODIFIED SECANT RIGIDITY ##
!

/TITLE,ANALYSIS OF A IRREGULAR PLATE USING MODIFIED SECANT
/TITLE,RIGIDITY
/GRA,POWER
/GST,ON
/PREP7

ET,1,SHELL63
*SET,THK,12.7                  ! THICKNESS IN MM
*SET,EM,206913.383             ! YOUNGS MODULUS
*SET,L,381                     ! LENGTH IN MM
*SET,B,254                     ! BREADTH IN MM
*SET,LZ,84                     ! LINE DIVISIONS ALONG LENGTH
*SET,BZ,54                     ! LINE DIVISIONS ALONG BREADTH
*SET,P,5                       ! PRESSURE LOAD IN NEWTON PER SQ.MM

R,1,THK, , , , , ,
UIMP,1,EX, , ,EM,
UIMP,1,NUXY, , ,.3,

k,1,0,0,0,
K,2,L,0,0
K,3,L,-B,0
K,4,0,-B,0

L,1,2
L,2,3
L,3,4
```

```
L,4,1

LESIZE,1, , ,LZ,1,              ! CHANGE TO VARY MESH SIZE
LESIZE,2, , ,BZ,1,          ! CHANGE TO VARY MESH SIZE
LESIZE,3, , ,LZ,1,              ! CHANGE TO VARY MESH SIZE
LESIZE,4, , ,BZ,1,              ! CHANGE TO VARY MESH SIZE

LSEL,ALL

AL,ALL

ASEL,ALL

AMESH,ALL

FINISH

/SOLU

NSEL,S,LOC,Y,0,
NSEL,R,LOC,X,0,L/3

D,ALL,ALL

NSEL,ALL

NSEL,S,LOC,Y,0
NSEL,R,LOC,X,2*L/3,L

D,ALL,ALL

NSEL,ALL

NSEL,S,LOC,Y,0,-B/3
NSEL,R,LOC,X,L

D,ALL,UZ

NSEL,ALL

NSEL,S,LOC,Y,-2*B/3,-B
NSEL,R,LOC,X,L

D,ALL,UZ
```

```
NSEL,ALL

NSEL,S,LOC,X,L/3,2*L/3
NSEL,R,LOC,Y,-B

D,ALL,ALL

NSEL,ALL

NSEL,S,LOC,Y,-B/3,-2*B/3
NSEL,R,LOC,X,0,

D,ALL,UZ

NSEL,ALL


SFA,ALL,1,PRES,P

SFTRAN
DTRAN

ANTYPE,0                ! DEFINE STATIC ANALYSIS
OUTRES,MISC,ALL
SAVE
SOLVE
FINISH

/INP,macro1             ! ## INPUT MACRO FOR ANALYSIS ###
```

A.2.2 Irregular plate partially fixed and partially simply supported.

```
/GRA,POWER
/GST,ON
/PREP7
/TITLE,ANALYSIS OF A IRREGULAR PLATE USING MODIFIED SECANT
/TITLE,RIGIDITY

ET,1,SHELL93

*SET,THK,10                    ! THICKNESS IN MM
*SET,EM,2e5                    ! YOUNGS MODULUS
*SET,L,1700                    ! LENGTH IN MM
*SET,B,1000                    ! BREADTH IN MM
*SET,P,5                       ! PRESSURE LOAD IN NEWTON PER SQ.MM

R,1,THK, , , , , ,
UIMP,1,EX, , ,EM,
UIMP,1,NUXY, , ,.3,

k,1,0,0,0,
k,2,L/3,0,0
K,3,L/3,-B/3,0
K,4,2*L/3,-B/3,0
K,5,2*L/3,0,0
K,6,L,0,0
K,7,L,-B/3,0
K,8,L,-B,0
K,9,L,-(B+L*TAN(0.2618))
K,10,0.75*L,-(B+0.75*L*TAN(0.2618)),0
K,11,0.25*L,-(B+0.25*L*TAN(0.2618)),0
K,12,0,-B,0
K,13,0,-2*B/3
K,14,0,-B/3

L,1,2
L,2,3
L,3,4
L,4,5
L,5,6
L,6,7
L,7,8
```

```
L,8,9
L,9,10
L,10,11
L,11,12
L,12,13
L,13,14
L,14,1


LESIZE,1, , ,25,1,
LESIZE,2, , ,25,1,
LESIZE,3, , ,25,1,
LESIZE,4, , ,25,1,
LESIZE,5, , ,25,1,
LESIZE,6, , ,25,1,
LESIZE,7, , ,50,1,
LESIZE,8, , ,15,1,
LESIZE,9, , ,20,1,
LESIZE,10, , ,55,1,
LESIZE,11, , ,20,1,
LESIZE,12, , ,25,1,
LESIZE,13, , ,15,1,
LESIZE,14, , ,25,1,

LSEL,ALL
AL,ALL
ASEL,ALL
AMESH,ALL

FINISH

/SOLU
DL,1,1,ALL
DL,5,1,ALL

DL,6,1,UX
DL,6,1,UY
DL,6,1,UZ

DL,8,1,UX
DL,8,1,UY
DL,8,1,UZ

DL,10,1,ALL
```

```
DL,13,1,UX
DL,13,1,UY
DL,13,1,UZ

SFA,ALL,1,PRES,-P

SFTRAN
DTRAN
ANTYPE,0              ! DEFINE STATIC ANALYSIS
OUTRES,ALL,ALL
SAVE
SOLVE
FINISH

/inp,macro1
```

A.3. ANALYSIS OF A CONTINUOUS PLATE

A.3.1 Continuous plate (3 X 3) with outer edge simply supported.

```
! # VALUES OF TA, TB, n, LA and LB may be changed to solve any panel size
! and divisions #

/GRA,POWER
/GST,ON
/PREP7
/TITLE,ANALYSIS OF A CONTINUOUS PLATE USING MODIFIED SECANT
/TITLE,RIGIDITY

ET,1,SHELL63

*SET,THK,10              ! THICKNESS IN MM
*SET,EM,2e5              ! YOUNGS MODULUS
*SET,P,10                ! PRESSURE LOAD IN NEWTON PER SQ.MM
*SET,TB,4500             ! OVERALL LENGTH, SHORT SPAN
*SET,TA,9000             ! OVERALL LENGTH, LONG SPAN
*SET,n,3                 ! NO OF PANELS DIVISIONS
*SET,LA,28               ! LINE DIVISIONS IN EACH PANEL
                         ! OF LONG SPAN
*SET,LB,18               ! LINE DIVISIONS IN EACH PANEL
                         ! OF SHORT SPAN
```

```
R,1,THK, , , , , ,
UIMP,1,EX, , ,EM,

b=TB/n
a=TA/n

k,1,0,0,0,
k,2,a,0,0
k,n+2,0,b,0

L,1,2,LA
LGEN,n,1,,,a,0,,1,

L,1,n+2,LB
LGEN,n,n+1,,,0,b,,n+1,

lsel,s,loc,x,0
LGEN,n+1,all,,,a,0,,1
lsel,all

lsel,s,loc,y,0
LGEN,n+1,all,,,0,b,,n+1
lsel,all

AL,1,(n+1),(((n+2)*n)+1),((2*n)+1)
agen,n,1,,,a,,,1
agen,n,all,,,0,b,,n+1

ASEL,ALL

AMESH,ALL

FINISH

/SOLU

*DO,SN,1,n,1

NSEL,ALL
NSEL,S,LOC,Y,0,
D,ALL,UZ

NSEL,ALL
NSEL,S,LOC,Y,SN*b,
```

```
D,ALL,UZ

NSEL,ALL
NSEL,S,LOC,X,0,
D,ALL,UZ

NSEL,ALL
NSEL,S,LOC,X,SN*a,
D,ALL,UZ

*ENDDO

NSEL,S,LOC,X,0
NSEL,R,LOC,Y,0
D,ALL,UX
NSEL,ALL

NSEL,S,LOC,X,n*a
NSEL,R,LOC,Y,0
D,ALL,UY
NSEL,ALL

NSEL,S,LOC,X,n*a
NSEL,R,LOC,Y,n*b
D,ALL,UX
NSEL,ALL

NSEL,S,LOC,X,0
NSEL,R,LOC,Y,n*b
D,ALL,UY
NSEL,ALL

ASEL,S,AREA,,1,n*n,2

SFA,ALL,1,PRES,-P          ! APPLY PRESSURE LOAD
SFTRAN
ANTYPE,0                   ! DEFINE STATIC ANALYSIS
OUTRES,ALL,ALL
SAVE
SOLVE
FINISH

/INP,macro1                ! ## INPUT MACRO FOR ANALYSIS ###
```

A.3.2 Continuous plate (3 X 3) with outer edge fixed.

```
! # VALUES OF TA,TB,n, LA and LB may be changed to solve any panel size
! and divisions #

/GRA,POWER
/GST,ON
/PREP7
/TITLE,ANALYSIS OF A CONTINUOUS PLATE USING MODIFIED SECANT
/TITLE,RIGIDITY

ET,1,SHELL63

*SET,THK,10                    ! THICKNESS IN MM
*SET,EM,2e5                    ! YOUNGS MODULUS
*SET,P,10                      ! PRESSURE LOAD IN NEWTON PER SQ.MM
*SET,TB,4500                   ! OVERALL LENGTH, SHORT SPAN
*SET,TA,9000                   ! OVERALL LENGTH, LONG SPAN
*SET,n,3                       ! NO OF PANELS DIVISIONS


*SET,LA,28                     ! LINE DIVISIONS IN EACH PANEL
                               ! OF LONG SPAN
*SET,LB,18                     ! LINE DIVISIONS IN EACH PANEL
                               ! OF SHORT SPAN

*SET,THK,10                    ! THICKNESS IN MM
*SET,EM,200000
*SET,P,10

R,1,THK, , , , , ,
UIMP,1,EX, , ,EM,

b=TB/n
a=TA/n

k,1,0,0,0,
k,2,a,0,0
k,n+2,0,b,0


L,1,2,LA
LGEN,n,1,,,a,0,,1,
```

```
L,1,n+2,LB
LGEN,n,n+1,,,0,b,,n+1,

lsel,s,loc,x,0
LGEN,n+1,all,,,a,0,,1
lsel,all

lsel,s,loc,y,0
LGEN,n+1,all,,,0,b,,n+1
lsel,all

AL,1,(n+1),(((n+2)*n)+1),((2*n)+1)

agen,n,1,,,a,,,1

agen,n,all,,,0,b,,n+1

ASEL,ALL

AMESH,ALL

FINISH

/SOLU

*DO,SN,1,n,1

NSEL,ALL
NSEL,S,LOC,Y,0,
D,ALL,UZ

NSEL,ALL
NSEL,S,LOC,Y,SN*b,
D,ALL,UZ

NSEL,ALL
NSEL,S,LOC,X,0,
D,ALL,UZ

NSEL,ALL
NSEL,S,LOC,X,SN*a,
D,ALL,UZ
```

```
*ENDDO

NSEL,S,LOC,X,0
D,ALL,ALL
NSEL,ALL

NSEL,S,LOC,X,TA
D,ALL,ALL
NSEL,ALL

NSEL,S,LOC,Y,TB
D,ALL,ALL
NSEL,ALL

NSEL,R,LOC,Y,0
D,ALL,ALL
NSEL,ALL


ASEL,S,AREA,,1,n*n,2

SFA,ALL,1,PRES,-P          ! APPLY PRESSURE LOAD
SFTRAN

ANTYPE,0                   ! DEFINE STATIC ANALYSIS
OUTRES,ALL,ALL
SAVE
SOLVE
FINISH

/INP,macro1                ! ## INPUT MACRO FOR ANALYSIS ###
```

APPENDIX B

B.1.MACRO FOR MODIFYING SECANT RIGIDITY

B.1.1 Tresca Yield Criterion

```
!
! ###### MACRO FOR MODIFYING SECANT RIGIDITY PROPERTIES ######
!
!
! ### THICKNESS OF PLATE IS DEFINED AS PARAMETER "THK" ###
! ### BELOW => THK=thickness of plate in 'mm'        ###

! INITIAL:    THK=10 mm
!             V=0.3
!             EM=2e5
!             D=(EM*THK**3)/(12*(1-V**2))

!
!             ENTER POST PROCESSOR AFTER FIRST ELASTIC ANALYSIS
!

*DO,IT,1,N                          ! N is the number of iterations

*GET,SZ,ELEM,0,COUNT

/POST1

CSYS,1                              ! Use this for Cylindrical co-ordinate system
CSYS,0                              ! Use this for Cartesian co-ordinate system

*DIM,COL1,ARRAY,1                   ! !!!!!!!!!!!!!!
*DIM,COL2,ARRAY,1                   ! !!!!!!!!!!!!!!
*DIM,COL3,ARRAY,1                   !
*DIM,COL4,ARRAY,1                   !   DEFINE
*DIM,COL5,ARRAY,1                   !   ARRAY
*DIM,COL6,ARRAY,1                   ! PARAMETERS
*DIM,COL7,ARRAY,1                   !
*DIM,COL8,ARRAY,1                   ! !!!!!!!!!!!!!!
*DIM,COL9,ARRAY,SZ                  ! !!!!!!!!!!!!!!
*DIM,COL10,ARRAY,SZ,1               !
*DIM,COL11,ARRAY,1                  ! !!!!!!!!!!!!!!
```

```
*DIM,COL12,ARRAY,1                    ! !!!!!!!!!!!!!!
*DIM,COL13,ARRAY,1                    ! !!!!!!!!!!!!!!

!
!       READING MOMENTS  Mxx, Myy, Mxy FROM FIRST ELASTIC ANALYSIS
!

SET,1
ETABLE,Mxx,SMISC,4                    ! Mxx
ETABLE,Myy,SMISC,5                    ! Myy
ETABLE,Mxy,SMISC,6                    ! Mxy

!
!       STORING ALL OUTPUT IN FILE  " result_first "
!

*SET,MN,2

*GET,MMAX1,ELEM,0,COUNT               ! Get max number of elements - MMAX1
*CFOPEN,result_first                  ! Open file " result_first "
*DO,KK,1,MMAX1,                       !

*IF,IT,EQ,1,then
NU=1
*ELSE
NU=MN
*ENDIF

*GET,cdnx,ELEM,KK,CENT,x              ! x coordinate
*GET,cdny,ELEM,KK,CENT,y              ! y coordinate
*GET,Mxx1,ELEM,KK,ETAB,Mxx           ! Mxx moment
*GET,Myy1,ELEM,KK,ETAB,Myy           ! Myy moment
*GET,Mxy1,ELEM,KK,ETAB,Mxy           ! Mxy moment
*GET,THK,RCON,NU,CONST,1             ! Get thicknesses

Meq1=abs(0.5*(Mxx1+Myy1)-((0.5*(Mxx1-Myy1))**2+(Mxy1)**2)**0.5)
Meq2=abs(0.5*(Mxx1+Myy1)+((0.5*(Mxx1-Myy1))**2+(Mxy1)**2)**0.5)

*IF,Meq1,GT,Meq2,THEN                 ! !!!!!!!!!!!!!!!!!!!!!!!!!!!!!!!!!!!!
Meq=Meq1                              !
*else                                 ! Choosing maximum of the two values of
Meq=Meq2                              ! Meq1 and Meq2
*endif                                !
THETA=0.5*ATAN((2*Mxy1)/(Mxx1-Myy1))*(180/3.1416)
```

```
COL1(1)=kk
COL2(1)=cdnx
COL3(1)=cdny
COL4(1)=Mxx1
COL5(1)=Myy1
COL6(1)=Mxy1
COL7(1)=Meq1
COL8(1)=Meq2
COL11(1)=Meq
COL12(1)=THETA
COL13(1)=THK

*VWRITE,COL1(1),COL2(1),COL3(1),COL4(1),COL5(1),COL6(1),COL7(1),COL8(1),
COL11(1),COL12(1),COL13(1)
(x,f8.1,e23.10,3x,e21.10,3x,e21.10,3x,e21.10,3x,e21.10,3x,e21.10,3x,e21.10,3x,e21.10,3
x,e21.10,3x,e21.10,3x,e21.10)

*SET,MN,MN+1
*ENDDO
*CFCLOS

!!!!     GETTING MAXIMUM EQUIVALENT MOMENT VALUE                !!!!

*VREAD,COL10(1,1),result_first,,,ij,SZ,1   ! Read Equivalent moments
(132x,e21.10)
*STAT,COL10(1,1)                          ! Print values in output file
*VSCFUN,COL9(1),MAX,COL10(1,1)      ! Maximum Meq       ! Get maximum value

        !x means one spacing
        !f6.1 means 6 digits and one decimal place (6 incl)
        !e21.10 means 21 digits and one decimal place(21 incl)

!     MODIFYING THICKNESS USING VALUES OF EQUIVALENT MOMENTS
!     AND STORING IN FILE " MODVAL1 "
!

*SET,MN,2

*CFOPEN,MODVAL1
*DO,J,1,MMAX1

*IF,IT,EQ,1,then
NU=1
```

```
*ELSE
NU=MN
*ENDIF

*GET,Mxx1,ELEM,J,ETAB,Mxx
*GET,Myy1,ELEM,J,ETAB,Myy
*GET,Mxy1,ELEM,J,ETAB,Mxy
*GET,THK,RCON,NU,CONST,1              ! Get thicknesses

Meq1=abs(0.5*(Mxx1+Myy1)-((0.5*(Mxx1-Myy1))**2+(Mxy1)**2)**0.5)
Meq2=abs(0.5*(Mxx1+Myy1)+((0.5*(Mxx1-Myy1))**2+(Mxy1)**2)**0.5)

*IF,Meq1,GT,Meq2,THEN
Meq=Meq1
*else
Meq=Meq2
*endif

*SET,GMODIF1,(COL9(1)/Meq)**(1/3)*THK
*CFWRITE,R,MN,GMODIF1
*CFWRITE,REAL,MN
*CFWRITE,EMODIF,J
*SET,MN,MN+1
*ENDDO
*CFCLOS

/sys,cat result_first >> results
/sys,rm result_first

!
!    ######  ENTER NEXT LINEAR ANALYSIS AFTER MODIFYING ! !
       !THICKNESS######
!

/PREP7                                ! ENTER PREPROCESSOR
RESUME                                ! RESUME .db file

!              ### USE MACRO MODVAL1 FOR ANALYSIS ###              !

*USE,MODVAL1
FINISH
/SOLU
SAVE
SOLVE
```

```
FINISH

/sys,rm MODVAL1

*ENDDO
!/inp,tmac
```

B.1.2 Von-Mises Yield Condition

```
!
! ###### MACRO FOR MODIFYING SECANT RIGIDITY ######
!
!
! ### THICKNESS OF PLATE IS DEFINED AS PARAMETER "THK" ###
! ### BELOW => THK=thickness of plate in 'mm'        ###

! INITIAL:    THK=10 mm
!             V=0.3
!             EM=2e5
!             D=(EM*THK**3)/(12*(1-V**2))
!
!             ENTER POST PROCESSOR AFTER FIRST ELASTIC ANALYSIS
!

*DO,IT,1,N                      ! N is the no. of iterations

*GET,SZ,ELEM,0,COUNT

/POST1

CSYS,1                          ! Use this for Cylindrical co-ordinate system
CSYS,0                          ! Use this for Cartesian co-ordinate system

*DIM,COL1,ARRAY,1               ! !!!!!!!!!!!!!!
*DIM,COL2,ARRAY,1               ! !!!!!!!!!!!!!!
*DIM,COL3,ARRAY,1               !
*DIM,COL4,ARRAY,1               !   DEFINE
*DIM,COL5,ARRAY,1               !   ARRAY
*DIM,COL6,ARRAY,1               !  PARAMETERS
*DIM,COL7,ARRAY,1               !
*DIM,COL8,ARRAY,1               ! !!!!!!!!!!!!!!
*DIM,COL9,ARRAY,SZ              ! !!!!!!!!!!!!!!
*DIM,COL10,ARRAY,SZ,1           !
```

```
*DIM,COL11,ARRAY,1              ! !!!!!!!!!!!!!!
*DIM,COL12,ARRAY,1              ! !!!!!!!!!!!!!!

!
!       READING MOMENTS  Mxx, Myy, Mxy FROM FIRST ELASTIC ANALYSIS
!

SET,1
ETABLE,Mxx,SMISC,4              ! Mxx
ETABLE,Myy,SMISC,5              ! Myy
ETABLE,Mxy,SMISC,6              ! Mxy

!
!       STORING ALL OUTPUT IN FILE  " result_first "
!

*SET,MN,2

*GET,MMAX1,ELEM,0,COUNT    ! Get max number of elements - MMAX1
*CFOPEN,result_first       ! Open file " result_first "
*DO,KK,1,MMAX1,            !

*IF,IT,EQ,1,then
NU=1
*ELSE
NU=MN
*ENDIF

*GET,cdnx,ELEM,KK,CENT,x       ! x coordinate
*GET,cdny,ELEM,KK,CENT,y       ! y coordinate
*GET,Mxx1,ELEM,KK,ETAB,Mxx ! Mxx moment
*GET,Myy1,ELEM,KK,ETAB,Myy ! Myy moment
*GET,Mxy1,ELEM,KK,ETAB,Mxy ! Mxy moment
*GET,THK,RCON,NU,CONST,1     ! Get thicknesses

Meq1=abs(0.5*(Mxx1+Myy1)-((0.5*(Mxx1-Myy1))**2+(Mxy1)**2)**0.5)
Meq2=abs(0.5*(Mxx1+Myy1)+((0.5*(Mxx1-Myy1))**2+(Mxy1)**2)**0.5)

Meq=((Meq1**2+Meq2**2-Meq1*Meq2)**0.5)

THETA=0.5*ATAN((2*Mxy1)/(Mxx1-Myy1))*(180/3.1416)

COL1(1)=kk
COL2(1)=cdnx
```

```
COL3(1)=cdny
COL4(1)=Mxx1
COL5(1)=Myy1
COL6(1)=Mxy1
COL7(1)=Meq1
COL8(1)=Meq2
COL11(1)=Meq
COL12(1)=THK

*VWRITE,COL1(1),COL2(1),COL3(1),COL4(1),COL5(1),COL6(1),COL7(1),COL8(1),
COL11(1),COL12(1)
(x,f6.1,e21.10,3x,e21.10,3x,e21.10,3x,e21.10,3x,e21.10,3x,e21.10,3x,e21.10,3x,e21.10,3
x,e21.10,3x,e21.10)

*SET,MN,MN+1
*ENDDO
*CFCLOS

!!!!    GETTING MAXIMUM EQUIVALENT MOMENT VALUE                !!!!

*VREAD,COL10(1,1),result_first,,,ij,SZ,1   ! Read Equivalent moments
(132x,e21.10)
*STAT,COL10(1,1)                          ! Print values in output file
*VSCFUN,COL9(1),MAX,COL10(1,1)      ! Maximum Meq       ! Get maximum value

        !x means one spacing
        !f6.1 means 6 digits and one decimal place (6 incl)
        !e21.10 means 21 digits and one decimal place(21 incl)

!
!    MODIFYING THICKNESS USING VALUES OF EQUIVALENT MOMENTS
!    AND STORING IN FILE " MODVAL1 "
!
*SET,MN,2

*CFOPEN,MODVAL1
*DO,J,1,MMAX1

*IF,IT,EQ,1,then
NU=1
*ELSE
NU=MN
*ENDIF
```

```
*GET,Mxx1,ELEM,J,ETAB,Mxx
*GET,Myy1,ELEM,J,ETAB,Myy
*GET,Mxy1,ELEM,J,ETAB,Mxy
*GET,THK,RCON,NU,CONST,1        ! Get thicknesses

Meq1=abs(0.5*(Mxx1+Myy1)-((0.5*(Mxx1-Myy1))**2+(Mxy1)**2)**0.5)
Meq2=abs(0.5*(Mxx1+Myy1)+((0.5*(Mxx1-Myy1))**2+(Mxy1)**2)**0.5)

Meq=((Meq1**2+Meq2**2-Meq1*Meq2)**0.5)

*SET,GMODIF1,(COL9(1)/Meq)**(1/3)*THK
*CFWRITE,R,MN,GMODIF1
*CFWRITE,REAL,MN
*CFWRITE,EMODIF,J
*SET,MN,MN+1
*ENDDO
*CFCLOS

/sys,cat result_first >> results
/sys,rm result_first

!
!     ######  ENTER NEXT LINEAR ANALYSIS AFTER MODIFYING
THICKNESS######
!

/PREP7        ! ENTER PREPROCESSOR
RESUME          ! RESUME .db file

!                ### USE MACRO MODVAL1 FOR ANALYSIS ###                !

*USE,MODVAL1
FINISH

/SOLU
SAVE
SOLVE
FINISH

/sys,rm MODVAL1

*ENDDO
```

APPENDIX C

C.1 Non-linear analysis of irregular plates

C.1.1 Rectangular plate partially fixed and partially simply supported.

```
!
! ## NON-LINEAR ANALYSIS OF A PARTIALLY FIXED AND
! PARTIALLY SIMPLY SUPPORTED RECTANGULAR PLATE USING MODIFIED
! SECANT RIGIDITY ##
!

/TITLE,NON-LINEAR ANALYSIS OF A IRREGULAR PLATE USING MODIFIED
/TITLE,SECANT RIGIDITY

/GRA,POWER
/GST,ON
/PREP7
/TITLE,ANALYSIS OF A IRREGULAR PLATE USING MODIFIED GEOMETRIC
PROPERTIES
ET,1,SHELL143

*SET,THK,12.7                    ! THICKNESS IN MM
*SET,EM,206.85e3

R,1,THK, , , , , ,
UIMP,1,EX, , ,EM,
UIMP,1,NUXY, , ,.3,

TB,BKIN,1, , , ,
TBMODIF,2,1,206.85
TBPLOT,BKIN,1,

B=254
L=381

k,1,0,0,0,
K,2,L,0,0
K,3,L,-B,0
K,4,0,-B,0

L,1,2
```

```
L,2,3
L,3,4
L,4,1

LESIZE,1, , ,81,1,
LESIZE,2, , ,54,1,
LESIZE,3, , ,81,1,
LESIZE,4, , ,54,1,

LSEL,ALL
AL,ALL

ASEL,ALL
AMESH,ALL

FINISH

/SOLU

NSEL,S,LOC,Y,0,
NSEL,R,LOC,X,0,L/3
D,ALL,ALL

NSEL,ALL

NSEL,S,LOC,Y,0
NSEL,R,LOC,X,2*L/3,L
D,ALL,ALL

NSEL,ALL

NSEL,S,LOC,Y,0,-B/3
NSEL,R,LOC,X,L
D,ALL,UZ

NSEL,ALL

NSEL,S,LOC,Y,-2*B/3,-B
NSEL,R,LOC,X,L
D,ALL,UZ

NSEL,ALL

NSEL,S,LOC,X,L/3,2*L/3
```

```
NSEL,R,LOC,Y,-B

D,ALL,ALL

NSEL,ALL

NSEL,S,LOC,Y,-B/3,-2*B/3
NSEL,R,LOC,X,0,

D,ALL,UZ

NSEL,ALL

SFA,ALL,1,PRES,20

SFTRAN

ANTYPE,0                        ! DEFINE STATIC ANALYSIS
NROPT,AUTO,,
time,1
NSUBST,50,
autots,on
NEQIT,100,
SSTIF,ON
pred,on,,on
OUTRES,ALL,ALL
SAVE
SOLVE
FINISH
```

C.1.2 Irregular plate partially fixed and partially simply supported.

```
!
! ## NON-LINEAR ANALYSIS OF A PARTIALLY FIXED AND
! PARTIALLY SIMPLY SUPPORTED IRREGULAR PLATE USING MODIFIED
! SECANT RIGIDITY ##
!

/GRA,POWER
/GST,ON
/PREP7
/TITLE,ANALYSIS OF A IRREGULAR PLATE USING MODIFIED SECANT
/TITLE,RIGIDITY
```

```
ET,1,SHELL143
R,1,10,,,,,,
UIMP,1,EX,,,200533.344724,
UIMP,1,NUXY,,,.3,

TB,MISO,1,,,,

TBMODIF,1,1,0.0017484
TBMODIF,1,2,350.6125

TBMODIF,2,1,0.095
TBMODIF,2,2,350.6125

B=1000
L=1700

k,1,0,0,0,
k,2,L/3,0,0
K,3,L/3,-B/3,0
K,4,2*L/3,-B/3,0
K,5,2*L/3,0,0
K,6,L,0,0
K,7,L,-B/3,0
K,8,L,-B,0
K,9,L,-(B+L*TAN(0.2618))
K,10,0.75*L,-(B+0.75*L*TAN(0.2618)),0
K,11,0.25*L,-(B+0.25*L*TAN(0.2618)),0
K,12,0,-B,0
K,13,0,-2*B/3
K,14,0,-B/3

L,1,2
L,2,3
L,3,4
L,4,5
L,5,6
L,6,7
L,7,8
L,8,9
L,9,10
L,10,11
L,11,12
L,12,13
L,13,14
```

```
L,14,1


LESIZE,1, , ,25,1,
LESIZE,2, , ,25,1,
LESIZE,3, , ,25,1,
LESIZE,4, , ,25,1,
LESIZE,5, , ,25,1,
LESIZE,6, , ,25,1,
LESIZE,7, , ,50,1,
LESIZE,8, , ,15,1,
LESIZE,9, , ,20,1,
LESIZE,10, , ,55,1,
LESIZE,11, , ,20,1,
LESIZE,12, , ,25,1,
LESIZE,13, , ,15,1,
LESIZE,14, , ,25,1,

LSEL,ALL

AL,ALL

ASEL,ALL

AMESH,ALL

FINISH

/SOLU

DL,1,1,ALL
DL,5,1,ALL

DL,6,1,UX
DL,6,1,UY
DL,6,1,UZ

DL,8,1,UX
DL,8,1,UY
DL,8,1,UZ

DL,10,1,ALL
DL,13,1,UX
DL,13,1,UY
```

```
DL,13,1,UZ

SFA,ALL,1,PRES,-0.5

SFTRAN
DTRAN

ANTYPE,0                    ! DEFINE STATIC ANALYSIS
NROPT,AUTO, ,
NSUBST,100,250
autots,on
kbc,0
EQSLV, , ,0,
NEQIT,100,
LNSRCH,ON
SSTIF,ON
OUTRES,ALL,ALL
SAVE
SOLVE
FINISH
```